

**University of Alberta**

Understanding the function of the JunB transcription factor in anaplastic  
lymphoma kinase-positive, anaplastic large cell lymphoma

by

Joel Dylan Pearson

A thesis submitted to the Faculty of Graduate Studies and Research  
in partial fulfillment of the requirements for the degree of

Doctor of Philosophy

in

Immunology

Medical Microbiology and Immunology

©Joel Dylan Pearson

Fall 2013

Edmonton, Alberta

Permission is hereby granted to the University of Alberta Libraries to reproduce single copies of this thesis and to lend or sell such copies for private, scholarly or scientific research purposes only. Where the thesis is converted to, or otherwise made available in digital form, the University of Alberta will advise potential users of the thesis of these terms.

The author reserves all other publication and other rights in association with the copyright in the thesis and, except as herein before provided, neither the thesis nor any substantial portion thereof may be printed or otherwise reproduced in any material form whatsoever without the author's prior written permission.

To my amazing wife Rachael, for supporting me throughout this entire  
endeavour.

## ABSTRACT

Anaplastic lymphoma kinase-positive, anaplastic large cell lymphoma (ALK+ ALCL) is a non-Hodgkin lymphoma thought to arise from an activated T lymphocyte. This lymphoma is characterized by the presence of chromosomal translocations involving the *ALK* tyrosine kinase, which generate oncogenic fusion proteins, most commonly nucleophosmin (NPM)-ALK. NPM-ALK activates many signalling pathways that drive the proliferation, survival and migration of ALK+ ALCL cells. One of the downstream effectors of NPM-ALK signalling is the activator protein-1 family transcription factor, JunB. JunB is highly expressed in ALK+ ALCL and was reported to promote proliferation of ALK+ ALCL cell lines. Despite this, transcriptional targets of JunB that are important in the pathogenesis of ALK+ ALCL were largely uncharacterized.

To better understand the function of JunB in ALK+ ALCL, we performed a quantitative mass spectrometry screen to identify JunB-regulated proteins in ALK+ ALCL cell lines. We identified the serine protease, Granzyme B (GzB), and the heat shock protein-90 co-chaperone, Cyclophilin 40 (Cyp40), as potential JunB-regulated proteins in ALK+ ALCL. Here, we demonstrate that *GzB* and *Cyp40* are JunB transcriptional targets, and that NPM-ALK and JunB signalling promotes GzB and Cyp40 expression in ALK+ ALCL. By regulating the expression of GzB and the related protein, Perforin, we show that NPM-ALK and JunB influence the cytotoxic phenotype observed in ALK+ ALCL.

Since the expression of GzB and Cyp40 was promoted by oncogenic signalling in ALK+ ALCL, we examined whether they play important roles in the pathogenesis of this lymphoma. Interestingly, we found that GzB expression actually sensitized ALK+ ALCL cell lines to apoptosis following treatment with apoptosis-inducing drugs. This finding is consistent with the observation that ALK+ ALCL patients are often successfully treated using standard chemotherapy regimens. We further found that Cyp40 promoted the viability of ALK+ ALCL cell lines. Together, our results shed light onto the function of an important transcription factor in ALK+ ALCL, and demonstrate that JunB regulates the expression of genes that contribute to multiple aspects of ALK+ ALCL biology. Furthermore, our findings uncover novel signalling events downstream of the NPM-ALK oncoprotein, and better clarify the molecular mechanisms underlying ALK+ ALCL phenotype and pathogenesis.

## **ACKNOWLEDGMENTS**

First, I would like to thank my supervisor, Dr. Robert Ingham, for giving me the opportunity to work in his lab and also for allowing me to move with him from the University of Victoria to the University of Alberta. He has been a great mentor and has always provided me with an amazing training environment with many different opportunities. Next, I would like to thank my supervisory committee, Drs. Troy Baldwin and Michele Barry for all of their guidance and suggestions during my time at the University of Alberta.

I would also like to thank the past and present Ingham lab members. In particular Jill Brandon who was a student in Dr. Ingham's lab when I began at UVic. She taught me so much about working in a lab when I first started. Jason Lee has been a great lab mate over the last 3.5 years, especially the times when we were a small lab just starting out. I am also grateful to all of our collaborators, in particular Dr. Julinor Bacani, Dr. Raymond Lai, Dr. Mike Gold and Spencer Freeman who have helped with various aspects of my project, as well as members of the Baldwin and Lai labs for many helpful ideas during lab meetings.

I would also like to thank all of the great friends I have made since joining the MMI department, in particular everyone from the first floor of MSB. You guys have made Grad school tons of fun, with various costume themes, Motorant trips, sushi lunches and lots of other great activities that I won't forget.

Finally, I want to thank all of my family. My mom and dad have always put a huge emphasis on education and I would not have made it to university without them. My little sister Ayla has always been an inspiration to me. My mother-in-law Leslie has also been a huge support and so encouraging ever since I have met her. Finally, my wonderful wife Rachael has probably been my biggest support during grad school and has put up with so much, from late nights and endless weekends in the lab, to night after night of work at home. She has been so supportive and amazing over this time and I couldn't have done this without her.

# TABLE OF CONTENTS

|  |          |
|--|----------|
| <b>CHAPTER 1: INTRODUCTION .....</b>   | <b>1</b> |
| 1.1: ANAPLASTIC LYMPHOMA KINASE-POSITIVE, ANAPLASTIC LARGE CELL LYMPHOMA (ALK+ ALCL) ..... | 2        |
| 1.1.1: Identification of ALK+ ALCL .....   | 2        |
| 1.1.2: Clinical features and course of ALK+ ALCL .....                                     | 2        |
| 1.1.3: Immunophenotype and morphology of ALK+ ALCL .....                                   | 4        |
| 1.1.3.1: <i>Cellular origin and morphology</i> .....                                       | 4        |
| 1.1.3.2: <i>CD30</i> .....   | 6        |
| 1.1.3.3: <i>Cytotoxic phenotype</i> .....  | 7        |
| 1.1.3.4: <i>Expression of ALK fusion proteins in ALK+ ALCL</i> .....                       | 10       |
| 1.2: ALK AND ALK FUSION PROTEINS .....   | 14       |
| 1.2.1: The physiological role of ALK .....   | 14       |
| 1.2.2: ALK ligands .....   | 15       |
| 1.2.3: Expression of ALK and ALK fusion proteins in cancer .....                           | 16       |
| 1.2.4: The role of the ALK fusion partner .....  | 18       |
| 1.2.5: Signalling pathways activated by NPM-ALK .....                                      | 21       |
| 1.3: THE AP-1 FAMILY OF TRANSCRIPTION FACTORS .....  | 23       |
| 1.4: THE JUNB TRANSCRIPTION FACTOR .....   | 24       |
| 1.4.1: Background .....  | 24       |
| 1.4.2: JunB is a positive and negative regulator of proliferation .....                    | 25       |
| 1.4.3: The role of JunB in development and differentiation .....                           | 26       |
| 1.4.4: The role of JunB in hematological malignancies .....                                | 28       |
| 1.4.5: JunB and AP-1 proteins in ALK+ ALCL .....   | 31       |
| 1.4.5.1: <i>Expression of AP-1 proteins in ALK+ ALCL</i> .....                             | 31       |

|                   |   |           |
|-------------------|---|-----------|
| 1.4.5.2:          | <i>The regulation and function of c-Jun in ALK+ ALCL</i>                            | 32        |
| 1.4.5.3:          | <i>Regulation and function of JunB in ALK+ ALCL</i>                                 | 34        |
| 1.5:              | HYPOTHESIS AND OBJECTIVES   | 38        |
| <b>CHAPTER 2:</b> | <b>MATERIALS AND METHODS</b>  | <b>40</b> |
| 2.1:              | CELL CULTURE AND TRANSFECTIONS  | 41        |
| 2.1.1:            | Cell lines  | 41        |
| 2.1.2:            | Transfection by electroporation   | 42        |
| 2.1.3:            | Generating stable cell lines using lentiviral transduction                          | 44        |
| 2.1.3.1:          | <i>Generating lentiviral particles</i>  | 44        |
| 2.1.3.2:          | <i>Infecting ALK+ ALCL cell lines with lentiviral particles</i>                     | 46        |
| 2.2:              | DNA METHODS   | 46        |
| 2.2.1:            | Genomic DNA Extraction  | 46        |
| 2.2.2:            | Polymerase chain reaction for cloning   | 47        |
| 2.2.3:            | Restriction endonuclease digestions   | 49        |
| 2.2.4:            | DNA ligations   | 49        |
| 2.2.5:            | Bacterial transformation  | 49        |
| 2.2.6:            | Isolation and purification of plasmid DNA   | 50        |
| 2.2.7:            | DNA sequencing and analysis   | 50        |
| 2.3:              | CLONING   | 51        |
| 2.3.1:            | Vectors   | 51        |
| 2.3.2:            | Cloning the FLAG- and Myc-tagged JunB constructs                                    | 51        |
| 2.3.3:            | Cloning the human <i>GzB</i> and <i>Cyp40</i> promoter-driven luciferase constructs | 53        |
| 2.3.4:            | Site-directed mutagenesis of AP-1 mutant promoter luciferase constructs             | 53        |

|          |  |    |
|----------|--|----|
| 2.4:     | PROTEIN METHODS.....   | 54 |
| 2.4.1:   | Cell lysis.....  | 54 |
| 2.4.2:   | Protein quantification using the bicinchoninic acid assay.....                           | 54 |
| 2.4.3:   | Quantitative mass spectrometry .....   | 55 |
| 2.4.4:   | Immunoprecipitations .....   | 55 |
| 2.4.5:   | Western blotting.....  | 56 |
| 2.4.6:   | Quantitative western blotting .....  | 57 |
| 2.4.7:   | Analysis of GzB expression using flow cytometry.....                                     | 59 |
| 2.5:     | RNA METHODS .....  | 59 |
| 2.5.1:   | Isolation of total RNA.....  | 59 |
| 2.5.2:   | DNase digestion and reverse transcription .....  | 59 |
| 2.5.3:   | PCR analysis of converted cDNA.....  | 60 |
| 2.5.4:   | Quantitative real-time PCR (qRT-PCR) .....   | 61 |
| 2.6:     | LUCIFERASE REPORTER ASSAYS .....   | 63 |
| 2.7:     | ELECTROPHORETIC MOBILITY SHIFT ASSAYS (EMSA) .....                                       | 63 |
| 2.7.1:   | Cytoplasmic and nuclear fractionation and Bradford assays .....                          | 63 |
| 2.7.2:   | EMSA experiments.....  | 64 |
| 2.7.2.1: | <i>Annealing duplex probes</i> .....   | 64 |
| 2.7.2.2: | <i>Binding reactions</i> .....   | 65 |
| 2.7.2.3: | <i>Electrophoresis and detection</i> .....   | 65 |
| 2.8:     | GRANZYME B RELEASE ASSAYS .....  | 66 |
| 2.9:     | EXPERIMENTS TO ASSESS GRANZYME B ACTIVITY.....   | 66 |
| 2.9.1:   | Cleavage of the synthetic GzB substrate, Ac-IEPD-pNA .....                               | 66 |
| 2.9.2:   | Cleavage of the extracellular matrix proteins vitronectin, fibronectin and decorin ..... | 67 |
| 2.9.3:   | Activity of released GzB .....   | 68 |

|   |           |
|---|-----------|
| 2.10: CELL TREATMENTS .....   | 68        |
| 2.10.1: 5-aza-2'-deoxycytidine (DAC) treatment .....  | 68        |
| 2.10.2: Staurosporine and doxorubicin treatments .....  | 69        |
| 2.10.3: Crizotinib treatments .....   | 69        |
| 2.11: IN VITRO INVASION ASSAYS .....  | 69        |
| 2.11.1: Preparing the collagen/fibronectin matrix .....   | 69        |
| 2.11.2: Invasion assay .....  | 70        |
| 2.12: APOPTOSIS ANALYSIS USING TERMINAL DEOXYNUCLEOTIDYL<br>TRANSFERASE dUTP NICK END LABELING (TUNEL).....                       | 71        |
| 2.13: MTS VIABILITY ASSAYS .....  | 71        |
| 2.14: STATISTICAL ANALYSIS.....   | 72        |
| <br>  |           |
| <b>CHAPTER 3: NPM-ALK AND THE JUNB TRANSCRIPTION FACTOR REGULATE<br/>THE EXPRESSION OF CYTOTOXIC MOLECULES IN ALK+ ALCL .....</b> | <b>73</b> |
| 3.1: INTRODUCTION .....   | 74        |
| 3.2: IDENTIFICATION OF GRANZYME B AS A POTENTIAL JUNB-REGULATED<br>PROTEIN IN ALK+ ALCL.....                                      | 75        |
| 3.3: GRANZYME B PROTEIN LEVELS ARE REDUCED FOLLOWING JUNB<br>KNOCK-DOWN IN ALK+ ALCL CELL LINES .....                             | 79        |
| 3.4: GRANZYME B IS A JUNB TRANSCRIPTIONAL TARGET IN ALK+ ALCL CELL<br>LINES .....   | 82        |
| 3.5: C-FOS ALSO BINDS THE AP-1 SITE IN THE <i>GRANZYME B</i> PROMOTER AND<br>ASSOCIATES WITH JUNB IN ALK+ ALCL CELL LINES.....    | 87        |
| 3.6: JUNB DOES NOT REGULATE PERFORIN EXPRESSION IN ALK+ ALCL.....   | 89        |
| 3.7: NPM-ALK REGULATES GRANZYME B AND PERFORIN EXPRESSION IN<br>ALK+ ALCL.....  | 92        |

|   |            |
|---|------------|
| 3.8: PERFORIN EXPRESSION IS SUPPRESSED BY DNA METHYLATION IN SUP-M2 AND SU-DHL-1 CELLS .....  | 96         |
| 3.9: DISCUSSION .....   | 98         |
| <b>CHAPTER 4: GRANZYME B SENSITIZES ALK+ ALCL CELL LINES TO DRUG-INDUCED APOPTOSIS.....</b>   | <b>101</b> |
| 4.1: INTRODUCTION .....   | 102        |
| 4.2: WHILE GRANZYME B IS CONSISTENTLY EXPRESSED IN ALK+ ALCL CELL LINES, GRANZYME A IS EXPRESSED ONLY AT LOW LEVELS AND EXPRESSION OF OTHER GRANZYMES IS NOT DETECTABLE IN THESE CELLS..... | 104        |
| 4.3: ALK+ ALCL CELL LINES EXPRESS ENZYMATICALLY ACTIVE GRANZYME B... ..   | 109        |
| 4.4: THE GRANZYME B EXPRESSED BY ALK+ ALCL CELLS PROMOTES CLEAVAGE OF ECM PROTEINS.....   | 114        |
| 4.5: ALK+ ALCL CELL LINES RELEASE ENZYMATICALLY ACTIVE GRANZYME B INTO THE CULTURE SUPERNATANT .....  | 120        |
| 4.6: KNOCK-DOWN OF GRANZYME B IN SUP-M2 CELLS DOES NOT OVERTLY EFFECT SUP-M2 INVASION INTO A COLLAGEN/FIBRONECTIN MATRIX.....   | 124        |
| 4.7: THE ELECTROPHORETIC MOBILITY OF $\alpha$ -TUBULIN IS ALTERED IN ALK+ ALCL CELLS FOLLOWING GRANZYME B KNOCK-DOWN.....   | 126        |
| 4.8: GRANZYME B SENSITIZES ALK+ ALCL CELL LINES TO STAUROSPORINE-INDUCED PARP CLEAVAGE.....   | 128        |
| 4.9: GRANZYME B SENSITIZES KARPAS 299 CELLS TO STAUROSPORINE-INDUCED DNA NICKING/FRAGMENTATION.....   | 133        |
| 4.10: GRANZYME B SENSITIZES SUP-M2 AND SR ALK+ ALCL CELL LINES TO DOXORUBICIN-INDUCED PARP CLEAVAGE .....   | 135        |
| 4.11: DISCUSSION .....  | 138        |

|   |            |
|---|------------|
| <b>CHAPTER 5: THE HEAT SHOCK PROTEIN-90 CO-CHAPERONE, CYCLOPHILIN 40, PROMOTES ALK+ ALCL VIABILITY AND ITS EXPRESSION IS REGULATED BY THE NPM-ALK ONCOPROTEIN .....</b> | <b>145</b> |
| 5.1: INTRODUCTION .....   | 146        |
| 5.2: JUNB PROMOTES CYP40, BUT NOT FKBP51 OR FKBP52, PROTEIN EXPRESSION IN ALK+ ALCL CELL LINES .....  | 148        |
| 5.3: JUNB PROMOTES <i>CYP40</i> TRANSCRIPTION IN ALK+ ALCL CELL LINES...  | 153        |
| 5.4: NPM-ALK PROMOTES CYP40 AND FKBP52, BUT NOT FKBP51, EXPRESSION .....  | 157        |
| 5.5: KNOCK-DOWN OF CYP40 REDUCES THE VIABILITY OF ALK+ ALCL CELL LINES .....  | 164        |
| 5.6: CYP40 KNOCK-DOWN DOES NOT AFFECT NPM-ALK LEVELS OR TYROSINE PHOSPHORYLATION, OR THE PHOSPHORYLATION OF CELLULAR PROTEINS..   | 168        |
| 5.7: DISCUSSION .....   | 171        |
| <br>  |            |
| <b>CHAPTER 6: DISCUSSION.....</b>   | <b>175</b> |
| 6.1: SUMMARY OF FINDINGS .....  | 176        |
| 6.2: OTHER POTENTIAL JUNB TARGETS IDENTIFIED IN THE ITRAQ SCREEN .....  | 180        |
| 6.3: JUNB REGULATES THE EXPRESSION OF PROTEINS THAT CONTRIBUTE TO MANY ASPECTS OF ALK+ ALCL BIOLOGY.....  | 182        |
| 6.4: EXAMINING THE ROLE OF JUNB IN OTHER LYMPHOMAS.....   | 186        |
| 6.5: THE FUNCTION OF JUNB IN OTHER ALK-EXPRESSING MALIGNANCIES  | 187        |
| 6.6: THE ROLE OF OTHER AP-1 PROTEINS WITH RELATION TO JUNB FUNCTION IN ALK+ ALCL .....  | 187        |
| 6.7: CONCLUSIONS .....  | 190        |

**CHAPTER 7: REFERENCES ..... 191**

**APPENDIX A: ADDITIONAL DATA..... 233**

## **LIST OF TABLES**

### **CHAPTER 1: INTRODUCTION**

|  |    |
|--|----|
| Table 1.1: ALK fusion proteins identified in ALK+ ALCL. .... | 12 |
| Table 1.2: ALK fusion proteins identified in cancer. ....    | 17 |

### **CHAPTER 2: MATERIALS AND METHODS**

|   |    |
|---|----|
| Table 2.1: siRNAs used in this study. ....            | 43 |
| Table 2.2: shRNA constructs used in this study. ....  | 45 |
| Table 2.3: Oligonucleotides used for cloning. ....    | 48 |
| Table 2.4: Vectors used in this study. ....           | 52 |
| Table 2.5: Antibodies used for western blotting. .... | 58 |
| Table 2.6: Primers used for RT-PCR. ....              | 62 |
| Table 2.7: Primers used for qRT-PCR. ....             | 62 |

### **CHAPTER 3: NPM-ALK AND THE JUNB TRANSCRIPTION FACTOR REGULATE THE EXPRESSION OF CYTOTOXIC MOLECULES IN ALK+ ALCL**

|  |    |
|--|----|
| Table 3.1: Summary of GzB quantitative mass spectrometry results. .... | 78 |
|--|----|

### **CHAPTER 5: THE HEAT SHOCK PROTEIN-90 CO-CHAPERONE, CYCLOPHILIN 40, PROMOTES ALK+ ALCL VIABILITY AND ITS EXPRESSION IS REGULATED BY THE NPM-ALK ONCOPROTEIN**

|  |     |
|--|-----|
| Table 5.1: Summary of Cyp40 quantitative mass spectrometry results. .... | 149 |
|--|-----|

### **APPENDIX A: ADDITIONAL DATA**

|  |     |
|--|-----|
| Appendix A3: Primers used for qRT-PCR analysis of additional JunB targets. ... | 236 |
|--|-----|

## LIST OF FIGURES

### CHAPTER 1: INTRODUCTION

|  |    |
|--|----|
| Figure 1.1: Staining of ALK+ ALCL tumour samples. ....   | 5  |
| Figure 1.2: The roles of Granzyme B and Perforin.....  | 9  |
| Figure 1.3: Chromosomal translocation that generates the NPM-ALK fusion protein in ALK+ ALCL. .... | 13 |
| Figure 1.4: Signalling pathways regulated downstream of NPM-ALK. ....                              | 22 |
| Figure 1.5: The regulation and function of c-Jun in ALK+ ALCL. ....                                | 33 |
| Figure 1.6: Regulation and function of JunB in ALK+ ALCL. ....                                     | 35 |

### CHAPTER 3: NPM-ALK AND THE JUNB TRANSCRIPTION FACTOR REGULATE THE EXPRESSION OF CYTOTOXIC MOLECULES IN ALK+ ALCL

|   |    |
|---|----|
| Figure 3.1: Identification of JunB-regulated proteins in ALK+ ALCL cell lines using quantitative iTRAQ mass spectrometry..... | 77 |
| Figure 3.2: siRNA-mediated knock-down of JunB reduces GzB protein levels.....   | 80 |
| Figure 3.3: Knock-down of JunB using shRNA results in reduced GzB protein levels. ....  | 81 |
| Figure 3.4: JunB knock-down reduces <i>GzB</i> mRNA expression in ALK+ ALCL cells.  | 83 |
| Figure 3.5: JunB promotes transcription from the <i>GzB</i> promoter. ....  | 84 |
| Figure 3.6: JunB can bind to the AP-1 site of the <i>GzB</i> promoter.....  | 86 |
| Figure 3.7: c-Fos can also bind to the AP-1 site of the <i>GzB</i> promoter.....  | 88 |
| Figure 3.8: JunB co-immunoprecipitates with c-Fos, Fra2 and other JunB molecules in ALK+ ALCL cell lines.....                 | 90 |
| Figure 3.9: JunB does not regulate Perforin expression in ALK+ ALCL. ....   | 91 |
| Figure 3.10: NPM-ALK promotes GzB expression in ALK+ ALCL. ....   | 93 |
| Figure 3.11: NPM-ALK regulates Perforin expression in Karpas 299 and SUP-M2 cells.....  | 94 |
| Figure 3.12: NPM-ALK promotes GzB expression but represses Perforin in SU-DHL-1 cells.....                                    | 95 |

|   |    |
|---|----|
| Figure 3.13: Inhibition of DNMTs results in elevated Perforin levels in SUP-M2 and SU-DHL-1 cells. .... | 97 |
|---|----|

**CHAPTER 4: GRANZYME B SENSITIZES ALK+ ALCL CELL LINES TO DRUG-INDUCED APOPTOSIS**

|  |     |
|--|-----|
| Figure 4.1: Examining expression of the Granzymes in ALK+ ALCL cell lines. ....  | 106 |
| Figure 4.2: ALK+ ALCL cell lines express greatly reduced <i>GzA</i> mRNA levels compared to NKL cells, while <i>GzB</i> is expressed more highly in ALK+ ALCL cells.   | 108 |
| Figure 4.3: ALK+ ALCL express enzymatically active <i>GzB</i> .....  | 110 |
| Figure 4.4: Examining <i>GzB</i> knock-down in Karpas 299 and SUP-M2 cells stably expressing <i>GzB</i> shRNA constructs.....  | 111 |
| Figure 4.5: Knock-down of <i>GzB</i> reduces cleavage of Ac-IEPD-pNA. ....   | 113 |
| Figure 4.6: A protein(s) expressed by ALK+ ALCL cell lines can cleave the ECM protein, vitronectin, and this is inhibited by the <i>GzB</i> inhibitor, Z-AAD-CMK. .... | 115 |
| Figure 4.7: Knock-down of <i>GzB</i> in Karpas 299 and SUP-M2 cells reduces appearance of the vitronectin cleavage bands.....  | 116 |
| Figure 4.8: Cleavage of the ECM protein fibronectin by Karpas 299 and SUP-M2 lysates is reduced by the <i>GzB</i> inhibitor Z-AAD-CMK.....                             | 118 |
| Figure 4.9: Decorin is cleaved in a <i>GzB</i> -dependent manner using Karpas 299 and SUP-M2 lysates. ....   | 119 |
| Figure 4.10: <i>GzB</i> is released by ALK+ ALCL cell lines.....   | 121 |
| Figure 4.11: <i>GzB</i> released by ALK+ ALCL cell lines possesses enzymatic activity. ....  | 123 |
| Figure 4.12: <i>GzB</i> knock-down does not affect invasion of SUP-M2 cells through a collagen/fibronectin matrix. ....  | 125 |
| Figure 4.13: <i>GzB</i> knock-down in ALK+ ALCL cell lines results in altered electrophoretic mobility of $\alpha$ -tubulin. ....                                      | 127 |
| Figure 4.14: Knock-down of <i>GzB</i> in Karpas 299 cells reduces PARP cleavage following treatment with the apoptosis-inducing drug, staurosporine. ....              | 130 |

|  |     |
|--|-----|
| Figure 4.15: Knock-down of GzB in SUP-M2 and SR cells results in reduced PARP cleavage following staurosporine treatment.....                        | 132 |
| Figure 4.16: GzB knock-down reduces TUNEL staining of Karpas 299 cells following staurosporine treatment.....  | 134 |
| Figure 4.17: SUP-M2 and SR cells stably expressing GzB shRNA have reduced PARP cleavage following doxorubicin treatment. ....                        | 136 |
| Figure 4.18: Knock-down of GzB in Karpas 299 cells does not reduce PARP cleavage following treatment with the apoptosis-inducing drug, doxorubicin . | 137 |

**CHAPTER 5: THE HEAT SHOCK PROTEIN-90 CO-CHAPERONE, CYCLOPHILIN 40, PROMOTES ALK+ ALCL VIABILITY AND ITS EXPRESSION IS REGULATED BY THE NPM-ALK ONCOPROTEIN**

|  |     |
|--|-----|
| Figure 5.1: JunB promotes Cyp40, but not FKBP51 or FKBP52, protein expression in ALK+ ALCL.....                            | 151 |
| Figure 5.2: shRNA-mediated knock-down of JunB results in reduced Cyp40 protein expression. ....                            | 152 |
| Figure 5.3: siRNA-mediated knock-down of JunB results in reduced <i>Cyp40</i> mRNA expression in ALK+ ALCL cells.....      | 154 |
| Figure 5.4: JunB promotes transcription from the Cyp40 promoter.....   | 155 |
| Figure 5.5: JunB binds to the AP-1 site of the <i>Cyp40</i> promoter. ....   | 156 |
| Figure 5.6: NPM-ALK promotes Cyp40 and FKBP52, but not FKBP51, protein expression in ALK+ ALCL cell lines.....             | 158 |
| Figure 5.7: NPM-ALK promotes Cyp40 and FKBP52 mRNA expression in ALK+ ALCL.....  | 159 |
| Figure 5.8: Crizotinib efficiently inhibits NPM-ALK activity in ALK+ ALCL cell lines. ....                                 | 161 |
| Figure 5.9: Inhibition of NPM-ALK activity results in a dose-dependent reduction in Cyp40 and FKBP52 protein levels. ....  | 162 |
| Figure 5.10: Inhibition of NPM-ALK activity results in a time-dependent reduction in Cyp40 and FKBP52 protein levels. .... | 163 |

|  |     |
|--|-----|
| Figure 5.11: Cyp40, but not FKBP51 or FKBP52, promotes ALK+ ALCL viability.  | 165 |
| Figure 5.12: Knock-down of Cyp40, FKBP51 and FKBP52 with individual siRNAs.<br>.....   | 166 |
| Figure 5.13: Knock-down of Cyp40, FKBP51 and FKBP52 in combination does not<br>reduce cell viability more than Cyp40 knock-down alone.....   | 167 |
| Figure 5.14: Cyp40 knock-down does not influence NPM-ALK expression or<br>tyrosine phosphorylation.....  | 169 |
| Figure 5.15: Knock-down of Cyp40 does not affect phosphorylation of total<br>cellular proteins or influence the phosphorylation and/or expression of STAT3,<br>ERK1/2, JunB, c-Jun or Akt in ALK+ ALCL cell lines..... | 170 |
| Figure 5.16: Pathways influencing expression of the immunophilin family of co-<br>chaperones in ALK+ ALCL. ....  | 172 |

**CHAPTER 6: DISCUSSION**

|   |     |
|---|-----|
| Figure 6.1: NPM-ALK and JunB regulate the expression of cytotoxic proteins in<br>ALK+ ALCL cell lines. .... | 177 |
| Figure 6.2: Regulation and function of the immunophilin co-chaperone proteins<br>in ALK+ ALCL.....          | 179 |
| Figure 6.3: JunB targets contribute to multiple aspects of ALK+ ALCL biology. .                             | 185 |

**APPENDIX A: ADDITIONAL DATA**

|   |     |
|---|-----|
| Appendix A1: Adhesion of Karpas 299 cells to fibronectin.....   | 234 |
| Appendix A2: Annexin A1 expression is repressed by JunB in ALK+ ALCL cells..  | 235 |
| Appendix A4: Analysis of potential JunB-regulated genes from proteins identified<br>in a single repeat of the iTRAQ screen..... | 237 |

## LIST OF ABBREVIATIONS

|             |   |
|-------------|---|
| 17-AAG      | 17-Allylamino-Demethoxygeldanamycin   |
| Ac-IEPD-pNA | N-Acetyl-Ile-Glu-Pro-Asp- <i>p</i> -nitroanilide  |
| ALCL        | anaplastic large cell lymphoma  |
| ALK         | anaplastic lymphoma kinase  |
| ALK- ALCL   | anaplastic lymphoma kinase-negative, anaplastic large cell lymphoma   |
| ALK+ ALCL   | anaplastic lymphoma kinase-positive, anaplastic large cell lymphoma   |
| AML         | acute myeloid leukemia  |
| AP-1        | activator protein-1   |
| ATF         | activating transcription factor   |
| ATIC-ALK    | 5-aminoimidazole-4-carboxamide ribonucleotide formyltransferase/IMP cyclohydrolase-anaplastic lymphoma kinase |
| BCA         | bicinchoninic acid  |
| BSA         | bovine serum albumin  |
| bZIP        | basic leucine zipper  |
| CHIP        | carboxyl-terminus of Hsp70-interacting protein  |
| CHOP        | cyclophosphamide, hydroxydaunorubicin (doxorubicin), oncovin, and prednisone                                  |
| CLTC-ALK    | clathrin heavy chain-anaplastic lymphoma kinase   |
| CML         | chronic myeloid leukemia  |
| CRE         | cyclic AMP response elements  |
| CTL         | cytotoxic T lymphocyte  |
| Cyp40       | Cyclophilin 40  |
| DAC         | 5-aza-2'-deoxycytidine  |
| DLBCL       | diffuse large B cell lymphoma   |

|                |   |
|----------------|---|
| DMEM           | Dulbecco's Modified Eagle's Medium  |
| DNA            | deoxyribonucleic acid   |
| DNMT           | DNA methyltransferase   |
| dNTP           | deoxynucleotide triphosphate  |
| <i>E. coli</i> | <i>Escherichia coli</i>   |
| ECM            | extracellular matrix  |
| EML4-ALK       | echinoderm microtubule-associated protein-like 4-anaplastic lymphoma kinase |
| EMSA           | electrophoretic mobility shift assay  |
| ERK            | extracellular signal-regulated kinase                                       |
| FBS            | fetal bovine serum  |
| FKBP51         | FK506-binding protein 51  |
| FKBP52         | FK506-binding protein 52  |
| GSK3 $\beta$   | Glycogen synthase kinase-3 $\beta$  |
| GzB            | Granzyme B  |
| HRP            | horseradish-peroxidase  |
| Hsp90          | heat shock protein-90   |
| ICAD           | inhibitor of caspase-activated deoxyribonuclease                            |
| IL             | interleukin   |
| IMT            | inflammatory myofibroblastic tumours  |
| iTRAQ          | isobaric tag for relative and absolute quantification                       |
| JAK            | Janus kinase  |
| JNK            | c-Jun N-terminal kinase   |
| LB             | Luria-Bertani   |
| MEK            | ERK kinase  |
| MSN-ALK        | moesin-anaplastic lymphoma kinase   |
| mTOR           | mammalian target of rapamycin   |

|                    |   |
|--------------------|---|
| MTS assay          | CellTiter 96 Aqueous Non-Radioactive Cell Proliferation Assay |
| NAPG               | N-ethylmaleimide-sensitive factor attachment protein, gamma   |
| NF- $\kappa$ B     | nuclear factor- $\kappa$ B                                    |
| NFAT               | nuclear factor of activated T cells                           |
| NK cell            | natural killer cell   |
| NPM                | nucleophosmin   |
| NPM-ALK            | nucleophosmin-anaplastic lymphoma kinase                      |
| NSCLC              | non-small cell lung carcinomas                                |
| PARP               | poly(ADP ribose) polymerase                                   |
| PBS                | phosphate-buffered saline                                     |
| PCR                | polymerase chain reaction                                     |
| PDGFR $\beta$      | platelet-derived growth factor receptor $\beta$               |
| PI-9               | proteinase inhibitor-9  |
| PI3K               | phosphatidylinositide 3-kinase                                |
| PIC                | protease inhibitor cocktail                                   |
| PLC $\gamma$       | phospholipase C- $\gamma$                                     |
| PMSF               | phenylmethyl sulfonyl fluoride                                |
| qRT-PCR            | quantitative real-time polymerase chain reaction              |
| RANBP2-ALK         | RAN binding protein 2-anaplastic lymphoma kinase              |
| RNA                | ribonucleic acid  |
| RPMI               | Roswell Park Memorial Institute                               |
| RPTP $\beta/\zeta$ | receptor tyrosine phosphatase $\beta/\zeta$                   |
| SDF-1 $\alpha$     | stromal cell-derived factor-1 $\alpha$                        |
| SDS-PAGE           | sodium dodecyl sulphate-polyacrylamide gel electrophoresis    |
| shRNA              | short hairpin RNA   |
| siRNA              | small interfering RNA   |

|              |   |
|--------------|---|
| STAT         | signal transducer and activator of transcription              |
| TBE buffer   | Tris/borate/EDTA buffer                                       |
| TBS          | Tris-buffered saline  |
| TBST         | Tris-buffered saline containing Tween-20                      |
| TCR          | T cell receptor   |
| TFG-ALK      | Trk-fused gene-anaplastic lymphoma kinase                     |
| TGF- $\beta$ | transforming growth factor $\beta$                            |
| TIA-1        | T cell restricted intracellular antigen-1                     |
| TPM3-ALK     | tropomyosin 3-anaplastic lymphoma kinase                      |
| TPM4-ALK     | tropomyosin 4-anaplastic lymphoma kinase                      |
| TPR-ALK      | translocated promoter region-anaplastic lymphoma kinase       |
| TRE          | 12-O-tetradecanoylphorbol-13-acetate (TPA) response elements  |
| TUNEL        | terminal deoxynucleotidyl transferase dUTP nick end labelling |
| TYMP         | Thymidine phosphorylase precursor                             |
| UGP2         | UTP-glucose-1-phosphate uridylyltransferase 1                 |

## CHAPTER 1: INTRODUCTION

Portions of this chapter were modified from a previously published manuscript:

**Pearson JD, Lee JKH, Bacani JTC, Lai R, and Ingham RJ.** (2012) NPM-ALK: the prototypic member of a family of oncogenic tyrosine kinases. *Journal of Signal Transduction*. **2012**:123253. (Review Article).

The original manuscript was drafted by J. Pearson, J. Lee and Dr. R. Ingham with input from Drs. J. Bacani and R. Lai.

## **1.1: ANAPLASTIC LYMPHOMA KINASE-POSITIVE, ANAPLASTIC LARGE CELL LYMPHOMA (ALK+ ALCL)**

### **1.1.1: Identification of ALK+ ALCL**

Anaplastic large cell lymphoma (ALCL) was first described by Stein and colleagues in 1985 as a Ki-1 (CD30)-positive non-Hodgkin lymphoma typically expressing T cell associated antigens, with a minor proportion expressing B cell associated antigen or neither B nor T cell markers (1). These tumour cells were described to have a range of morphologies, with some being large cells possessing large pleomorphic nuclei and abundant cytoplasm (1), what are now referred to as “hallmark cells.” Several subsequent studies identified a common t(2;5)(p23;q35) chromosomal translocation in some cell lines derived from patients with CD30-positive ALCL (2, 3), and in tumour cells from some patients with CD30-positive ALCL (4-7). It was later demonstrated in 1994 that this translocation resulted in the fusion of the *nucleophosmin (NPM)* gene on chromosome 5 to a previously unidentified tyrosine kinase on chromosome 2 (8, 9). This kinase was subsequently named *anaplastic lymphoma kinase (ALK)* given its common expression in ALCL. In several large studies it has been demonstrated that between 30-60% of ALCLs express ALK fusion proteins (10-17); however, when only childhood and adolescent cases of ALCL were examined, approximately 90% were found to possess ALK fusions (17-19). These lymphomas are referred to as ALK-positive ALCL (ALK+ ALCL), and are now classified as a distinct clinical entity by the World Health Organization (20, 21).

### **1.1.2: Clinical features and course of ALK+ ALCL**

ALK+ ALCL is predominantly observed in children and young adults, where the majority of ALK+ ALCL patients present in their first three decades of life (10, 11, 16, 20, 22), with average ages of presentation reported between 16-22 years (10, 11, 22). Even when childhood cases (less than 18 years of age) were excluded the

mean age of ALK+ ALCL patients at diagnosis is still quite young, and ranges from 34-37 years old (12-14). This is in contrast to ALK-negative ALCL (ALK- ALCL), in which the average age of presentation has been reported between 43 and 58 years (10-14). ALK+ ALCL accounts for 10-20% of childhood non-Hodgkin lymphoma, whereas it accounts for only ~3% of adult non-Hodgkin lymphomas (20), and this lymphoma has also been demonstrated to have a slightly male predominance (11-14, 18-20, 22). While ALK+ ALCL tumour cells are typically thought to originate in lymph nodes, patients often (53-73% of cases) present at advanced stages of the disease (stage III-IV) with extranodal infiltration of lymphoma cells and B symptoms (11-14, 18, 19). The most common extranodal sites of involvement include skin, bone, spleen, liver and lung, with spread to the digestive tract and nervous system being rare (11, 13, 18).

Despite the aggressive nature of this lymphoma and late stage of presentation, treatment of ALK+ ALCL patients with standard CHOP (cyclophosphamide, hydroxydaunorubicin (doxorubicin), oncovin, and prednisone) or CHOP-like chemotherapy regimens is typically quite successful (11, 12, 14, 18). Overall 5 year survival rates for ALK+ ALCL patients have been shown to range from 70-85% (10-14, 18, 23), and 5 year event/failure-free survival rates range from 60-75% (12-14, 18). A significant correlation between younger age of diagnosis (less than 60 years of age) and better overall survival has also been noted (23). In contrast to ALK+ ALCL, ALK- ALCL has significantly lower overall 5 year survival rates (30-50%) (10-14) and event/failure-free survival rates (~35%) (12-14). Furthermore, ALK+ ALCL was shown to have a better prognosis compared to several other non-Hodgkin lymphomas (12, 14), with the only exception being primary cutaneous ALCL, which was found to have a higher overall survival, although lower failure-free survival rate, compared to ALK+ ALCL (14). It has also been demonstrated that ALK+ ALCL patients have a significantly improved outcome when treated with anthracycline (doxorubicin)-containing chemotherapy compared to non-anthracycline-containing regimens (14).

Another study found that the combination of CHOP therapy and the apoptosis-inducing agent, etoposide, reduced the relapse rate (although not the overall survival) of ALK+ ALCL patients compared to CHOP therapy alone (12).

### **1.1.3: Morphology and immunophenotype of ALK+ ALCL**

#### **1.1.3.1: Cellular origin and morphology**

ALK+ ALCL tumour cells are often found to express different T cell markers; however, some cells lack expression of common T cell markers, which has led to ALK+ ALCL being described as having a T or null-cell immunophenotype (20, 22, 24). Despite the presence of some T cell markers in many of these tumours, many do not express common T cell proteins, such as TCR- $\beta$ , CD3, LAT, SLP-76, ZAP70 and CD4/CD8 (19, 22, 25-27); however, the majority of these cells, as well as cells of a null immunophenotype possess clonal TCR gene rearrangements (19, 26, 28). This finding suggests that these tumours likely originate from cells of T cell origin. One explanation for why many common T cell markers are not expressed by ALK+ ALCL tumours, is that the genes encoding for several of these proteins are silenced by DNA methylation in ALK+ ALCL cell lines (25).

ALK+ ALCL tumour cells have been described to have a variety of different morphologies; however, ALK+ ALCL patients are characterized by the presence of a certain proportion of so call “hallmark cells” (20, 22, 29, 30). These “hallmark cells” are typically large cells with kidney or horseshoe shaped nuclei and abundant cytoplasm (20, 22, 29, 30) (Figure 1.1). In addition to the presence of “hallmark cells,” the expression of several proteins is commonly associated with ALK+ ALCL. These include CD30, cytotoxic proteins (Granzyme B (GzB), Perforin and T cell restricted intracellular antigen-1 (TIA-1)), and most importantly, ALK-containing fusion proteins.

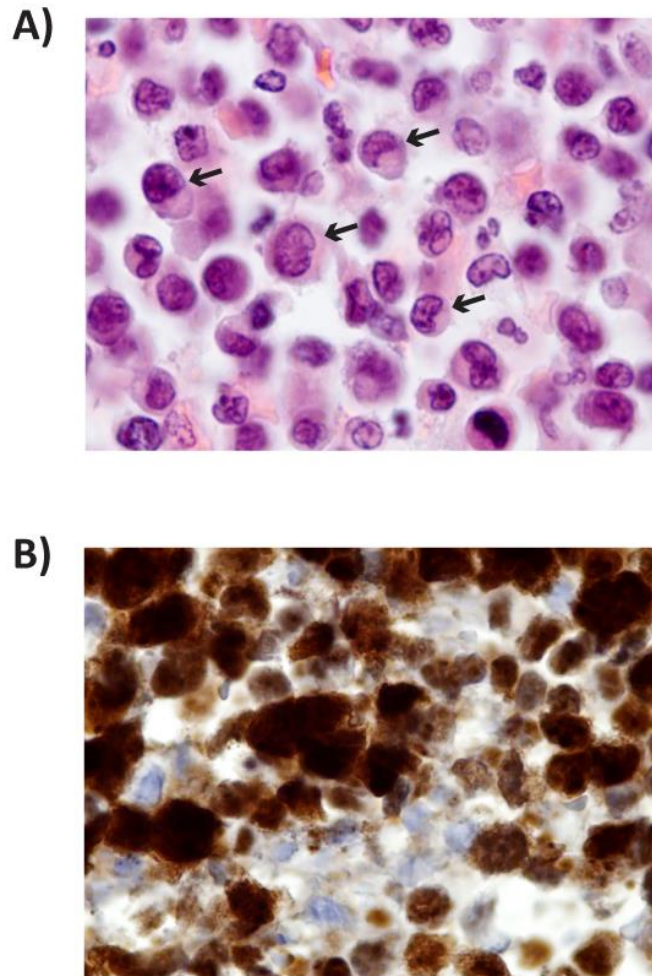


**Figure 1.1: Staining of ALK+ ALCL tumour samples.**

**(A)** Haematoxylin and eosin staining of a tumour biopsy section from a patient with ALK+ ALCL. Some of the “hallmark” cells containing irregularly shaped nuclei and abundant cytoplasm are indicated with arrows. **(B)** Immunohistochemical staining for ALK in an ALK+ ALCL tumour section. Images are from different fields of different sections from the same patient. Original images were 100X magnification, and the image in **(A)** was further enlarged in Photoshop. Images were provided by Dr. Julinor Bacani (University of Alberta).

### **1.1.3.2: CD30**

ALCL was initially identified because it expresses the CD30 (Ki-1) antigen (1), and it is now well established that CD30 is commonly expressed by ALK+ ALCL tumour cells (20, 24, 27, 30, 31). CD30 was first identified as an antigen expressed by Hodgkin lymphoma cells (32, 33), and since then CD30 expression has been noted in several hematological malignancies. These include ALK+ ALCL, ALK- ALCL, a subset of diffuse large B cell lymphomas (DLBCL), multiple myeloma, as well as various other T and B cell lymphomas and leukemias (1, 34-37). CD30 is a member of the tumour necrosis factor receptor family (38) and is typically expressed by activated T and B cells (34-36). Ligation of CD30 typically results in activation of nuclear factor- $\kappa$ B (NF- $\kappa$ B) (39, 40) and signalling initiated by CD30 can have pleiotropic effects depending on the cellular context. CD30 has been shown to have a role in T cell co-stimulation, to promote cytokine secretion, to enhance proliferation and survival and also to promote apoptosis (35, 36).

In ALK+ ALCL the role of CD30 is somewhat controversial. It has been demonstrated by several studies that stimulation of CD30 using anti-CD30 antibodies or CD30 ligand inhibits proliferation of the Karpas 299 ALK+ ALCL cell line (41-48), while one of these studies also observed reduced proliferation of several other ALK+ ALCL cell lines following CD30 stimulation (41). In several instances there was no effect on apoptosis of ALK+ ALCL cells stimulated through CD30 (44-47). However, other groups have demonstrated that stimulation of CD30 promotes the apoptosis of Karpas 299 cells (41-43, 49-51), while one study also observed a minor induction of apoptosis in the SR ALK+ ALCL cell line (51).

The reason for the differing results of CD30 stimulation on ALK+ ALCL biology is currently unclear, but it was suggested that the means by which cells were stimulated may affect the outcome. Stimulation of CD30 using plate-bound antibodies was found to promote apoptosis of Karpas 299 cells, whereas soluble antibodies did not promote apoptosis of these cells (50). However, these findings

do not entirely explain the differing results from these studies, as one group has not observed an induction of apoptosis in Karpas 299 cells following stimulation of CD30 with plate-bound antibodies (44, 45, 52).

Another factor contributing to the discrepancy in results may be related to the level of NF- $\kappa$ B activity induced by CD30 stimulation. It was demonstrated that CD30 stimulation does not activate NF- $\kappa$ B in Karpas 299 cells (49, 53), and it was proposed that this may be due to NPM-ALK-mediated suppression of NF- $\kappa$ B activation downstream of CD30 (53). However, several other groups have shown that NF- $\kappa$ B is activated down-stream of CD30 in ALK+ ALCL cell lines (43, 46, 47, 52). Interestingly, it was found that inhibition of NF- $\kappa$ B resulted in apoptosis of CD30-stimulated Karpas 299 cells (43, 47, 52). Thus, these findings suggest that the presence of NF- $\kappa$ B activity following CD30 stimulation may protect cells from apoptosis and that in situations where NF- $\kappa$ B is not activated downstream of CD30, CD30 signalling may promote apoptosis of ALK+ ALCL cells. However, the reason for why CD30 stimulation activates NF- $\kappa$ B in some studies but not others is not clear, but could be due to stimulation or culture conditions or intrinsic differences in the cell clones used in the experiments. In spite of the differing findings regarding the exact role of CD30 in ALK+ ALCL, it does appear that CD30 signalling is largely detrimental to ALK+ ALCL tumour cells, as it inhibits proliferation and may promote apoptosis of these cells.

### **1.1.3.3: Cytotoxic phenotype**

ALK+ ALCL tumour cells have been described to have a cytotoxic phenotype because they often express the cytotoxic-related proteins GzB, Perforin and TIA-1 (19, 27, 28, 54-56). GzB is a member of the Granzyme family of proteins, which in humans also consists of Granzymes A, H, K and M (57). These proteins are typically found within specialized vesicles (called granules) of natural killer (NK) cells and activated cytotoxic T lymphocytes (CTLs), and are used by these cells to kill virally infected or transformed cells (57-60). To accomplish this, Granzymes

function as serine proteases to cleave a variety of proteins within the target cell, ultimately resulting in death of the targeted cell (57-59) (Figure 1.2). The pore-forming protein Perforin is another component of the cytolytic granules present in CTL and NK cells (61-64), and is important for Granzyme-mediated target cell death, as Perforin is thought to facilitate entry of Granzymes into the cytosol of the target cell (65-69) (Figure 1.2). TIA-1 is a RNA-binding protein that is expressed by various cell types (70, 71) and has a variety of cellular functions (71-77). For example, TIA-1 is present in the cytotoxic granules of CTL and NK cells (78) and it has been shown that purified TIA-1 has the ability to induce DNA fragmentation in permeabilized cells, suggesting that it may represent a cytotoxic protein used by CTL and NK cells to kill target cells (72).

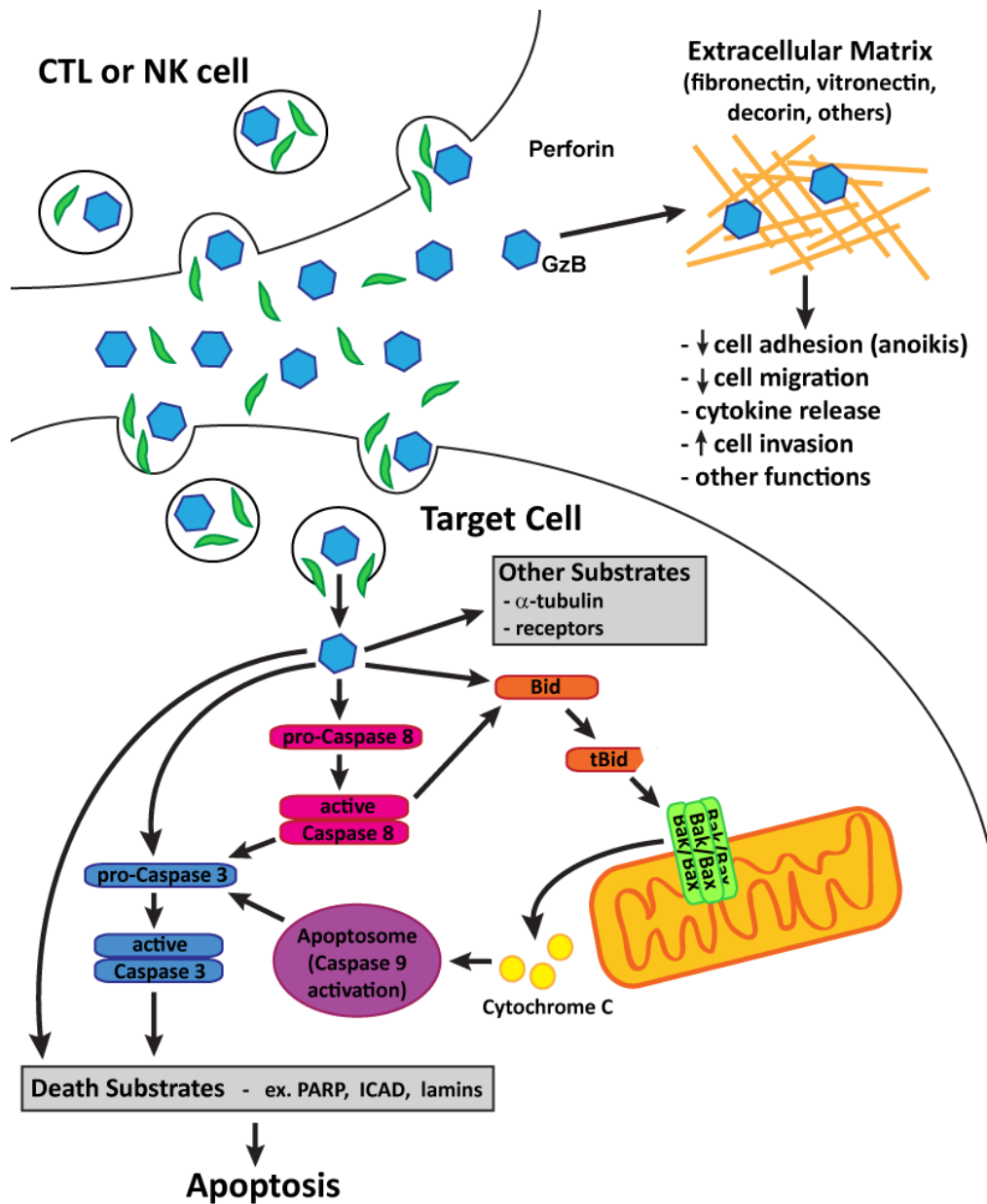


**Figure 1.2: The roles of Granzyme B and Perforin.**

GzB released by a CTL or NK cell can enter a target cell with the assistance of the pore-forming protein, Perforin. Once in the cytosol of the target cell, GzB cleaves many substrates, such as Bid and Caspases to induce apoptosis of the targeted cell. GzB that is released by CTL and NK cells can also cleave extracellular matrix proteins, such as fibronectin, vitronectin and decorin, which can influence the interaction of different cells with these proteins.

When GzB, Perforin and TIA-1 expression was examined in 68 ALK+ ALCL patient samples, approximately 95% of patients possess tumour cells that expressed at least one of these cytotoxic markers (19). In several smaller studies where only two of the cytotoxic proteins were examined, 78-92% of patients were found to possess tumour cells that express at least one cytotoxic molecule, with only 1-2 patients staining negative for both proteins examined in each study (28, 55, 56). These findings have demonstrated a common cytotoxic phenotype in ALK+ ALCL, and have led to the suggestion that ALK+ ALCL may arise from cells of CTL origin. However, it is interesting to note that ALK+ ALCL tumour cells are more commonly positive for the helper T cell marker CD4, opposed to the CTL marker CD8 (19), and a gene expression profiling study found that ALK+ ALCL tumour cells have a genetic signature that is equally similar to activated CD4+ and activated CD8+ cells (79). It is also interesting that the intracellular serpin inhibitor of Granzyme B, proteinase inhibitor-9 (PI-9), that is usually expressed by CTLs (80) has been reported to be absent in tumour cells from ALK+ ALCL patients (81). Furthermore, it has been demonstrated that NPM-ALK signalling induces a regulatory T cell phenotype in ALK+ ALCL, characterized by expression of interleukin (IL)-10, transforming growth factor  $\beta$  (TGF- $\beta$ ) and FoxP3 (82). ALK+ ALCL cells have also been found to express IL-17 (83, 84), and NPM-ALK signalling has been suggested to promote a Th17-like phenotype in ALK+ ALCL by up-regulating expression of microRNA-135b (83). microRNA-135b then suppressed expression STAT6 and GATA3, two transcription factors that promote Th2 differentiation and are thought to repress Th17 differentiation (83). These latter findings suggest that ALK+ ALCL may not necessarily arise from a CTL and that other factors may be contributing to the cytotoxic phenotype observed in this lymphoma.

#### **1.1.3.4: Expression of ALK fusion proteins in ALK+ ALCL**

While the presence of “hallmark cells” and the expression of CD30 and cytotoxic proteins is characteristic of ALK+ ALCL, this cancer is defined by the presence of

fusion proteins involving the ALK tyrosine kinase (Table 1.1) that arise from various chromosomal translocations. The most common of these fusion proteins is NPM-ALK, which is present in 75-84% of ALK+ ALCL tumours, while tropomyosin 3 (TPM3)-ALK has been observed in 12-18% of ALK+ ALCL cases and a variety of other ALK fusion proteins have been identified in a limited number (<2%) of ALK+ ALCL cases (20, 31, 85). In all ALK fusion proteins, an N-terminal partner is fused to the C-terminal intracellular domain of ALK including the ALK kinase domain (Figure 1.3). Since full length ALK is typically not expressed in lymphocytes (8), these translocations put the *ALK* fusions under transcriptional control of the regulatory regions of the fusion partner, allowing for the aberrant expression of the ALK kinase in ALK+ ALCL. It is now well established that these ALK fusion proteins have potent transforming capabilities using *in vitro* cell line models (86-90) and *in vivo* transgenic mouse models (91-96). As will be discussed in the following sections, these ALK fusion proteins play critical roles in the pathogenesis of ALK+ ALCL, as well as several other malignancies.

**Table 1.1: ALK fusion proteins identified in ALK+ ALCL.**

| <b>ALK fusion protein</b> | <b>Chromosomal abnormality</b> | <b>Reference(s)</b> |
|---------------------------|--------------------------------|---------------------|
| NPM-ALK                   | t(2;5)(p23;q35)                | (8, 9)              |
| TPM3-ALK                  | t(1;2)(q25;p23)                | (97, 98)            |
| TFG-ALK                   | t(2;3)(p23;q21)                | (99, 100)           |
| ATIC-ALK                  | Inv(2)(p23;q35)                | (88, 89, 101)       |
| CLTC-ALK                  | t(2;17)(p23;q23)               | (102)               |
| TPM4-ALK                  | t(2;19)(p23;p13.1)             | (103)               |
| MSN-ALK                   | t(X;2)(q11;p23)                | (104, 105)          |
| ALO17-ALK                 | t(2;17)(p23;q25)               | (106)               |
| MYH9-ALK                  | t(2;22)(p23;q11.2)             | (107)               |

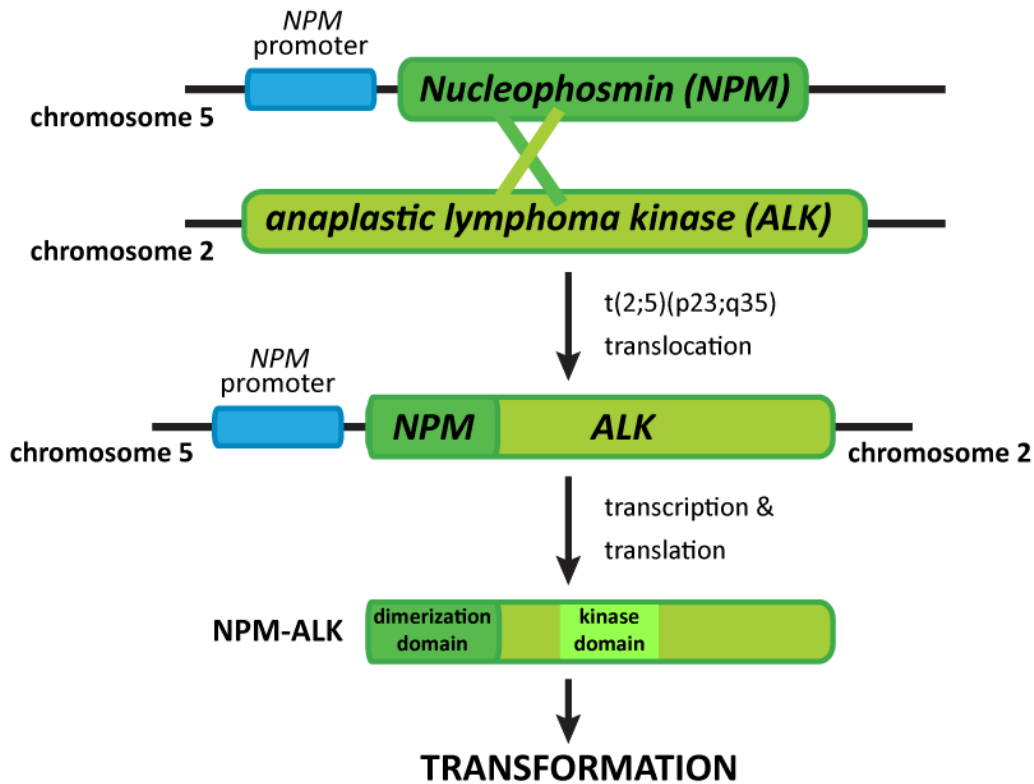


**Figure 1.3: Chromosomal translocation that generates the NPM-ALK fusion protein in ALK+ ALCL.**

A common  $t(2;5)(p23;q35)$  chromosomal translocation in ALK+ ALCL between the *ALK* gene on chromosome 2 and *NPM* gene on chromosome 5 results in the generation of the NPM-ALK fusion protein. *NPM-ALK* consists of the first 4 exons of the *NPM* gene and exons 20-29 of *ALK*, resulting in a protein containing the NPM dimerization domain and ALK kinase domain and intracellular tail. Most other ALK fusion proteins are generated in a similar manner.

## 1.2: ALK AND ALK FUSION PROTEINS

### 1.2.1: The physiological role of ALK

ALK is a receptor tyrosine kinase that belongs to the insulin receptor superfamily and is most closely related to leukocyte tyrosine kinase (8, 9). In mice and humans ALK expression is largely restricted to the brain and nervous system (15, 108-110), where it appears to be more prevalent in the developing nervous system (108, 109). This has suggested a role for ALK in the development and/or function of the nervous system. Furthermore, *in vitro* studies have supported a role for ALK in development of the nervous system, as ALK can promote neurite outgrowth in different *in vitro* models (111-114). However, differences in the role of ALK in neurogenesis have been observed *in vivo*. In one study it was found that adult (but not younger) *ALK* knockout mice have increased neurogenesis of some subsets of neurons and enhanced proliferation of hippocampal progenitor cells (115). However, another group observed reduced neurogenesis in similar subsets of neurons in *ALK* knockout mice (116). The reason for these differences is not clear, but could be due to differences in the targeting sequences used to generate the different mice. In *Drosophila melanogaster*, ALK is expressed in different tissues including the developing visual system. Furthermore, its expression in target neurons is required for proper formation of the retina in these organisms (117), further supporting a role for ALK in neuronal function.

Although ALK may have a role in neurogenesis, in mice it does not appear to be required for development of the nervous system (or other tissues), as several groups have independently generated *ALK* knockout mice that do not appear to have any obvious developmental or anatomical defects (115, 116, 118, 119). However, *ALK*-deficient mice have been suggested to have some behavioural abnormalities. These mice perform better on tests of cognitive ability, have enhanced spatial memory retention and have reduced anxiety and depression compared to wild-type littermates (115, 116). *ALK* knockout mice also display enhanced consumption of alcohol in a binge drinking model and have an altered

sensitivity to alcohol (118). Interestingly, flies with transposon insertions in *dALK* have increased resistance to the sedating effect of alcohol, and in humans several single nucleotide polymorphisms in *ALK* have been identified that correlate with decreased alcohol sensitivity (118) and alcohol dependence (120). These findings suggest a common role of ALK in influencing alcohol sensitivity and consumption in various organisms. Single nucleotide polymorphisms in *ALK* were also correlated with schizophrenia patients in a Japanese population (121).

### **1.2.2: ALK ligands**

In *Drosophila melanogaster*, jelly belly has been well characterized as a ligand for ALK (122-124). However, mammals do not appear to express a jelly belly homologue, suggesting that another protein may function as the ligand for ALK in higher organisms. The secreted proteins, pleiotrophin (125-128) and midkine (129-131), have now been described as activating ligands for human ALK. However, some studies have argued that these proteins may not be true ALK stimulating ligands (112, 113, 132), and an alternative means by which pleiotrophin may stimulate ALK signalling was recently suggested. It was shown that through binding to its known receptor, receptor tyrosine phosphatase  $\beta/\zeta$  (RPTP  $\beta/\zeta$ ), pleiotrophin can relieve the inhibitory dephosphorylation of ALK by RPTP  $\beta/\zeta$ , resulting in ALK activation (133). However, there is data that also questions this hypothesis, as pleiotrophin could still activate ALK signalling in glioblastoma cell lines with undetectable levels of RPTP  $\beta/\zeta$  (128). Furthermore, it has been demonstrated that through stimulating ALK, midkine can protect glioma cells from apoptosis induced by cannabinoids (131). In these studies, significant knock-down of RPTP  $\beta/\zeta$  was found to have no impact on this apoptosis protection in some cell lines and only a minimal impact in others (131), suggesting that RPTP  $\beta/\zeta$  was not required for midkine to activate ALK in these cells. It has also been demonstrated that ALK may function as a dependence

receptor (134), which are receptors that suppress apoptosis when bound to their ligand but promote apoptosis of cells when they are not ligand-bound (135).

### **1.2.3: Expression of ALK and ALK fusion proteins in cancer**

While ALK expression is typically restricted to the nervous system, aberrant expression of ALK has been noted in several malignancies. Expression of the NPM-ALK oncoprotein was first noted in ALK+ ALCL, and since then, at least 19 different ALK fusion proteins have been described in ALK+ ALCL and other malignancies (31, 136). ALK fusion proteins have now been identified in rare cases of DLBCL (137-143) and extramedullary plasmacytoma (144), as well as several solid tumours (Table 1.2). Most notably, ALK fusions have been found in 1-11% of non-small cell lung carcinomas (NSCLC), with echinoderm microtubule-associated protein-like 4 (EML4)-ALK being the most common fusion in this cancer (145-150). Within patients with NSCLC, ALK fusions are more common in patients with adenocarcinoma (148, 151, 152), and in patients who are non-smokers (146, 148). ALK fusions have also been observed in about 50% of inflammatory myofibroblastic tumours (IMT) (106, 153-159), as well as rare cases of colon cancer (147, 160), breast cancer (147), and renal cell carcinoma (161-163). Mass spectrometry data has also suggested the presence of tropomyosin 4 (TPM4)-ALK in esophageal squamous cell carcinoma (164, 165). In addition to ALK fusion proteins, full length ALK is expressed in some breast cancers (166) and *ALK* gene amplifications have been observed in esophageal cancer (167). *ALK* gene amplifications and several ALK activating mutations have also been identified in cases of familial and sporadic neuroblastoma (168-173) and thyroid cancer (174). Because of the expression and importance of ALK fusions in various cancers, ALK inhibitors have been developed and the ALK inhibitor, Crizotinib, has shown efficacy in treating patients with ALK+ ALCL (175), ALK+ NSCLC (176-178) and ALK+ IMT (179). Various other ALK inhibitors are also being tested for their efficacy and safety in patients with ALK-expressing tumours (180).

**Table 1.2: ALK fusion proteins identified in cancer.**

| <b>Cancer</b>                      | <b>ALK fusion protein</b> | <b>Reference(s)</b> |
|------------------------------------|---------------------------|---------------------|
| ALCL                               | NPM-ALK                   | (8, 9)              |
| ALCL                               | TPM3-ALK                  | (97, 98)            |
| ALCL                               | TFG-ALK                   | (99, 100)           |
| ALCL                               | ATIC-ALK                  | (88, 89, 101)       |
| ALCL                               | CLTC-ALK                  | (102)               |
| ALCL                               | TPM4-ALK                  | (103)               |
| ALCL                               | MSN-ALK                   | (104, 105)          |
| ALCL                               | ALO17-ALK                 | (106)               |
| ALCL                               | MYH9-ALK                  | (107)               |
| DLBCL                              | NPM-ALK                   | (137)               |
| DLBCL                              | CLTC-ALK                  | (138-140)           |
| DLBCL                              | SEC31L1-ALK               | (141, 142)          |
| DLBCL                              | SQSTM1-ALK                | (143)               |
| NSCLC                              | EML4-ALK                  | (149, 150)          |
| NSCLC                              | TFG-ALK                   | (150)               |
| NSCLC                              | KIF5B-ALK                 | (181)               |
| NSCLC                              | KLC1-ALK                  | (182)               |
| IMT                                | TPM3-ALK                  | (154)               |
| IMT                                | TPM4-ALK                  | (154)               |
| IMT                                | CLTC-ALK                  | (156)               |
| IMT                                | CARS-ALK                  | (106, 183)          |
| IMT                                | ATIC-ALK                  | (155)               |
| IMT                                | RANBP2-ALK                | (157)               |
| IMT                                | SEC31L1-ALK               | (158)               |
| IMT                                | PPFIBP1-ALK               | (159)               |
| colorectal cancer                  | EML4-ALK                  | (147)               |
| colorectal cancer                  | C2orf44-ALK               | (160)               |
| breast cancer                      | EML4-ALK                  | (147)               |
| renal cell carcinoma               | VCL-ALK                   | (161, 162)          |
| renal cell carcinoma               | TPM3-ALK                  | (163)               |
| renal cell carcinoma               | EML4-ALK                  | (163)               |
| extramedullary plasmacytoma        | CLTC-ALK                  | (144)               |
| esophageal squamous cell carcinoma | TPM4-ALK                  | (164, 165)          |

#### **1.2.4: The role of the ALK fusion partner**

The ALK fusion partner has been shown to play an essential role in the activation and transforming ability of ALK fusion proteins. It was found that deletions in the NPM portion of NPM-ALK resulted in a protein that lost the ability to transform NIH 3T3 (86) or Fischer Rat 3T3 cells (87). Furthermore, an engineered ALK fusion protein, translocated promoter region (TPR)-ALK, that contains the fusion partner of the TPR-MET oncogene (184), was able to transform cells almost as efficiently as NPM-ALK (87). This demonstrated that while an ALK fusion partner is required for transformation, it does not have to be NPM. The NPM domain was also required for NPM-ALK phosphorylation (87) and for NPM-ALK to associate with the adapter proteins Shc, insulin receptor substrate 1 and Grb2 (86). NPM was known to form hexamers and other oligomers (185, 186), suggesting that, like the TPR region of TPR-MET (184), NPM might facilitate dimerization/oligomerization of the NPM-ALK fusion protein. Indeed, NPM-ALK fusion proteins could form multimeric complexes, a process that required the NPM portion of the fusion protein (86, 87). These findings suggested that NPM-ALK fusion proteins dimerize/oligomerize through the NPM portion of the protein, which allows for activation of the ALK kinase domain, potentially through a transphosphorylation event. Interestingly, NPM-ALK was shown to dimerize with endogenous NPM, and it was suggested that this may explain why a portion of NPM-ALK can be found in the nucleus (87). Taken together, the findings of these studies suggested that the NPM fusion partner provides a critical dimerization domain required for the oncogenic activity of NPM-ALK.

Many of the ALK fusion partners other than NPM also possess known dimerization or oligomerization domains that likely function to facilitate activation of the given ALK fusion protein. For example, EML4 functions as a dimerization domain for EML4-ALK (149), and this is probably mediated by the coiled-coil motif within the EML4 basic domain (187). Many of the other ALK fusion partners also contain coiled-coil motifs (97, 99, 107, 154, 159, 181), as

well as various other domains thought to facilitate multimerization and activation of the fusion protein (102, 143, 157, 158). However, not all ALK fusion partners contain a known multimerization domain. For example, the ALK fusion partner moesin (MSN) does not possess a known dimerization domain, but instead was hypothesized to promote activation of MSN-ALK through co-localization to cellular membranes (104). Therefore, it appears that dimerization, oligomerization or co-localization through the ALK fusion partner is a common event that is required for activation and the transforming ability of ALK fusion proteins.

Full length ALK is a transmembrane receptor; however, in ALK fusion proteins the transmembrane and extracellular domains of ALK are lost, and it appears that the ALK fusion partner can dictate the subcellular localization of the fusion protein. For example, NPM-ALK localizes to both the cytoplasm and nucleus (87, 188), while MSN-ALK localizes to the plasma membrane (104), and many other ALK fusions are found only in the cytoplasm (31, 188). However, some fusions also have a distinct distribution within the cytoplasm: RAN binding protein 2 (RANBP2)-ALK localizes to the periphery of the nucleus (157) and clathrin heavy chain (CLTC)-ALK localizes to granular structures in the cytoplasm (102). Localization of CLTC-ALK to these structures is thought to be a result of the CLTC portion of the fusion binding to clathrin-coated vesicles (102). These findings demonstrate that in addition to mediating oligomerization, the ALK fusion partner also controls the sub-cellular localization of the fusion protein. Since the different ALK fusions are able to drive transformation, it suggests that controlling the sub-cellular localization is not the primary function of the ALK fusion partner. However, for certain fusions this may be important, as it is thought that that the MSN and CLTC fusion partners function by co-localizing the ALK fusions allowing for their activation.

While the different ALK fusion proteins all possess transforming ability, it is possible that these proteins vary in their ability to activate different signalling pathways and drive different biological processes. To address this question, Armstrong and colleagues stably expressed the NPM-, TPM3-, CLTC-, 5-aminoimidazole-4-carboxamide ribonucleotide formyltransferase/IMP cyclohydrolase (ATIC)-, or Trk-fused gene (TFG)-ALK fusion proteins in NIH 3T3 cells and examined the ability of these proteins to activate signalling pathways and regulate different cellular processes (90). It was found that TPM3-ALK expressing cells proliferated less robustly under low serum conditions compared to cells expressing other fusions; however, the TPM3-ALK expressing cells were more migratory and invasive than other cells. In contrast, other fusions could promote proliferation to a comparable level, but varied in their ability to promote invasion and migration. NPM-ALK and TFG-ALK expressing cells were able to form tumours more readily than cells expressing other fusions when injected into nude mice. The ability to activate different signalling pathways also varied amongst the different fusion proteins, as ATIC-ALK expression did not activate Akt, but was able to promote STAT3 phosphorylation to a much greater extent than the other ALK fusions. Alternatively, CLTC-ALK could strongly activate Akt but was unable to (or could only very weakly) promote STAT3 phosphorylation, while NPM-ALK was able to moderately activate both Akt and STAT3. In a more recent study, TPM3-ALK expressing NIH 3T3 cells were shown to have a higher metastatic potential compared to cells expressing NPM-ALK using an experimental lung metastasis assay (189). TPM3-ALK expressing cells also had alterations in the architecture of the actin cytoskeleton (189), which may be due to the ability of TPM3-ALK, but not NPM-ALK, to associate with components of the cytoskeleton (189). These findings raise the interesting possibility that while the primary function of the ALK fusion partner is to mediate dimerization allowing for activation of the fusion protein, the different partners may have subtle effects on the biology of the different fusion proteins. While the

different ALK fusions may have some biological differences, ultimately this may not be clinically relevant as no significant difference in patient outcome was observed for patients expressing NPM-ALK compared to other ALK fusion proteins (27). However, these conclusions may be affected by the relatively small number of patients with ALK fusions other than NPM-ALK (27).

#### **1.2.5: Signalling pathways activated by NPM-ALK**

Dimerization/oligomerization of NPM-ALK allows for constitutive phosphorylation and activation of ALK kinase activity, which allows NPM-ALK to initiate a variety of signalling pathways that drive the proliferation, survival, migration, and phenotype of lymphoma cells (Figure 1.4). These pathways are not limited to, but include the JAK/STAT, PI3K/Akt, MEK/ERK, JNK and PLC $\gamma$  pathways. These pathways contribute to various aspects of ALK+ ALCL biology and have been reviewed extensively in several recent publications (24, 30, 31, 136, 190). One family of proteins that is up-regulated/activated downstream of NPM-ALK signalling is the activator protein-1 (AP-1) family of transcription factors. Most notably are JunB and c-Jun, which are members of the Jun sub-family of AP-1 proteins. JunB expression is up-regulated downstream of the MEK/ERK (191, 192) and PI3K/Akt (191, 193) pathways, while c-Jun is regulated downstream of the JNK pathway in ALK+ ALCL (194). Importantly, c-Jun (194) and JunB (191) have been demonstrated to promote the proliferation of ALK+ ALCL cell lines, and elucidating the function of JunB in ALK+ ALCL will be the focus of my thesis project.

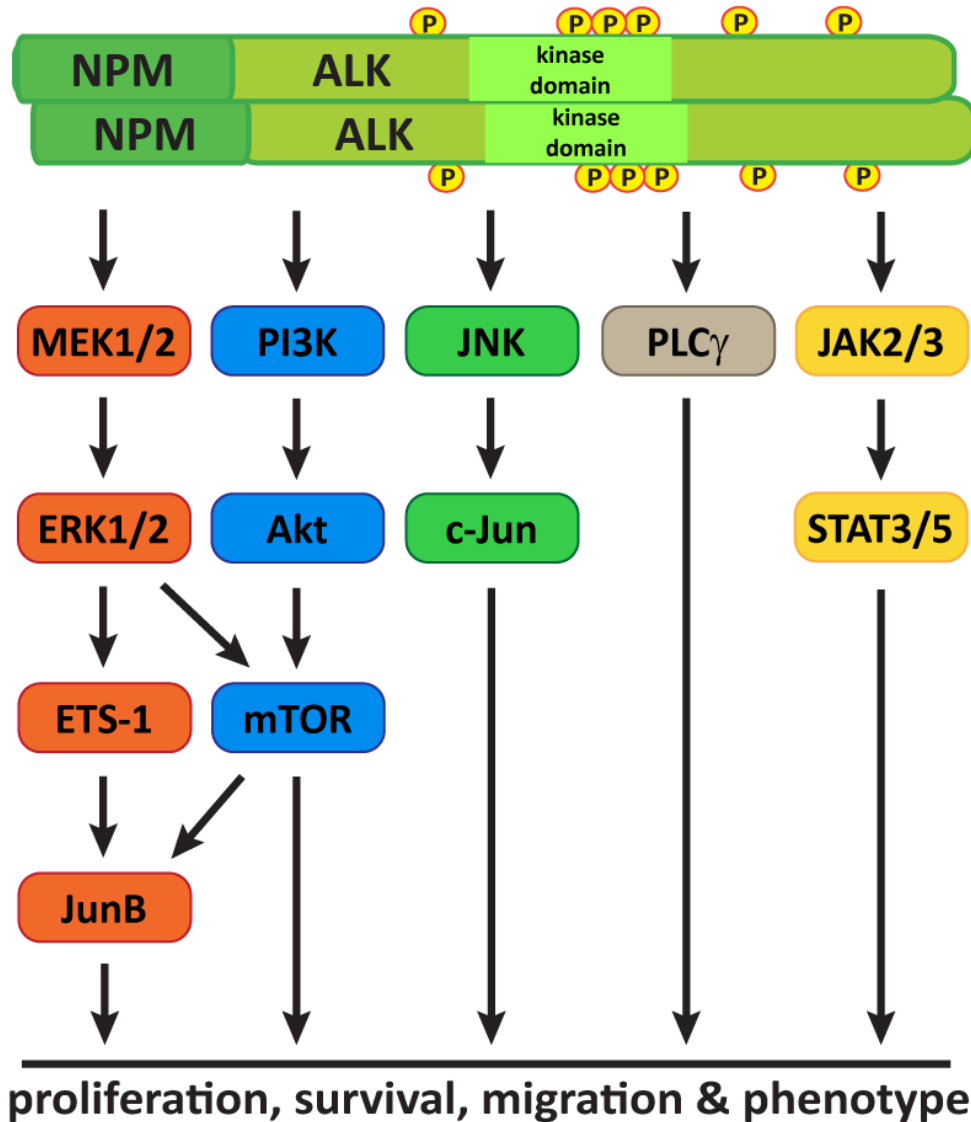


**Figure 1.4: Signalling pathways regulated downstream of NPM-ALK.**

NPM-ALK promotes proliferation, survival and migration of ALK+ ALCL cells and influences the phenotype of this lymphoma through the activation of various signalling pathways, such as the MEK/ERK, PI3K/Akt, JNK, PLC $\gamma$  and JAK/STAT pathways. The AP-1 transcription factors, JunB and c-Jun, are downstream effectors of some of these pathways. c-Jun activity and expression is promoted downstream of JNK. *JunB* transcription is enhanced downstream of MEK/ERK through the ETS-1 transcription factor and JunB translation is up-regulated through an mTOR-dependent mechanism.

### **1.3: THE AP-1 FAMILY OF TRANSCRIPTION FACTORS**

The AP-1 family of transcription factors consists of members of the Jun, Fos/Fra, activating transcription factor (ATF) and Maf sub-families, which are characterized by the presence of a conserved basic leucine zipper (bZIP) domain (195-197). These proteins form homo- and heterodimers through their leucine zipper, which allows them to bind to specific DNA sequences through their basic domain (198-202). AP-1 transcriptional complexes can then regulate the expression of various genes involved in biological processes such as apoptosis, proliferation, differentiation, migration and the immune response (195-197). AP-1 dimers typically bind to 12-O-tetradecanoylphorbol-13-acetate (TPA) response elements (TRE; consensus sequence: TGAG/CTCA) (198, 203, 204) or cyclic AMP response elements (CRE; consensus sequence: TGACGTCA) (199, 200) in the promoter regions of various genes. It is thought that the composition of the AP-1 dimers determines the specific AP-1 sites which they bind to, thereby controlling the specific genes that are regulated (205, 206). It has also been demonstrated that dimers consisting of only Jun proteins are much less stable than heterodimers between Jun and Fos proteins, resulting in the Jun/Fos heterodimers having higher DNA-binding affinity (198, 200, 202) and transcriptional activity (207, 208).

In addition to the leucine zipper and basic domain, AP-1 proteins also possess a nuclear localization signal within the basic domain, which targets these transcription factors to the nucleus (209). Some AP-1 family members also possess a transactivation domain that contains various phosphorylation sites or binding sites for cofactors that regulate their transcriptional activity. For example, phosphorylation of c-Jun on serine 63 and 73 within the transactivation domain by JNK is required for optimal c-Jun transcriptional activity (210-212). Furthermore, it was shown that the presence of the transcriptional cofactor p300 is required for JunB to promote transcription from the AP-1 site in the *dentin matrix protein 1* promoter in the MC3t3-E1 preosteoclast cell line (213).

Importantly, phosphorylation of JunB on serine 79 by the p38 kinase was required for association of JunB with p300 and for activation of the *dentin matrix protein 1* promoter (213). The Jun family members, c-Jun, JunB and JunD all have N-terminal transactivation domains (214), whereas within the Fos/Fra family, the presence of transactivation domains is variable (215-218).

## **1.4: THE JUNB TRANSCRIPTION FACTOR**

### **1.4.1: Background**

JunB was initially identified in 1988, shortly following the identification of the related family member, c-Jun (219). In mice, *JunB* message and protein can be detected early in embryogenesis (220, 221) and *JunB* message was detected in all adult tissues tested, including tissues of the reproductive system and digestive tract, as well as in lymphoid organs, lung, heart and brain tissue (221, 222). In normal cells JunB expression is tightly regulated throughout the cell cycle. In quiescent cells JunB is expressed at very low levels, but upon serum stimulation and entry into the G1 phase of the cell cycle JunB levels are rapidly up-regulated (223). However, JunB synthesis gradually declines as cells transition through the G1 and S phase of the cell cycle (223), and JunB protein is rapidly degraded as cells enter the G2/M phase, likely due to proteasomal degradation of JunB by the skip/cullin/F-box<sup>Fbxw7</sup> E3 ubiquitin ligase complex (193).

JunB was initially demonstrated to be a much weaker activator of transcription than c-Jun (224, 225), and it was demonstrated that minor differences in their DNA binding and dimerization domains accounted for these differences in transcriptional activity (224). However, another study suggested that the weaker transcriptional activity of JunB is due to differences between the transactivation domains of JunB and c-Jun (225). Furthermore, JunB was demonstrated to be a potent inhibitor of c-Jun activity in several studies. JunB over-expression could efficiently block AP-1-dependent transcription activated by over-expression of c-

Jun (224-227). JunB can also inhibit transformation of rat embryonic fibroblasts induced by expression of c-Jun and activated Ras (226). However, it was also found that expression of JunB along with active Ras could very weakly transform cells, and JunB could synergize with c-Fos to enhance transformation of rat embryonic fibroblasts that were transfected with active Ras (226). Interestingly, ectopic expression of JunB in *c-Jun* knockout mice rescued the embryonic lethality and defects in organ development observed in *c-Jun* knockout mice (221). Thus, the ability of JunB to inhibit AP-1-dependent transcription appears to be dependent on the AP-1 proteins present within a cell, and may also depend on the specific cell type or target gene examined.

#### **1.4.2: JunB is a positive and negative regulator of proliferation**

JunB impinges on a variety of biological processes including proliferation, development, differentiation, immune function and transformation. JunB has been shown to be both a positive and negative regulator of cell cycle transition and proliferation. It was demonstrated that microinjection of a JunB antibody into synchronized or asynchronously growing Swiss 3T3 fibroblasts resulted in a significant inhibition in DNA synthesis (228). Furthermore, isolated embryonic fibroblasts from *JunB* knockout mice have delayed progression through the S phase of the cell cycle, and it was argued that this defect was at least in part due to a failure of JunB to promote transcription of *cyclin A* in these cells (229). Furthermore, ectopic expression of JunB in *c-Jun* knockout mice is able to largely rescue the proliferation defect of embryonic fibroblasts from *c-Jun* knockout mice (221), and *JunB*-deficient osteoblasts and osteoclasts have reduced proliferation compared to wild type cells (230).

However, JunB has also been demonstrated to inhibit cell cycle progression. In NIH 3T3 cells over-expressing a JunB-estrogen receptor fusion protein, treatment with  $\beta$ -estradiol (to activate the fusion protein) resulted in reduced proliferation

of cells (227). JunB over-expression in mouse embryonic fibroblasts induced senescence of these cells, and could also inhibit proliferation of immortalized fibroblasts (231). In both of these cases, reduced proliferation was accompanied by an increased proportion of cells in the G0/G1 stage of the cell cycle (227, 231). Furthermore, mice lacking *JunB* specifically in cells of the myeloid lineage develop a myeloproliferative disorder, and myeloid progenitor cells from these mice proliferate more robustly compared wild type cells (232). Consistent with an anti-proliferative role for JunB, it was found that JunB over-expression reduced *cyclin D1* transcription and protein expression (227) and promoted transcription of the cyclin-dependent kinase inhibitor  $p16^{INK4\alpha}$  (231). It was further suggested that  $p16^{INK4\alpha}$  represented a critical JunB target that suppressed proliferation, because JunB over-expression did not inhibit proliferation of  $INK4\alpha^{-/-}$  cells (231). Taken together, these studies suggest that JunB can have both anti- and pro-proliferative effects on cells, and that the specific effect may be cell-type and context specific. Furthermore, these results suggest that JunB may slow progression of cells through the G0/G1 phase of the cell cycle, but is then required for efficient progression through S phase. This indicates that the proper regulation of JunB expression throughout the cell cycle is likely critical for proper cell cycle transition.

### **1.4.3: The role of JunB in development and differentiation**

A role for JunB in various aspects of development and differentiation has also been noted. The first demonstration of this was the observation that *JunB* knockout in mice is embryonic lethal between day E8.5 and E10 (220). It was also noted that prior to loss of the embryo, *JunB* knockout embryos were severely retarded in their growth, a defect that did not appear to be due to reduced cellular proliferation (220). It was instead suggested that the reduced growth and lethality in these embryos was likely due to defects in formation and vascularization of extra-embryonic tissues such as the yolk sac and placenta

(220). This hypothesis was further supported by the finding that conditional deletion of *JunB* in the embryo (but not extra-embryonic tissues) does not result in embryonic lethality and that these mice are born seemingly normal (230).

Following birth, JunB has also been demonstrated to play roles in the proper development of certain tissues and cell types. Mice with conditional deletion of *JunB* in only the embryo (which are born phenotypically normal) develop osteopenia and have defects in bone resorption, which is accompanied by significantly decreased numbers of osteoblast and osteoclast cells (230). It was also found that differentiation and proliferation of osteoblast and osteoclast cells *in vitro* was inhibited in cells isolated from *JunB*-deficient mice. Furthermore, mice with specific deletion of *JunB* in cells of the macrophage-osteoclast lineage developed an osteopetrosis-like disease and contained osteoclast cells with reduced proliferative capability (230). Interestingly, *c-Fos* knockout mice also develop osteopetrosis (233, 234), likely due to a defect in the development of osteoclast cells (235).

JunB also contributes to appropriate differentiation of cells in the myeloid lineage. It has been shown that loss of JunB in cells of the myeloid lineage results in an age-dependent myeloproliferative disorder in mice that resulted in dramatically increased numbers of neutrophils (232). In some mice this disorder was found to resemble human chronic myeloid leukemia (CML) (232). Consistent with these *in vivo* observations, *in vitro* it was found that compared to wild type cells, *JunB*-deficient stem cells differentiated more readily into granulocytes, and *JunB*-deficient myeloid progenitors proliferated more robustly than wild type cells (232). Hematopoietic stem cells from *JunB*-deficient have also been shown to proliferate more robustly than wild type cells, which is likely a major contributor to the myeloproliferative disease in mice lacking *JunB* (236, 237).

JunB can also influence differentiation of T lymphocytes. CD4<sup>+</sup> cells are able to differentiate into different subsets of helper T cells, which are able to mediate

different types of immune responses. Two of these subsets are Th1 and Th2 cells, which preferentially facilitate cell-mediated or humoral immune responses, respectively (238). These cell types mediate their different effects largely by secreting different types of cytokines, which help to shape the specific immune response (238). It was found that Th2 cells express higher levels of JunB compared to Th1 cells (239), and consistent with this expression pattern, JunB was found to play a role in promoting a Th2-type phenotype. Transgenic expression of *JunB* in T lymphocytes (using the *CD4* promoter) did not overtly affect thymocyte development; however, differentiation of CD4<sup>+</sup> cells into Th1 or Th2 cells was altered in these mice (239). Even under Th1-polarizing conditions *in vitro* or *in vivo*, CD4<sup>+</sup> T cells from *JunB* transgenic mice still produced Th2-type cytokines, such as IL-4, IL-5 and IL-10 (239). Furthermore, JunB could synergize with c-Maf to promote *IL-4* transcription, which likely contributes to the Th2-skewing of *JunB* transgenic T cells. These findings are also consistent with the suggestion that deregulation of JunB expression is likely a contributing factor to the Th2 phenotype and severe inflammatory disorder observed in mice deficient in the E3 ubiquitin ligase Itch, an E3 ligase that was shown to regulate JunB protein stability (240, 241).

#### **1.4.4: The role of JunB in hematological malignancies**

Given the pro- and anti-proliferative functions of JunB in various cell types, it is not surprising that JunB has been demonstrated to play roles in different hematological malignancies. JunB expression is low or absent in many patients with a variety of B cell leukemias and non-Hodgkin lymphomas (242, 243), suggesting that reduced JunB expression may be important in these cancers. Consistent with this, it was found that mice over-expressing *JunB* under control of a ubiquitous promoter have reduced numbers of B cells, while T cell numbers were not affected (242). JunB over-expressing B cells were found to have substantially reduced proliferation compared to wild type B cells, which likely

contributes to the reduced B cell numbers observed in JunB over-expressing mice (242). Importantly, B cells over-expressing JunB were more resistant to v-Abl-induced transformation *in vitro*, and mice expressing a *JunB* transgene survived significantly longer than wild type mice following infection with Abelson murine leukemia virus (242). Using a complimentary approach, Ott *et al* examined Abelson-induced leukemias in *JunB*-deficient mice (244). They found that *JunB*-deficient mice infected with the Abelson murine leukemia virus developed B cell leukemia and succumbed to the disease more rapidly than infected wild type mice. By 13 weeks, all *JunB*-deficient mice had succumbed to the leukemia, while only 40% of wild type mice had. Furthermore, when *JunB*-deficient B cell lines stably transfected with the BCR-Abl oncogene were injected into *Rag2*<sup>-/-</sup> mice, these mice also developed B cell leukemia and died much more rapidly than when mice were injected with wild type cells transfected with BCR-Abl (244). While the transformed *JunB*-deficient cells did not have altered levels of apoptosis or differences in apoptosis sensitivity, they did have significantly increased proliferation accompanied by increased cdk6 expression and reduced expression of the cell cycle inhibitors p27<sup>Kip1</sup>, p21<sup>Cip1</sup> and p16<sup>INK4α</sup> (244).

In addition to B cell leukemias and lymphomas, it has also been demonstrated that leukemic stem cells from patients with acute myeloid leukemia (AML) have significantly lower *JunB* message compared to non-leukemic stem cells (245). *JunB* expression in AML appears to be regulated by two important transcription factors in this disease. One of these transcription factors is PU.1, which, when knocked-down in mice results in the development of AML (246). It was demonstrated that PU.1 promotes the transcription of *JunB*, and that JunB levels were significantly decreased in PU.1 knock-down mice (245). Importantly, restoration of JunB expression in PU.1 knock-down cells reduced proliferation and colony formation and enhanced apoptosis of these cells *in vitro*, and blocked leukemia development *in vivo* (245). Furthermore, a correlation between *JunB* and *PU.1* expression was noted in human AML patients (245). The second

transcription factor found to regulate *JunB* expression in AML is HOXA9, a protein that is often found to be activated in AML patients (247, 248) and that when over-expressed with the Meis1 transcription factor can lead to the development of AML in mice (249). It was found that HOXA9 can repress *JunB* transcription in leukemic cell lines, and that JunB and HOXA9 levels were inversely correlated in AML patient samples (250). While the importance of JunB down-regulation was not assessed in this system, given the tumour suppressor-like role of JunB in PU.1 knock-down leukemic cells, down-regulation of JunB by HOXA9 is also likely an important event in HOXA9 over-expressing leukemic cells.

Like AML, it has also been demonstrated that patients with CML have reduced JunB levels, and it was proposed that this was due to methylation of the *JunB* promoter in this disease (251). However, two other studies suggested that JunB down-regulation was specific to patients with advanced phases of CML, and that this was not likely due to methylation of the *JunB* promoter (252, 253). Together, these studies demonstrate that JunB expression is down-regulated in at least a subset of CML patients. Given that mice deficient in *JunB* in cells of the myeloid lineage develop an age-dependent myeloproliferative disorder that resembles CML (232), it is quite possible that loss or down-regulation of JunB plays a role in the pathogenesis of human CML.

While many studies have demonstrated a tumour suppressor-like role for JunB in hematological malignancies, JunB is also highly expressed in various lymphomas. These include ALK+ ALCL (242, 254, 255), Hodgkin lymphoma (254, 255), ALK- ALCL (255) and CD30+ DLBCL (but not CD30- DLBCL) (255), as well as the cutaneous lymphoproliferative disorder, CD30+ lymphomatoid papulosis (255). The role of JunB in influencing the pathogenesis and phenotype of ALK+ ALCL has been the best studied of these lymphomas and will be discussed in depth below (see section 1.4.5.3). The role of JunB in Hodgkin lymphoma has also been briefly investigated. It has been demonstrated in Hodgkin lymphoma that JunB

promotes the transcription of *CD30*, which is a common phenotypic marker of this cancer (256-258). JunB similarly regulates *CD30* expression in ALK+ ALCL (51, 256, 257), and given that JunB is commonly expressed in CD30+ lymphomas (255), it suggests that the ability of JunB to promote CD30 expression is likely a common feature of these CD30+ cancers. In Hodgkin lymphoma, CD30 signalling promotes constitutive NF- $\kappa$ B activation, which plays an important role in promoting the proliferation and survival of tumour cells (41, 259-261), suggesting that the up-regulation of CD30 plays an important role in Hodgkin lymphoma. Interestingly, NF- $\kappa$ B signalling has been demonstrated to promote JunB expression in Hodgkin lymphoma (254), suggesting an auto-regulatory loop between CD30, NF- $\kappa$ B and JunB in this cancer. Finally, AP-1 activity has been shown to play an important role in promoting proliferation of the Hodgkin lymphoma cell line, L428, as over-expression of the AP-1 dominant negative, A-Fos (262), reduced proliferation of these cells (254); however, the specific AP-1 factors that are important for proliferation of these cells were not examined in this study.

#### **1.4.5: JunB and AP-1 proteins in ALK+ ALCL**

##### **1.4.5.1: Expression of AP-1 proteins in ALK+ ALCL**

It has been well documented that JunB and c-Jun are highly expressed in ALK+ ALCL (242, 254, 255, 263, 264). In addition to c-Jun and JunB, other AP-1 family proteins have been described as being commonly or highly expressed in ALK+ ALCL tumour samples. Immunohistochemistry experiments demonstrated strong staining for ATF1 and ATF2 in ALK+ ALCL patient samples, although this was not specific to ALK+ ALCL, as samples from various other lymphomas showed similar staining (264). In this same study it was also demonstrated that c-Fos was highly expressed in ALK+ ALCL patient samples compared to several other lymphomas (264). Furthermore, ALK+ ALCL cell lines and patient samples have been shown to consistently express high levels of Fra2 compared to non-malignant tissues,

which may be partly due to an increase in *Fra2* gene copy number in this cancer (265). These findings in ALK+ ALCL patient samples are consistent with the finding that ectopic expression of NPM-ALK in HEK293 cells enhanced general AP-1 transcriptional activity as well as DNA binding activity of all Jun, Fos and Fra family proteins (266). This finding suggested that AP-1 proteins are up-regulated and/or have increased activity in ALK-expressing cells. The importance of enhanced AP-1 signalling in ALK+ ALCL was first demonstrated by Mathas *et al* who found that over-expression of the AP-1 dominant negative, A-Fos (262), in the Karpas 299 ALK+ ALCL cell line resulted in the induction of apoptosis (254).

#### **1.4.5.2: The regulation and function of c-Jun in ALK+ ALCL**

It has been suggested that the expression of c-Jun in ALK+ ALCL is a consequence of NPM-ALK signalling (Figure 1.5). Ectopic expression of NPM-ALK in different cell types resulted in up-regulation of c-Jun (191, 194) protein and mRNA expression, and also enhanced c-Jun activation as measured by phosphorylation of c-Jun on serine 73 and c-Jun DNA binding activity (194, 266). Data suggests that NPM-ALK promotes c-Jun expression and phosphorylation, at least in part, through the activation of JNK. JNK was found to be activated in ALK+ ALCL cell lines and patient samples, and NPM-ALK was able to promote JNK activation (194). Furthermore, small interfering RNA (siRNA)-mediated knock-down or pharmacological inhibition of JNK resulted in a slight reduction in c-Jun protein levels and dramatically reduced c-Jun phosphorylation (194). Activation of the JNK/c-Jun pathway in ALK+ ALCL was demonstrated to be functionally important, as knock-down of c-Jun in ALK+ ALCL cell lines resulted in reduced cell viability and proliferation (194). The decreased proliferation of these cells was accompanied by reduced expression of cyclin A and D3 and up-regulation of the cyclin-dependent kinase inhibitor p21<sup>Cip1</sup> (194), suggesting that c-Jun may regulate the expression of these molecules in ALK+ ALCL. However, a study by Staber *et al* demonstrated no effect on proliferation of Karpas 299 cells following c-Jun knock-down (191), bringing into question the role of c-Jun in this cancer.

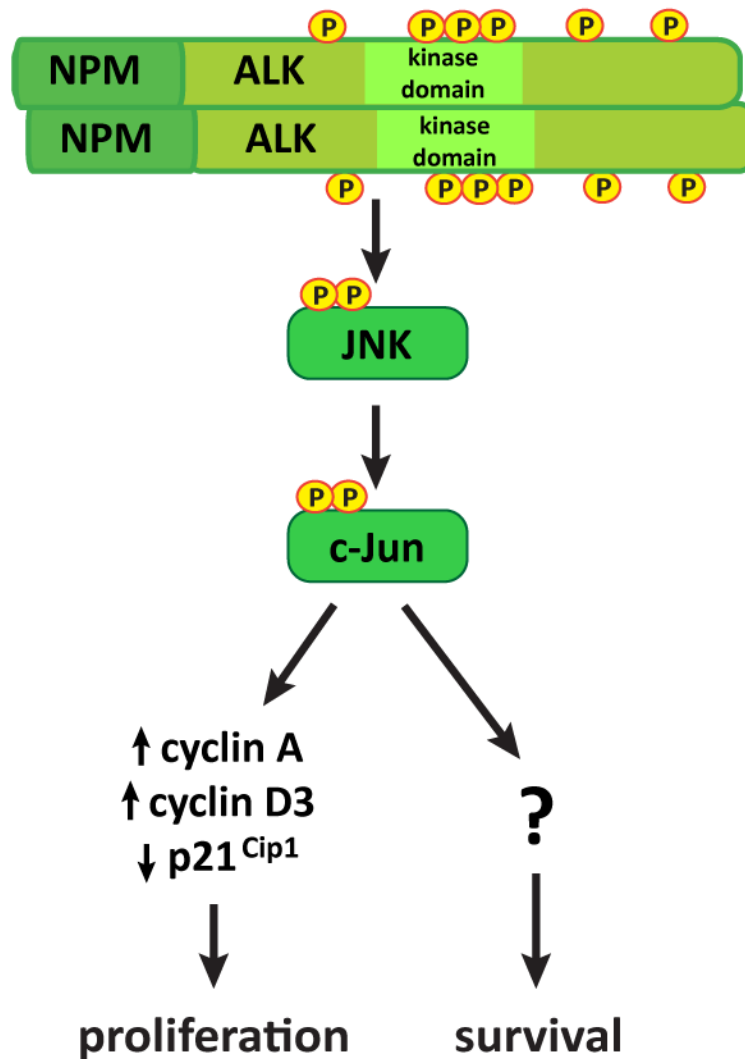


**Figure 1.5: The regulation and function of c-Jun in ALK+ ALCL.**

NPM-ALK promotes JNK activation, which in turn promotes the expression and activation of c-Jun in ALK+ ALCL. Furthermore, c-Jun promotes the proliferation and survival of ALK+ ALCL cell lines. It is thought that c-Jun, at least in part, promotes proliferation by promoting cyclin A and D3 expression and repressing p21<sup>Cip1</sup> expression.

### 1.4.5.3: Regulation and function of JunB in ALK+ ALCL

The pathways regulating JunB expression in ALK+ ALCL have been well characterized, and are a consequence of NPM-ALK signalling (Figure 1.6). It was demonstrated that knock-down of NPM-ALK in ALK+ ALCL cell lines resulted in reduced JunB expression (51, 192, 267), and ectopic expression of NPM-ALK in different cell types promoted JunB protein and mRNA expression (51, 191). NPM-ALK signalling can activate the MEK/ERK (191, 268-270), PI3K/Akt (271-274) and mTOR (191, 274, 275) pathways, and all of these pathways contribute to the elevated expression of JunB in ALK+ ALCL. Treatment of ALK+ ALCL cells or Ba/F3 cells ectopically expressing NPM-ALK with the MEK inhibitor, U0126, resulted in reduced JunB protein and mRNA levels (191), suggesting that *JunB* transcription is promoted downstream of MEK/ERK signalling. It was further suggested that the ETS-1 transcription factor may function downstream of MEK/ERK to promote *JunB* transcription in ALK+ ALCL (192). CD30 signalling also promotes JunB transcription in ALK+ ALCL, likely through a MEK/ERK/ETS-1 signalling pathway (192, 256). Interestingly, it was shown that treatment of ALK+ ALCL cells or Ba/F3 cells expressing NPM-ALK with the mTOR inhibitor, rapamycin, resulted in reduced JunB protein levels but did not affect *JunB* mRNA expression (191). It was further demonstrated that mTOR promotes JunB translation by targeting *JunB* mRNA to highly translationally active polysomes (191). Since both the MEK/ERK (274) and PI3K/Akt (275) pathways can promote mTOR activation in ALK+ ALCL, it suggests that both of these pathways may contribute to elevated JunB translation.

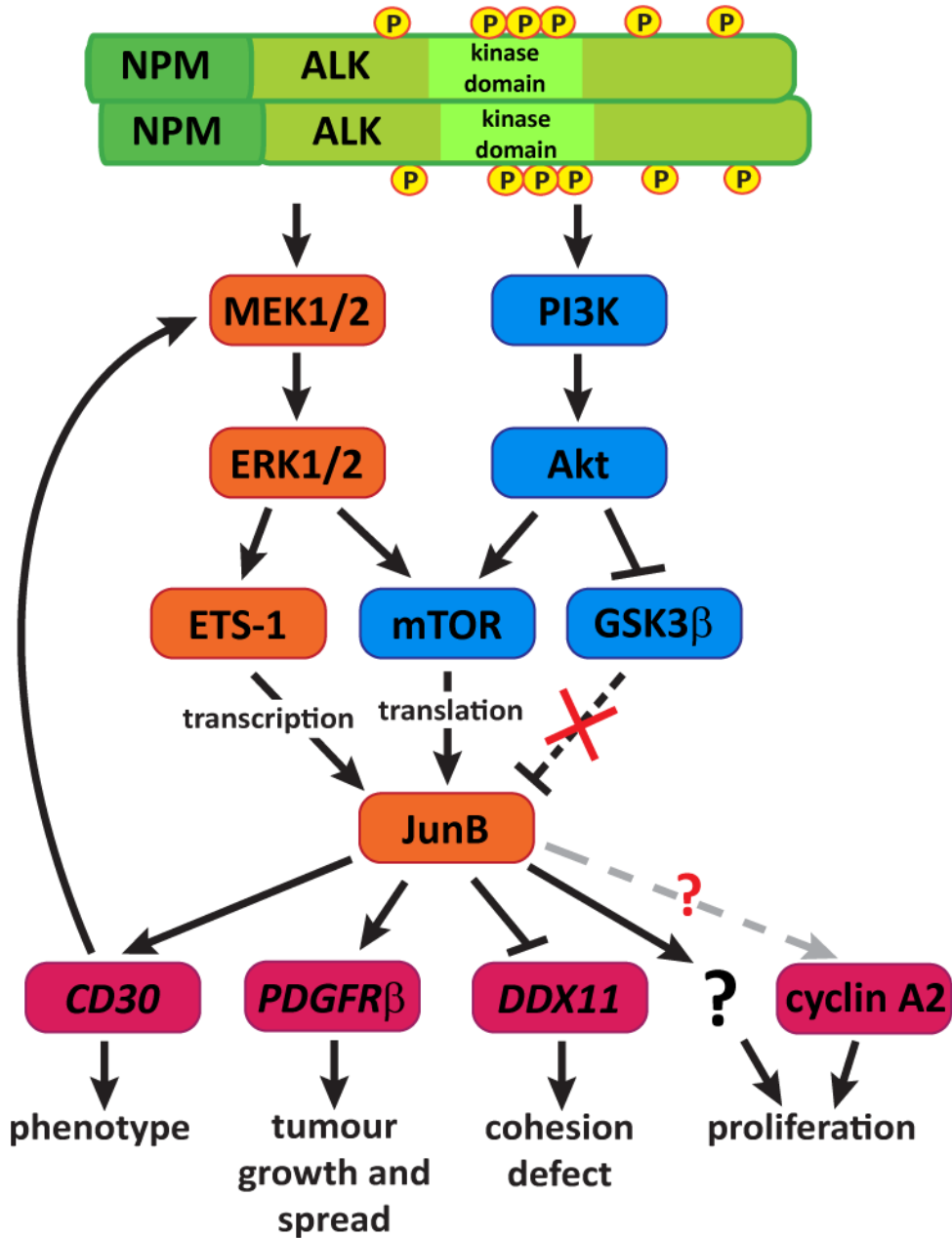


**Figure 1.6: Regulation and function of JunB in ALK+ ALCL.**

NPM-ALK promotes activation of the MEK/ERK pathway, which promotes *JunB* transcription through the ETS-1 transcription factor. NPM-ALK also activates the PI3K/Akt pathway, which results in inhibition of GSK3β, and protects JunB from proteasomal degradation. mTOR activation promotes JunB expression by enhancing JunB translation. JunB can both promote and repress the expression of several genes that contribute to the pathogenesis and phenotype of NPM-ALK expressing tumours, although there are likely many important JunB-regulated genes yet to be identified in ALK+ ALCL. JunB also appears to regulate cyclin A2 expression, but whether this is a direct relationship was not examined.

More recently, it has also been suggested that PI3K/Akt signalling may promote JunB expression through stabilizing JunB protein levels (193). It was shown that the E3 ubiquitin ligase skip/cullin/F-box<sup>Fbxw7</sup> can target JunB for ubiquitin-mediated proteasomal degradation following phosphorylation of JunB by glycogen synthase kinase (GSK) 3 $\beta$ , which was important for degradation of JunB as cells progress through the cell cycle (193). Akt is known to inhibit GSK3 $\beta$  by phosphorylating GSK3 $\beta$  on serine 9 (276), and it has been shown that NPM-ALK can promote phosphorylation of GSK3 $\beta$  through the PI3K/Akt pathway (277), so the authors examined whether the constitutive Akt activation in ALK+ ALCL stabilized JunB expression in this cancer. Indeed, it was found that inhibiting PI3K in ALK+ ALCL cell lines resulted in reduced JunB protein levels, which could be blocked by treatment of these cells with a proteasome inhibitor (193), suggesting that PI3K/Akt signalling stabilizes JunB protein expression in ALK+ ALCL cell lines.

The elevated expression of JunB in ALK+ ALCL has been demonstrated to play important roles in this cancer (Figure 1.6). Knock-down of JunB in Karpas 299 cells was shown to result in reduced cell numbers (191). This was accompanied by an increased proportion of cells in the G1/G0 stage of the cell cycle and a reduced percentage of cells in the G2/M stage, suggesting a proliferation defect. Furthermore, reduced cell numbers were observed following JunB knock-down in Ba/F3 cells stably expressing an inducible NPM-ALK construct (191). Under these conditions no caspase 3 activation was observed, suggesting the reduction in cell number was a result of reduced proliferation.

In addition to promoting proliferation of ALK+ ALCL cell lines, it has been demonstrated that JunB contributes to the phenotype of ALK+ ALCL by promoting transcription of *CD30* in this cancer. Using electrophoretic mobility shift assays, it was demonstrated that JunB binds to an AP-1 site present in a microsatellite region of the *CD30* promoter, while no other AP-1 family proteins were found to bind this site (256). Furthermore, in ALK+ ALCL cell lines, over-

expressed JunB (51, 256), but not c-Jun (256), was able to promote transcription through the AP-1 site in the *CD30* promoter. JunB knock-down also resulted in reduced transcription from this promoter (256). The ability of JunB to promote *CD30* transcription in ALK+ ALCL is thought to be enhanced due to hypomethylation of CpG islands in the promoter region, first exon and first intron of the *CD30* gene in ALK+ ALCL (257). Because CD30 signalling promotes JunB expression (192, 256), it suggests an auto-regulatory mechanism whereby JunB promotes CD30 expression, which in turn enhances JunB expression. Interestingly, the regulation of *CD30* transcription by JunB in ALK+ ALCL is very similar to the regulation of *CD30* in Hodgkin lymphoma (256-258), suggesting that JunB may have similar functions in these two malignancies where JunB is highly expressed.

It has also been shown that JunB represses the transcription of the DNA helicase, *DDX11* (193), a protein required for proper sister chromatid cohesion in cells undergoing mitosis (278). A failure of JunB to be targeted for ubiquitin-mediated degradation in ALK+ ALCL cells was postulated to prevent up-regulation of DDX11 in mitotic cells, therefore resulting in a cohesion defect in ALK+ ALCL cells (193). Consistent with the notion that JunB may repress DDX11 expression in mitotic ALK+ ALCL cells, it was found that JunB knock-down resulted in increased DDX11 levels in Karpas 299 cells in the G2/M phase of the cell cycle (193). The authors postulated that this may contribute to the chromosomal abnormalities often observed in ALK+ ALCL. It was also observed that JunB knock-down in ALK+ ALCL cells resulted in a slight reduction in cyclin A2 protein levels, but whether this was directly mediated by JunB or merely an indirect result of the reduced proliferation following JunB knock-down was not investigated (193).

The importance of c-Jun and JunB in NPM-ALK-driven pathogenesis has also been demonstrated *in vivo* (279). Knockout of both *c-Jun* and *JunB* reduced proliferation and enhanced apoptosis of NPM-ALK-expressing tumour cells

arising in transgenic mice expressing *NPM-ALK* under control of the *CD4* promoter. This was accompanied by prolonged survival of these mice. Interestingly, this effect was mediated by both JunB and c-Jun, as knockout of only *JunB* or *c-Jun* had no significant effect on survival of *NPM-ALK* transgenic mice. This finding suggests there is likely some functional redundancy between c-Jun and JunB in *NPM-ALK*-driven tumours. In these mice it was found that c-Jun and JunB promoted transcription of *platelet-derived growth factor receptor β* (*PDGFRβ*). Up-regulation of *PDGFRβ* was functionally important in these cancers because treatment of *NPM-ALK*-expressing mice with the *PDGFR* inhibitor, imatinib, resulted in reduced proliferation and enhanced apoptosis of tumour cells and substantially prolonged survival of these mice. Interestingly, *PDGFRβ* expression was not observed in human *ALK+* ALCL cell lines, but tumour cells in about 75% of human *ALK+* ALCL patients expressed *PDGFRβ* (279). Most importantly, *PDGFRβ* was found to be a clinically relevant target, as treatment of one *ALK+* ALCL patient (that was resistant to conventional chemotherapy) with imatinib resulted in complete clinical remission for 22 months at the time of the publication (279).

### **1.5: HYPOTHESIS AND OBJECTIVES**

When we began this project, JunB was known to be highly expressed in *ALK+* ALCL and play an important role in promoting proliferation of *ALK+* ALCL cell lines *in vitro*. However, the transcriptional targets of JunB were largely uncharacterized in this lymphoma, and it was only known that JunB promoted the transcription of *CD30* in *ALK+* ALCL, a common phenotypic marker for this cancer. Given that AP-1 sites are present throughout the human genome, we hypothesized that there are many unidentified JunB transcriptional targets in *ALK+* ALCL. Furthermore, we hypothesized that these JunB transcriptional targets

play an important role in the pathogenesis of ALK+ ALCL and/or contribute to the phenotype of this lymphoma.

The specific objectives of my thesis project were to:

1. Identify novel JunB targets in ALK+ ALCL cell lines.
2. Characterize the regulation of these targets by JunB.
3. Examine the function of these JunB targets in ALK+ ALCL pathogenesis.

## **CHAPTER 2: MATERIALS AND METHODS**

## **2.1: CELL CULTURE AND TRANSFECTIONS**

### **2.1.1: Cell lines**

The ALK+ ALCL cell line SR (280) was obtained from the American Type Culture Collection (ATCC, Manassas, VA). The ALK+ ALCL cell lines, Karpas 299 (2) (used in Chapters 1 and 2), SUP-M2 (3) (used in Chapters 1 and 2), SU-DHL-1 (3) and UCONN (8) were generously provided by Dr. Raymond Lai (University of Alberta). The Karpas 299 and SUP-M2 cells used in Chapter 3 and to generate the JunB shRNA stable cell lines used in Chapters 1 and 2 were from the Leibniz Institute DSMZ-German Collection of Microorganisms and Cell Cultures (Braunschweig, Germany). All ALK+ ALCL cell lines were originally generated from cells isolated from human lymphoma patients and possess the t(2;5)(p23;q35) chromosomal translocation (281). The Hodgkin lymphoma cell line, KM-H2 (282), was generously provided by Dr. Hesham Amin (University of Texas M. D. Anderson Cancer Center, Houston, TX). KM-H2 and ALK+ ALCL cell lines were cultured in Roswell Park Memorial Institute (RPMI) 1640 media (Gibco; Burlington, ON, Canada) supplemented with 10% heat-inactivated fetal bovine serum (FBS), 1 mM sodium pyruvate (Sigma-Aldrich; St Louis, MO), 2 mM L-glutamine (Gibco), and 50  $\mu$ M 2-mercaptoethanol (BioShop; Burlington, ON, Canada). The human leukemic NK cell line, NKL, and the non-Hodgkin lymphoma NK cell line, NK-92, were generously provided by Dr. Debby Burshtyn (University of Alberta). NKL cells were cultured in Iscove's media (Life Technologies) supplemented with 2 mM L-glutamine, 10% FBS and 200 U/ml recombinant human interleukin (IL)-2 (Sigma-Aldrich). NK-92 cells were cultured in Iscove's media supplemented with 2 mM L-glutamine, 12.5% FBS, 12.5% horse serum, 36  $\mu$ g/ml inositol (Sigma Aldrich), 17.6  $\mu$ g/ml folic acid (Sigma-Aldrich), 100  $\mu$ M 2-mercaptoethanol and 100 U/ml recombinant human IL-2. HEK 293T cells were from Dr. Tony Pawson (Samuel Lunenfeld Research Institute, Toronto, ON, Canada), and were cultured in Dulbecco's Modified Eagle's Medium (DMEM) supplemented with 10% FBS, 1

mM sodium pyruvate and 2 mM L-glutamine. All cells were maintained at 37°C in a 5% CO<sub>2</sub> atmosphere.

### **2.1.2: Transfection by electroporation**

ALK+ ALCL cell lines were transiently transfected with siRNAs or cDNA constructs using electroporation. For siRNA experiments, cells were counted and suspended to  $8 \times 10^6$  cells/ml in complete RPMI. Five hundred microliters ( $4 \times 10^6$  cells) were then transferred to a 4 mm gap cuvette (VWR International; Mississauga, ON, Canada) and transfected with 100 nM siRNA (600 nM for the iTRAQ mass spectrometry experiment) using a BTX ECM 830 square wave electroporator (BTX; San Diego, CA) with the following settings: 225V, 3 pulses of 8 msec each with 1 sec between pulses. The siRNAs used were siGENOME or ON-TARGETplus from Dharmacon RNAi Technologies (Thermo Scientific; Waltham, MA) and are listed in Table 2.1. Unless stated otherwise, siRNA pools were used to target the indicated genes. After transfection, cells were transferred to 12-15 ml of complete RPMI and incubated at 37°C in a 5% CO<sub>2</sub> atmosphere for 48 hrs prior to analysis. For electroporations involving cDNA constructs,  $1 \times 10^7$  cells were transfected (in 500 µl of complete RPMI) with the amount of each cDNA indicated for that specific experiment using the conditions described above. Cells were then transferred to 10-12 ml of complete RPMI and incubated at 37°C in a 5% CO<sub>2</sub> atmosphere for 24 hrs prior to analysis. For luciferase experiments involving siRNAs,  $1 \times 10^7$  cells were transfected with 100 nM siRNA and the indicated amount of each cDNA. After transfection, cells were transferred to 10-12 ml of RPMI and incubated at 37°C in a 5% CO<sub>2</sub> atmosphere for 24 hrs prior to analysis for luciferase activity.

**Table 2.1: siRNAs used in this study.**

| Target  | Product                 | Catalogue Number   |
|---|-------------------------|--|
| control (non-targeting) pool #1                   | siGENOME SMARTpool      | D-001206-13-20   |
| JunB pool*  | siGENOME SMARTpool      | M-003269-01-0010   |
| JunB individual #1                                | siGENOME                | D-003269-05  |
| JunB individual #2                                | siGENOME                | D-003269-06  |
| JunB individual #3                                | siGENOME                | D-003269-07  |
| JunB individual #4                                | siGENOME                | D-003269-08  |
| c-Fos pool <sup>#</sup>                           | ON-TARGETplus           | LU-003265-00-0002  |
| Alk pool*   | ON-TARGETplus SMARTpool | L-003103-00-0005   |
| Granzyme B pool*                                  | siGENOME SMARTpool      | M-005889-02-0005   |
| Cyp40 pool <sup>#</sup>                           | siGENOME                | MU-008888-00-0002  |
| FKBP51 pool <sup>#</sup>                          | siGENOME                | MU-004224-01-0002  |
| FKBP52 pool <sup>#</sup>                          | siGENOME                | MU-006410-02-0002  |
| Cyp40 individual #1                               | siGENOME                | D-008888-01  |
| Cyp40 individual #2                               | siGENOME                | D-008888-02  |
| Cyp40 individual #3                               | siGENOME                | D-008888-03  |
| Cyp40 individual #4                               | siGENOME                | D-008888-04  |
| FKBP51 individual #1                              | siGENOME                | D-004224-01  |
| FKBP51 individual #2                              | siGENOME                | D-004224-02  |
| FKBP51 individual #3                              | siGENOME                | D-004224-04  |
| FKBP51 individual #4                              | siGENOME                | D-004224-05  |
| FKBP52 individual #1                              | siGENOME                | D-006410-05  |
| FKBP52 individual #2                              | siGENOME                | D-006410-07  |
| FKBP52 individual #3                              | siGENOME                | D-006410-20  |
| FKBP52 individual #4                              | siGENOME                | D-006410-21  |
| Cyp40, FKBP51 & FKBP52 combined pool <sup>‡</sup> | siGENOME                | Cyp40 – D-008888-01<br>– D-008888-02<br>FKBP51 – D-004224-01<br>– D-004224-02<br>FKBP52 – D-006410-05<br>– D-006410-07 |

\* SMARTpool siRNAs were purchased as equal molar amounts of 4 different siRNAs to target the gene of interest.

<sup>#</sup> c-Fos, Cyp40, FKBP51 and FKBP52 pools were generated by combining 4 different individual siRNAs to target each gene.

<sup>‡</sup> The Cyp40, FKBP51 and FKBP52 combined pool was generated by combining 2 siRNAs to target each of the 3 genes.

### **2.1.3: Generating stable cell lines using lentiviral transduction**

#### **2.1.3.1: Generating lentiviral particles**

HEK 293T cells were used to generate lentiviral vectors using the MISSION short hairpin RNA (shRNA) lentiviral system (Sigma-Aldrich). One day prior to transfection, 1 ml of HEK 293T cells from a confluent 10 cm plate were seeded into 10 ml of DMEM in a T25 flask. On the day of transfection, the media was removed from the cells and replaced with 5 ml of complete DMEM. A mixture for each transfection was prepared with the lentiviral packaging vector (1.53 µg), the vesicular stomatitis virus G-protein (pCMV-VSV-G) envelope vector (170 ng) and 1.13 µg of pLKO.1 vector containing the shRNA of interest. The lentiviral packaging vector and pCMV-VSV-G were kindly provided by Dr. Maya Shmulevitz (University of Alberta) and the MISSION shRNA vectors were purchased from Sigma-Aldrich and are listed in Table 2.2. In a separate tube, 7 µl of FuGENE HD (Promega; Madison, WI) was added to 79 µl of serum-free DMEM for each transfection. Eighty-six microliters of the DMEM/FuGENE HD mixture was then added to the DNA mixture, followed by incubation at room temperature for 15 min. The entire mixture was transferred to a flask of HEK 293T cells and the cells then incubated at 37°C. Approximately 24 hrs after transfection, media was removed from the cells and replaced with 10 ml of fresh complete DMEM. Approximately 40 hrs after transfection, the media was again removed from the HEK 293T cells and replaced with 3.5 ml of fresh complete DMEM. After 8 hrs of incubation at 37°C, the media was collected and cells removed by centrifugation followed by filtration through a 0.45 µm low protein-binding syringe filter to generate lentivirus-containing supernatants.

**Table 2.2: shRNA constructs used in this study.**

| <b>Name</b>                                  | <b>Vector</b>         | <b>TRC identifier/<br/>catalogue number</b> | <b>Sequence</b>  |
|--|-----------------------|---|--|
| IPTG-inducible control (non-targeting) shRNA | pLKO-puro-IPTG-3xLacO | SHC332                                      | CCG <b>GGC GCG</b> ATA GCG<br>CTA ATA ATT TCT CGA<br>GAA ATT ATT AGC GCT<br>ATC <b>GCG</b> CTT TTT               |
| IPTG-inducible JunB shRNA                    | pLKO-puro-IPTG-3xLacO | TRCN0000014943                              | CCG <b>GCA GAC</b> TCG ATT<br>CAT ATT <b>GAA</b> TCT CGA<br>GAT TCA ATA TGA ATC<br><b>GAG</b> TCT GTT TTT        |
| control (non-targeting) shRNA                | pLKO.1-puro           | SHC002                                      | CCG <b>GCA ACA</b> AGA TGA<br>AGA <b>GCA CCA</b> ACT CGA<br>GTT GGT GCT CTT CAT<br>CTT <b>GTT</b> GTT TTT        |
| GzB shRNA #1                                 | pLKO.1-puro           | TRCN0000006445                              | CCG <b>GCG AAT</b> CTG ACT<br>TAC <b>GCC</b> ATT ACT CGA<br>GTA ATG <b>GCG</b> TAA GTC<br>AGA <b>TTC</b> GTT TTT |
| GzB shRNA #2                                 | pLKO.1-puro           | TRCN0000006448                              | CCG <b>GCA TTG</b> TCT CCT<br>ATG <b>GAC GAA</b> ACT CGA<br>GTT TCG TCC ATA GGA<br><b>GAC</b> AAT GTT TTT        |
| GzB shRNA #3                                 | pLKO.1-puro           | TRCN0000006449                              | CCG <b>GGC TTC</b> CTG ATA<br>CAA <b>GAC GAC</b> TCT CGA<br>GAG TCG TCT TGT ATC<br>AGG <b>AAG</b> CTT TTT        |

Targeting sequences are bolded.

### **2.1.3.2: Infecting ALK+ ALCL cell lines with lentiviral particles**

Prior to infection, ALK+ ALCL cell lines were counted, centrifuged and suspended to  $5 \times 10^5$  cells/ml in complete RPMI. One millilitre of lentivirus-containing supernatant was added to 1 ml of ALK+ ALCL cells, and polybrene (Sigma-Aldrich) was added to a concentration of 8  $\mu\text{g/ml}$ . Cells were then incubated at 37°C for approximately 24 hrs, collected, washed twice with 10 ml RPMI, resuspended in fresh RPMI and incubated at 37°C. After approximately 24 hrs, cells were split as needed into RPMI (to maintain cells at a density below  $6 \times 10^5$  cells/ml) and puromycin (Sigma-Aldrich) was added to a final concentration of 0.5  $\mu\text{g/ml}$  to select for stable transfectants. After 3 days in selection, the efficiency of knock-down was assessed using flow cytometry and western blotting (for cells stably expressing GzB shRNA). Karpas 299 cells stably expressing an IPTG-inducible control (non-targeting) or JunB shRNA were generated by Dr. Robert Ingham and Joyce Wu, and JunB knock-down was assessed by treating cells with various concentrations of IPTG for 48 or 72 hrs followed by western blotting. Stable cells were continuously cultured in RPMI containing 0.5  $\mu\text{g/ml}$  puromycin to maintain stable transfectants.

## **2.2: DNA METHODS**

### **2.2.1: Genomic DNA Extraction**

Genomic DNA was isolated from  $5 \times 10^6$  Karpas 299 cells using the DNeasy Blood and Tissue Kit (Qiagen; Mississauga, ON, Canada) according to the manufacturer's protocol. Briefly, cells were collected, washed with 1X phosphate-buffered saline (PBS) then incubated in buffer AL with proteinase K for 10 min at 56°C. One-third volume (200  $\mu\text{l}$ ) of 100% ethanol was then added and the genomic DNA bound to the DNeasy Mini spin column. The column was washed with buffers AW1 and AW2, then DNA eluted from the column with

buffer AE. The concentration of eluted DNA was quantified using a NanoDrop ND-1000 spectrophotometer (Thermo Scientific).

### **2.2.2: Polymerase chain reaction for cloning**

Polymerase chain reactions (PCR) were performed in 50  $\mu$ l reaction volumes containing the appropriately supplied reaction buffer, 0.8 mM deoxynucleotide triphosphate (dNTP) mix (Fermentas), 4 mM MgCl<sub>2</sub> (*Taq* polymerase) or MgSO<sub>4</sub> (*Pfu* polymerase), 0.3  $\mu$ M forward and reverse primers (Table 2.3), and 2.5U of *Pfu* polymerase (Fermentas) or 1U of High Fidelity *Taq* polymerase (Invitrogen). To generate the *Cyp40* promoter construct, 2% (v/v) DMSO was also added to the PCR reaction. To generate the JunB or AP-1 mutant luciferase constructs, 50 ng of plasmid DNA was used as a template and to generate the wild-type *GzB* or *Cyp40* promoter constructs, 30 ng of Karpas 299 genomic DNA was used as a template. PCR reactions were performed using either a PTC-100 Peltier thermal cycler (Bio-Rad; Hercules, CA) or a Biometra T-gradient thermal cycler (Biometra; Goettingen Germany). The PCR cycling parameters used for cloning were an initial denaturing step at 95°C for 3 min followed by 35-40 cycles of denaturing at 95°C for 30 sec, annealing at 52-60°C for 30 sec, and extension at 72°C for 1-2 min, followed by a final extension step at 72°C for 5 min. Generation of a PCR product of the expected size was confirmed by agarose gel electrophoresis using a 1% (w/v) agarose gel prepared in 1X TAE buffer (40 mM Tris, 20 mM acetic acid, 1 mM EDTA) containing 1:10,000 SYBR Safe DNA gel stain (Invitrogen). PCR products were then purified using the QIAquick PCR Purification kit (Qiagen) as per manufacturer's instructions.

**Table 2.3: Oligonucleotides used for cloning.**

| Name                                 | Sequence  | Enzyme Site  | Description   |
|--------------------------------------|---|--------------|---|
| JunB 5' (FLAG tag)                   | TTT TTT <u>GAA TTC</u><br>ATG CAC TAA AAT<br>GGA A            | <i>EcoRI</i> | Used to generate the JunB cDNA for cloning into pFLAG-CMV2 vector                           |
| JunB 5' (Myc tag)                    | TTT TTT <u>GAA TTC</u><br>TGC ACT AAA ATG<br>GAA              | <i>EcoRI</i> | Used to generate the JunB cDNA for cloning into pBS-Myc2 vector                             |
| JunB 3'                              | TTT TTT <u>GTC GAC</u><br>TCA GAA GGC<br>GTG TCC              | <i>Sall</i>  | Used to generate the JunB cDNA for cloning into pFLAG-CMV2 or pBS-Myc2 vectors              |
| <i>GzB</i> promoter 5'               | TTT TTT <u>GGT ACC</u><br>GAC CCC AGC CTA<br>CCC AAA GTG      | <i>KpnI</i>  | Used to generate the full length <i>GzB</i> promoter to clone into the pBSII SK(+) vector   |
| <i>GzB</i> promoter 3'               | TTT TTT <u>CTC GAG</u><br>AGG AAG GCT<br>GCC CTG GTT<br>GGA G | <i>XhoI</i>  | Used to generate the full length <i>GzB</i> promoter to clone into the pBSII SK(+) vector   |
| <i>Cyp40</i> promoter 5'             | TTT TTT <u>GAG CTC</u><br>ACC ACC ACG CCC<br>GGG TGA TTT      | <i>SacI</i>  | Used to generate the full length <i>Cyp40</i> promoter to clone into the pBSII SK(+) vector |
| <i>Cyp40</i> promoter 3'             | TTT TTT <u>CTC GAG</u><br>CCC GGG CCG<br>CCC AAA CTC CAG      | <i>XhoI</i>  | Used to generate the full length <i>Cyp40</i> promoter to clone into the pBSII SK(+) vector |
| <i>GzB</i> promoter AP-1 mutant 5'   | TCC ACT <b>CTT</b> AGT<br>TAT CAG CTG                         | n/a          | Used to generate the AP-1 mutant <i>GzB</i> promoter construct                              |
| <i>GzB</i> promoter AP-1 mutant 3'   | CAG CTG <b>ATA</b> ACT<br><b>AAG</b> AGT GGA                  | n/a          | Used to generate the AP-1 mutant <i>GzB</i> promoter construct                              |
| <i>Cyp40</i> promoter AP-1 mutant 5' | GGC ATT GTA CTA<br><b>ACT</b> <b>AAT</b> GTC TTT<br>AAT C     | n/a          | Used to generate the AP-1 mutant <i>Cyp40</i> promoter construct                            |
| <i>Cyp40</i> promoter AP-1 mutant 3' | GAT TAA AGA<br>CAT <b>TAG</b> TTA GTA<br>CAA TGC C            | n/a          | Used to generate the AP-1 mutant <i>Cyp40</i> promoter construct                            |

Restriction sites in the oligonucleotides are underlined. Nucleotides that were mutated to generate the AP-1 mutation in the *GzB* and *Cyp40* promoter sequences are bolded. n/a – not applicable.

### **2.2.3: Restriction endonuclease digestions**

To perform restriction endonuclease digestions, 0.5-2 µg of PCR product or plasmid DNA was incubated with 0.5-1.0 µl of the desired restriction enzyme(s) in 1X NEBuffer (New England BioLabs; Ipswich, MA) or 1X FastDigest buffer (Fermentas) in 20 µl volumes. When recommended by the manufacturer, bovine serum albumin (BSA) was also included in the reaction at a final concentration of 100 µg/ml. Digests were incubated at 37°C for 1-3 hrs and then the DNA purified using the QIAquick PCR Purification kit (Qiagen) as per manufacturer's instructions.

### **2.2.4: DNA ligations**

Ligations were performed in 10 µl reaction volumes using 1U of T4 DNA ligase (New England BioLabs or Fermentas) in the supplied T4 DNA ligase buffer (New England BioLabs or Fermentas) with 50 ng of digested vector and the appropriate amount of insert to give an insert to vector molar ratio of 3:1. Ligations were incubated overnight at room temperature then the entire reaction was transformed into chemically competent DH5α *Escherichia coli* (*E. coli*).

### **2.2.5: Bacterial transformation**

Chemically competent DH5α *E. coli* were transformed with plasmid DNA or ligation reactions using heat shock transformation. Competent DH5α *E. coli* were incubated with DNA on ice for 20-40 min, followed by heat shocked at 42°C for 2 min. Cells were then allowed to recover for 5 min on ice and plated on Luria-Bertani (LB) agar plates (1% (w/v) tryptone, 0.5% (w/v) yeast extract, 1% (w/v) NaCl, 1.5% (w/v) agar, pH 7.4) containing 100 µg/ml ampicillin (Sigma-Aldrich). LB plates were then incubated at 37°C for 16-20 hrs.

### **2.2.6: Isolation and purification of plasmid DNA**

Plasmid DNA was isolated from *E. coli* using either the Qiagen Qiaprep Spin Miniprep or the Qiagen Plasmid Maxiprep kit as outlined in the manufacturer's protocols. Briefly, an overnight culture (100 ml for maxipreps and 2 ml for minipreps) of DH5 $\alpha$  *E. coli* grown in LB media (1% (w/v) tryptone, 0.5% (w/v) yeast extract, 1% (w/v) NaCl, pH 7.4) containing 100 $\mu$ g/ml ampicillin was harvested by centrifugation. Bacterial cells were then lysed under alkaline conditions, the lysate neutralized and the DNA bound to an anion-exchange column. Following several washes, the DNA was eluted from the column, and the DNA concentration quantified using a NanoDrop ND-1000 spectrophotometer (Thermo Scientific).

### **2.2.7: DNA sequencing and analysis**

DNA sequencing of FLAG-tagged JunB was performed at the Centre for Biomedical Research DNA Sequencing Facility (University of Victoria; Victoria, BC) using the CMV 30-forward and CMV 24-reverse sequencing primers supplied by the facility. Sequencing of other constructs was performed at The Applied Genomics Centre (TAGC) (University of Alberta) using the T7-forward and bovine growth hormone (BGH)-reverse sequencing primers (Myc-tagged JunB) or the M13-forward and reverse primers (*GzB* and *Cyp40* promoters) supplied by TAGC. DNA sequences were analysed using the basic local alignment search tool (BLAST) (National Center for biotechnology Information (NCBI)) and sequence chromatograms were analysed using Chromas 2 (<http://technelysium.com.au>).

## **2.3: CLONING**

### **2.3.1: Vectors**

The vectors used in this study are outlined in Table 2.4. The pFLAG-CMV2 expression vector was purchased from Sigma-Aldrich and the pcDNA3.1A/Myc-His(-) expression vector was from Invitrogen. The pBluescriptII (pBSII) SK(+) cloning/sequencing vector and the pBlueScript (pBS)-Myc2 cloning vector were from Stratagene (La Jolla, CA). The pGL2 basic firefly luciferase and pRL-TK *Renilla* luciferase vectors were obtained from Promega.

### **2.3.2: Cloning the FLAG- and Myc-tagged JunB constructs**

To generate the N-terminal FLAG-tagged human JunB construct, JunB was PCR amplified from a JunB-containing cloning vector using the JunB 5' (FLAG tag) and 3' primers. JunB was then cloned into the *EcoRI* and *Sall* sites of the pFLAG-CMV2 expression vector. JunB possessing an N-terminal double Myc-tag was generated by PCR amplifying JunB from the FLAG-tagged JunB cDNA using the JunB 5' (Myc tag) and 3' primers. JunB was then digested with *EcoRI* and *Sall* and ligated into the *EcoRI* and *XhoI* sites of the pBS-Myc2 vector to add a double Myc-tag to the 5' end of the JunB cDNA (Note: the *Sall/XhoI* restriction sites were destroyed). The Myc-JunB was then removed from the pBS-Myc2 vector using the *KpnI* and *Sall* restriction sites of the pBS-Myc2 vector and cloned into the *KpnI* and *XhoI* restriction sites of the pcDNA3.1A/Myc-His(-) eukaryotic expression vector (Note: the *Sall/XhoI* restriction sites were destroyed). A translational stop site was included at the end of the JunB cDNA sequence so that the C-terminal Myc/His tag of the pcDNA3.1A/Myc-His(-) vector was not expressed. The sequence of both of these constructs was verified by DNA sequencing.

**Table 2.4: Vectors used in this study.**

| <b>Plasmid</b>                         | <b>Characteristics</b>  | <b>Source</b> |
|--|---|---------------|
| pFLAG-CMV2                             | Mammalian expression vector containing N-terminal FLAG tag and CMV promoter   | Sigma-Aldrich |
| pBluescript-Myc2                       | Cloning vector containing N-terminal double Myc tag   | Stratagene    |
| pcDNA3.1A/Myc-His(-)                   | Mammalian expression vector containing CMV promoter   | Invitrogen    |
| pFLAG-CMV2-JunB                        | Expression vector containing FLAG-tagged JunB   | This study    |
| pcDNA3.1A-Myc2-JunB                    | Expression vector containing double Myc-tagged JunB   | This study    |
| pBluescriptII SK(+)                    | Cloning/sequencing vector with sites for M13-forward and reverse primers  | Stratagene    |
| pGL2 basic                             | Promoter-less firefly luciferase vector   | Promega       |
| pGL2- <i>GzB</i> promoter              | Firefly luciferase vector under control of the human <i>GzB</i> proximal promoter   | This study    |
| pGL2- <i>Cyp40</i> promoter            | Firefly luciferase vector under control of the human <i>Cyp40</i> proximal promoter   | This study    |
| pGL2-AP-1 mutant <i>GzB</i> promoter   | Firefly luciferase vector under control of the human <i>GzB</i> proximal promoter containing a mutation in the AP-1 site                            | This study    |
| pGL2-AP-1 mutant <i>Cyp40</i> promoter | Firefly luciferase vector under control of the human <i>Cyp40</i> proximal promoter containing a mutation in the AP-1 site                          | This study    |
| phRL-TK                                | Vector containing the <i>Renilla</i> luciferase gene under control of the constitutively active herpes simplex virus thymidine kinase (TK) promoter | Promega       |

### **2.3.3: Cloning the human *GzB* and *Cyp40* promoter-driven luciferase constructs**

To generate the firefly luciferase reporter construct under control of the human *GzB* promoter, the human *GzB* proximal promoter (-728 to +59 relative to the transcriptional start site) was PCR amplified from Karpas 299 genomic DNA using the *GzB* promoter 5' and 3' primers and first cloned into the *KpnI* and *XhoI* sites of the pBSII SK(+) cloning/sequencing vector. The *GzB* promoter sequence was verified by DNA sequencing and then sub-cloned from the pBSII SK(+) vector to the pGL2 basic luciferase vector using the *KpnI* and *XhoI* restriction sites. To generate the *Cyp40* promoter-driven firefly luciferase reporter construct, the human *Cyp40* proximal promoter (-691 to +62 relative to the transcriptional start site) was PCR amplified from Karpas 299 genomic DNA using the *Cyp40* promoter 5' and 3' primers. The *Cyp40* promoter was then cloned into the *SacI* and *XhoI* restriction sites of the pBSII SK(+) vector, sequenced and finally sub-cloned into the pGL2 basic luciferase vector using these same restriction sites.

### **2.3.4: Site-directed mutagenesis of AP-1 mutant promoter luciferase constructs**

The AP-1 mutant promoter luciferase constructs were generated by site-directed mutagenesis where the AP-1 site in the *GzB* promoter was mutated from TGAGTCA to TTAGTTA using the pGL2-*GzB* promoter construct as a template. The *Cyp40* promoter AP-1 site was mutated from TGATTCA to TAACTAA using the pGL2-*Cyp40* promoter construct as a template. Point mutations were incorporated into each PCR product by overlap extension PCR using primers containing the desired mutation. Each half of the PCR product was PCR amplified using a 5' flanking primer and a 3' mutagenic primer or a 5' mutagenic primer and a 3' flanking primer. After PCR amplification, a small amount of the two PCR products were mixed and used as a template to PCR amplify the full length mutant construct using the *GzB* promoter or *Cyp40* promoter 5' and 3' flanking

primers. Mutant constructs were then cloned into the pBSII SK(+) vector, verified by DNA sequencing and sub-cloned into the pGL2 firefly luciferase vector in the same manner as the wild-type constructs (see section 2.3.3).

## **2.4: PROTEIN METHODS**

### **2.4.1: Cell lysis**

Cells were collected by centrifugation for 5 min at ~650 *g* and washed once in 1X PBS. Cells were then resuspended in 1% Nonidet P-40 (NP-40) lysis buffer (1% NP-40, 50 mM Tris pH 7.4, 150 mM NaCl, 2 mM EDTA, 10% glycerol) containing 1 mM phenylmethyl sulfonyl fluoride (PMSF; BioShop), 1 mM sodium orthovanadate (Sigma-Aldrich), and protease inhibitor cocktail (PIC; Sigma-Aldrich), and incubated for 10 min at 4°C on a nutator. Cell lysates were then cleared of detergent-insoluble material by centrifugation at ~20,000 *g* for 10 min.

### **2.4.2: Protein quantification using the bicinchoninic acid assay**

The protein concentration of cleared cell lysate was determined using the Pierce bicinchoninic acid (BCA) Protein Assay Kit (Thermo Scientific). Cell lysates or lysis buffer alone (blank measurement) were first diluted 1:4 in water, then 10 µl of diluted sample or lysis buffer was plated in triplicate in a 96-well plate. A standard curve of known concentrations of BSA was also prepared and plated in the 96-well plate. The BCA reagent was then prepared by mixing Reagent A with Reagent B at a 50:1 ratio, and 90 µl added to the samples/standards in the 96-well plate. The plate was incubated at 37°C for 30 min or 2hrs at room temperature, and the absorbance measured at 544 nm using a FLUOstar OPTIMA microplate reader (BMG Labtech; Ortenberg, Germany). The absorbance of the lysis buffer blank was subtracted from all samples and standards and the protein concentration of each sample quantified using a standard curve generated from

the BSA standards. Samples within a given experiment were then diluted to equal protein concentration in sample buffer (2% (w/v) SDS, 10% (w/v) glycerol, 5% (v/v) 2-mercaptoethanol, 0.002% (w/v) bromophenol blue, 62.5 mM Tris (pH 6.8)).

#### **2.4.3: Quantitative mass spectrometry**

Protein lysates collected from Karpas 299 or SUP-M2 cells transfected with control (non-targeting) or JunB siRNA were submitted for isobaric tag for relative and absolute quantification (iTRAQ) mass spectrometry analysis (283) at the University of Victoria/Genome BC Proteomics Centre (Victoria, BC, Canada). Proteins were precipitated with acetone and reduced and alkylated before being subjected to “in solution” trypsin digestion. Tryptic fragments were then labelled with the specific iTRAQ labels (Applied Biosystems; Foster City, CA) and analysed by liquid chromatography tandem mass spectrometry using a quadrupole time-of-flight mass spectrometer (QStar Pulsar i, Applied Biosystems). Data was analysed using Protein Pilot 2.0 software (284) (Applied Biosystems).

#### **2.4.4: Immunoprecipitations**

Anti-Alk immunoprecipitations were performed by incubating cleared cell lysates with 0.5 µg of anti-Alk antibody (Dako; Burlington, ON, Canada) and 10 µl of packed Protein A-Sepharose beads (Sigma-Aldrich) for 1-2 hrs at 4°C on a nutator. For other immunoprecipitations, cleared lysates were incubated with 2 µg of anti-JunB (C-11; Santa Cruz Biotechnology), anti-c-Fos (C-10; Santa Cruz Biotechnology), anti-FLAG M2 (Sigma-Aldrich) or an irrelevant isotype control antibody along with 10 µl of packed Protein G-Sepharose beads (Sigma-Aldrich) for 1-2 hrs at 4°C on a nutator. Beads were then washed 3 times with 500 µl of NP-40 lysis buffer and bound proteins eluted by boiling in sample buffer.

#### **2.4.5: Western blotting**

Prior to loading, cell lysates or immunoprecipitates were heated at ~95°C for 5 min prior to separation using sodium dodecyl sulphate-polyacrylamide gel electrophoresis (SDS-PAGE). Samples were resolved on SDS gels containing 8-12% polyacrylamide (Bio-Rad; Hercules, CA) using a Hoefer SE260 mini-vertical gel electrophoresis unit (Hoefer; Holliston, MA) at 25 mA/gel constant current (maximum 200 V) for approximately 1.5 hrs, or until desired protein separation was achieved. Gels were resolved in running buffer containing 25 mM Tris base, 192 mM glycine and 0.1% SDS. PageRuler prestained protein ladder (Thermo Scientific) was used as a molecular mass indicator.

After electrophoresis, gels and nitrocellulose membranes (Bio-Rad) were equilibrated in 1X transfer buffer (25 mM Tris base, 192 mM glycine, and 20% (v/v) methanol) for 5 min prior to transfer. Proteins were then transferred to the nitrocellulose membranes using a Bio-Rad Trans-Blot SD Semi-Dry transfer cell run at a constant voltage of 15 V (maximum 500 mA) for 30-60 min. Following transfer, membranes were stained with Ponceau S (0.1% (w/v) Ponceau S in 5% glacial acetic acid) (Sigma-Aldrich) to assess protein loading and the quality of transfer. The Ponceau S stain was removed by washing membranes with 0.05% TBST (1X Tris-buffered saline (TBS) containing 0.05% (w/v) Tween-20).

Membranes were blocked at room temperature for 0.5-2 hrs in 5% non-fat milk powder in 1X TBS. Membranes were then washed and incubated with primary antibody (described in Table 2.5) for 1-3 hrs at room temperature or overnight at 4°C with shaking. Non-specifically bound antibody was removed by washing membranes three times for 10 min each in 0.05% or 0.1% TBST, and membranes probed with horseradish-peroxidase (HRP)-conjugated secondary antibodies (Bio-Rad) for 30-60 min at room temperature. Membranes were then washed three times for 10 min each in 0.05% or 0.1% TBST and blots visualized by incubating membranes for 5 min with SuperSignal West Pico Chemiluminescent

Substrate (Thermo Scientific), followed by exposure to autoradiography film (Clonex; Markham, ON, Canada). Films were developed using an M35A X-OMAT (Kodak; Rochester, NY) or AGFA CP1000 (AGFA Healthcare; Greenville, SC) film processor. To reprobe blots, membranes were first stripped for 30-60 min at room temperature in stripping solution (0.1% TBST, pH 2), followed by washing in 0.05% TBST. Membranes were then incubated with a new primary antibody and probed as described above.

#### **2.4.6: Quantitative western blotting**

For quantitative western blotting experiments, samples were resolved by SDS-PAGE and proteins transferred to nitrocellulose membranes as described above. Following transfer, membranes were blocked in Odyssey blocking buffer (LI-COR Biosciences; Lincoln, NE) for 2 hrs at room temperature or 4°C overnight. Membranes were then washed and incubated with primary antibody as described above. Following three washes of 10 min each in 0.1% TBST, membranes were incubated with IRDye-conjugated secondary antibodies (Rockland Immunochemical Inc.; Gilbertsville, PA) for 30 min. Membranes were then washed three times for 10 min each in 0.1% TBST and once in 1X PBS before bands were quantified on a LI-COR Odyssey Infrared Imager (LI-COR Biosciences). For quantification, band intensity of the protein of interest was normalized to  $\beta$ -actin or  $\alpha$ -tubulin for each sample. Membranes were then incubated with HRP-conjugated secondary antibodies and visualized by chemiluminescence as described above.

**Table 2.5: Antibodies used for western blotting.**

| <b>Antibody</b>                                     | <b>Species</b> | <b>Dilution</b> | <b>Source</b>            |
|---|----------------|-----------------|--------------------------|
| β-actin (AC15)                                      | mouse          | 1:5000          | Santa Cruz               |
| Akt (#9272)   | rabbit         | 1:1000          | Cell Signaling           |
| Alk (ALK1)  | mouse          | 1:1000          | Dako                     |
| Phospho-Alk (Tyr 338, 342 & 343 of NPM-ALK) (#3983) | rabbit         | 1:1000          | Cell Signaling           |
| Annexin A1 (EH17a)                                  | mouse          | 1:200           | Santa Cruz               |
| c-Fos (C-10)  | mouse          | 1:200           | Santa Cruz               |
| c-Jun (60A8)  | rabbit         | 1:1000          | Cell Signaling           |
| Cyp40 (H185)  | rabbit         | 1:500           | Santa Cruz               |
| Decorin (clone 115402)                              | mouse          | 1 µg/ml         | R&D Systems              |
| ERK1/2 (137F5)                                      | rabbit         | 1:1000          | Cell Signaling           |
| Phospho-ERK1/2 (Thr202/Tyr204) (20G11)              | rabbit         | 1:1000          | Cell Signaling           |
| Fibronectin (F 3648)                                | rabbit         | 1:1000          | Sigma-Aldrich            |
| FKBP51 (D4)   | mouse          | 1:200           | Santa Cruz               |
| FKBP52/Hsp56 (329.1)                                | mouse          | 1:200           | Santa Cruz               |
| FLAG M2   | mouse          | 1:1000          | Sigma-Aldrich            |
| FosB (102)  | rabbit         | 1:200           | Santa Cruz               |
| Fra2 (Q-20)   | rabbit         | 1:200           | Santa Cruz               |
| Granzyme A (#4928)                                  | rabbit         | 1:1000          | Cell Signaling           |
| Granzyme B (2C5)                                    | mouse          | 1:500           | Santa Cruz               |
| JunB (C-11)   | mouse          | 1:200           | Santa Cruz               |
| Myc (9E10)  | mouse          | 1:200           | Santa Cruz               |
| NPM (NA24)  | mouse          | 1:1000          | Thermo Scientific        |
| PARP-1 (C2-10)                                      | mouse          | 1:5000          | Santa Cruz               |
| Perforin (F-1)                                      | mouse          | 1:200           | Santa Cruz               |
| Phospho-tyrosine (4G10)                             | mouse          | 1 µg/ml         | Millipore                |
| STAT3 (F-2)   | mouse          | 1:1000          | Santa Cruz               |
| Phospho-STAT3 (Tyr 705) (B-7)                       | mouse          | 1:1000          | Santa Cruz               |
| α-tubulin (DM1A)                                    | mouse          | 1:5000          | Santa Cruz               |
| Vitronectin (H-270)                                 | rabbit         | 1:200           | Santa Cruz               |
| anti-mouse IgG HRP conjugate (172-1011)             | goat           | 1:10,000        | Bio-Rad                  |
| anti-rabbit IgG HRP conjugate (172-1019)            | goat           | 1:10,000        | Bio-Rad                  |
| anti-mouse IRDye800CW (610-131-121)                 | goat           | 1:20,000        | Rockland Immunochemicals |
| anti-rabbit IRDye700DX (611-130-122)                | goat           | 1:20,000        | Rockland Immunochemicals |

#### **2.4.7: Analysis of GzB expression using flow cytometry**

To analyse GzB protein expression in cells stably expressing GzB shRNA,  $\sim 4 \times 10^5$  cells were collected by centrifugation and washed once with PBS. Cells were then resuspended in 100  $\mu$ l of BD Cytofix/Cytoperm solution (BD Biosciences; Mississauga, ON) and incubated for 20 min on ice. Fixed cells were washed once in 1X BD Perm/Wash buffer (BD Biosciences), and resuspended in 100  $\mu$ l of BD Perm/Wash buffer containing 1:250 diluted APC-conjugated anti-GzB (clone GB12) or isotype control antibody (Invitrogen). Cells were incubated with antibody for 30 min on ice in the dark, followed by washing in BD Perm/Wash buffer. Stained cells were then resuspended in 500  $\mu$ l of FACS buffer (1X PBS containing 1% (v/v) FBS) and analysed by flow cytometry using a FACSCalibur flow cytometer (BD Biosciences). Data was analysed using CellQuest Pro software (BD Biosciences) and the mean fluorescence intensity of GzB staining determined for each sample.

### **2.5: RNA METHODS**

#### **2.5.1: Isolation of total RNA**

Total RNA was collected from cells using the RNeasy Mini Kit (Qiagen) as outlined in the manufacturer's protocol. Briefly,  $3-7 \times 10^6$  cells were collected by centrifugation, resuspended in buffer RLT and lysed using QIAshredder spin columns (Qiagen). RNA was then bound to RNeasy spin columns, washed with buffers RW1 and RPE and eluted in water. The concentration of eluted RNA was determined using a NanoDrop ND-1000 spectrometer (Thermo Scientific) and the RNA stored at  $-80^\circ\text{C}$ .

#### **2.5.2: DNase digestion and reverse transcription**

Isolated RNA was first subjected to DNase digestion to remove any contaminating genomic DNA. Two micrograms of total RNA was incubated with

1U of DNase I, amplification grade (Invitrogen) in 1X DNase I reaction buffer (10 µl final volume) for 15 min at room temperature. One microliter of 25 mM EDTA was then added and the DNase I inactivated by heating at 65°C for 10 min. mRNA was then reverse transcribed to cDNA using the Superscript II Reverse Transcriptase System (Invitrogen). To the RNA mixture, 1 µl of 10 mM dNTPs and 1 µg of random primers (Invitrogen) were added, and the reaction heated at 65°C for 5 min then cooled 2 min on ice. To the mixture, first-strand buffer (Invitrogen) was added to a final concentration of 1X along with 5 mM DTT, 200U of Superscript II reverse transcriptase (Invitrogen) and 40U of the RNaseOUT ribonuclease inhibitor (Invitrogen). The reaction was then incubated for 5 min at 25°C, followed by 1 hr at 50°C and 15 min at 70°C. The resulting cDNA was then diluted 1:4 in water for PCR analysis or 1:64 for quantitative real-time PCR (qRT-PCR) analysis.

### **2.5.3: PCR analysis of converted cDNA**

To analyse mRNA expression of the different *Granzymes* in ALK+ ALCL cell lines, PCR reactions were performed on cDNA generated from the different ALK+ ALCL cell lines, or the NKL and NK92 cell lines as positive controls. PCR reactions were performed as described in section 2.2.2, with the exception that 1 µl of 1:4 diluted cDNA was used as a template and low fidelity *Taq* polymerase (Biological Sciences Fermentation Unit, University of Alberta) was used in the reaction. The primers used for these reactions are listed in Table 2.6. PCR cycling parameters used were an initial denaturing step at 95°C for 5 min followed by 35-40 cycles of denaturing at 95°C for 50 sec, annealing at 52°C for 50 sec, and extension at 72°C for 45 sec, followed by a final extension step at 72°C for 5 min. PCR products were then visualized by agarose gel electrophoresis using a 1% (w/v) agarose gel prepared in 1X TAE buffer containing 1:10,000 SYBR Safe DNA gel stain (Invitrogen).

#### **2.5.4: Quantitative real-time PCR (qRT-PCR)**

Quantitative real-time PCR (qRT-PCR) was performed to quantify relative mRNA expression using PerfeCTa SYBR Green FastMix (Quanta Biosciences; Gaithersburg, MD). White-walled 96-well real-time PCR plates (VWR) were plated in triplicate with 2.5  $\mu$ l of 1:64 diluted cDNA samples (or water alone as a blank control), 2.5  $\mu$ l of 1.2  $\mu$ M mixed forward and reverse primers (listed in Table 2.7) and 5  $\mu$ l of 2X PerfeCTa SYBR Green FastMix. Reactions were then performed using an Eppendorf Mastercycler realplex<sup>4</sup> thermal cycler (Eppendorf; Mississauga, ON, Canada) or a Bio-Rad CFX96 Real-Time PCR Detection System (Bio-Rad). Cycling conditions used were an initial denaturing step at 95°C for 2 min followed by 40-45 cycles of denaturing at 95°C for 15 sec, annealing at 52°C for 20 sec, and extension at 68°C for 30 sec. Fluorescence measurements were made following each cycle, and a final melting curve analysis was performed to ensure the purity of the final product. Expression of the gene of interest was normalized to  $\beta$ -actin, GAPDH or  $\beta$ -tubulin (as indicated) and relative expression determined using the  $\Delta\Delta$ -CT method (285).

**Table 2.6: Primers used for RT-PCR.**

| <b>Target gene</b> | <b>Forward primer sequence</b>    | <b>Reverse primer sequence</b> | <b>Expected product size (bp)</b> |
|--------------------|-----------------------------------|--------------------------------|-----------------------------------|
| <i>Granzyme B</i>  | TGC GAA TCT GAC<br>TTA CGC CAT    | GGA GGC ATG CCA<br>TTG TTT CG  | 164                               |
| <i>Granzyme A</i>  | CAT CTG TGC TGG<br>GGC TTT GA     | GAG GCT TCC AGC<br>ACA AAC CA  | 448                               |
| <i>Granzyme H</i>  | GCA AGA GAA GAG<br>TCG GAA GAG G  | AAC CCC AGC CAG<br>CCA CAC     | 323                               |
| <i>Granzyme K</i>  | CGT TTG TGG AGG<br>TGT TCT GAT TG | CAG TGA CTT CTC<br>GCA GGG TG  | 368                               |
| <i>Granzyme M</i>  | GCG GGG GTG TCC<br>TGG TG         | ATG CTG GGG GAG<br>AGG CTG     | 418                               |
| <i>GAPDH</i>       | GAC AGT CAG CCG<br>CAT CTT CT     | TTA AAA GCA GCC<br>CTG GTG AC  | 127                               |

**Table 2.7: Primers used for qRT-PCR.**

| <b>Target gene</b>               | <b>Forward primer sequence</b>    | <b>Reverse primer sequence</b>     | <b>Expected product size (bp)</b> |
|----------------------------------|-----------------------------------|------------------------------------|-----------------------------------|
| <i>Granzyme B</i>                | TGC GAA TCT GAC<br>TTA CGC CAT    | GGA GGC ATG CCA<br>TTG TTT CG      | 164                               |
| <i>Perforin</i>                  | TGG AGT GCC GCT<br>TCT ACA GTT    | CCG TAG TTG GAG<br>ATA AGC CTG A   | 139                               |
| <i>Granzyme A</i>                | CAT CTG TGC TGG<br>GGC TTT GA     | TCT GTT TTG TTG GCT<br>CTT CCC T   | 125                               |
| <i>Cyp40</i>                     | TCG AGT CTT CTT TGA<br>CGT GGA    | CAG TCG TGT GTC<br>CAA TGC CTT     | 140                               |
| <i>FKBP51</i>                    | AAG AGT GGG GAA<br>TGG TGA GG     | GCA CAG TAA ATG<br>GCA TAT CTC TCC | 208                               |
| <i>FKBP52</i>                    | TGC TGA AGG TCA<br>TCA AGA GAG AG | ATG GTG GCT ATG<br>GCA ATG TC      | 193                               |
| <i>β-actin</i>                   | AGA AAA TCT GGC<br>ACC ACA CC     | TAG CAC AGC CTG<br>GAT AGC AA      | 173                               |
| <i>GAPDH</i>                     | GAC AGT CAG CCG<br>CAT CTT CT     | TTA AAA GCA GCC<br>CTG GTG AC      | 127                               |
| <i>β-tubulin, class I (TUBB)</i> | CAG GCT GGT CAG<br>TGT GGC A      | CAG GAT GGC ACG<br>AGG AAC         | 174                               |

## **2.6: LUCIFERASE REPORTER ASSAYS**

Karpas 299 cells were transfected with 10 µg of the indicated pGL2 luciferase construct and 1 µg of a constitutively expressed *Renilla* luciferase construct (to control for transfection efficiency). In luciferase experiments involving siRNAs, cells were also transfected with 100 nM pooled control (non-targeting), JunB or Alk siRNA. For luciferase assays performed on Karpas 299 cells over-expressing JunB, cells were transfected with the luciferase constructs as described above along with 5 µg of FLAG- or Myc-tagged JunB or empty vector. Cells were then incubated for 24 hrs at 37°C prior to analysis of luciferase activity using the Dual-Glo Luciferase Assay System (Promega) and a BMG LabTech FLUOstar OPTIMA microplate reader. One million cells were analysed in triplicate for *GzB* promoter- or *Cyp40* promoter-driven firefly luciferase activity by mixing cells at a 1:1 ratio with the Dual-Glo luciferase reagent in a white-walled 96-well plate. The plate was incubated at room temperature for 10 min prior to measuring luminescence. The firefly luminescence was then quenched and *Renilla* luciferase determined by adding the Dual-Glo Stop & Glo reagent (1:100 dilution of the Stop & Glo substrate in Stop & Glo buffer), followed by incubation for 10 min at room temperature and luminescence measurement. The ratio of firefly to *Renilla* luciferase activity was calculated for each well and the triplicate measurements for each sample averaged.

## **2.7: ELECTROPHORETIC MOBILITY SHIFT ASSAYS (EMSA)**

### **2.7.1: Cytoplasmic and nuclear fractionation and Bradford assays**

Nuclear extracts used for EMSA experiments were collected using the ProteoJET cytoplasmic and nuclear protein extraction kit (Fermentas) as outlined in the manufacturer's protocol. Briefly, Karpas 299 cells were collected by centrifugation, washed in 1X PBS, and cell pellets resuspended in the supplied cell lysis buffer containing 1 mM PMSF and PIC. This was then incubated on ice

for 10 min. The nuclear fraction was separated from the cytoplasmic fraction by centrifugation at 500 *g* for 7 min at 4°C. The cytoplasmic fraction (supernatant) was then collected and centrifuged at ~20,000 *g* for 15 min to fully remove any insoluble material. Nuclear pellets were washed twice in the supplied nuclei wash buffer (containing 1 mM PMSF and PIC) and resuspended in the nuclei storage buffer (containing 1 mM PMSF and PIC). Nuclei lysis reagent was then added and the samples incubated on a nutator at 4°C for 15 min followed by centrifugation for 5 min at ~20,000 *g* to remove insoluble material. Nuclear fractions were aliquoted and immediately stored at -80°C until use. The protein concentration of nuclear fractions was quantified using the Bradford assay (286). Samples were diluted 1:2 in water, and 5 µl incubated with 250 µl of Quick Start Bradford dye reagent (Bio-Rad) in a 96-well plate. A standard curve of BSA standards was also prepared. Reactions were incubated ~5 min at room temperature and absorbance measured at 584 nm using a BMG Labtech FLUOstar OPTIMA microplate reader. Protein concentration of the nuclear fraction was then determined using the equation generated from the BSA standard curve.

## **2.7.2: EMSA experiments**

### **2.7.2.1: Annealing duplex probes**

The biotinylated probes and the unlabelled competitors used for EMSA experiments were based on the 20 nucleotide DNA sequence surrounding the AP-1 site in the human *GzB* proximal promoter (CCACTCTGAGTCATCAGCTG) or the human *Cyp40* proximal promoter (TTGTACTGATTCATGTCTTT). The unlabelled AP-1 mutant competitors possessed the same mutation as described for the luciferase reporter construct (see section 2.3.4). Duplex probes or competitors were generated by annealing antiparallel DNA oligonucleotides (IDT). Oligonucleotides were mixed at a 1:1 molar ratio in annealing buffer (50 mM

NaCl, 10 mM Tris, pH 7.5), heated to 95°C for 5 min and slowly cool to room temperature for ~1 hr. Annealed duplexes were stored at -80°C.

### **2.7.2.2: Binding reactions**

EMSA experiments were performed using the LightShift Chemiluminescent EMSA kit (Thermo Scientific) virtually as outlined in the manufacturer's protocol. Binding reactions (20 µl volumes) were performed with ~4 µg (*GzB* promoter probe) or ~7.5 µg (*Cyp40* promoter probe) of nuclear protein extract, 20 fmol (*GzB* promoter probe) or 100 fmol (*Cyp40* promoter probe) of biotinylated probe and 1 µg of poly(dI:dC) in 1X binding buffer. For competitor experiments, a 200-fold (*GzB* promoter probe) or 50-fold (*Cyp40* promoter probe) molar excess of unlabelled wild-type or AP-1 mutant probe was included in the binding reaction. Binding reactions were incubated for 20 min at room temperature, followed by the addition of 5 µl of 5X loading buffer. For super-shift experiments, 1 µg of an isotype control or specific antibody was pre-incubated with the reaction mixture for 15 min on ice prior to addition of the biotinylated probe. The JunB (C-11) mAb (Santa Cruz Biotechnology) was used for super-shift experiments with the *GzB* promoter probe, while the JunB (204C4a) mAb (Santa Cruz Biotechnology) was used for super-shift experiments with the *Cyp40* promoter probe. For the panel of AP-1 antibodies used for super-shifting the *GzB* promoter probe, we used: JunB (C-11), JunD (329), c-Fos (C-10), FosB (102), and Fra2 (Q-20) (all from Santa Cruz Biotechnology).

### **2.7.2.3: Electrophoresis and detection**

Binding reactions were resolved on non-denaturing gels prepared in 0.5X Tris/borate/EDTA (TBE) buffer (45 mM Tris base, 45 mM boric acid, 1.6 mM EDTA) containing 5% acrylamide. Gels were electrophoresed at a constant voltage of 100V for ~1 hr in 0.5X TBE buffer. Following electrophoresis, the gel and BrightStar-Plus positively charged nylon membrane (Life Technologies) were equilibrated in 0.5X TBE buffer for 5 min, and DNA complexes transferred to the

nylon membrane using a Bio-Rad Trans-Blot SD Semi-Dry transfer cell run at 400 mA constant amperage for 25 min. DNA was then cross-linked to the membrane by placing the membrane face-down on a UV transilluminator equipped with a 312 nm bulb for 15 min. Following DNA crosslinking, membranes were visualized using the Nucleic Acid Detection Module included with the LightShift EMSA kit. Membranes were blocked for 15 min in Blocking Buffer, followed by incubation with Stabilized Streptavidin-Horseradish Peroxidase Conjugate diluted 1:300 in Blocking Buffer for 15 min. Membranes were then washed four times for 5 min each with 1X Wash Buffer and incubated in Substrate Equilibration Buffer for 5 min. EMSAs were visualized by incubating membranes for 5 min with the chemiluminescent substrate, followed by exposure to autoradiography film (Clonex). Film was developed using an M35A X-OMAT (Kodak) or AGFA CP1000 (AGFA Healthcare) film processor.

## **2.8: GRANZYME B RELEASE ASSAYS**

Cells were counted, collected by centrifugation and resuspended to  $5 \times 10^5$  cells/ml in fresh RPMI 1640 media. When indicated, Brefeldin A (Sigma-Aldrich) was added to the media at a concentration of 1  $\mu\text{g/ml}$ . Cells were incubated for 24 hrs at 37°C, then supernatants collected and cell lysates prepared for western blotting as described in section 2.4.

## **2.9: EXPERIMENTS TO ASSESS GRANZYME B ACTIVITY**

### **2.9.1: Cleavage of the synthetic GzB substrate, Ac-IEPD-pNA**

Activity of GzB present in ALK+ ALCL cell line lysates was assessed by measuring cleavage of the synthetic GzB substrate, N-Acetyl-Ile-Glu-Pro-Asp-*p*-nitroanilide (Ac-IEPD-pNA) (287). Cells were lysed at a concentration of  $5 \times 10^7$  cells/ml as described in section 2.4.1, with the exception that protease inhibitors were

omitted from the lysis buffer. Samples were prepared in triplicate by diluting 50  $\mu$ l of cell lysate or lysis buffer alone to 100  $\mu$ l in cleavage buffer (50 mM HEPES pH 7.5, 10% (w/v) sucrose, 0.05% (w/v) CHAPS). Ac-IEPD-pNA (Sigma-Aldrich) was then added to a final concentration of 200  $\mu$ M. For blank measurements, samples were similarly prepared, except that Ac-IEPD-pNA was not included. Reactions were then incubated at 37°C for 0.5-1 hr and absorbance measured at 405 nm using a BMG Labtech FLUOstar OPTIMA microplate reader. Triplicate samples were then averaged and blank measurements were subtracted for each sample.

### **2.9.2: Cleavage of the extracellular matrix proteins vitronectin, fibronectin and decorin**

The extracellular matrix (ECM) proteins used as GzB substrates in this study were human fibronectin (BD Biosciences), human vitronectin (BD Biosciences) and human decorin (Gly17-Lys359) (R&D Systems; Minneapolis, MN). To assess cleavage of the ECM proteins by GzB, wells of a 96-well plate were coated with 0.5  $\mu$ g of the desired ECM protein (suspended in 50  $\mu$ l of 1X PBS) at 4°C overnight. Wells were then blocked with 2% BSA (in 50  $\mu$ l of 1X PBS) for 1 hr at 37°C and excess BSA removed by washing the wells twice with 100  $\mu$ l of 1X PBS. Cells were lysed at  $5 \times 10^7$  cells/ml in lysis buffer lacking protease inhibitors, and 50  $\mu$ l of cell lysate or lysis buffer alone was added to the coated wells. When indicated, the GzB inhibitor, Z-AAD-CMK (Calbiochem; Billerica, MA), was included in the reactions at a concentration of 100  $\mu$ M. Plates were then incubated at 37°C for the indicated times, at which time reactions were stopped by adding sample buffer to the wells. Samples were then collected, resolved using SDS-PAGE and cleavage of the ECM proteins detected by western blotting.

### **2.9.3: Activity of released GzB**

Supernatant samples were collected as described in section 2.8 and assayed for GzB activity using the QuickZyme Granzyme B activity assay kit (QuickZyme Bioscience; Leiden, Netherlands) as described in the manufacturer's protocol. Briefly, 96-well plates were coated with 0.2 µg of the supplied anti-GzB antibody at 4°C overnight, washed then incubated with supernatant samples or media alone (in triplicate) for 1 hr at room temperature. Wells were then washed, the detection reagent (consisting of the supplied detection enzyme and chromogenic substrate) added and the absorbance at 405 nm measured immediately using a BMG Labtech FLUOstar OPTIMA microplate reader (this was then used for a background correction). When indicated, the GzB inhibitor, Z-AAD-CMK (100 µM), was included in the reactions. Plates were then incubated at 37°C for 48 hrs and absorbance again measured at 405 nm. The initial background measurement was subtracted from the 48 hr measurement and triplicate samples averaged.

## **2.10: CELL TREATMENTS**

### **2.10.1: 5-aza-2'-deoxycytidine (DAC) treatment**

To examine the role of DNA methylation in regulating Perforin expression in ALK+ ALCL cell lines, cells were treated with the DNA methyltransferase inhibitor, 5-aza-2'-deoxycytidine (DAC) (Sigma-Aldrich). Karpas 299, SUP-M2 or SU-DHL-1 cells were suspended to  $\sim 4 \times 10^4$  cells/ml then treated with 1 µM DAC and incubated at 37°C for 0, 48 or 96 hrs. Alternatively, cells were treated with 0.1% (v/v) DMSO alone for 96hrs. After 72 hrs, cells were split into fresh media containing 0.1% DMSO or 1 µM DAC to maintain cells in logarithmic growth. Cell lysates were collected after the indicated times and Perforin protein expression examined using quantitative western blotting as described in section 2.4.

### **2.10.2: Staurosporine and doxorubicin treatments**

To induce apoptosis in ALK+ ALCL cell lines, cells were suspended to  $4-6 \times 10^5$  cells/ml in complete RPMI. Cells were then treated with 0.1% DMSO (untreated) or the indicated concentrations of staurosporine (Enzo Life Sciences; Plymouth Meeting, PA) for 6 hrs at 37°C. Alternatively, cells were treated with 0.1% water (untreated) or the indicated concentrations of doxorubicin (Sigma-Aldrich) for 12 hrs at 37°C. After treatment, cells were collected and lysates prepared for western blotting as described in section 2.4 or analyzed for apoptosis using TUNEL labeling (see section 2.12).

### **2.10.3: Crizotinib treatments**

The Alk inhibitor, Crizotinib, used to inhibit NPM-ALK activity in ALK+ ALCL cell lines was kindly provided by Pfizer (176, 270, 288). For dose-course experiments, Karpas 299 or SUP-M2 cells were diluted to  $\sim 1 \times 10^5$  cells/ml in complete RPMI 1640 media and treated with 0.1% (v/v) DMSO (untreated) or with 25, 50 or 75 nM Crizotinib. Cells were incubated at 37°C for 48 hrs prior to lysis. For time-course experiments, cells were diluted to  $\sim 2 \times 10^5$  cells/ml in complete RPMI 1640. Cells were then treated with 0.1% (v/v) DMSO (untreated) or 75 nM Crizotinib and incubated at 37°C for 24, 48 or 72 hrs. For time-course experiments, cells were split into fresh Crizotinib-containing media after 24 and 48 hrs to maintain the cells in logarithmic growth. After the indicated times cell lysates were prepared and examined by western blotting.

## **2.11: IN VITRO INVASION ASSAYS**

### **2.11.1: Preparing the collagen/fibronectin matrix**

To prepare a collagen/fibronectin matrix for cell invasion assays, rat tail collagen Type I (BD Biosciences) and human fibronectin (BD Biosciences) were diluted to 2 mg/ml and 25 µg/ml, respectively, in sterile 1X PBS containing 5 mM NaOH. The

collagen mixture was prepared on ice, and then 200  $\mu$ l added to pre-warmed 8.0  $\mu$ m cell culture transwell inserts (VWR cat# 353097) in a 24-well plate. The collagen/fibronectin mixture was allowed to set at 37°C for 30-45 min, hydrated with 500  $\mu$ l of serum-free RPMI for 30-45 min at 37°C, and then stained overnight at 37°C with 500  $\mu$ l of serum-free RPMI containing 10  $\mu$ M CellTracker Green CMFDA (Invitrogen). After staining, the collagen/fibronectin matrix was washed three times with 750  $\mu$ l of serum-free RPMI.

### **2.11.2: Invasion assay**

SUP-M2 cells expressing control shRNA or GzB shRNA #1 were collected and suspended to  $2 \times 10^6$  cells/ml in PBS containing 10  $\mu$ M CellTracker Red CMTPX (Invitrogen). Cells were stained for 20 min at 37°C, and then washed once with serum-free RPMI. Stained cells were suspended to  $2 \times 10^6$  cell/ml in serum-free RPMI, and 750  $\mu$ l ( $1.5 \times 10^6$  cells) were added to the top of the collagen/fibronectin matrix. To the lower chamber of the transwell, 1 ml of serum-free RPMI (no attractant) or RPMI containing 10% FBS and 100 ng/ml stromal cell-derived factor-1 $\alpha$  (SDF-1 $\alpha$ ) (R&D Systems) was added and plates incubated at 37°C for ~20 hrs. Following incubation the media was removed from the upper chamber of the transwell, and then the collagen/fibronectin matrix containing invading cells was fixed at 4°C overnight in 4% paraformaldehyde (Electron Microscopy Sciences; Hatfield, PA). The fixed collagen/fibronectin matrices were washed twice in 1X PBS and then frozen on dry ice. The frozen matrix was then removed from the transwell insert, embedded in Tissue-Tek O.C.T. compound (Electron Microscopy Sciences) on dry ice, and 40  $\mu$ M sections prepared using a Leica CM1900 UV Cryostat (Leica; Wetzlar, Germany). The invasive depth of the 4-5 most invasive cells in a given field (10X magnification) of each section was measured using a Zeiss Axiovert 200M inverted widefield fluorescent microscope (Zeiss; Oberkochen, Germany). The average invasive depth was then determined by averaging the invasive depth of the 4-5 most

invasive cells in each field, and then the average invasive depth of 8-12 different sections was averaged to give the invasive depth for each sample.

#### **2.12: APOPTOSIS ANALYSIS USING TERMINAL DEOXYNUCLEOTIDYL TRANSFERASE dUTP NICK END LABELING (TUNEL)**

Apoptosis was analysed by terminal deoxynucleotidyl transferase dUTP nick end labelling (TUNEL) using the *In Situ* Cell Death Detection Kit, Fluorescein (Roche Applied Science; Laval, QC, Canada) as outlined in the manufacture's protocol. After staurosporine treatment, cells were collected and washed twice in 1X PBS. Cells were then fixed in 200 µl of 2% paraformaldehyde for 1 hr at room temperature with shaking. Fixed cells were washed once with 500 µl of 1X PBS and permeabilized in 100 µl 0.1% Triton X-100 (in 0.1% sodium citrate) for 2 min on ice. Cells were then washed twice with 500 µl of 1X PBS and resuspended in 50 µl of the supplied Label Solution (negative control) or Enzyme Solution diluted 1:10 in Label Solution. Reactions were incubated for 1 hr at 37°C then washed twice with 500 µl of 1X PBS. Washed cells were resuspended in ~300 µl of FACS buffer (1X PBS containing 1% FBS) and analysed for the percentage of dUTP-positive cells using a FACSCalibur flow cytometer (BD Biosciences).

#### **2.13: MTS VIABILITY ASSAYS**

After transfection with the indicated pooled siRNAs, cells were suspended to  $4 \times 10^4$  cells/ml in RPMI 1640 media and incubated at 37°C for 48 hrs. The number of viable cells in each sample was then determined in triplicate using the CellTiter 96 Aqueous Non-Radioactive Cell Proliferation Assay (MTS assay) (Promega). One hundred microliters of cells were plated in triplicate in a 96-well plate and 20 µl of MTS reagent was added. Cells were then incubated at 37°C for 1-2 hrs and absorbance at 492 nm measured using a BMG Labtech FLUOstar OPTIMA

microplate reader. Triplicate measurements were averaged and the percentage of viable cells determined relative to cells transfected with control siRNA. Each experiment was performed in quadruplicate.

#### **2.14: STATISTICAL ANALYSIS**

Statistical analysis was performed using either paired or unpaired *t*-tests, as indicated in figure legends.

## **CHAPTER 3: NPM-ALK AND THE JUNB TRANSCRIPTION FACTOR REGULATE THE EXPRESSION OF CYTOTOXIC MOLECULES IN ALK+ ALCL**

A portion of this chapter has been published:

**Pearson JD, Lee JKH, Bacani JTC, Lai R, and Ingham RJ.** (2011) NPM-ALK and the JunB transcription factor regulate the expression of cytotoxic molecules in ALK-positive, anaplastic large cell lymphoma. *International Journal of Clinical and Experimental Pathology*. **4**:124-133.

All experiments contained within this chapter were performed by J. Pearson. J. Lee assisted with the analysis of mass spectrometry data (Figure 3.1B). Joyce Wu and Dr. R. Ingham generated the JunB shRNA stable Karpas 299 cell lines used in Figure 3.3. The original manuscript was written by J. Pearson, and Dr. R. Ingham with minor editorial input from J. Lee, Dr. J. Bacani and Dr. R. Lai.

### 3.1: INTRODUCTION

The JunB transcription factor is known to be up-regulated downstream of the NPM-ALK oncoprotein via increased transcription through a MEK/ERK/ETS1 pathway (191, 192), and increased translation via an mTOR-dependent pathway (191). Importantly, JunB has been demonstrated to promote proliferation of the Karpas 299 ALK+ ALCL cell line, as siRNA-mediated knock-down of JunB in these cells resulted in reduced cell numbers (191). This was accompanied by an increased proportion of cells in the G1/G0 stage of the cell cycle and a reduced percentage of cells in the G2/M stage, suggesting a proliferation defect. JunB has also been demonstrated to cooperate with c-Jun to promote the pathogenesis of tumours in a *NPM-ALK* transgenic mouse model (279). While a few JunB transcriptional targets have been described in ALK+ ALCL (51, 193, 256, 279), these do not likely explain the proliferation defect observed in ALK+ ALCL cell lines after JunB knock-down. This suggests that there are important JunB transcriptional targets yet to be identified in ALK+ ALCL. Therefore, we used siRNA to knock-down the expression of JunB in the Karpas 299 and SUP-M2 ALK+ ALCL cell lines, and performed a quantitative mass spectrometry screen to identify proteins whose expression is regulated by JunB in these cells. As will be discussed in this chapter, one protein whose expression was found to be reduced after JunB knock-down was the serine protease, Granzyme B (GzB).

GzB belongs to the Granzyme family of serine protease enzymes, which in humans also consists of four other members: Granzyme A, H, K and M (57). These proteins are typically expressed by CTL and NK cells, and along with the pore-forming protein Perforin are used by CTL and NK cells to kill virally infected or cancerous cells (57, 58, 60). We were particularly intrigued by the finding that GzB expression might be regulated by JunB because it has been noted by several groups that ALK+ ALCL tumour cells often express GzB (19, 28, 54). ALK+ ALCL cells also often express Perforin and TIA-1 (19, 28, 54, 55), and the expression of these proteins along with GzB gives rise to a common cytotoxic phenotype in

ALK+ ALCL. These observations are one piece of evidence suggesting that ALK+ ALCL tumour cells may arise from a CTL. Here, we demonstrate that JunB and NPM-ALK influence the cytotoxic phenotype of ALK+ ALCL by promoting the expression of GzB. Furthermore, we show that NPM-ALK signalling also influences the expression of Perforin in ALK+ ALCL cell lines where it promoted the expression of Perforin in one cell line, but repressed Perforin expression in others.

### **3.2: IDENTIFICATION OF GRANZYME B AS A POTENTIAL JUNB-REGULATED PROTEIN IN ALK+ ALCL**

In order to better understand the function of JunB in ALK+ ALCL, the Karpas 299 and SUP-M2 ALK+ ALCL cell lines were transfected with a pooled control (non-targeting) siRNA or pooled siRNA to target JunB. We found that transfection of these cells with JunB siRNA resulted in down-regulation of JunB protein levels compared to cells transfected with control siRNA (Figure 3.1A). Lysates were then collected from Karpas 299 or SUP-M2 cells transfected with control or JunB siRNA and submitted for quantitative mass spectrometry using isobaric tag for relative and absolute quantification (iTRAQ) labelling (283) to identify proteins whose expression was altered in cells transfected with JunB siRNA compared to control siRNA. In two independent experiments we obtained quantitative data for 744 (experiment 1) and 871 (experiment 2) total proteins; 342 of these proteins were commonly identified in both experiments (Figure 3.1B). We found that the expression of the majority of these proteins was not substantially altered following JunB knock-down. In order to identify proteins that were likely to be general JunB targets in ALK+ ALCL, we concentrated on proteins whose expression was similarly altered in both experiments and in both cell lines after JunB knock-down. Based on these criteria, we identified GzB as one protein that had reduced expression following JunB knock-down. We identified three

(experiment 1) and five (experiment 2) down-regulated peptides that corresponded to GzB in samples with JunB knock-down (Table 3.1). Since GzB expression is a well-known phenotypic characteristic of ALK+ ALCL (19, 28) we were intrigued by this finding, and we decided to further examine whether JunB promotes the expression of GzB in ALK+ ALCL.

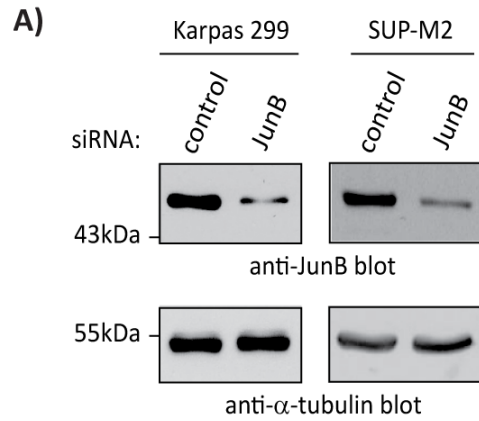


**Figure 3.1: Identification of JunB-regulated proteins in ALK+ ALCL cell lines using quantitative iTRAQ mass spectrometry.**

**(A)** Western blot of JunB knock-down in Karpas 299 or SUP-M2 ALK+ ALCL cell lines transfected with 600 nM pooled control (non-targeting) or pooled JunB siRNAs. **(B)** Total number (n) of proteins in which quantitative data for at least one tryptic peptide was obtained in each of the two independent iTRAQ mass spectrometry experiments.

|              | Granzyme B peptides used for quantification | Karpas 299                |                  | SUP-M2                    |                  |
|--------------|---|---------------------------|------------------|---------------------------|------------------|
|              |   | Relative Granzyme B level | Rank             | Relative Granzyme B level | Rank             |
| Experiment 1 | 3   | 0.6365                    | 4 <sup>th</sup>  | 0.7889                    | 9 <sup>th</sup>  |
| Experiment 2 | 5   | 0.7387                    | 21 <sup>st</sup> | 0.8401                    | 27 <sup>th</sup> |

**Table 3.1: Summary of GzB quantitative mass spectrometry results.**

The summarized GzB results from the two independent iTRAQ experiments are shown. The “relative Granzyme B level” is the ratio of GzB protein in the JunB siRNA-treated cell lysate compared to control siRNA-treated cells. “Rank” indicates the rank order of GzB on the list of down-regulated proteins in the Karpas 299 or SUP-M2 JunB siRNA-treated cell lysates for the indicated experiment.

### **3.3: GRANZYME B PROTEIN LEVELS ARE REDUCED FOLLOWING JUNB KNOCK-DOWN IN ALK+ ALCL CELL LINES**

To confirm the findings of the mass spectrometry screen, we used quantitative western blotting to examine GzB protein levels in lysates from Karpas 299 and SUP-M2 ALK+ ALCL cells treated with either pooled JunB or non-targeting (control) siRNA. These experiments confirmed that reducing JunB expression resulted in decreased GzB protein levels (Figure 3.2A). To rule out potential off-targeting effects of the pooled JunB siRNAs, we performed similar experiments using individual siRNAs directed against JunB. We found that GzB protein levels were reduced in cells treated with each of the four individual JunB siRNAs (Figure 3.2B). Moreover, the decrease in GzB levels directly correlated with the degree of JunB silencing observed with the individual siRNAs.

As an alternative approach, we used lentiviral transduction to generate Karpas 299 cells stably expressing a JunB shRNA under control of an IPTG-inducible promoter. Treatment these cells with increasing concentrations of IPTG resulted in a dose-dependent decrease in JunB protein levels over 48 and 72 hrs (Figure 3.3), whereas treatment of cells expressing a control (non-targeting) shRNA had no effect on JunB levels. Importantly, we also observed a substantial dose-dependent decrease in GzB protein levels 48 and 72 hrs after IPTG treatment in cells expressing the JunB shRNA (Figure 3.3). In these experiments we did observe a modest reduction in GzB levels after 72 hrs of IPTG treatment in cells expressing a control shRNA; however, this decrease was much less than what was observed for cells expressing the JunB shRNA. Taken together, these results demonstrate that JunB promotes GzB protein expression in ALK+ ALCL.

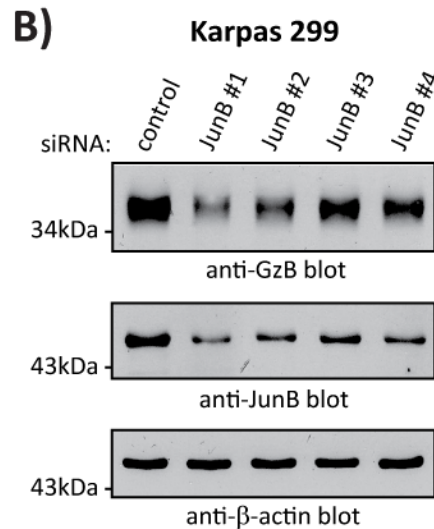
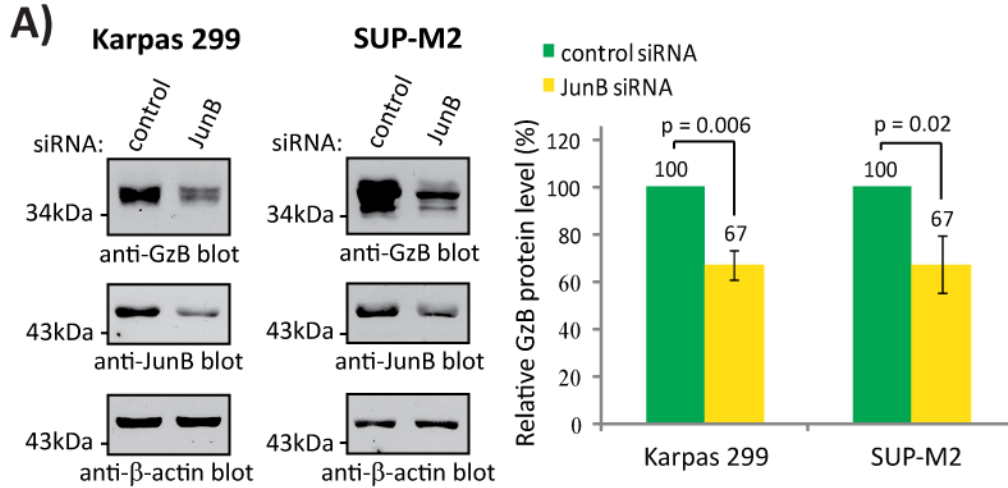


**Figure 3.2: siRNA-mediated knock-down of JunB reduces GzB protein levels.**

**(A)** Western blot analysis of GzB (upper panel) and JunB (middle panel) expression in cell lysates of Karpas 299 or SUP-M2 cells transfected with 100 nM of pooled non-targeting (control) or JunB siRNAs (left). Relative GzB protein levels were quantified using the LI-COR Odyssey Infrared imager (right). The results shown are the mean and standard deviation of three independent experiments. *p* values were obtained using paired, one-tailed *t*-tests. **(B)** Western blot analysis of GzB (upper panel) and JunB (middle panel) expression in lysates from Karpas 299 cells transfected with 100 nM of a non-targeting (control) or individual JunB siRNAs. The anti-β-actin western blots demonstrate equivalent protein loading. Molecular mass markers are indicated to the left of the blots.

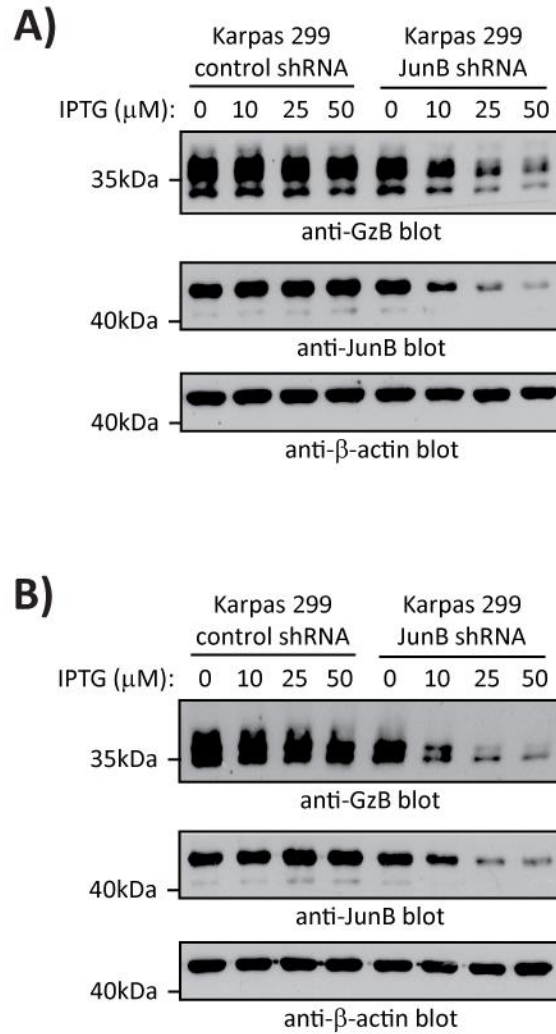


**Figure 3.3: Knock-down of JunB using shRNA results in reduced GzB protein levels.**

Karpas 299 cells expressing an IPTG-inducible control (non-targeting) or JunB shRNA were left untreated or were treated with 10, 25 or 50  $\mu\text{M}$  IPTG for 48 hrs **(A)** or 72 hrs **(B)** to induce the shRNA. Lysates were then collected and JunB and GzB levels were examined by western blotting. The anti- $\beta$ -actin western blots demonstrate equivalent protein loading. Molecular mass markers are indicated to the left of the blots.

### **3.4: GRANZYME B IS A JUNB TRANSCRIPTIONAL TARGET IN ALK+ ALCL CELL LINES**

Since JunB is a transcription factor, we next examined whether it promotes *GzB* transcription in ALK+ ALCL. Using qRT-PCR we demonstrated that *GzB* mRNA levels were reduced in ALK+ ALCL cell lines transfected with JunB siRNA (Figure 3.4), consistent with the hypothesis that JunB promotes *GzB* transcription. The human *GzB* promoter contains an AP-1 binding site as well as CRE, Ikaros, CBF, ETS, and NFAT recognition sites (289). This AP-1 site is conserved in mice and is required for maximal *GzB* promoter activity in both murine and human activated T cells (290, 291). Because the *GzB* promoter contains an AP-1 site that could be recognized by JunB, we investigated whether JunB could promote the expression of a luciferase reporter construct under control of the human *GzB* proximal promoter. Treatment of Karpas 299 cells with JunB siRNA (Figure 3.5A) significantly reduced *GzB* promoter-driven luciferase activity, and over-expression of FLAG-tagged JunB enhanced *GzB* promoter luciferase activity in Karpas 299 cells (Figure 3.5B). This established that JunB promotes transcription from the *GzB* proximal promoter in ALK+ ALCL cells. Furthermore, we found that mutation of the AP-1 site in the *GzB* proximal promoter significantly reduced activity compared to the wild-type promoter construct (Figure 3.5C). This demonstrated that similar to activated T cells (290, 291) AP-1 activity is also an important regulator of *GzB* transcription in ALK+ ALCL. Interestingly, we observed that JunB knock-down reduced luciferase activity to a greater extent than mutation of the AP-1 site in the *GzB* proximal promoter. This suggests that JunB may be able to promote transcription from this promoter through a second AP-1 site, or that it can indirectly promote transcription from the *GzB* proximal promoter. In support of the former possibility, it has been suggested that the human *GzB* proximal promoter contains another (non-canonical) AP-1 site that can promote transcription from this promoter (292, 293).

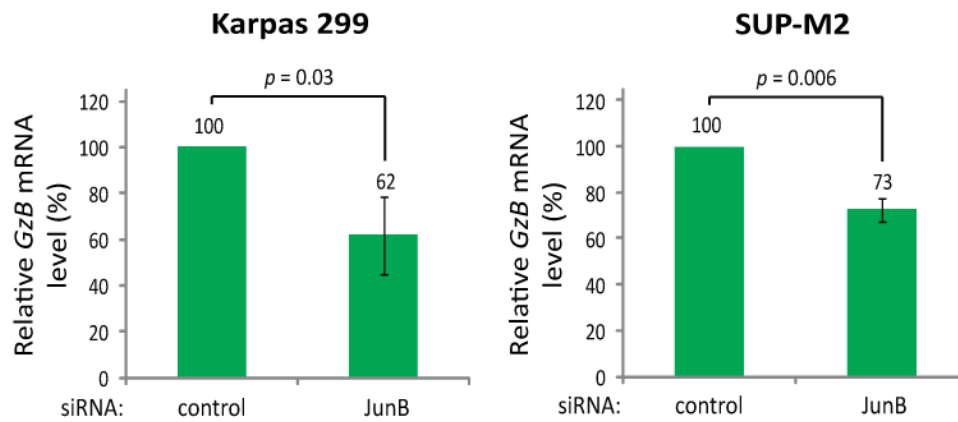


**Figure 3.4: JunB knock-down reduces *GzB* mRNA expression in ALK+ ALCL cells.**

qRT-PCR analysis of *GzB* mRNA levels in Karpas 299 (left) and SUP-M2 (right) cells transfected with 100 nM of the indicated pooled siRNAs. *GzB* mRNA levels were normalized to the housekeeping gene  $\beta$ -*actin* and the quantification represents the mean and standard deviation of three independent experiments. *p* values were determined using paired, one-tailed *t*-tests. Note: these experiments were performed on the mRNA extracted from cells transfected in Figure 3.2A.

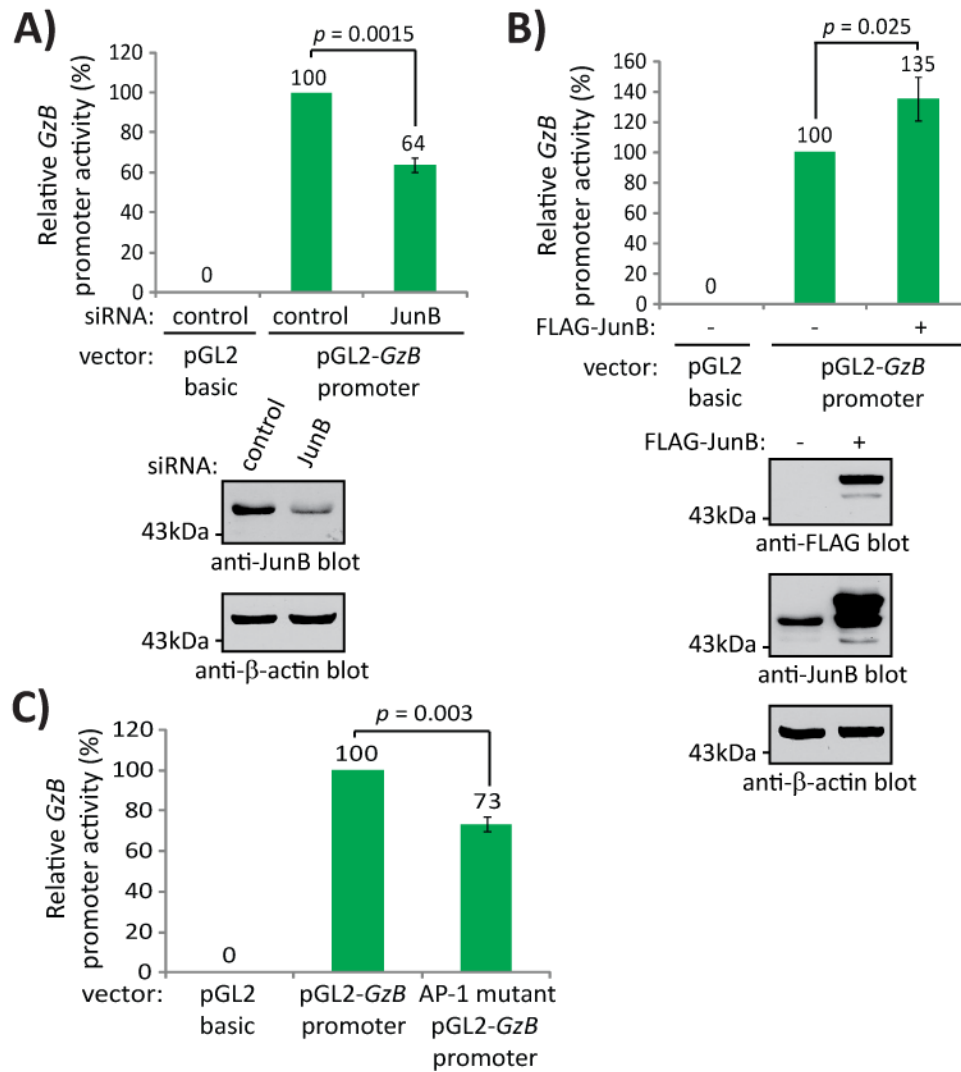


**Figure 3.5: JunB promotes transcription from the GzB promoter.**

**(A)** Luciferase activity was measured in Karpas 299 cells transfected with a promoter-less luciferase construct (pGL2 basic) or a luciferase construct under control of the *GzB* proximal promoter (pGL2-*GzB* promoter) and the indicated siRNAs. Luciferase activity is expressed relative to the cells transfected with the pGL2-*GzB* promoter and control siRNA. A western blot demonstrating JunB knock-down is shown below. **(B)** Karpas 299 cells were transfected with the indicated luciferase constructs and FLAG-tagged JunB (+) or empty vector (-). Luciferase activity is expressed relative to the pGL2-*GzB* promoter and empty vector-transfected cells. FLAG and JunB western blots demonstrate JunB over-expression (bottom). **(C)** Luciferase activity was measured in Karpas 299 cells transfected with the pGL2 basic, pGL2-*GzB* promoter, or AP-1 mutant pGL2-*GzB* promoter luciferase constructs. Luciferase activity is expressed relative to the pGL2-*GzB* promoter transfected cells. *p* values were determined using paired, one-tailed *t*-tests.

Since JunB promoted transcription from the *GzB* promoter and the AP-1 site was required for maximal activity from this promoter, we next performed electrophoretic mobility shift assays (EMSAs) to test whether JunB can bind the AP-1 site in the *GzB* proximal promoter. A protein(s) present in Karpas 299 nuclear extract associated with a biotin-labelled probe based on a 20 nucleotide sequence surrounding the AP-1 site in the *GzB* promoter (Figure 3.6). Moreover, this binding was out-competed by a molar excess of an unlabelled *GzB* AP-1 probe, but not with an unlabelled probe containing a mutation in the AP-1 site (Figure 3.6), demonstrating that binding to this probe is mediated by the AP-1 site. We also observed an almost complete super-shift of the protein/probe complex by the addition of an anti-JunB antibody, but not by an irrelevant control antibody (Figure 3.6). This latter result demonstrates that not only is JunB present in these probe/protein complexes, but that almost all probe/protein complexes associating with the AP-1 site in the *GzB* promoter in these assays contain JunB. Taken together, these findings suggest that JunB binds the AP-1 site in the *GzB* promoter and functions as a direct activator of *GzB* transcription in ALK+ ALCL.

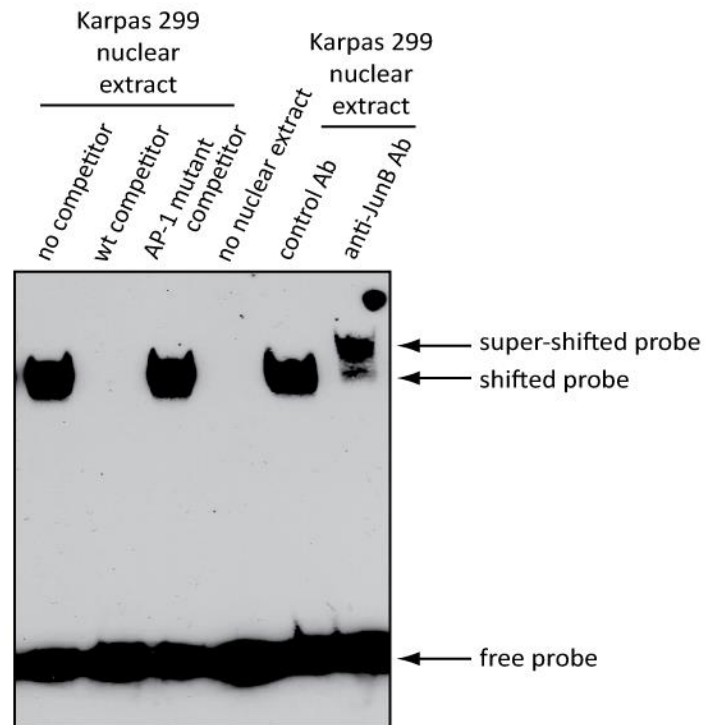


**Figure 3.6: JunB can bind to the AP-1 site of the *GzB* promoter.**

EMSAs were performed with Karpas 299 nuclear extracts using a biotinylated probe based on the sequence of the AP-1 site in the *GzB* proximal promoter (*GzB* AP-1 probe). For competitor experiments, a 200-fold molar excess of unlabelled *GzB* AP-1 probe (wt competitor) or an unlabelled *GzB* AP-1 probe with a mutation in the AP-1 binding site (AP-1 mutant competitor) were included in the reaction. For super-shift experiments, 1  $\mu$ g of the indicated antibody (Ab) was included in the reaction.

### **3.5: C-FOS ALSO BINDS THE AP-1 SITE IN THE *GRANZYME B* PROMOTER AND ASSOCIATES WITH JUNB IN ALK+ ALCL CELL LINES**

In one study, JunB was suggested to function largely as a homodimer to promote *CD30* expression in ALK+ ALCL (256). Similarly, in another study using EMSA experiments, JunB was suggested to be the major AP-1 component with DNA-binding activity in ALK+ ALCL cell lines (191). However, it has also been demonstrated that JunB and Fra2 were the major AP-1 components active in ALK+ ALCL cell lines, and that JunB and Fra2 co-immunoprecipitate in these cells (265). This suggests that different JunB dimers may be important for regulating the expression of different genes in ALK+ ALCL. To test which AP-1 family members may function with JunB to promote *GzB* expression in ALK+ ALCL, we performed EMSA super-shift experiments using the *GzB* promoter AP-1 probe and antibodies to several AP-1 family members. Of the antibodies tested, the only one other than JunB that was able to noticeably super-shift the probe/protein complex was the antibody specific to c-Fos (Figure 3.7). Of note, the c-Fos antibody was able to strongly super-shift the probe/protein complex, suggesting it is a major component of the AP-1 factor(s) bound to this probe. While we cannot rule out that the lack of super-shift by other antibodies is due to the fact that they do not work for EMSA experiments, others have successfully used these same antibodies in EMSA super-shift experiments (265, 294-297).

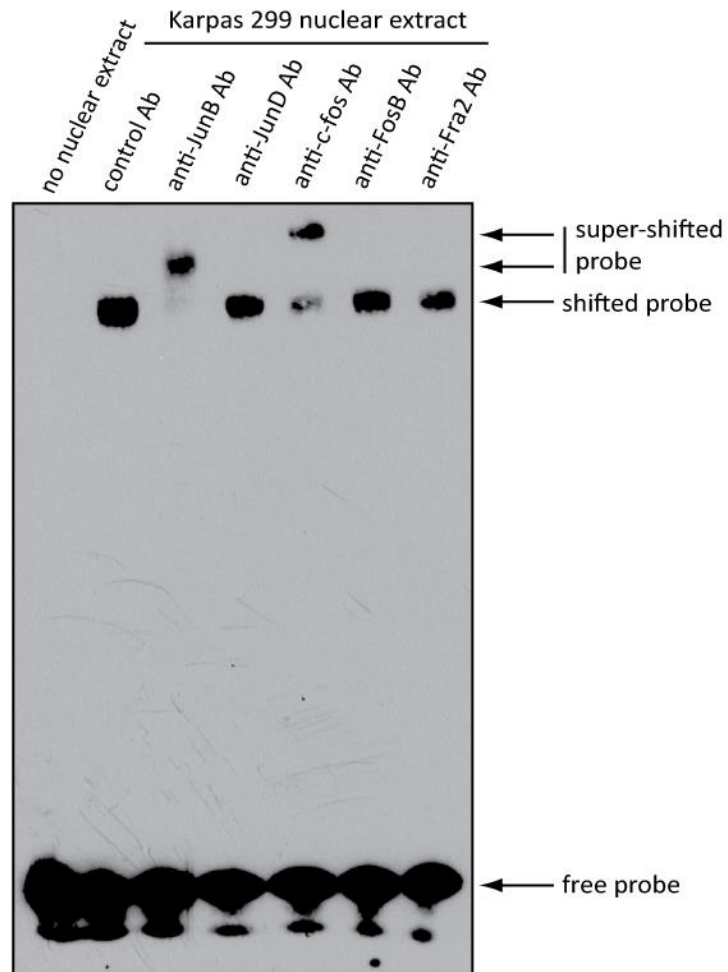


**Figure 3.7: c-Fos can also bind to the AP-1 site of the *GzB* promoter.**

EMSAs were performed with Karpas 299 nuclear extracts using a biotinylated probe based on the sequence of the AP-1 site in the *GzB* proximal promoter. An irrelevant control antibody (Ab) or antibodies specific for the indicated AP-1 family proteins were used to super-shift the biotinylated probe.

We next performed co-immunoprecipitation experiments to test whether JunB and c-Fos can associate in ALK+ ALCL cell lines. Using either anti-JunB (Figure 3.8A) or anti-c-Fos (Figure 3.8B) immunoprecipitations we found that endogenous JunB and c-Fos co-precipitate in Karpas 299 and SUP-M2 cells. Taken together with the EMSA experiments, these results suggest that JunB may function as a heterodimer with c-Fos to regulate GzB expression in ALK+ ALCL. Unfortunately, we have been unable to silence c-Fos expression in ALK+ ALCL cell lines using siRNA (Figure 3.8C) to determine whether c-Fos does promote GzB expression in these cells. We also found that Fra2 associates with JunB (Figure 3.8A) in ALK+ ALCL cells; however, we observed no association of FosB or c-Jun with JunB (Figure 3.8A). Using FLAG- and Myc-tagged JunB constructs, we further found that when ectopically expressed in Karpas 299 cells, Myc-JunB can co-immunoprecipitate with FLAG-JunB (Figure 3.8D). These results suggest that JunB may also function as a heterodimer with Fra2 or as a homodimer in ALK+ ALCL.

### **3.6: JUNB DOES NOT REGULATE PERFORIN EXPRESSION IN ALK+ ALCL**

GzB is just one component of cytotoxic granules. Perforin, a pore forming protein that functions with GzB to allow CTL and NK cells to kill target cells, is also expressed in ALK+ ALCL tumour cells (19, 28, 55). Since the *Perforin* promoter contains an AP-1 binding site (289), we postulated it may also be regulated by JunB in this lymphoma. However, western blotting experiments revealed that Perforin protein levels were not significantly altered in cells treated with JunB siRNA (Figure 3.9). Therefore, while JunB is an important transcriptional activator of *GzB* in ALK+ ALCL, it is not a major regulator of Perforin expression in this lymphoma.

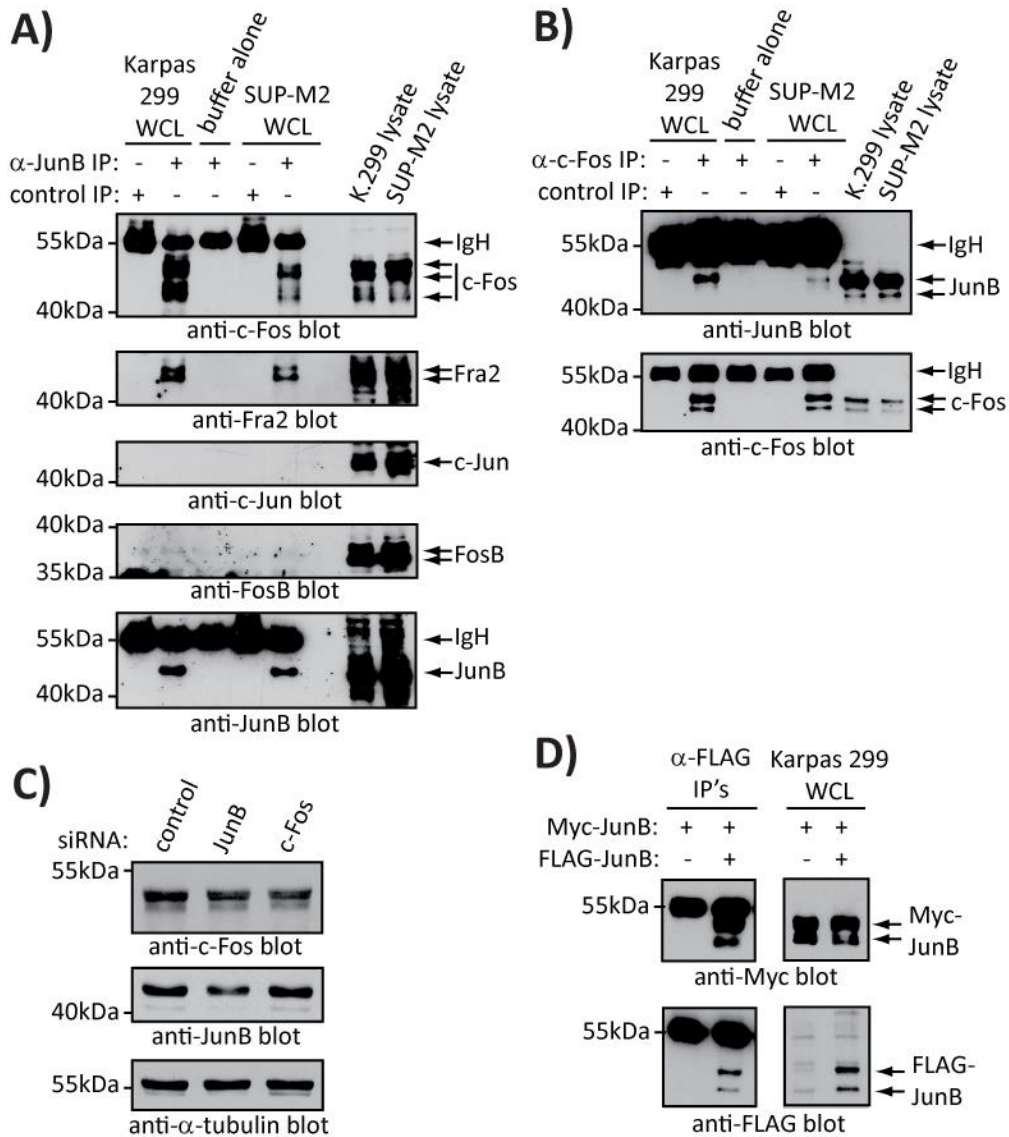


**Figure 3.8: JunB co-immunoprecipitates with c-Fos, Fra2 and other JunB molecules in ALK+ ALCL cell lines.**

Anti-JunB **(A)** or anti-c-Fos **(B)** immunoprecipitations (IPs) were performed with Karpas 299 or SUP-M2 cell lysates. Control IP represents an IP using an irrelevant isotype control antibody. These IPs or cell lysates were then western blotted with the indicated antibodies. **(C)** Karpas 299 cells were transfected with the indicated pooled siRNAs then lysates collected and western blotted with the indicated antibodies. The anti-α-tubulin blot demonstrates equal protein loading. **(D)** Karpas 299 cells were transfected with Myc- or FLAG-tagged JunB as indicated. Lysates were then prepared and immunoprecipitated with the anti-FLAG M2 antibody followed by anti-FLAG and anti-Myc western blotting. Molecular mass markers are indicated to the left of the western blots.

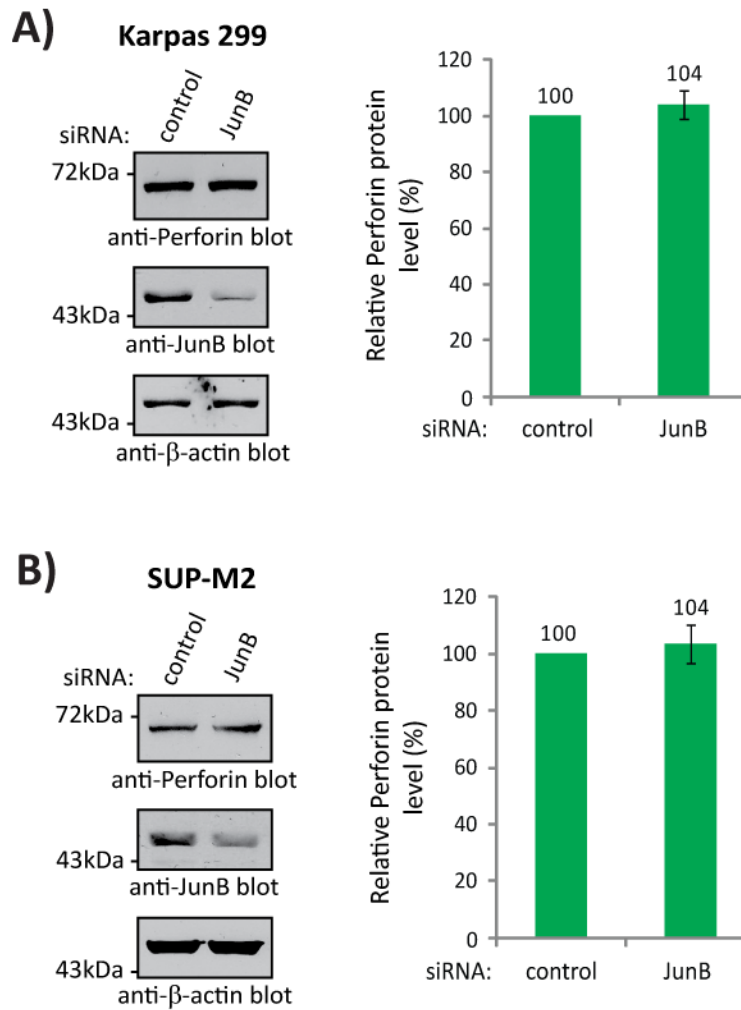


**Figure 3.9: JunB does not regulate Perforin expression in ALK+ ALCL.**

Western blot (left) and quantification (right) of Perforin expression in cell lysates from Karpas 299 **(A)** and SUP-M2 **(B)** cells transfected with pooled control (non-targeting) or JunB siRNAs. Results are the mean and standard deviation of three independent experiments. There was no statistical difference in Perforin levels between control and JunB siRNA-treated samples (paired, two-tailed *t*-tests;  $p > 0.15$ ). Anti- $\beta$ -actin blots demonstrate equal protein loading. Molecular mass markers are indicated to the left of the western blots.

### **3.7: NPM-ALK REGULATES GRANZYME B AND PERFORIN EXPRESSION IN ALK+ ALCL**

Since NPM-ALK promotes the expression of JunB (51, 191) we examined whether NPM-ALK also promotes GzB expression. Knock-down of NPM-ALK using siRNA in Karpas 299 and SUP-M2 cells resulted in a reduction of GzB protein levels by at least 50% (Figure 3.10A). Similar to previous studies (51, 267) we found that JunB levels were decreased in cells following ALK knock-down (Figure 3.10A), consistent with the notion that JunB might function downstream of NPM-ALK to promote GzB expression. Knock-down of NPM-ALK in Karpas 299 and SUP-M2 cells also resulted in reduced *GzB* mRNA expression (Figure 3.10B), and we observed a reduction in *GzB* promoter-driven luciferase activity in Karpas 299 cells co-transfected with the *GzB* promoter-driven luciferase reporter construct and ALK siRNA (Figure 3.10C). These latter findings suggest that NPM-ALK signalling promotes the transcription of *GzB* in ALK+ ALCL.

We next investigated whether NPM-ALK influences Perforin expression. In Karpas 299 cells, Perforin protein (Figure 3.11A) and mRNA (Figure 3.11B) levels were decreased in ALK siRNA-treated cells. In contrast, NPM-ALK knock-down in SUP-M2 cells led to a significant increase in Perforin protein and mRNA levels (Figure 3.11A and B, respectively). In light of these results, we examined how NPM-ALK knock-down affected Perforin levels in the SU-DHL-1 ALK+ ALCL cell line. Similar to SUP-M2 cells, we found that SU-DHL-1 cells treated with ALK siRNA had increased Perforin protein and mRNA levels (Figure 3.12A and B, respectively). Similar to both Karpas 299 and SUP-M2 cells, we found that NPM-ALK promoted GzB and JunB expression in SU-DHL-1 cells (Figure 3.12A and B). These results demonstrate that NPM-ALK is an important activator of *GzB* transcription in ALK+ ALCL, and that this oncogene can either promote or repress the expression of Perforin in a cell-line specific manner.

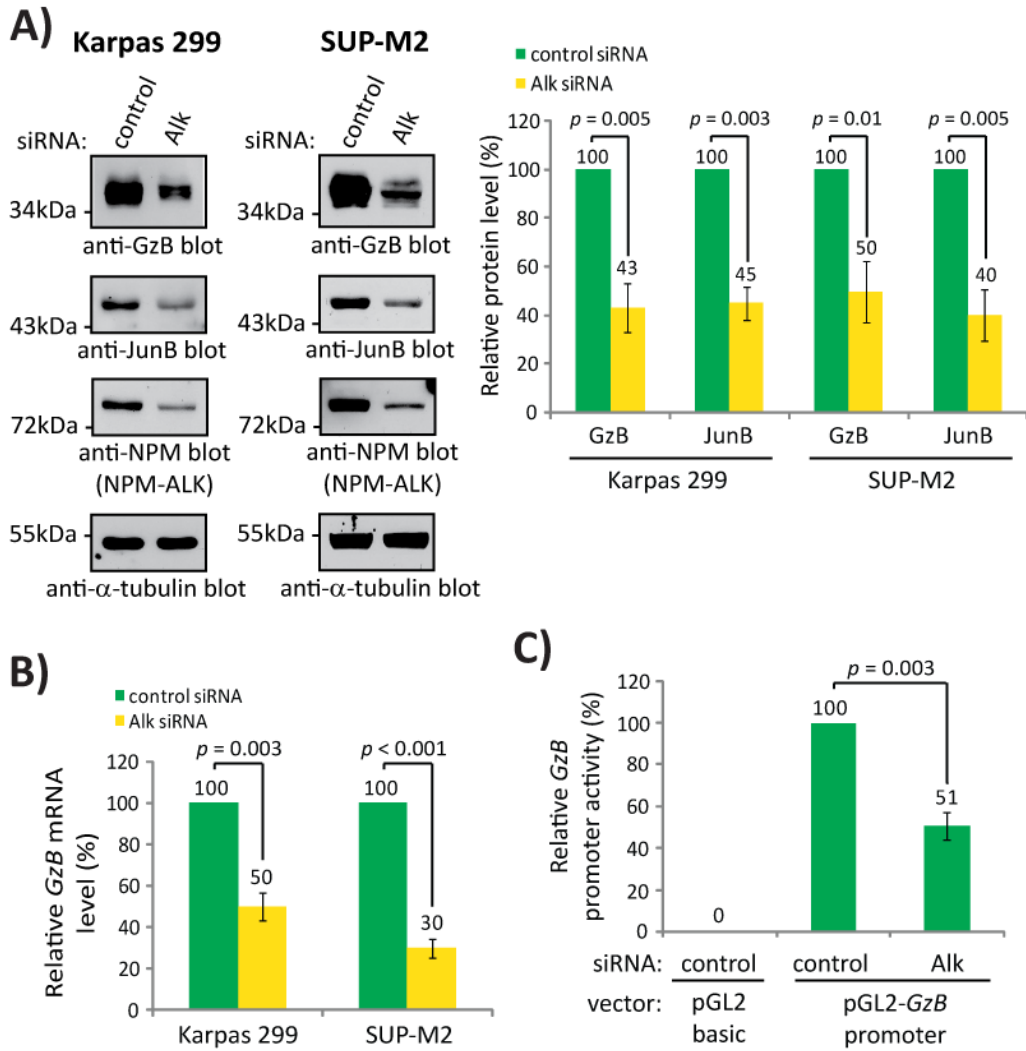


**Figure 3.10: NPM-ALK promotes GzB expression in ALK+ ALCL.**

**(A)** Western blots (left) and quantification (right) of GzB and JunB expression in lysates from Karpas 299 or SUP-M2 cells transfected with the indicated pooled siRNAs. The anti-NPM blots demonstrate NPM-ALK silencing. Molecular mass markers are indicated to the left of the blots. **(B)** qRT-PCR analysis of *GzB* mRNA expression in Karpas 299 and SUP-M2 cells transfected with the indicated siRNAs. *GzB* mRNA levels were normalized to  $\beta$ -actin. Note: these experiments were performed on the mRNA extracted from cells transfected in **(A)**. **(C)** *GzB* promoter-driven luciferase activity was measured in Karpas 299 cells transfected with non-targeting (control) or ALK siRNA. Luciferase activity is expressed relative to the activity present in cells transfected with the pGL2-*GzB* promoter and control siRNA. In all experiments, the quantification represents the mean and standard deviation of three independent experiments. *p* values were obtained using paired, one-tailed *t*-tests.

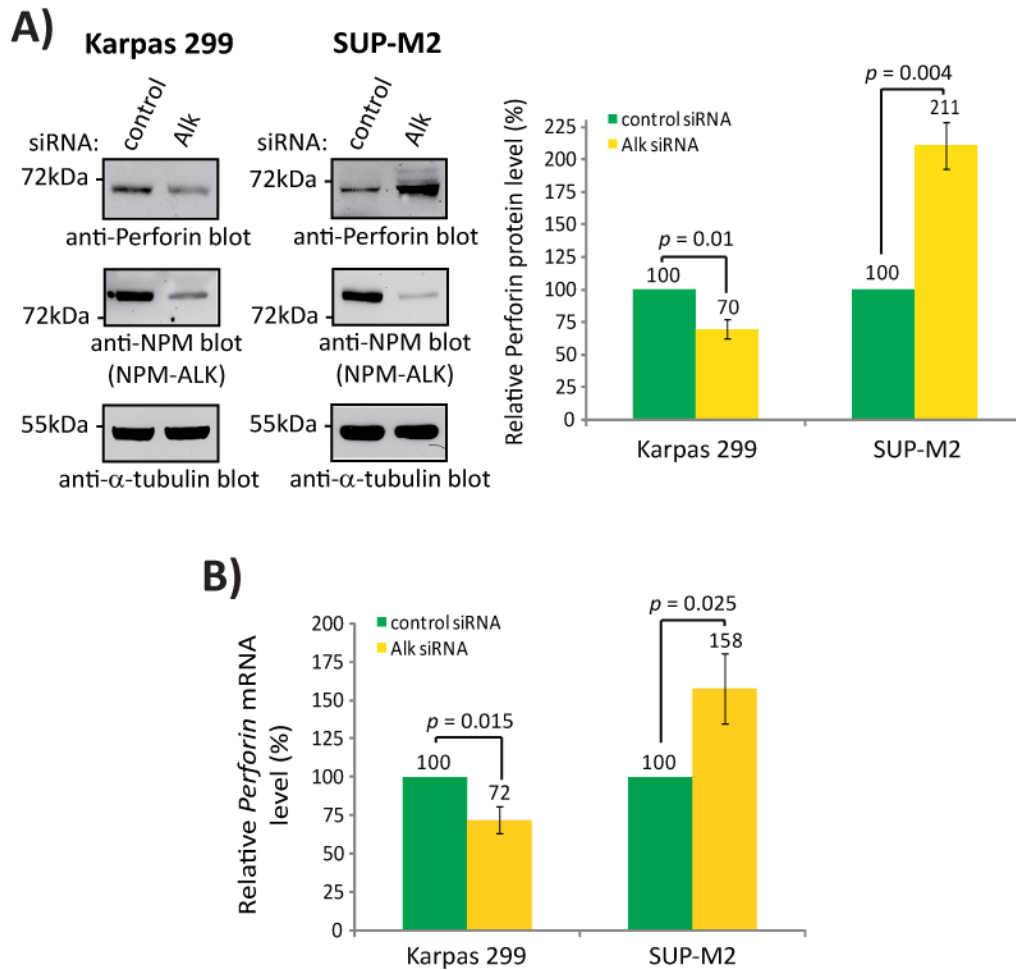


**Figure 3.11: NPM-ALK regulates Perforin expression in Karpas 299 and SUP-M2 cells.**

**(A)** Western blots (left) and quantification (right) of Perforin expression in lysates from Karpas 299 or SUP-M2 cells transfected with non-targeting (control) or ALK siRNA. The anti-NPM blots demonstrate NPM-ALK silencing. Molecular mass markers are indicated to the left of the western blots. **(B)** qRT-PCR analysis of *Perforin* mRNA expression in Karpas 299 and SUP-M2 cells transfected with non-targeting (control) or ALK siRNA. *Perforin* mRNA was normalized to the housekeeping gene  $\beta$ -actin. Note: these experiments were performed on the mRNA extracted from cells transfected in **(A)**. In all experiments, the quantification represents the mean and standard deviation of three independent experiments.  $p$  values were obtained using paired, one-tailed  $t$ -tests.

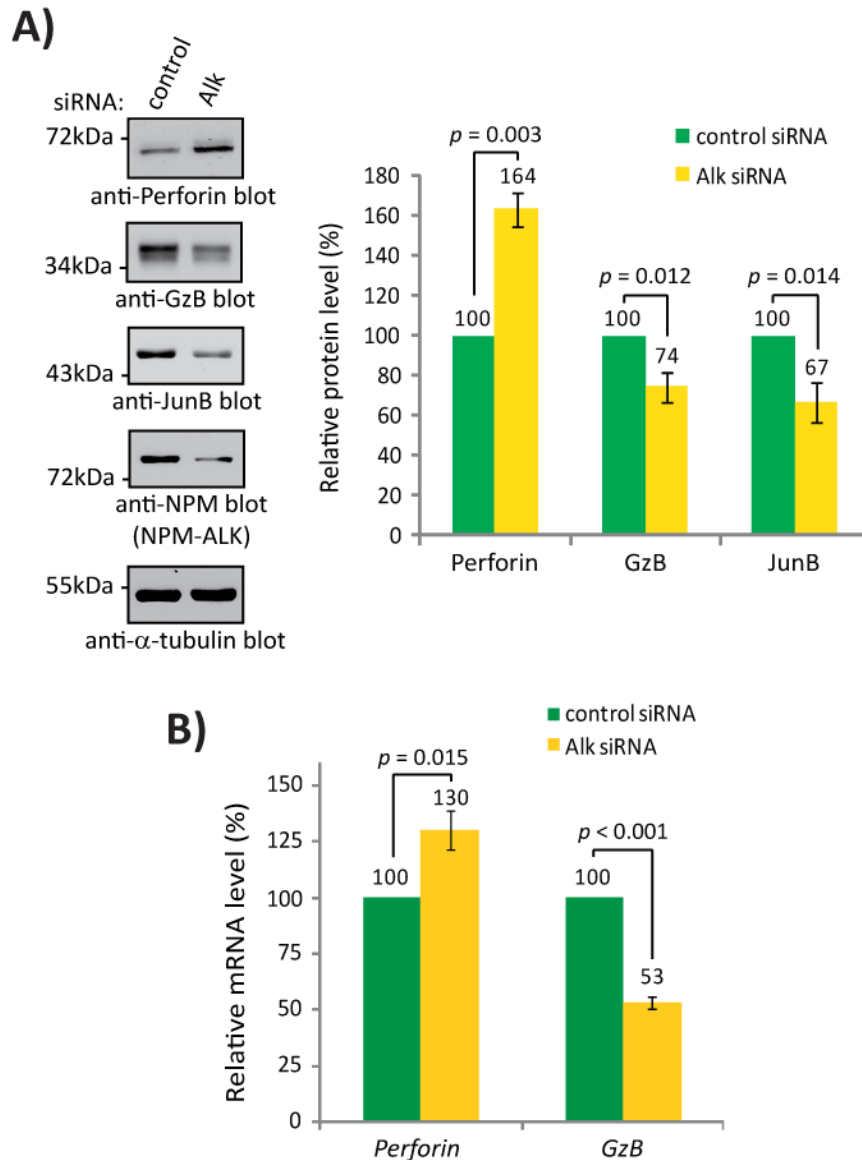


**Figure 3.12: NPM-ALK promotes GzB expression but represses Perforin in SU-DHL-1 cells.**

**(A)** Western blots (left) and quantification (right) of the indicated proteins in lysates from SU-DHL-1 cells transfected with non-targeting (control) or ALK siRNA. Note that the anti-NPM blot demonstrates NPM-ALK silencing. **(B)** qRT-PCR analysis of *Perforin* and *GzB* mRNA expression in SU-DHL-1 cells transfected with non-targeting (control) or ALK siRNA. mRNA levels were normalized to the housekeeping gene  $\beta$ -actin. These experiments were performed on the mRNA extracted from cells transfected in **(A)**. Molecular mass markers are indicated to the left of the western blots. In all experiments, the quantification represents the mean and standard deviation of three independent experiments.  $p$  values were obtained using paired, one-tailed  $t$ -tests.

### **3.8: PERFORIN EXPRESSION IS SUPPRESSED BY DNA METHYLATION IN SUP-M2 AND SU-DHL-1 CELLS**

A variety of genes are known to be silenced by DNA methylation in ALK+ ALCL (25, 298-301), and NPM-ALK can silence gene expression in ALK+ ALCL cell lines by promoting DNA methylation (25, 298). NPM-ALK signalling up-regulates the expression of DNA methyltransferases (DNMTs) (25), which in turn repress several T cell-associated genes (e.g. *CD3ε*, *SLP-76*, *ZAP-70*, *LAT*) in ALK+ ALCL (25). Furthermore, the downstream target of NPM-ALK signalling, STAT3, has been suggested to recruit DNMTs to the promoter of the *IL-2 receptor γ-chain* (298) and the promoter of the phosphatase, *SHP-1* (299), thereby silencing the expression of these genes in ALK+ ALCL. Therefore, we investigated whether the increased Perforin expression observed in SUP-M2 and SU-DHL-1 cells treated with ALK siRNA could be due to relieving methylation of the *Perforin* promoter. To determine whether Perforin expression is repressed by DNA methylation in ALK+ ALCL cells, we treated ALK+ ALCL cell lines with the DNMT inhibitor, 5-Aza-2'-deoxycytidine (DAC), and examined how this affected Perforin protein expression. In SUP-M2 cells, where Perforin expression was highly up-regulated when NPM-ALK expression was reduced (Figure 3.11), we found that DAC treatment significantly increased Perforin expression (Figure 3.13). Likewise, a more modest, and transient, increase in Perforin expression was observed in SU-DHL-1 cells treated with DAC (Figure 3.13). Thus, the increase in Perforin expression observed in SUP-M2 and SU-DHL-1 cells treated with ALK siRNA may partly be due to relieving the epigenetic silencing of *Perforin* transcription. Consistent with our observation that NPM-ALK does not repress Perforin expression in Karpas 299 cells (Figure 3.11), we observed no increase in Perforin expression when these cells were treated with DAC (Figure 3.13).

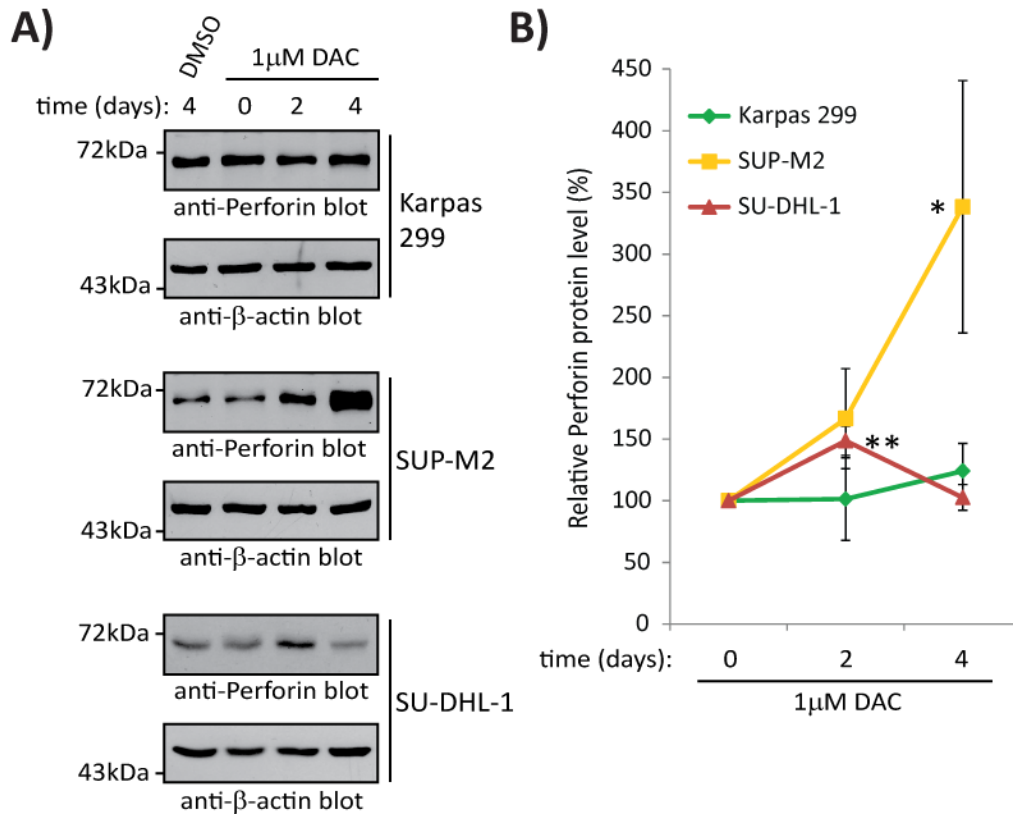


**Figure 3.13: Inhibition of DNMTs results in elevated Perforin levels in SUP-M2 and SU-DHL-1 cells.**

**(A)** Western blot analysis of Perforin levels in cell lysates from Karpas 299, SUP-M2 or SU-DHL-1 cells treated for the indicated times with 0.1% DMSO or 1 μM DAC. Anti-β-actin western blots demonstrate protein loading and molecular mass markers are indicated to the left of the western blots. **(B)** Quantification of Perforin levels from western blots in (A). Perforin expression was normalized to β-actin expression for each time point and expressed relative to the starting time point (day 0), which was set at 100%. Results represent the mean and standard deviation of three independent experiments. *p* values comparing perforin levels in DAC-treated cells at the indicated time point to perforin levels in cells at day 0 were obtained using paired, one-tailed *t*-tests; \* *p* < 0.05, \*\* *p* < 0.01.

### 3.9: DISCUSSION

The expression of GzB and Perforin is a common feature of ALK+ ALCL and one piece of evidence that has led to the suggestion by some that these tumour cells may be derived from a CTL. However, our results reveal that the expression of these proteins is not just a remnant of the potential CTL origin of this lymphoma. We demonstrate that the NPM-ALK oncoprotein and JunB transcription factor promote the transcription of *GzB* in ALK+ ALCL cell lines. When JunB expression was transiently knocked-down using siRNAs we observed an approximately 30% reduction in GzB protein levels (Figure 3.2), which we believe is likely an underestimation of the contribution that JunB makes to GzB expression because the siRNAs are able to only partially reduce JunB expression. Consistent with this, when we were able to reduce JunB expression more efficiently using the inducible JunB shRNA we observed a greater reduction in GzB protein levels than with the siRNA treatment (compare Figures 3.2 to 3.3). We believe our findings demonstrating that NPM-ALK and JunB promote GzB expression helps explain why the majority of ALK+ ALCL tumours are positive for GzB expression (19, 28, 56). Furthermore, these findings may also contribute to why a gene expression profiling study found that *GzB* was one of the most highly expressed genes in ALK+ ALCL tumour samples compared to normal activated T cells (79). In addition to GzB, we also found that while Perforin expression was not regulated by JunB, its expression can either be promoted or repressed by NPM-ALK in a cell line-specific manner. Taken together, these novel findings demonstrate that oncogenic signalling influences the expression of cytotoxic molecules in ALK+ ALCL.

Since NPM-ALK promotes JunB expression ((51, 191, 267) and Figures 3.10A and 3.12A), we postulate that NPM-ALK likely promotes *GzB* transcription in large part through JunB. However, NPM-ALK knock-down had a more dramatic effect on GzB expression than JunB knock-down (compare Figures 3.2, 3.4 and 3.5 with Figure 3.10), so it is likely that NPM-ALK activates other signalling pathways that

promote *GzB* transcription. One possibility is the Jak/STAT pathway. NPM-ALK activates Jak/STAT signalling (24, 190) and since this pathway promotes *GzB* expression in other cell types (302-305), it may also contribute to *GzB* expression in ALK+ ALCL. Since JunB can function as both a homo- and hetero-dimer, we investigated if JunB may be functioning with other AP-1 family transcription factors to regulate *GzB* expression. Our EMSA experiments suggest that c-Fos may be one such family member, as it was also found to bind the AP-1 site in the *GzB* proximal promoter (Figure 3.7). In further support of this, we found that JunB and c-Fos can associate in ALK+ ALCL cell lines using co-immunoprecipitation experiments (Figure 3.8A and B). Unfortunately, we have been unable to silence c-Fos expression using siRNA (Figure 3.8C), so we have been unable to determine whether c-Fos does promote *GzB* expression in ALK+ ALCL cell lines.

NPM-ALK was found to promote Perforin expression in Karpas 299 cells, but interestingly repressed Perforin expression in SUP-M2 and SU-DHL-1 cells (Figure 3.11 and 3.12). Treatment of SUP-M2 and SU-DHL-1 cells with a DNMT inhibitor resulted in increased Perforin protein levels, whereas treatment of Karpas 299 cells had no effect on Perforin expression (Figure 3.13). Because of this, we believe that the repression of Perforin by NPM-ALK in SUP-M2 and SU-DHL-1 cells may be due to the ability of NPM-ALK signalling to silence gene expression by promoting DNA methylation (25, 298). In SU-DHL-1 cells we observed a transient increase in Perforin expression following DAC treatment, whereas in SUP-M2 cells Perforin levels continued to increase throughout the duration of the treatment (Figure 3.13). The reason for the transient increase in Perforin levels in SU-DHL-1 cells is currently unknown, but it could be that treatment of SU-DHL-1 cells with DAC for longer periods of time affected the expression of another protein that is important for promoting or stabilizing Perforin expression in SU-DHL-1 cells. Why NPM-ALK differentially regulates *Perforin* gene expression in ALK+ ALCL cell lines is unclear. However, these results are consistent with the

observation that other genes known to be silenced by NPM-ALK through DNA methylation are not uniformly silenced in ALK+ ALCL patient samples and cell lines (25).

The fact that GzB expression is actively promoted by oncogenic signalling in ALK+ ALCL raises the question as to whether GzB could be important in the pathogenesis of this lymphoma. While GzB is best characterized as an effector molecule used by CTL or NK cells to kill virally infected or cancerous cells, several other functions of GzB have been demonstrated. Both CTL and NK cells constitutively release GzB (306), and GzB has been shown to cleave various ECM proteins resulting in different outcomes (307-309). Furthermore, GzB has been demonstrated to cleave the extracellular domains of membrane proteins (310). These studies demonstrate that the GzB expressed by ALK+ ALCL cells could have a variety of functions that would be beneficial to tumour cells. We are very interested in whether GzB may play a beneficial role in the pathogenesis of ALK+ ALCL and the following chapter will discuss our characterization of Granzyme proteins in ALK+ ALCL and examination of potential functions of GzB in this lymphoma.

## **CHAPTER 4: GRANZYME B SENSITIZES ALK+ ALCL CELL LINES TO DRUG-INDUCED APOPTOSIS**

A manuscript using a portion of this data is currently under preparation.

The majority of experiments presented in this chapter were performed by J. Pearson. Experiments presented in Figure 4.3 and 4.5B were performed by Katelynn Rowe, an undergraduate summer student mentored by J. Pearson. Figures 4.6B and C, 4.8, 4.9 and 4.10C were provided by Kayla Thew, an undergraduate honours student mentored by J. Pearson. Some repeats of Figures 4.8 and 4.9 and 4.14 were performed by Cathy Zhang, and some repeats of Figure 4.14 were performed by Brandon Maser. J. Pearson wrote this chapter with major editorial input from Dr. R. Ingham.

#### **4.1: INTRODUCTION**

Several publications have demonstrated that the majority of ALK+ ALCL patients possess tumour cells that express the cytotoxic proteins perforin and/or GzB (19, 28, 54, 55), and we have demonstrated that NPM-ALK signalling regulates the expression of these proteins (see Chapter 3). Since GzB expression is promoted by oncogenic signalling in ALK+ ALCL, we hypothesized that it plays an important role in the pathogenesis of this cancer.

The GzB expressed by CTL and NK cells is typically contained within granules along with Perforin, and these proteins are used by CTL and NK cells to induce apoptosis of virally infected or transformed target cells (57, 58, 60) (see Figure 1.2). To do this, GzB functions as a serine protease to cleave a variety of pro- and anti-apoptotic proteins. While there are some differences in the substrates recognized by human and mouse GzB, GzB can cleave and activate the pro-apoptotic protein Bid (311-315), and can cleave the anti-apoptotic protein Mcl-1, resulting in release of the pro-apoptotic protein Bim (316). GzB can also directly cleave and activate pro-caspase 3 (311, 317-319), as well as various other caspases (311, 317, 320, 321). Furthermore, GzB shares some substrates with caspases, and has been shown to cleave important proteins involved in the apoptotic process, such as the nuclear membrane protein lamin B (322), the inhibitor of caspase-activated deoxyribonuclease (ICAD) (311, 323), and poly(ADP ribose) polymerase (PARP) (324).

In addition to its well characterized role as a pro-apoptotic protein, GzB has been demonstrated or proposed to have a variety of other functions. Activated CTL and NK cells can release GzB (306), suggesting a potential extracellular role for GzB. Consistent with this notion, purified GzB has been demonstrated to cleave different extracellular proteins. GzB secreted by activated T cells cleaves the extracellular domain of the GluR3 glutamate receptor from the surface of these cells in an autocrine and/or paracrine fashion (310). This is functionally

important as it renders T cells unable to adhere to laminin in response to glutamate treatment (310). The cleavage of ECM proteins by GzB has also been demonstrated to have several functions. The cleavage of matrix proteins such as aggrecan (309), fibronectin, vitronectin and laminin (307) inhibits cells from adhering to or migrating on matrices composed of these proteins. Cleavage of some ECM proteins by GzB can also result in detachment-induced death (anoikis) of adherent cell lines (307). Recently, GzB has been demonstrated to cleave the ECM proteins decorin, biglycan and betaglycan, and in doing so is able to release TGF- $\beta$  bound by these ECM proteins (308). Importantly, this released TGF- $\beta$  possessed biological activity, as it was able to activate TGF- $\beta$  signalling in human coronary artery smooth muscle cells as measured by phosphorylation of SMAD-3 (308), a downstream target of the TGF- $\beta$  receptor.

GzB has also been demonstrated to have a biological role in tumour cell invasiveness. In a panel of 56 tissue samples obtained from patients with urothelial carcinoma, 42 (75%) patients were found to have tumour cells expressing GzB (325). Furthermore, about half of the bladder cancer cell lines tested were found to express GzB. Interestingly, no perforin expression was detected in primary urothelial carcinoma or bladder cancer cell lines (325). In this study it was observed that GzB expression is associated with a greater level of tumour spreading as well as invasive potential in patients with urothelial carcinoma (325). It was also demonstrated that the GzB expressed by bladder cancer cell lines possessed enzymatic activity and could cleave the ECM protein, vitronectin (325). Finally, GzB was found to promote the invasion of bladder cancer cell lines *in vitro*, as knock-down of GzB in these cells significantly inhibited their invasion through matrigel (325). Whether ALK+ ALCL cell lines use GzB to similarly promote invasion through matrix is an interesting possibility and could be one factor that contributes to why this lymphoma is widely disseminated in patients at clinical presentation (11, 18, 23). A recent report demonstrating that ALK+ ALCL cell lines use matrix metalloproteinase-9 to

efficiently migrate through matrigel (326), supports the notion that these tumour cells use proteases to invade through ECM.

In humans, GzB belongs to a family of five different Granzyme proteins, which also includes GzA, K, H and M (57). We found that while GzB was commonly expressed by all ALK+ ALCL cell lines tested, we did not detect expression of *GzK*, *H* or *M* message in these cells, and could detect only low levels of *GzA*. Because GzB is commonly expressed in ALK+ ALCL, and its expression is promoted by NPM-ALK signalling, we examined whether GzB promotes the pathogenesis of ALK+ ALCL by influencing invasion of ALK+ ALCL cell lines. While we found that ALK+ ALCL cell lines release enzymatically active GzB, there was no effect on invasion of SUP-M2 ALK+ ALCL cells following knock-down of GzB under the conditions tested. Interestingly, we show evidence that there may be active GzB in the cytoplasm of ALK+ ALCL cell lines and that GzB appears to sensitize ALK+ ALCL cell lines to apoptosis following treatment with apoptosis-inducing agents. These findings suggest that the expression of GzB by ALK+ ALCL cells may be one factor contributing to why patients with ALK+ ALCL are successfully treated with standard chemotherapy (11-14, 29, 85), and why tumour cells have been observed to have high levels of apoptosis compared to several other lymphomas (81, 327-329).

#### **4.2: WHILE GRANZYME B IS CONSISTENTLY EXPRESSED IN ALK+ ALCL CELL LINES, GRANZYME A IS EXPRESSED ONLY AT LOW LEVELS AND EXPRESSION OF OTHER GRANZYMES IS NOT DETECTABLE IN THESE CELLS**

Since the expression of GzB is a well-established characteristic of ALK+ ALCL but the expression of other Granzymes had yet to be investigated, we examined which Granzymes are expressed by ALK+ ALCL cell lines. We first examined expression of the five human Granzymes (*GzA*, *GzB*, *GzH*, *GzK* and *GzM*) at the mRNA level in five ALK+ ALCL cell lines (Karpas 299, SUP-M2, SU-DHL-1, SR and

UCONN). As positive controls, we used the human NK cell lines, NKL and NK92, both of which have been shown to express the human Granzymes at the mRNA level (330, 331). Reverse transcriptase-PCR analysis of RNA collect from each of the cell lines demonstrated that all five of the ALK+ ALCL cell lines express *GzB* mRNA and that four of the ALK+ ALCL cell lines (Karpas 299, SU-DHL-1, SR and UCONN) express detectable levels of *GzA* mRNA (Figure 4.1A). In contrast to *GzA* and *GzB*, we did not detect *GzH*, *GzK* or *GzM* mRNA in any of the ALK+ ALCL cell lines (Figure 4.1A), suggesting that they are not expressed in these ALK+ ALCL cells or that they are expressed below our limit of detection. Because *GzA* and *GzB* mRNA was expressed by most of the cell lines tested, we examined whether these cells also expressed *GzA* and *GzB* protein using western blotting. In these experiments we used lysate from NKL cells as a positive control and lysate from the Granzyme-negative Hodgkin lymphoma cell line, KM-H2, as a negative control. While we could clearly see the presence of *GzA* in NKL cells, we did not observe *GzA* protein in any of the ALK+ ALCL cell lines (Figure 4.1B). As expected, *GzB* protein was expressed in all ALK+ ALCL cell lines tested, as well as the NKL cells (Figure 4.1B).

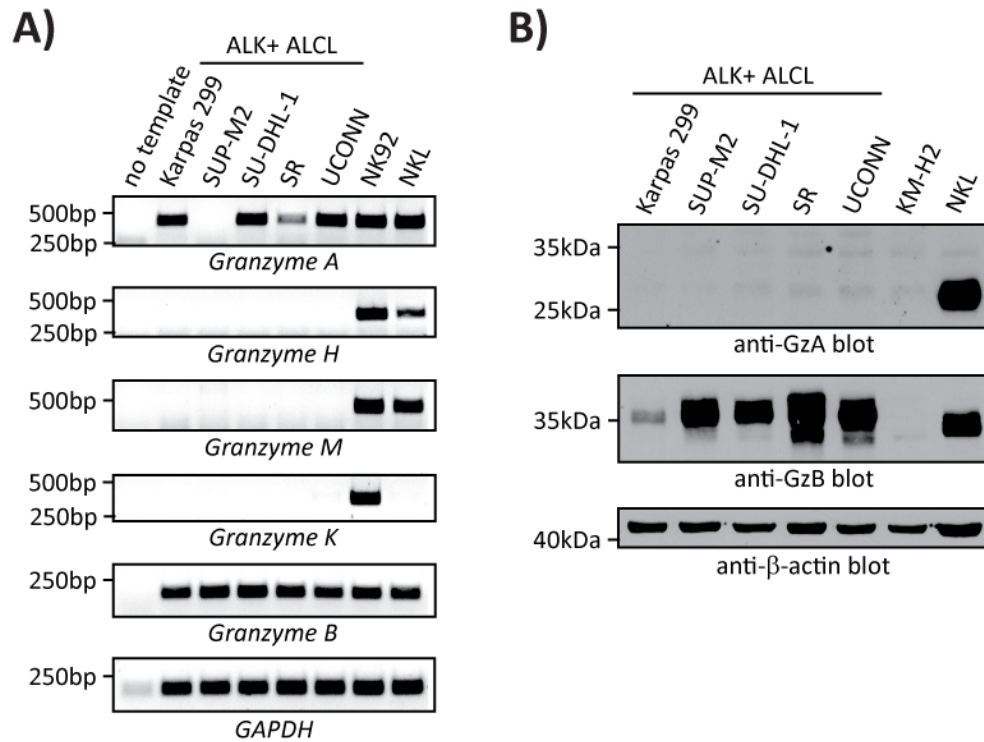


**Figure 4.1: Examining expression of the Granzymes in ALK+ ALCL cell lines.**

**(A)** Reverse transcriptase-PCR analysis of *GzA*, *GzH*, *GzK*, *GzM* and *GzB* mRNA expression in the Karpas 299, SUP-M2, SU-DHL-1, SR and UCONN ALK+ ALCL cell lines. NK92 and NKL cells lines were used as positive controls. "No template" represents a negative control where no cDNA template was included in the PCR reaction. **(B)** Western blot analysis of GzA and GzB protein expression in ALK+ ALCL cell lines. NKL cells were used as a positive control for GzA expression and the Hodgkin lymphoma cell line, KM-H2, was used as a negative control. Equal amounts of protein were loaded for each sample as assessed by BCA assay, and the anti- $\beta$ -actin blot demonstrates protein loading. Molecular mass markers are shown to the left of the blots.

The lack of observed GzA protein in ALK+ ALCL cell lines, despite most cells expressing GzA mRNA, could be because the GzA protein is expressed below our detection limit in these cells. To determine if the lack of GzA protein expression in the ALK+ ALCL cell lines may be because GzA transcript is expressed at low levels, we quantified GzA mRNA levels in the ALK+ ALCL cell lines compared to NKL cells using qRT-PCR (Figure 4.2A). Because the cell lines may express different levels of housekeeping genes, we normalized our data to both *GAPDH* and  $\beta$ -*tubulin*. Although there were some differences in the results when the two different housekeeping genes were used, both did show a similar trend. All ALK+ ALCL cell lines were found to express substantially lower levels of GzA mRNA compared to NKL cells. The SU-DHL-1 and UCONN cells expressed 80-90% less GzA mRNA than the NKL cells. GzA mRNA expression was even lower in the other ALK+ ALCL cell lines, with Karpas 299 cells expressing about 2% of the GzA mRNA that NKL cells express, and the SR cells expressing less than 1%. Similar to the reverse transcriptase-PCR, GzA message was not detected in SUP-M2 cells. These results suggest that our inability to detect GzA protein in the ALK+ ALCL cell lines by western blotting could be because they express substantially lower GzA message compared to the NKL cells. Interestingly, when we examined GzB mRNA levels in the ALK+ ALCL cells compared to NKL cells, the ALK+ ALCL cell lines expressed substantially higher levels than the NKL cells (Figure 4.2B). Karpas 299 cells expressed 3-4 times more GzB mRNA compared to NKL cells (Figure 4.2B), despite the fact that the Karpas 299 cells express lower GzB protein levels (Figure 4.1B). The other four ALK+ ALCL cell lines expressed 10-30 times more GzB mRNA than the NKL cells (Figure 4.2B), although their GzB protein levels were comparable with some ALK+ ALCL cell lines expressing only slightly more GzB protein than the NKL cells (Figure 4.1B).

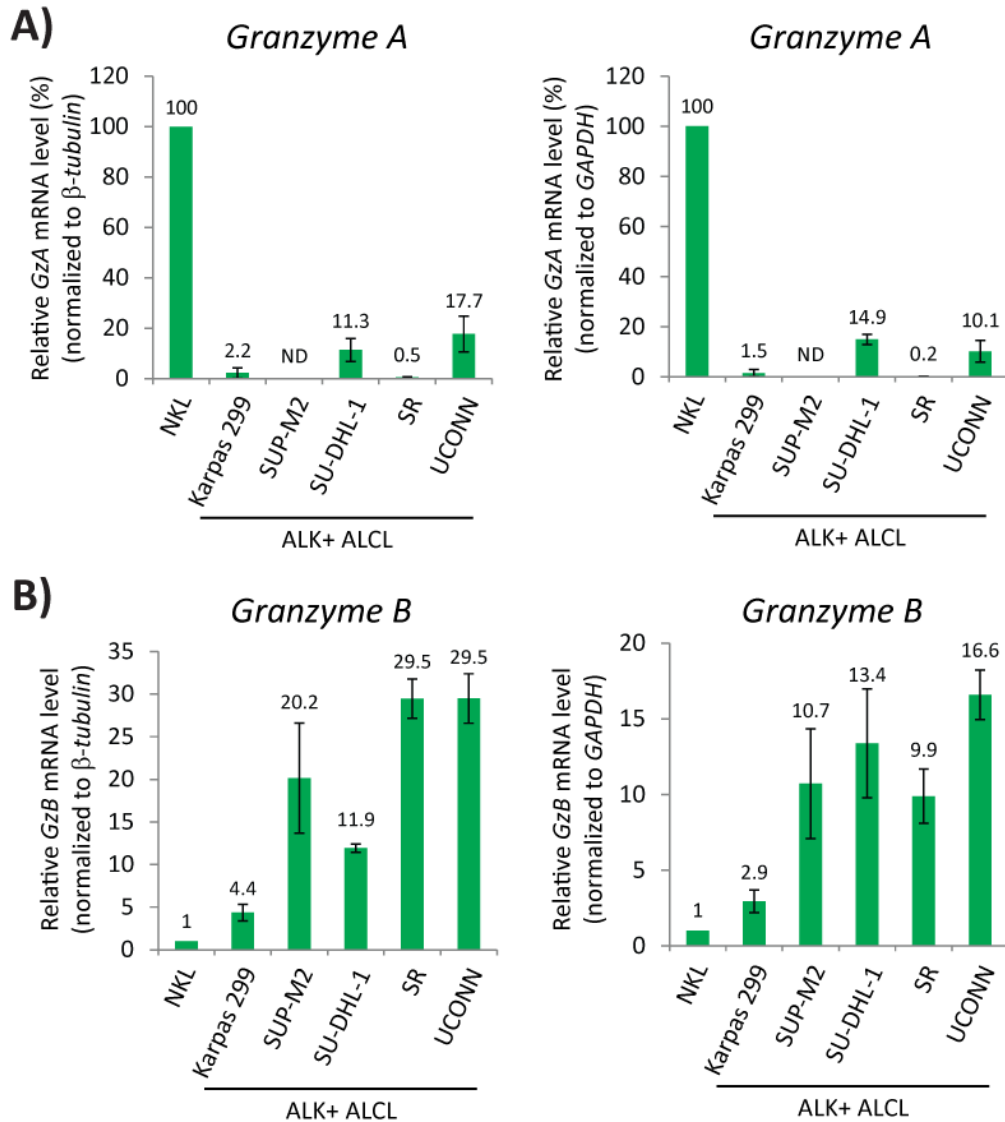


**Figure 4.2: ALK+ ALCL cell lines express greatly reduced GzA mRNA levels compared to NKL cells, while GzB is expressed more highly in ALK+ ALCL cells.**

qRT-PCR analysis of GzA (**A**) and GzB (**B**) mRNA expression in ALK+ ALCL cell lines compared to NKL cells. Expression was normalized to  $\beta$ -tubulin (left) and GAPDH (right) housekeeping genes. Results represent the mean and standard deviation of three (GzA) or two (GzB) independent experiments. mRNA levels are expressed relative to the mRNA present in NKL cells for the given target gene (which was set to 100% for GzA or to a value of 1 for GzB). ND - none detected.

#### **4.3: ALK+ ALCL CELL LINES EXPRESS ENZYMATICALLY ACTIVE GRANZYME B**

In cells, GzB is produced as an inactive pro-enzyme that is activated by proteolytic cleavage of the N-terminus activation dipeptide (Glycine-Glutamic acid) (332-334). This is primarily accomplished by an enzyme known as Cathepsin C (dipeptidyl peptidase I) (333-336), although it has also been shown that Cathepsin H can make a minor contribution to GzB activation (337). To determine whether GzB is involved in the pathogenesis of ALK+ ALCL, we first wanted to determine whether the GzB expressed by ALK+ ALCL cell lines possesses enzymatic activity. We collected cell lysates from the Karpas 299, SUP-M2, SR and UCONN ALK+ ALCL cell lines, or the GzB-negative Hodgkin lymphoma cell line, KM-H2. These lysates were then incubated with the colourimetric GzB substrate Ac-IEPD-pNA, and the relative level of GzB activity quantified by monitoring release of the *p*-nitroanilide group (by measuring absorbance at 405 nm). In these experiments we observed significant cleavage of Ac-IEPD-pNA using lysates from all four ALK+ ALCL cell lines, but not with lysate from the KM-H2 cells (Figure 4.3). Interestingly, the level of GzB activity did not correlate with the level of GzB expression in the lysate of the ALK+ ALCL cell lines (Figure 4.3).

To confirm that the observed activity was due to GzB, we generated Karpas 299 cell lines stably expressing three different GzB shRNA constructs (#1-3) or SUP-M2 cells with two different GzB shRNA constructs (#1 and #3). When compared to cells expressing a control (non-targeting) shRNA construct, all cells expressing a GzB shRNA had reduced GzB protein levels, with GzB shRNA#1 and #3 giving better knock-down than GzB shRNA#2 in Karpas 299 cells (Figure 4.4A). We next quantified the extent of GzB knock-down in these stable cell lines using flow cytometry (Figure 4.4B). In Karpas 299 cells, GzB levels were reduced by >70% using GzB shRNA sequences #1 and #3, while GzB shRNA #2 gave an approximately 50% reduction in GzB protein levels. In SUP-M2 cells, we observed an approximately 65% reduction in GzB protein levels with GzB shRNA #1 and #3.

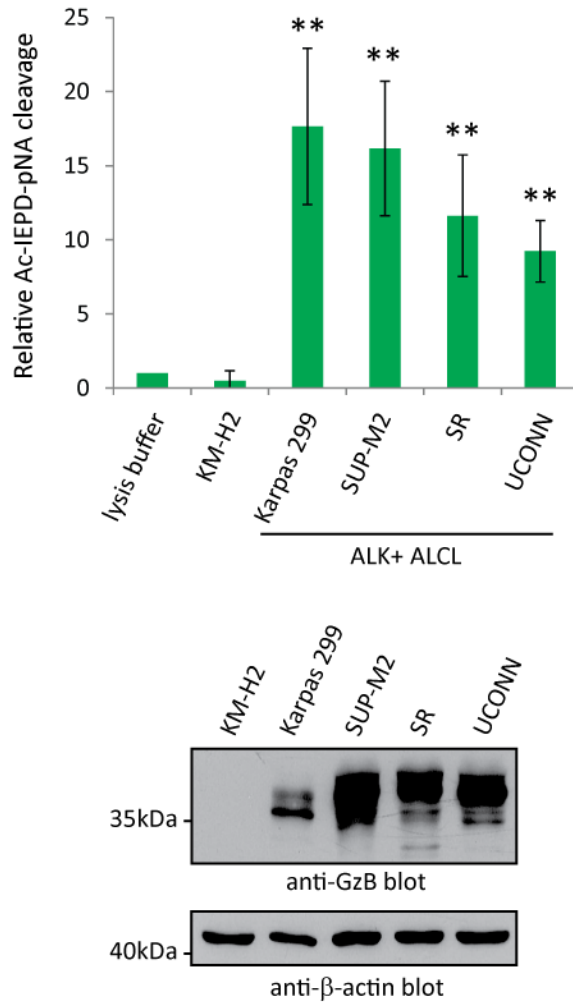


**Figure 4.3: ALK+ ALCL express enzymatically active GzB.**

GzB activity present in the lysate of ALK+ ALCL cell lines or the GzB-negative Hodgkin lymphoma cell line, KM-H2, was assessed by incubating lysates with the GzB substrate Ac-IEPD-pNA and measuring absorbance at 405 nm after 1hr (top). Results are presented relative to background absorbance of lysis buffer incubated with Ac-IEPD-pNA, which was set to a value of 1. Error bars represent the standard deviation of four independent experiments.  $p$  values comparing Ac-IEPD-pNA cleavage in lysis buffer alone to cleavage by the different lysates were determined using paired, one-tailed  $t$ -tests; \*\*  $p < 0.01$ . A western blot demonstrating GzB expression in the respective cell lysates is shown below. The anti-β-actin western blot demonstrates protein loading. Molecular mass markers are indicated to the left of the blots.

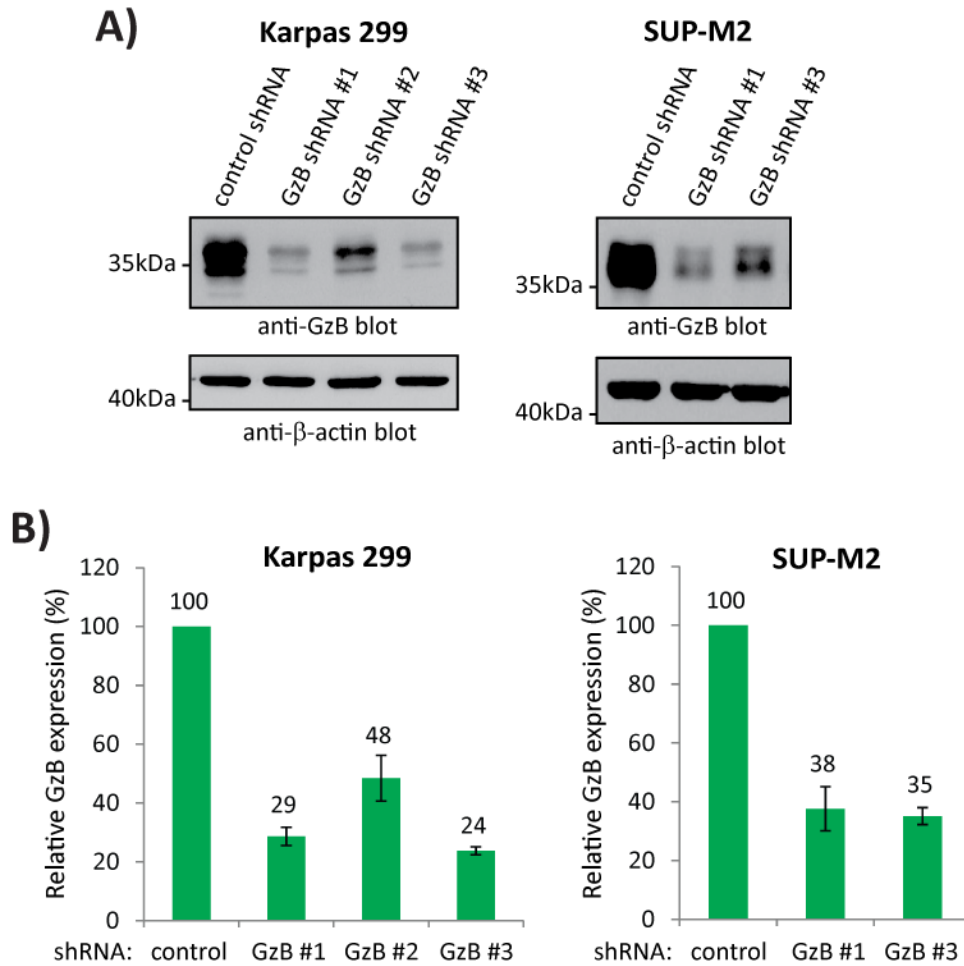


**Figure 4.4: Examining GzB knock-down in Karpas 299 and SUP-M2 cells stably expressing GzB shRNA constructs.**

**(A)** Western blot demonstrating knock-down of GzB in Karpas 299 cells stably expressing control shRNA or three different GzB shRNA sequences (labelled #1-3) (left). Western blot demonstrating GzB knock-down in SUP-M2 cells expressing control shRNA or GzB shRNA constructs #1 and #3 (right). Anti- $\beta$ -actin blots demonstrate equal protein loading. Molecular mass markers are shown to the left of the western blots. **(B)** GzB expression in the different stable cell lines was quantified using flow cytometry (mean fluorescence intensity) and is expressed relative to cells expressing control shRNA (which was set to 100%). Results represent the mean and standard deviation of three independent experiments.

We next asked whether knock-down of GzB affects Ac-IEPD-pNA cleavage in ALK+ ALCL cells. When lysates were collected from Karpas 299 and SUP-M2 cells with stable GzB knock-down and analyzed for Ac-IEPD-pNA cleavage, we observed a significant reduction in Ac-IEPD-pNA cleavage compared to cells expressing control shRNA (Figure 4.5A). In Karpas 299 cells, the degree of reduction in Ac-IEPD-pNA cleavage was similar to the degree of GzB knock-down, with GzB shRNA #1 and #3 giving a greater reduction than GzB shRNA #2. In SUP-M2 cells, the reduction in Ac-IEPD-pNA cleavage was similar for both GzB shRNA #1 and #3 compared to control shRNA. Using pooled siRNAs to transiently knock-down GzB expression in Karpas 299 and SR cells, we similarly observed a reduction in the extent of Ac-IEPD-pNA cleavage (Figure 4.5B). Taken together, these results suggest that the GzB expressed by ALK+ ALCL cell lines possesses enzymatic activity.

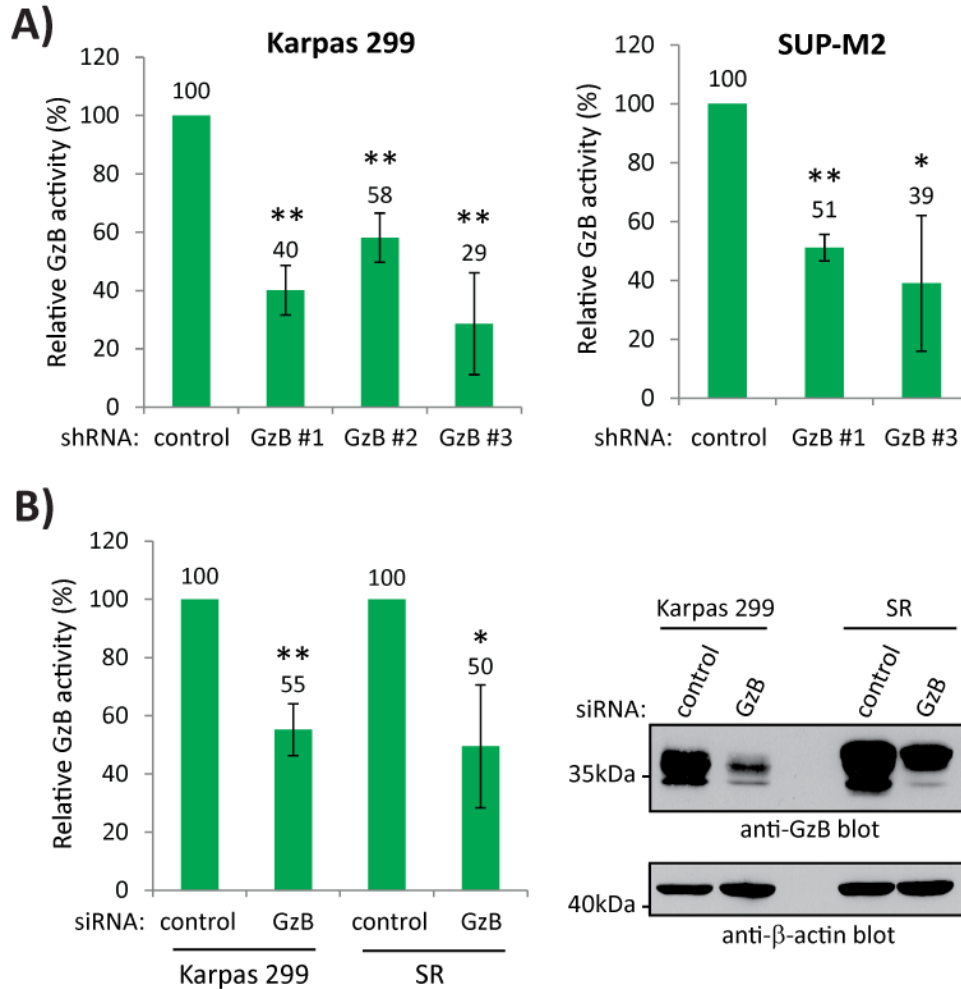


**Figure 4.5: Knock-down of GzB reduces cleavage of Ac-IEPD-pNA.**

**(A)** GzB activity was assessed by incubating lysates from Karpas 299 (left) or SUP-M2 (right) cells expressing control or GzB shRNA with Ac-IEPD-pNA for 30 min followed by absorbance measurement. GzB activity is presented relative to absorbance of samples with control shRNA (which was set to 100%). **(B)** GzB activity in Karpas 299 or SR cells transiently transfected with pooled control or GzB siRNAs was examined (left). Lysates from Karpas 299 or SR cells transfected with the indicated siRNAs were incubated with Ac-IEPD-pNA for 1 hr and absorbance was measured. Results are presented relative to the activity present in Karpas 299 or SR cells transfected with control siRNA (which was set to 100%). A western blot demonstrating GzB knock-down in the respective cell lysates is also included (right). Molecular mass markers are indicated to the left of the blots. For all experiments, quantification represents the mean and standard deviation of three independent experiments.  $p$  values comparing GzB shRNA or siRNA to control shRNA or siRNA were determined using paired, one-tailed  $t$ -tests; \*  $p < 0.05$ , \*\*  $p < 0.01$ .

#### **4.4: THE GRANZYME B EXPRESSED BY ALK+ ALCL CELLS PROMOTES CLEAVAGE OF ECM PROTEINS**

Since the GzB expressed by ALK+ ALCL cell lines possessed enzymatic activity, we next examined whether it could cleave biologically relevant substrates. GzB has been shown to cleave various ECM proteins, such as vitronectin, fibronectin, laminin (307), decorin, betaglycan and biglycan (308), and cleavage of these substrates by GzB has been implicated in various aspects of ECM remodelling (307, 308, 325). We first examined cleavage of vitronectin using lysates from Karpas 299 and SUP-M2 cells. Lysates were incubated with plate-bound vitronectin, then vitronectin cleavage assessed by western blotting. We observed the appearance of a lower molecular weight anti-vitronectin immunoreactive band over time in these experiments when vitronectin was incubated with Karpas 299 or SUP-M2 lysate, but not when lysis buffer alone or KM-H2 lysate was used (Figure 4.6A). This suggests that the vitronectin is being cleaved by a protein(s) present in Karpas 299 and SUP-M2 lysates. To test whether this may be due to GzB, we performed similar experiments in the presence of the GzB inhibitor, Z-AAD-CMK. Inclusion of Z-AAD-CMK in these reactions strongly inhibited the appearance of the lower molecular weight anti-vitronectin band(s) (Figure 4.6B and C), suggesting that the vitronectin was being cleaved in a GzB-dependent manner. We also observed a reduction in the appearance of the vitronectin cleavage products when lysates from Karpas 299 or SUP-M2 cells expressing GzB shRNA #1 or #3 were used in these assays (Figure 4.7). Taken together, these results are consistent with the hypothesis that the GzB expressed by ALK+ ALCL cells can cleave the ECM protein, vitronectin. However, from these experiments we cannot rule out that the vitronectin is being cleaved in a GzB-dependent manner, but not directly by GzB.

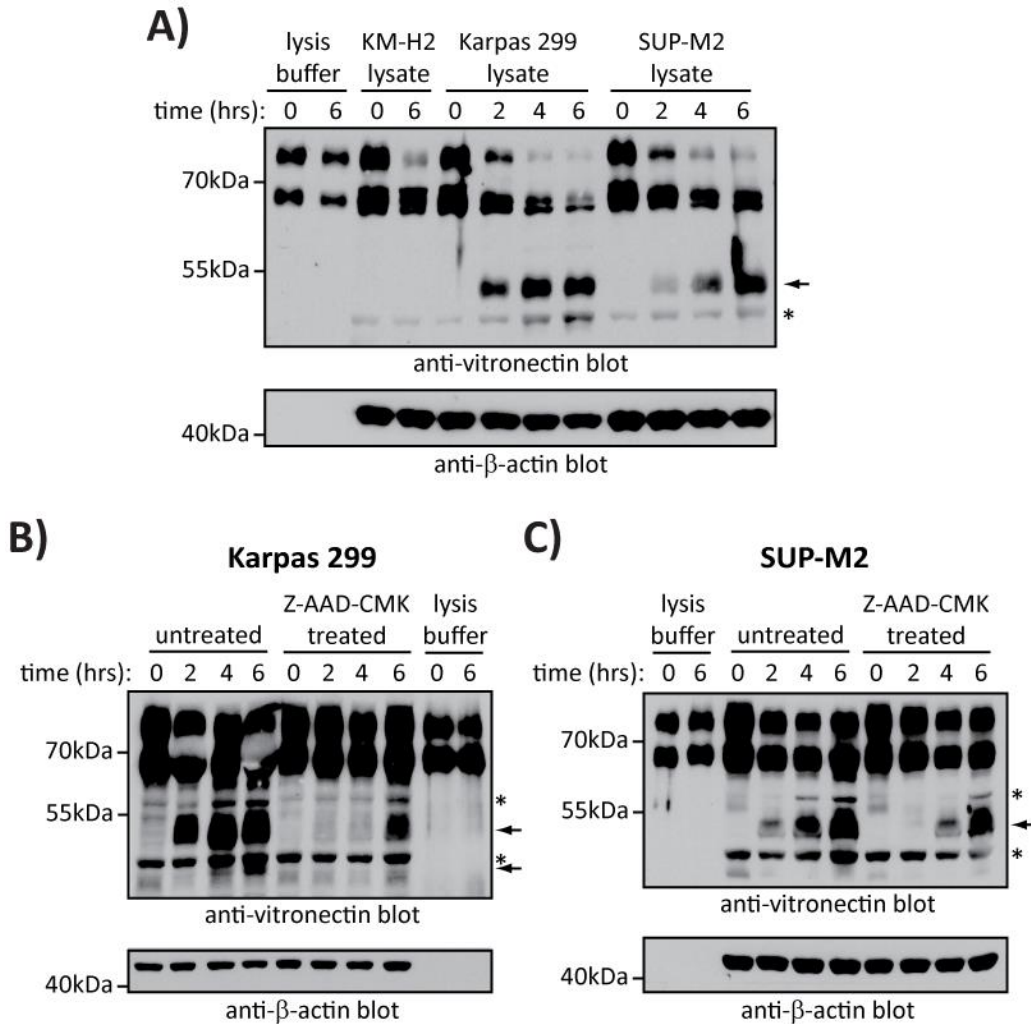


**Figure 4.6: A protein(s) expressed by ALK+ ALCL cell lines can cleave the ECM protein, vitronectin, and this is inhibited by the GzB inhibitor, Z-AAD-CMK.**

**(A)** Lysates from the indicated cell lines or lysis buffer alone were incubated with plate-bound vitronectin for the indicated times. Samples were then collected and subjected to western blotting with an anti-vitronectin antibody to examine vitronectin cleavage. **(B & C)** Lysates from Karpas 299 **(B)** or SUP-M2 **(C)** cells were incubated with plate-bound vitronectin for the indicated times in the absence (untreated) or presence of the GzB inhibitor, Z-AAD-CMK (Z-AAD-CMK treated). Samples were then collected and western blotted as in **(A)**. β-actin blots demonstrate that equivalent amounts of lysate were used for each sample. Arrows indicate the band(s) corresponding to the vitronectin cleavage product(s). \* indicates non-specific bands that were sometimes observed in cell lysates upon longer exposures. Molecular mass markers are shown to the left of the western blots.

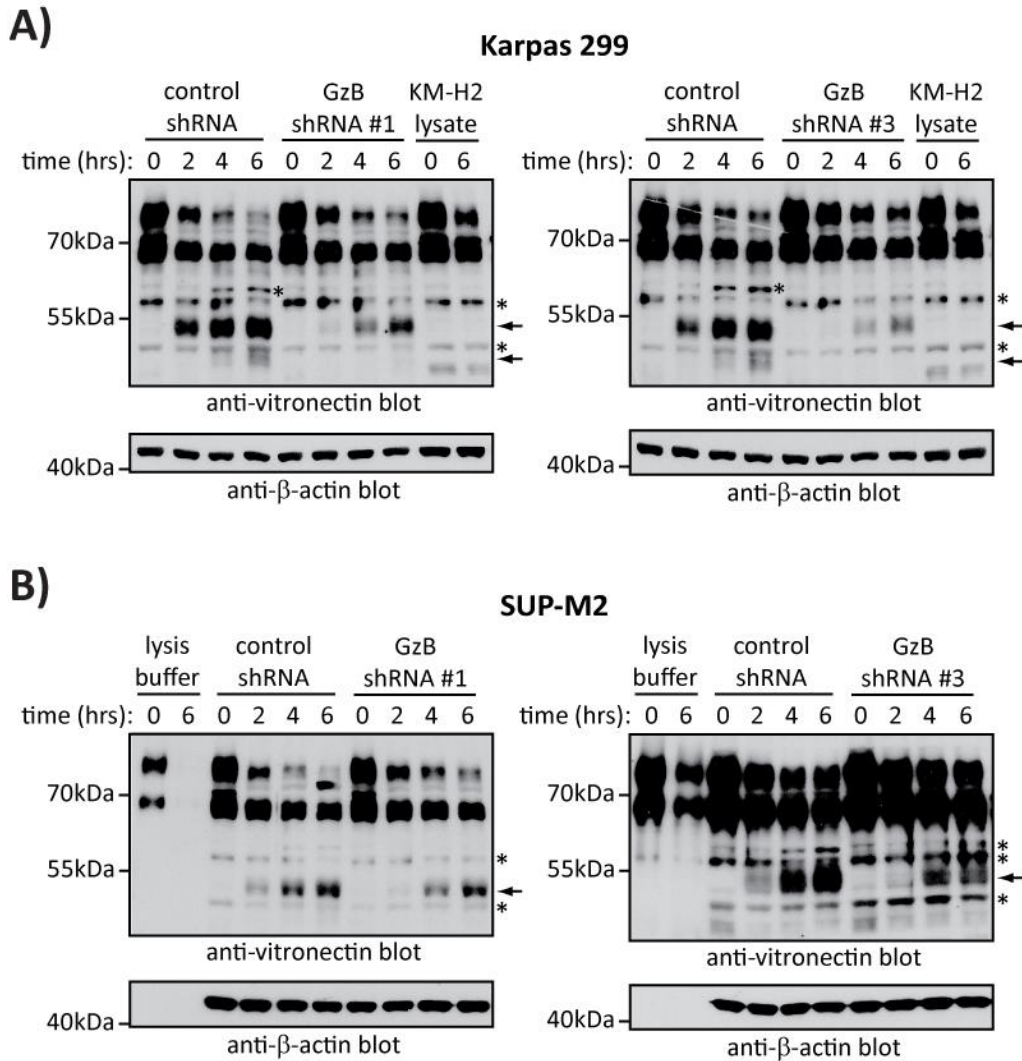


**Figure 4.7: Knock-down of GzB in Karpas 299 and SUP-M2 cells reduces appearance of the vitronectin cleavage bands.**

Lysates from Karpas 299 **(A)** or SUP-M2 **(B)** cells expressing control or GzB shRNA #1 or #3 were incubated with plate-bound vitronectin for the indicated times. Samples were then collected and vitronectin cleavage assessed by western blotting (anti-vitronectin blot). As negative controls, lysate from the GzB-negative Hodgkin lymphoma cell line, KM-H2 **(A)**, or lysis buffer alone **(B)** was incubated with vitronectin for 6 hrs. Arrows indicate vitronectin cleavage products. \* indicates non-specific bands from the cell lysates that we sometimes observe on longer exposures.  $\beta$ -actin blots demonstrate that equivalent amounts of lysate were used for each sample. Molecular mass markers are shown to the left of the western blots.

We next examined cleavage of fibronectin using lysates collected from ALK+ ALCL cell lines. When lysate from Karpas 299 or SUP-M2 cells was incubated with fibronectin, we observed the appearance of several lower molecular weight bands that had similar electrophoretic mobility as the fibronectin cleavage bands induced by purified GzB (Figure 4.8A). Importantly, we did not observe these same bands when fibronectin was incubated with lysis buffer alone or with lysate from the GzB-negative cell line, KM-H2 (Figure 4.8A). Furthermore, we found that inclusion of the GzB inhibitor, Z-AAD-CMK, in these cleavage assays reduced the appearance of fibronectin cleavage bands (Figure 4.8B and C), suggesting that the cleavage of fibronectin by a protein(s) expressed by Karpas 299 and SUP-M2 cells is dependent on GzB.

It was recently demonstrated that purified GzB can cleave the proteoglycans biglycan, betaglycan and decorin (308). We therefore examined the cleavage of decorin using lysates from ALK+ ALCL cells. Similar to vitronectin and fibronectin, we observed the appearance of decorin cleavage products following incubation of plate-bound decorin with Karpas 299 or SUP-M2 lysates (Figure 4.9A). The decorin cleavage bands observed were not seen when the purified decorin was incubated with lysate from the GzB-negative Hodgkin lymphoma cell line, KM-H2, or with lysis buffer alone (Figure 4.9A). Furthermore, the decorin cleavage products had the same mobility as the bands observed following incubation of decorin with purified GzB (Figure 4.9A). Importantly, we found that inclusion of a GzB inhibitor in these cleavage assays dramatically reduced appearance of the decorin cleavage products (Figure 4.9B and C). These findings are consistent with the notion that the GzB expressed by ALK+ ALCL cell lines can cleave decorin, and taken together with earlier results (Figure 4.6 to 4.8) suggests that this GzB can cleave (or at least promote the cleavage of) various ECM proteins.

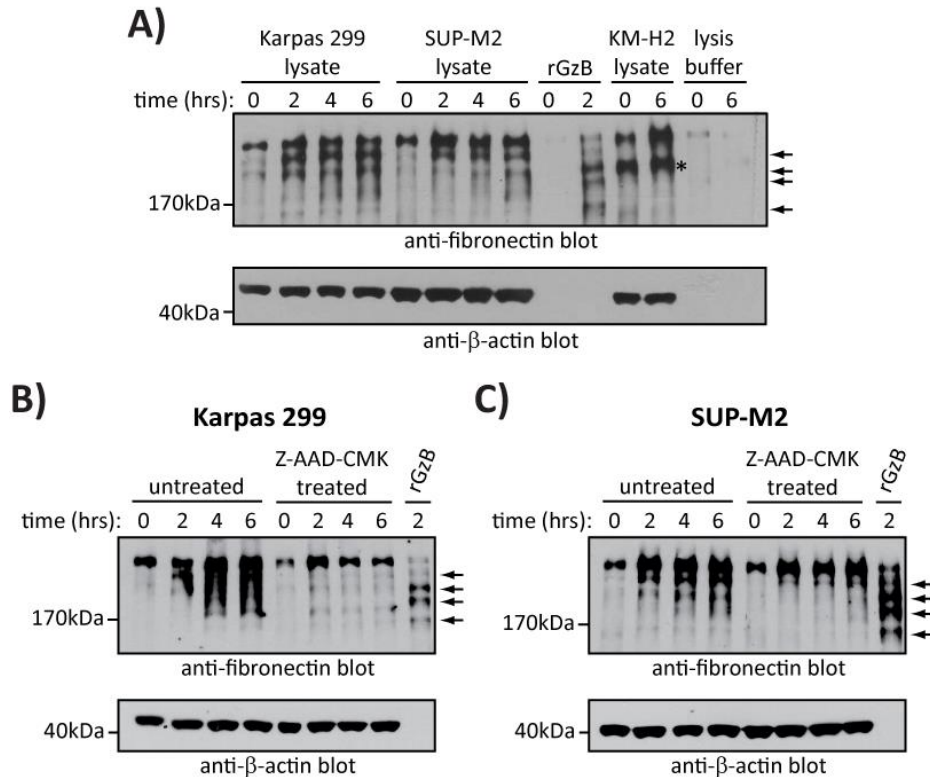


**Figure 4.8: Cleavage of the ECM protein fibronectin by Karpas 299 and SUP-M2 lysates is reduced by the GzB inhibitor Z-AAD-CMK.**

**(A)** Purified human fibronectin was incubated with lysate from the indicated cell lines, recombinant active human GzB (rGzB; 100 nM) or lysis buffer for the indicated times. Samples were then collected by the addition of SDS-PAGE sample buffer and subjected to western blotting with an anti-fibronectin antibody to examine fibronectin cleavage. \* indicates a non-specific band from the KM-H2 lysate. **(B & C)** Lysates from Karpas 299 **(B)** or SUP-M2 **(C)** cells were incubated with plate-bound fibronectin for 2, 4 or 6 hrs in the absence (untreated) or presence of the GzB inhibitor, Z-AAD-CMK (Z-AAD-CMK treated). Samples were then collected and western blotted as in **(A)**. Fibronectin incubated with recombinant human GzB (rGzB) for 2 hrs is included to indicate the mobility of fibronectin cleavage products. β-actin blots demonstrate that equivalent amounts of lysate were used for each sample. Arrows indicate bands corresponding to the fibronectin cleavage products. Molecular mass markers are shown to the left of the blots.

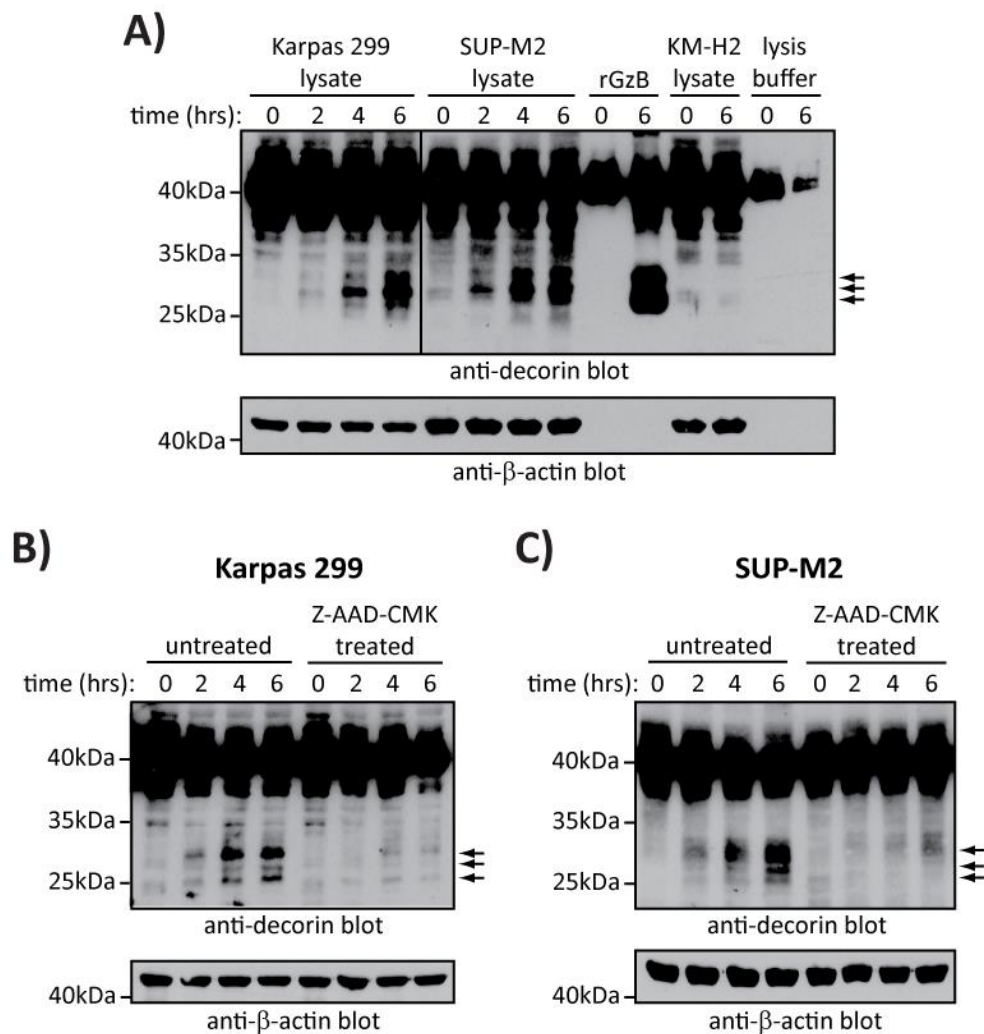


**Figure 4.9: Decorin is cleaved in a GzB-dependent manner using Karpas 299 and SUP-M2 lysates.**

**(A)** Lysates from the indicated cell lines, recombinant active human GzB (rGzB; 75 nM) or lysis buffer alone were incubated with plate-bound decorin for the indicated times. Samples were then collected and subjected to western blotting with an anti-decorin antibody to examine decorin cleavage. The split decorin blot represents different exposures of the same membrane. **(B & C)** Lysates from Karpas 299 **(B)** or SUP-M2 **(C)** cells were incubated with plate-bound decorin for the indicated times in the absence (untreated) or presence of the GzB inhibitor, Z-AAD-CMK (Z-AAD-CMK treated). Samples were then collected and western blotted as in **(A)**. β-actin blots demonstrate that equivalent amounts of lysate were used for each sample. Arrows indicate bands corresponding to the decorin cleavage products. Molecular mass markers are shown to the left of the western blots.

#### **4.5: ALK+ ALCL CELL LINES RELEASE ENZYMATICALLY ACTIVE GRANZYME B INTO THE CULTURE SUPERNATANT**

Both CTL and NK cells constitutively release GzB (306), and a variety of functions have been suggested for this released GzB. We therefore asked whether ALK+ ALCL cell lines are able to release GzB into the culture supernatant. Western blotting of supernatants from Karpas 299, SUP-M2, SR and UCONN cells showed that GzB is present in the supernatants of these cell lines (Figure 4.10A). The amount of GzB present in the supernatants was roughly proportional to the amount of GzB typically observed in the lysate of the respective cell lines, although the GzB in the supernatant appears to be over-represented in UCONN cells (Figure 4.10B). To rule out that non-specific cell lysis was resulting the observed GzB in the supernatant, we treated cells with Brefeldin A. Brefeldin A blocks secretion by interfering with protein transport through the endoplasmic reticulum/Golgi network (338). When cells were treated with Brefeldin A we observed a substantial reduction in the level of GzB present in the culture supernatant, arguing that GzB is being released by these cells (Figure 4.10C). We also observed an accumulation of GzB protein in SUP-M2, SR and UCONN cell lysates after Brefeldin A treatment, while we observed similar GzB levels in Karpas 299 lysates before and after Brefeldin A treatment (Figure 4.10C). This demonstrated that the reduced GzB observed in the supernatants from ALK+ ALCL cell lines after Brefeldin A treatment was not due to reduced GzB expression and further supports the notion that these ALK+ ALCL cell lines actively release GzB.

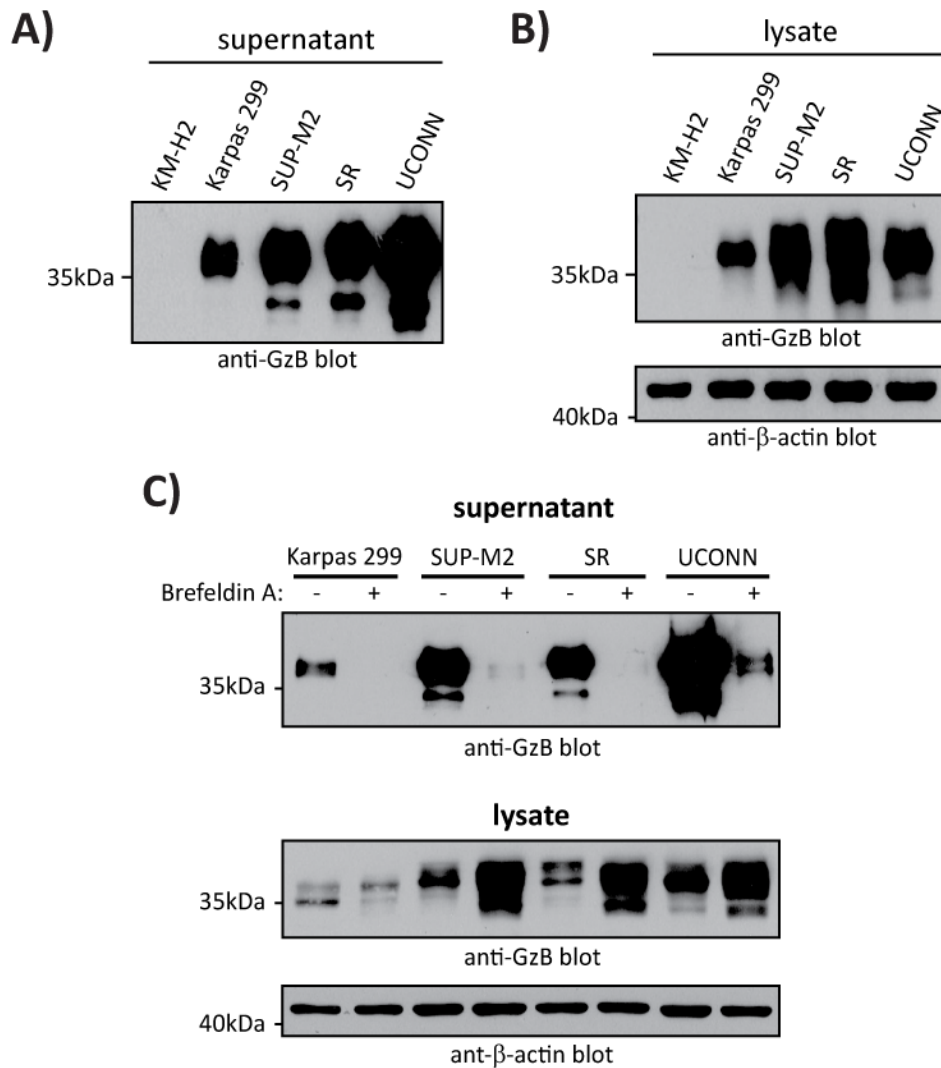


**Figure 4.10: GzB is released by ALK+ ALCL cell lines.**

**(A)** Anti-GzB western blot of culture supernatants collected from the indicated cell lines. **(B)** Western blot for GzB expression in lysates collected from the indicated cell lines. **(C)** GzB western blot of tissue culture supernatants (upper panel) or lysates (middle panel) collected from the indicated cell lines treated with DMSO (-) or Brefeldin A (+) for 24 hrs. Anti-β-actin blots on lysates demonstrate equivalent protein loading. Molecular mass markers are indicated to the left of the western blots.

We next examined whether the GzB released by ALK+ ALCL cell lines is enzymatically active. Using a GzB-specific activity assay, we assessed GzB activity in supernatant samples collected from ALK+ ALCL cell lines. We observed significant levels of GzB activity in the supernatants from all four ALK+ ALCL cell lines, but not in supernatant collected from the GzB-negative Hodgkin lymphoma cell line, KM-H2 (Figure 4.11A). The activity we observed did not correlate with GzB levels, but did roughly correlate with the level of activity we observed in the respective cell lysates (see Figure 4.3), with the exception that GzB activity in the UCONN supernatant appeared to be lower relative to the other cell lines compared to what was observed for the cell lysates. Importantly, activity in these supernatants was strongly inhibited by the GzB inhibitor, Z-AAD-CMK (Figure 4.11B). Furthermore, when supernatants from Karpas 299 or SUP-M2 cells stably expressing the GzB shRNA constructs were used in these assays, we observed strongly reduced GzB activity compared to cells expressing a control shRNA construct (Figure 4.11C). Taken together, these results suggest that ALK+ ALCL cell lines release enzymatically active GzB.

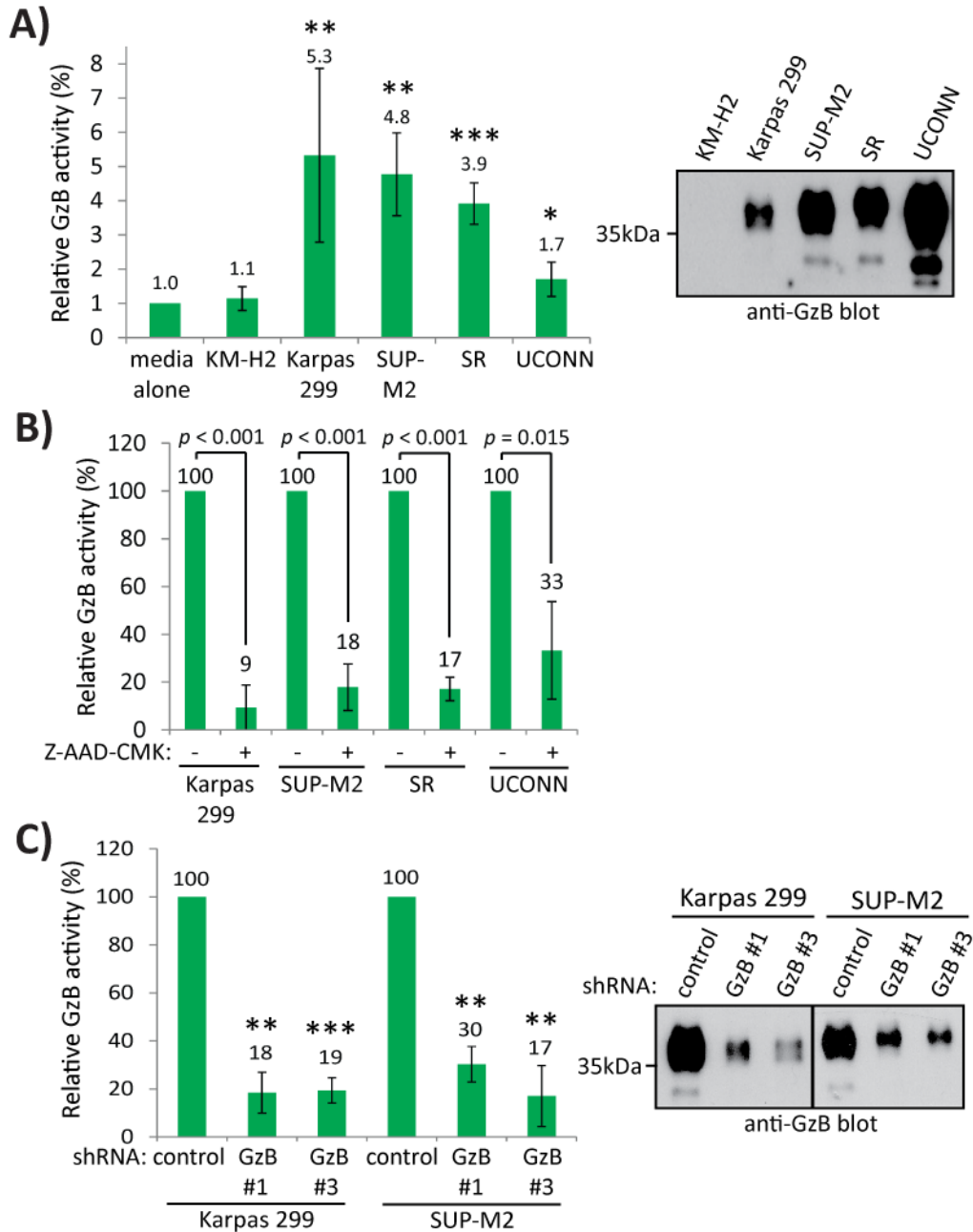


**Figure 4.11: GzB released by ALK+ ALCL cell lines possesses enzymatic activity.**

**(A)** GzB activity was assessed in supernatants from the indicated cell lines. Error bars represent the standard deviation of five (SUP-M2) or six (other cell lines) experiments. **(B)** GzB activity was determined in supernatants incubated with (+) or without (-) the GzB inhibitor, Z-AAD-CMK. **(C)** GzB activity was examined in supernatants collected from Karpas 299 or SUP-M2 cells expressing the indicated shRNAs. The results in **(B)** and **(C)** are the mean and standard deviation of three independent experiments. All *p* values were determined using paired, one-tailed *t*-tests; \* *p* < 0.01, \*\* *p* < 0.005, \*\*\* *p* < 0.001.

#### **4.6: KNOCK-DOWN OF GRANZYME B IN SUP-M2 CELLS DOES NOT OVERTLY EFFECT SUP-M2 INVASION INTO A COLLAGEN/FIBRONECTIN MATRIX**

The demonstration that ALK+ ALCL cell lines release enzymatically active GzB suggested that this GzB might be involved in interaction of these cells with the ECM. The GzB expressed by some bladder cancer cell lines has recently been shown to promote their invasion through ECM, and the expression of GzB in urothelial carcinoma correlates with tumour spreading and invasive potential (325). Several studies have demonstrated that ALK+ ALCL cell lines can invade through matrix *in vitro* (326, 339, 340), so we examined whether GzB is a factor contributing to this invasion. We developed an *in vitro* invasion assay to examine invasion of SUP-M2 cells through a collagen/fibronectin matrix towards a chemoattractant of 10% FBS and SDF-1 $\alpha$ , similar to what has been previously used to examine invasion of ALK+ ALCL cell lines (326, 339). Under these conditions, we observed an increased invasive depth of SUP-M2 cells towards the FBS and SDF-1 $\alpha$  chemoattractant compared to when no chemoattractant was used (Figure 4.12). When the invasive depth of SUP-M2 stably expressing GzB shRNA #1 was compared to cells expressing control shRNA, we observed no difference (Figure 4.12), suggesting that GzB does not affect ALK+ ALCL invasion under the conditions tested.

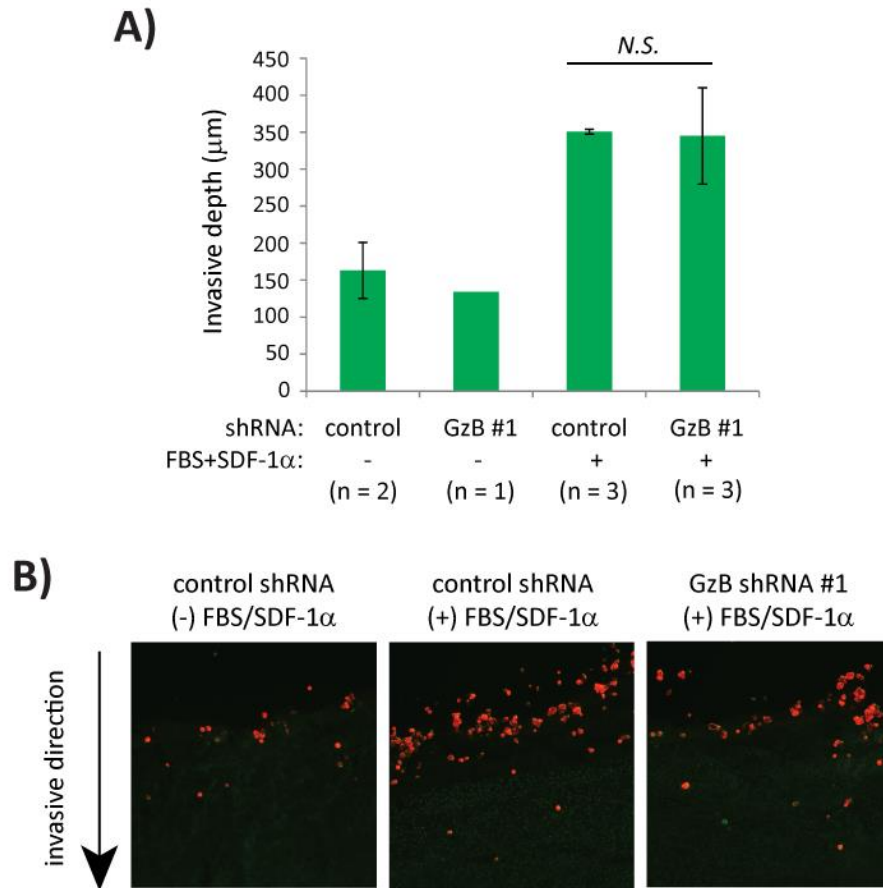


**Figure 4.12: GzB knock-down does not affect invasion of SUP-M2 cells through a collagen/fibronectin matrix.**

**(A)** The average invasive depth (in  $\mu\text{m}$ ) of SUP-M2 cells stably expressing control shRNA or GzB shRNA #1 through a collagen/fibronectin matrix is shown. Cells were allowed to invade towards no chemoattractant (-) or towards FBS and SDF-1 $\alpha$  (+). Results represent the mean and standard deviation of the indicated number of experiments (n). No significant difference (N.S.) in invasive depth was observed between cells with control shRNA or GzB shRNA #1 when allowed to invade towards FBS + SDF-1 $\alpha$  (unpaired, two-tailed *t*-test). **(B)** Sample images demonstrating invasion of CMTPIX-labelled (red) SUP-M2 cells with control or GzB shRNA into a collagen/fibronectin matrix (green) towards no chemoattractant ((-) FBS/SDF-1 $\alpha$ ) or towards a FBS + SDF-1 $\alpha$  chemoattractant ((+) FBS/SDF-1 $\alpha$ ).

#### **4.7: THE ELECTROPHORETIC MOBILITY OF $\alpha$ -TUBULIN IS ALTERED IN ALK+ ALCL CELLS FOLLOWING GRANZYME B KNOCK-DOWN**

When we generated ALK+ ALCL cell lines with stable GzB knock-down we made the interesting observation that there was a reduction in the lower molecular weight  $\alpha$ -tubulin band that we observe on long exposures of western blots (Figure 4.13A and B). In Karpas 299 cells this reduction correlated with the degree of GzB silencing (Figure 4.13A). We also observed a similar effect on the  $\alpha$ -tubulin banding pattern in SR cells stably expressing GzB shRNA #1 (Figure 4.13C), although the proportion of the lower molecular weight  $\alpha$ -tubulin band was reduced in SR cells compared to other cells.  $\alpha$ -tubulin is known to be cleaved by GzB *in vitro* and in cells undergoing CTL or NK cell-mediated apoptosis (341, 342). GzB cleaves  $\alpha$ -tubulin at aspartic acid 438 to remove 13 amino acids from its carboxyl-terminus (341, 342). In one study it was suggested that cleaved  $\alpha$ -tubulin is not associated with polymerized microtubules (341); however, another study showed that cleaved  $\alpha$ -tubulin polymerized more readily than uncleaved  $\alpha$ -tubulin (342). The molecular mass of the lower molecular weight  $\alpha$ -tubulin band we observed in ALK+ ALCL cell lines is consistent with the reported size of the fragment generated by GzB-mediated cleavage (341, 342), suggesting that this band might be due to GzB-mediated cleavage of  $\alpha$ -tubulin in ALK+ ALCL cell lines. Consistent with this, the lower molecular weight  $\alpha$ -tubulin band observed in Karpas 299 cell lysates had the same electrophoretic mobility as the  $\alpha$ -tubulin band observed after incubation of Karpas 299 lysate with purified GzB (Figure 4.13D). While we cannot exclude the possibility that GzB activates another protein responsible for the altered mobility of  $\alpha$ -tubulin in ALK+ ALCL cells, our results suggest that there is active GzB in the cytoplasm of ALK+ ALCL cell lines. Of note, the lysates from these experiments contained three serine protease inhibitors (aprotinin, PMSF and 4-(2-Aminoethyl)benzenesulfonyl fluoride hydrochloride), that would be expected to inhibit GzB activity. This argues that  $\alpha$ -tubulin is being cleaved in the cytoplasm of intact cells, as opposed to post-lysis.

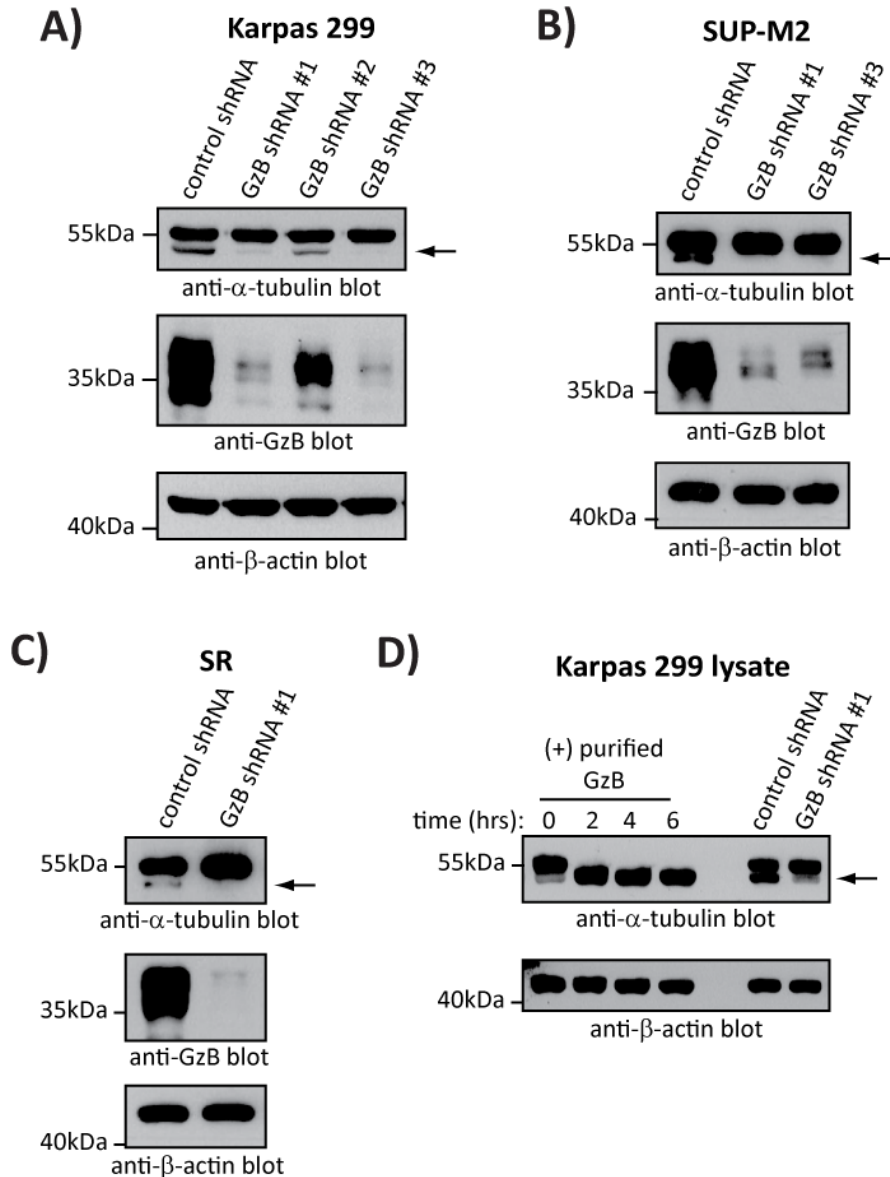


**Figure 4.13: GzB knock-down in ALK+ ALCL cell lines results in altered electrophoretic mobility of  $\alpha$ -tubulin.**

Anti- $\alpha$ -tubulin western blots were performed on lysates from Karpas 299 (A), SUP-M2 (B) and SR (C) cells stably expressing the indicated shRNA constructs. GzB western blots demonstrate GzB knock-down. (D) Lysates from Karpas 299 cells were incubated with 100 nM recombinant human GzB for the indicated times. These samples were then run beside lysates from Karpas 299 cells stably expressing control or GzB shRNA #1 and western blotted for  $\alpha$ -tubulin. Note: the experiment in (D) was performed only once. In all panels, arrows indicate the lower molecular weight  $\alpha$ -tubulin band that is reduced following GzB knock-down. Anti- $\beta$ -actin western blots demonstrate equal protein loading and molecular mass markers are indicated to the left of the western blots.

#### **4.8: GRANZYME B SENSITIZES ALK+ ALCL CELL LINES TO STAUROSPORINE-INDUCED PARP CLEAVAGE**

While the GzB expressed by ALK+ ALCL could play a role in promoting the pathogenesis of this cancer under certain circumstances, it may also play a detrimental role in this cancer. Once GzB is released toward a target cell by a CTL or NK cell, GzB enters the target cell and initiates apoptosis by cleaving a variety of proteins, such as caspases (311, 317-321), Bid (311-315), Mcl-1 (316) and ICAD (311, 323). Although the ability of human and murine GzB to cleave these different substrates has been shown to vary (311), in humans it has been suggested that Bid represents the major GzB target in cells (315). Recently it has been shown that the expression of GzB in nasal-type NK/T cell lymphoma tumour cells correlates with increased apoptosis (343). Furthermore, in the one nasal-type NK/T cell lymphoma cell line tested there was a substantial level of PARP cleavage and apoptosis in resting cells that could be partially blocked by treatment of cells with the GzB inhibitor, Z-AAD-CMK (343). It has also been found that GzB can leak out of granules and into the cytoplasm of NK cells, and this was proposed to promote activation-induced death of NK cells (344). Because of these findings, and our observation that there is likely active GzB present in the cytoplasm of ALK+ ALCL cells, we hypothesised that the GzB expressed by ALK+ ALCL cell lines sensitizes these cells to apoptosis. To test this, we first examined cleavage of PARP (using western blotting) following treatment of ALK+ ALCL cell lines with low doses of the apoptosis-inducing agent, staurosporine. PARP is a caspase substrate that is cleaved by executioner caspases in apoptotic cells (345-350). PARP is also known to be cleaved by GzB; however, cleavage of PARP by GzB generates different sized fragments (~42-64kDa) compared to caspase 3 (~90 and 24kDa) (324), so the caspase cleavage products of PARP can be easily distinguished from those generated by GzB. In Karpas 299 cells treated with staurosporine we observed a dose-dependent increase in PARP cleavage (Figure 4.14A and B). The molecular mass of the

cleaved PARP band suggests that this PARP cleavage was mediated by Caspase 3 and not directly by GzB. Interestingly, when we compared PARP cleavage in Karpas 299 cells expressing control shRNA to cells expressing two different GzB shRNA constructs, we observed reduced PARP cleavage in cells with GzB knock-down when treated with low doses (0.15 and 0.2  $\mu\text{M}$ ) of staurosporine (Figure 4.14A and B). However, at a high staurosporine concentration (1  $\mu\text{M}$ ), we observed complete PARP cleavage in all cells whether GzB was knock-down or not. These findings suggest that the presence of GzB sensitizes Karpas 299 cells to staurosporine-induced PARP cleavage.

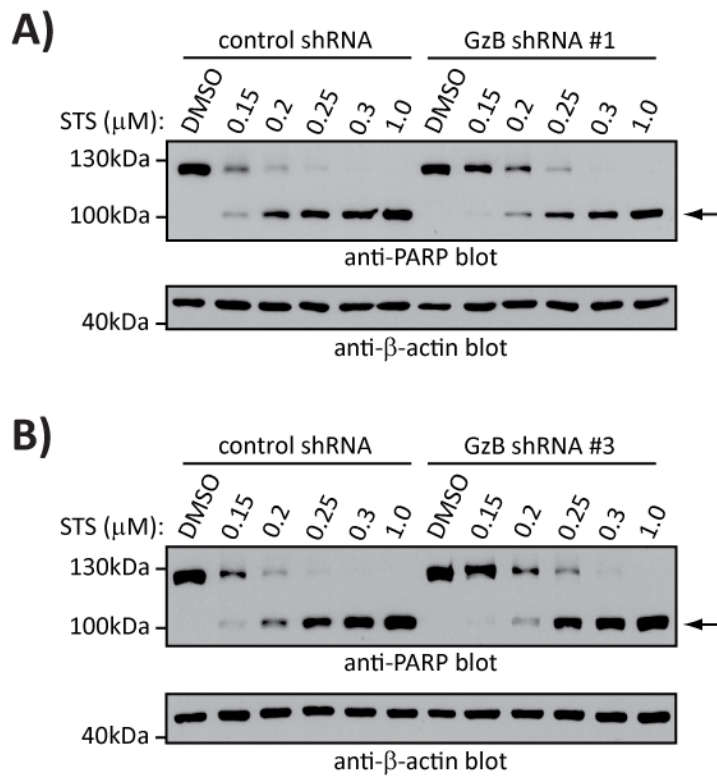


**Figure 4.14: Knock-down of GzB in Karpas 299 cells reduces PARP cleavage following treatment with the apoptosis-inducing drug, staurosporine.**

Karpas 299 cells stably expressing control shRNA or GzB shRNA #1 (A) or #3 (B) were left untreated (DMSO) or were treated with increasing concentrations of staurosporine (STS) for 6 hrs. Lysates were then prepared and subjected to anti-PARP western blotting to examine PARP cleavage. Arrows indicate the cleaved PARP band following staurosporine treatment. Anti- $\beta$ -actin blots demonstrate protein loading. Molecular mass markers are indicated to the left of western blots.

We next examined PARP cleavage in SUP-M2 and SR cells following GzB knock-down. We found that the SUP-M2 and SR cell lines were more sensitive to staurosporine than Karpas 299 cells, so lower doses were used to achieve a dose-dependent response. Similar to Karpas 299 cells, we observed dose-dependent PARP cleavage following low doses of staurosporine treatment in SUP-M2 and SR cells (Figure 4.15). Importantly, in SUP-M2 cells we observed that knock-down of GzB using two different shRNA constructs resulted in a modest reduction in the appearance of cleaved PARP; however, it did not obviously affect the disappearance of the full-length PARP band (Figure 4.15A and B). Furthermore, in SR cells stably expressing GzB shRNA #1, we also observed a minor reduction in PARP cleavage compared to cells expressing control shRNA following staurosporine treatment (Figure 4.15C). Similar to Karpas 299 cells, we still observed similar levels of PARP cleavage at higher staurosporine concentrations in SUP-M2 and SR cells. Taken together these results demonstrate that GzB sensitizes ALK+ ALCL cell lines to staurosporine-induced PARP cleavage and are consistent with the hypothesis that GzB sensitizes these cells to drug-induced apoptosis.

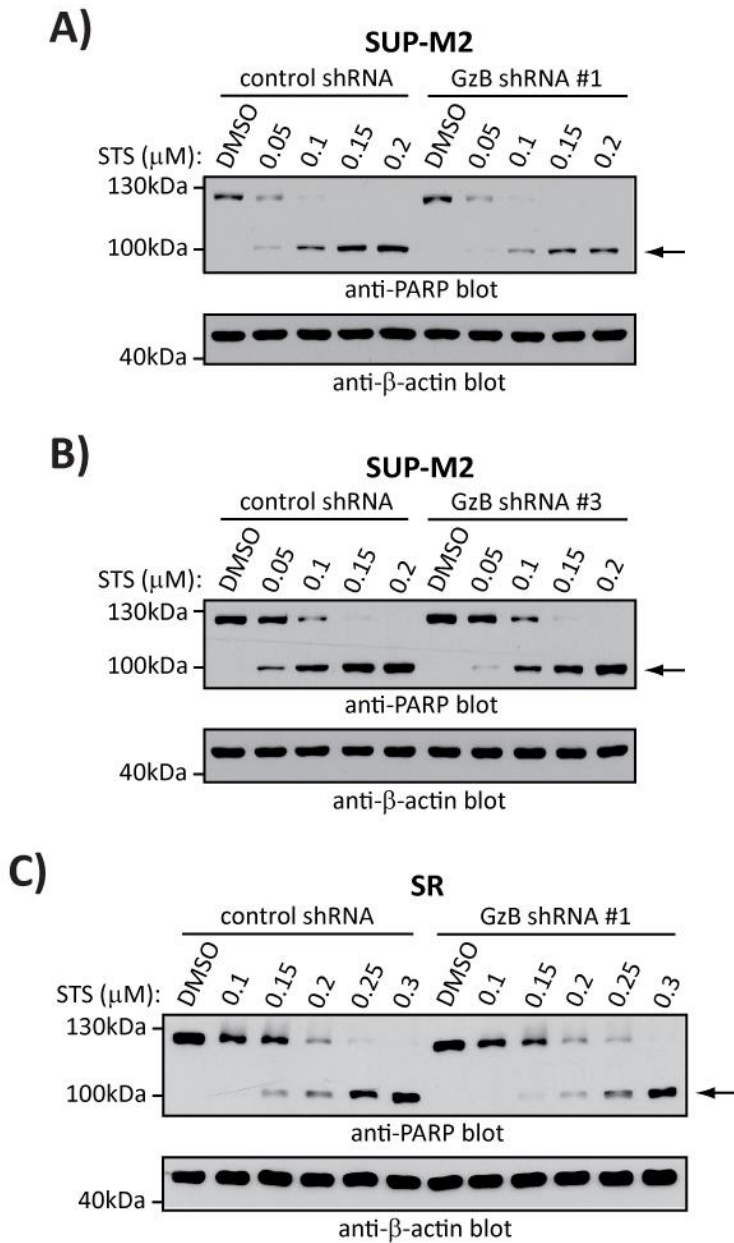


**Figure 4.15: Knock-down of GzB in SUP-M2 and SR cells results in reduced PARP cleavage following staurosporine treatment.**

**(A & B)** SUP-M2 cells stably expressing control shRNA or GzB shRNA #1 **(A)** or #3 **(B)** were left untreated (DMSO) or were treated with the indicated concentrations of staurosporine (STS). Lysates were prepared and western blotted to examine PARP cleavage. **(C)** SR cells expressing control or GzB shRNA #1 were treated and western blotted as in **(A)** and **(B)**. Arrows indicate PARP cleavage following staurosporine treatment. Anti- $\beta$ -actin blots demonstrate equal protein loading and molecular mass markers are shown to the left of the western blots.

#### **4.9: GRANZYME B SENSITIZES KARPAS 299 CELLS TO STAUROSPORINE-INDUCED DNA NICKING/FRAGMENTATION**

While cleavage of PARP is one event that occurs in apoptotic cells, there are a variety of other events associated with apoptotic cells. One of these is the nicking and fragmentation of genomic DNA, and this can be measured using terminal deoxynucleotidyl transferase dUTP nick end labelling (TUNEL) (351-353). To determine if GzB sensitizes ALK+ ALCL cell lines to aspects of apoptosis other than PARP cleavage, we performed TUNEL staining in Karpas 299 cells treated with staurosporine. We observed a dose-dependent increase in the percentage of cells positive for TUNEL staining (TUNEL-positive cells) following treatment with increasing concentrations of staurosporine (Figure 4.16). In Karpas 299 cells expressing GzB shRNA #1 we observed a significant reduction in the percentage of TUNEL-positive cells following treatment with low concentrations of staurosporine (0.15 and 0.2  $\mu$ M) compared to cells expressing control shRNA (Figure 4.16). When cells expressing GzB shRNA #3 were compared to control cells, we observed only a very minor reduction in TUNEL-positive cells when cells were treated with 0.15  $\mu$ M staurosporine; however, a more substantial reduction in the proportion of TUNEL-positive cells was observed following treatment with 0.2  $\mu$ M staurosporine (Figure 4.16). The reduction in TUNEL-positive cells with 0.2  $\mu$ M staurosporine observed with GzB shRNA #3 was comparable to that observed for GzB shRNA #1. Similar to what was observed for PARP cleavage, we observed no difference in the percentage of TUNEL-positive cells following treatment with 0.3  $\mu$ M staurosporine. These findings suggest that GzB sensitizes ALK+ ALCL cell lines to multiple aspects of apoptosis following treatment of cells with the apoptosis-inducing agent, staurosporine.

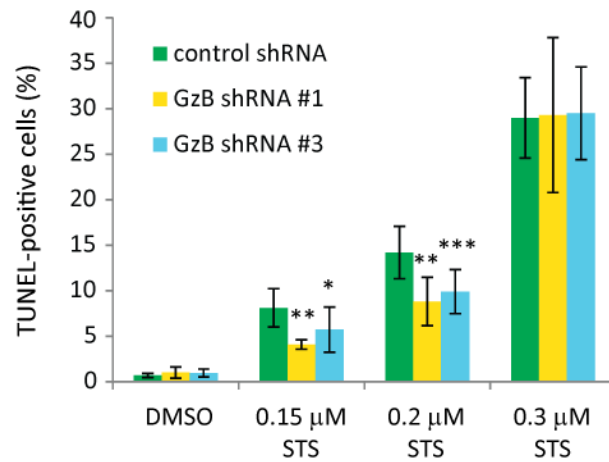


**Figure 4.16: GzB knock-down reduces TUNEL staining of Karpas 299 cells following staurosporine treatment.**

Karpas 299 cells stably expressing control, GzB #1 or GzB #3 shRNA were left untreated (DMSO) or treated with the indicated concentrations of staurosporine (STS) for 6 hrs. Following treatment, cells were collected and analysed by TUNEL staining and flow cytometry. Results are presented as the percentage of total cells that were positive for TUNEL staining. Results represent the mean and standard deviation of at least four independent experiments. All *p* values were determined using paired, one-tailed *t*-tests; \* *p* < 0.05, \*\* *p* < 0.005, \*\*\* *p* < 0.001.

#### **4.10: GRANZYME B SENSITIZES SUP-M2 AND SR ALK+ ALCL CELL LINES TO DOXORUBICIN-INDUCED PARP CLEAVAGE**

To determine if the apoptosis sensitivity conferred by GzB expression is common to other apoptosis-inducing drugs, we examined if GzB sensitizes ALK+ ALCL cells to PARP cleavage induced by doxorubicin. Doxorubicin is a DNA damaging agent that promotes apoptosis in ALK+ ALCL cell lines (328, 354), and is one component of the CHOP chemotherapy regimen often used to treat ALK+ ALCL patients (11, 12, 18). When SUP-M2 cells expressing control shRNA were treated with doxorubicin we observed efficient PARP cleavage (Figure 4.17A and B). When this was compared to SUP-M2 cells expressing GzB shRNA we observed reduced PARP cleavage following doxorubicin treatment in SUP-M2 cells with GzB knock-down (Figure 4.17A and B). Using SR cells expressing GzB shRNA #1, we also observed reduced PARP cleavage after treatment with doxorubicin when compared to cells expressing control shRNA (Figure 4.17C). When PARP cleavage was examined in Karpas 299 cells treated with doxorubicin, we actually observed more efficient PARP cleavage in cells with GzB shRNA #1 compared to control shRNA, suggesting that GzB knock-down might sensitize Karpas 299 to doxorubicin-induced PARP cleavage (Figure 4.18A). However, we observed comparable levels of PARP cleavage when we compared Karpas 299 cells expressing control shRNA to those with GzB shRNA #3 (Figure 4.18B). These results suggest that GzB expression does not sensitize Karpas 299 cells to doxorubicin-induced PARP cleavage, unlike what was observed for SUP-M2 and SR cells treated with doxorubicin or for staurosporine-treated cells. In sum, although we found GzB knock-down did not reduce PARP cleavage following doxorubicin treatment in Karpas 299 cells, GzB did sensitize SUP-M2 and SR cells to doxorubicin-induced PARP cleavage. This suggests that the reduced apoptosis observed after GzB knock-down in staurosporine-treated cells is not restricted to the apoptosis-inducing agent staurosporine, and under most conditions tested, GzB sensitized ALK+ ALCL cell lines to drug-induced apoptosis.

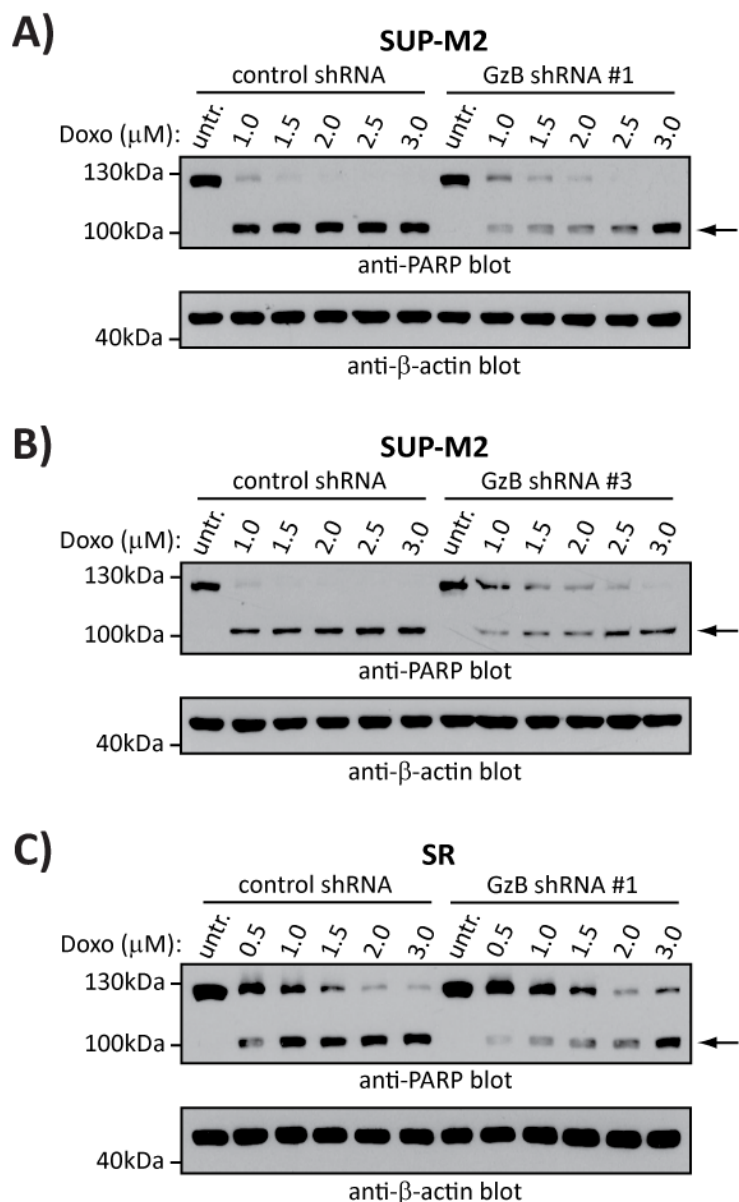


**Figure 4.17: SUP-M2 and SR cells stably expressing GzB shRNA have reduced PARP cleavage following doxorubicin treatment.**

**(A & B)** SUP-M2 cells stably expressing control shRNA and GzB shRNA #1 **(A)** or GzB shRNA #3 **(B)** were left untreated (untr.) or were treated with the indicated concentrations of doxorubicin (Doxo). Lysates were then prepared from these cells and PARP cleavage was examined using anti-PARP western blotting. **(C)** SR cells expressing control or GzB shRNA #1 were treated and western blotted as described in **(A)** and **(B)**. Arrows indicate the PARP cleavage band following doxorubicin treatment. Anti- $\beta$ -actin blots demonstrate loading. Molecular mass markers are included to the left of the western blots.

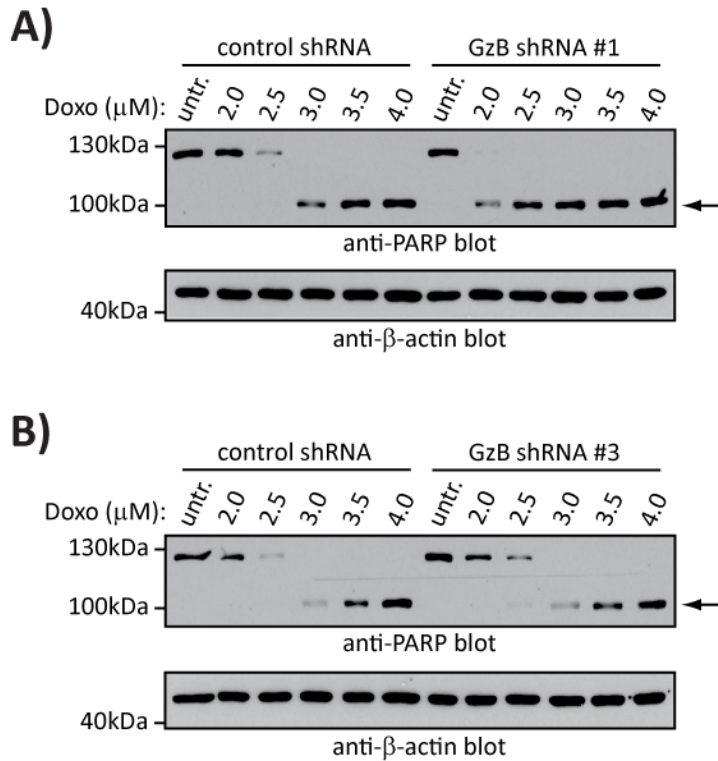


**Figure 4.18: Knock-down of GzB in Karpas 299 cells does not reduce PARP cleavage following treatment with the apoptosis-inducing drug, doxorubicin.**

Karpas 299 cells stably expressing control shRNA and GzB shRNA #1 **(A)** or GzB shRNA #3 **(B)** were left untreated (untr.) or were treated with increasing concentrations of doxorubicin (Doxo) for 12 hrs. PARP cleavage was then examined in lysates from these cells using anti-PARP western blotting. Arrows indicate the cleaved PARP band following doxorubicin treatment. Anti- $\beta$ -actin blots demonstrate equal protein loading and molecular mass markers are indicated to the left of the blots.

#### 4.11: DISCUSSION

The expression of the serine protease GzB is a common feature in ALK+ ALCL (19, 28, 54), and it has been suggested that GzB is more highly expressed in ALK+ ALCL tumour cells compared to normal activated T lymphocytes (79). In contrast to GzB, we demonstrate here that some ALK+ ALCL cell lines express only low levels of *GzA* mRNA (Figure 4.2A) and undetectable levels of GzA protein (Figure 4.1B). Additionally, we found that these cells do not express detectable levels of the other Granzymes at the mRNA level (Figure 4.1A). We are currently working on developing staining protocols to examine expression of the various Granzymes in ALK+ ALCL patient samples using immunohistochemistry to confirm our findings in the ALK+ ALCL cell lines. The finding that ALK+ ALCL cell lines express GzB, while other Granzymes are either not expressed or are expressed at very low levels is an interesting observation. Activated CTLs have been reported to express GzA, GzB, GzK and GzM (355-357), and gene expression profiling has suggested that ALK+ ALCL cells have a genetic signature that most closely resembles an activated T lymphocyte (79). Therefore it might be thought that at least some of the other Granzymes would be expressed by the ALK+ ALCL cell lines. NPM-ALK signalling has been demonstrated to repress a variety of T cell-associated genes through promoting their epigenetic silencing (25), so it would be interesting to examine whether NPM-ALK signalling represses the expression of the Granzymes (other than GzB) in ALK+ ALCL. If expression of other Granzymes is repressed by NPM-ALK, while GzB expression is promoted by NPM-ALK signalling, it would raise the important question as to why GzB is selectively expressed in this cancer.

When we compared GzB protein expression in ALK+ ALCL cell lines to that of NKL cells we found that Karpas 299 had lower GzB protein levels, while SUP-M2 and SU-DHL-1 had similar levels and SR and UCONN cells had slightly higher levels compared to NKL cells (Figure 4.1B). However, when we examined *GzB* mRNA levels in these cells, we found that all ALK+ ALCL cell lines had higher *GzB*

message compared to NKL cells, with SUP-M2, SU-DHL-1, SR and UCONN cells expressing 10-30 times more *GzB* message than NKL cells (Figure 4.2B). The reason for why NKL cells express higher *GzB* protein levels than Karpas 299 cells and comparable levels to other ALK+ ALCL cell lines, while expressing substantially lower *GzB* mRNA levels is not known. However, it could be that the ALK+ ALCL cells release much more *GzB* protein into the culture supernatant than NKL cells, resulting in the different cell lines having comparable levels remaining inside the cell. Consistent with this notion, human blood-derived CTL cells were found to release a much greater proportion of their total *GzB* than blood-derived NK cells or two different NK cell lines (306). It was suggested that this may be because of differential glycosylation of *GzB* in the different cells (306). It is also possible that the NKL cells translate the *GzB* message at a higher rate than the ALK+ ALCL cell lines.

Another interesting observation of our study was that the level of *GzB* expression in the different ALK+ ALCL cell lines did not correlate with the level of *GzB* activity in the respective cell lysates (Figure 4.3). Most notably, Karpas 299 cells, which express substantially lower *GzB* levels, had equivalent or even higher *GzB* activity compared to other cell lines. Also, in other cell lines with similar *GzB* protein levels, there are variable levels of activity with UCONN cells having the lowest level of *GzB* activity. This suggests that the *GzB* might be activated more efficiently in some cells compared to other cell lines. This could potentially be due to different expression levels of Cathepsins, the enzymes that activate *GzB* (333-337), in the different cell lines. Alternatively, it may be due to differential trafficking of *GzB* in the various cell lines, so that in some cells the *GzB* is not efficiently trafficked to lytic granules where it can become activated. *GzB* is thought to be targeted to these granules through the mannose-6-phosphate receptor (358). Therefore, differences in the glycosylation machinery in different cell lines may affect the trafficking, and therefore the activation, of *GzB*. Consistent with this possibility, it was shown that *GzB* from blood-derived NK

cells or different NK cell lines was modified with different combinations of mannose or complex carbohydrate chains (306), demonstrating that GzB can be differently modified in different cell lines that presumably arise from the same cell type. Consistent with this notion, members of our lab have observed different glycosylation patterns of GzB in the different ALK+ ALCL cell lines (Kayla Thew, personal communication).

Since we found that oncogenic signalling promotes GzB expression in ALK+ ALCL we hypothesized that GzB contributes to the pathogenesis of this lymphoma. GzB has been previously demonstrated to promote invasion of bladder cancer cell lines that express GzB, likely through the degradation of ECM proteins (325). Consistent with the possibility that ALK+ ALCL cell lines use GzB to degrade ECM proteins to promote invasion, we found that the GzB expressed by ALK+ ALCL cell lines has the ability to promote cleavage of ECM proteins (Figures 4.6 to 4.9) and that these cells release enzymatically active GzB (Figure 4.11). When we tested whether GzB influences ALK+ ALCL invasion, we found that SUP-M2 ALK+ ALCL cells do invade into a collagen/fibronectin matrix; however, we observed no effect on invasion of these cells following GzB knock-down (Figure 4.12). While we did not observe any effect of GzB knock-down on invasion in these assays, we cannot exclude the possibility that ALK+ ALCL cells use GzB to promote invasion under conditions different than the ones tested in our *in vitro* assay. The conditions used in the invasion assays were chosen because data had demonstrated that SUP-M2 cells invaded very well into a collagen/fibronectin matrix, and importantly, a strong correlation was observed between the level of GzB expression and invasive depth of individual cells (personal communication with Spencer Freeman; University of British Columbia). At the time that we performed the invasion assays we were still working on developing conditions for examining *in vitro* cleavage of the different ECM proteins. However, our results of these cleavage assays suggest that vitronectin and decorin may be better substrates than fibronectin for the GzB expressed by ALK+ ALCL cells (see

Figures 4.6 to 4.9). Furthermore, the major ECM protein that was used to prepare the matrix for the invasion assays was collagen, which is not cleaved by GzB (307). So, while GzB did not appear to affect invasion of SUP-M2 cells into a collagen/fibronectin matrix, it may be that invasion through a matrix consisting of other ECM proteins could be more dependent on GzB. Therefore, we feel that whether GzB can influence ALK+ ALCL invasion *in vitro*, or more importantly *in vivo*, is still an unanswered question and warrants further investigation.

In addition to regulating cell invasion, there are other roles that GzB could play in the pathogenesis of ALK+ ALCL. For example, GzB released by ALK+ ALCL cells could cleave cell surface receptors (310) on tumour cells or surrounding normal cells to influence the biology of the different cells. Alternatively, this GzB could cleave different ECM proteins to affect adhesion of cells to these ECM proteins (307), or could result in the release of cytokines or growth factors that are bound by these ECM proteins (308). This could affect ALK+ ALCL tumour cells or other cells within the tumour microenvironment in a manner that benefits the tumour cells. For example, Karpas 299 cells have been demonstrated to adhere to the ECM protein fibronectin (359). We therefore examined whether GzB might affect adhesion of Karpas 299 cells to fibronectin, hypothesizing that GzB would reduce adhesion of cells by cleaving the fibronectin. When Karpas 299 cells expressing control shRNA were incubated on plates coated with fibronectin we found that about 7.5% of the total cells adhered to the plate, opposed to the <1% that adhered to a plate coated with BSA alone (Appendix A1). When Karpas 299 cells expressing three different GzB shRNA sequences were compared to control cells, two cell lines with GzB knock-down (GzB shRNA #1 and #2) adhered better to the fibronectin matrix. However, the other cell line with GzB knock-down (GzB shRNA #3) actually had a similar (or even slightly reduced) percentage of adhering cells compared to the control cells (Appendix A1). Because integrin  $\beta$ 1 has been shown to mediate adhesion of Karpas 299 cells to fibronectin (359), we next examined whether differences in integrin  $\beta$ 1 levels on the different stable

cell clones might explain the differences we observed in adhesion of these cells. We found that cells with GzB shRNA #1 and #2 had increased integrin  $\beta$ 1 expression compared to control cells, whereas, cells expressing GzB shRNA #3 did not (Appendix A1). The level of integrin  $\beta$ 1 expression appeared to correlate with the proportion of adhering cells for the different cell lines, suggesting that the integrin  $\beta$ 1 expression levels may be a factor contributing to the differences we observed in cell adhesion. Whether GzB might be regulating integrin  $\beta$ 1 levels is unknown, but given that integrin  $\beta$ 1 levels did not correlate with the level of GzB knock-down, this seems unlikely. The differing levels of adhesion and the differences in integrin  $\beta$ 1 expression between the different stable cell lines with GzB knock-down ultimately makes it difficult to conclude whether GzB influences the adhesion of Karpas 299 cells to fibronectin. Whether GzB influences some of the other above mentioned processes is currently an unanswered question; however, a more important question is whether GzB affects ALK+ ALCL pathogenesis *in vivo*. Future work could focus on developing mouse models to address whether GzB promotes ALK+ ALCL pathogenesis *in vivo*. If GzB is found to promote pathogenesis, more work could examine whether it does so by degrading ECM proteins, cell surface receptors or other proteins, and which biological processes this affects.

Our finding that the GzB expressed by ALK+ ALCL cell lines sensitizes these cells to PARP cleavage (Figures 4.14, 4.15 and 4.17) and DNA fragmentation (Figure 4.16) following treatment with apoptosis-inducing drugs suggests that the expression of GzB in ALK+ ALCL may sensitize these cells to drug-induced apoptosis. These findings would be consistent with the fact that patients with ALK+ ALCL are often treated successfully using standard chemotherapy regimens (11-14, 29, 85). Interestingly, we did not observe any reduction in PARP cleavage in Karpas 299 cells with GzB knock-down following doxorubicin treatment, and in one stable cell line with GzB knock-down we actually observed enhanced PARP cleavage compared to control cells (Figure 4.18). The reason for this is not clear;

however, we found that GzB knock-down reduced PARP cleavage (Figure 4.14) and TUNEL staining (Figure 4.16) in Karpas 299 cells treated with staurosporine, and that GzB knock-down reduced PARP cleavage in SUP-M2 and SR cells treated with staurosporine (Figure 4.15) or doxorubicin (Figure 4.17). Taken together, the sensitization to apoptosis by GzB appears to be a common feature of ALK+ ALCL cells, although this could be examined in other cell lines and with other apoptosis-inducing agents to strengthen this argument. Furthermore, whether GzB sensitizes ALK+ ALCL cells to drug-induced apoptosis *in vivo* could also be tested using mouse models.

Although our results suggest that the expression of GzB sensitizes ALK+ ALCL cell lines to drug-induced apoptosis, the mechanism by which GzB does this is currently unknown. Our results demonstrating that the electrophoretic mobility  $\alpha$ -tubulin is altered in ALK+ ALCL cells following GzB knock-down, suggests that there may some active GzB present in the cytoplasm of these cells, or that a portion of cells have active GzB present in their cytoplasm. Normal lymphocytes typically express the endogenous GzB inhibitor, proteinase inhibitor-9, which would protect these cells from GzB if it did “leak” into their cytoplasm (80). However, it has been reported that proteinase inhibitor-9 is not expressed by tumour cells from ALK+ ALCL patients (81), which is consistent with the notion that active GzB is present in the cytoplasm of ALK+ ALCL cells. Another possibility is that GzB is released from granules into the cytosol of cells upon apoptosis induction, which increases the amount of GzB present in the cytoplasm allowing it accelerate apoptosis of the cells. If there is active GzB present or released into the cytoplasm of ALK+ ALCL cell lines, it is likely that it has the ability to cleave various proteins that could be enhancing drug-induced apoptosis in these cells. GzB has been shown to cleave and activate pro-apoptotic proteins, such as caspases (311, 317-321) and Bid (311-315). Furthermore, GzB can cleave and inactivate anti-apoptotic proteins, such as Mcl-1 (316), ICAD (311, 323) and PARP (324). Cleavage of any of these proteins could be contributing the apoptosis

sensitivity conferred by GzB in ALK+ ALCL cell lines. It is also possible that other pro- or anti-apoptotic proteins are cleaved directly by GzB to regulate their activity. Alternatively, GzB has the ability to cleave a variety of signalling proteins, such as the Notch1 transcription factor (360, 361), receptors (360), heat-shock proteins (362, 363) and the ubiquitin fusion degradation protein-2E4 E4 ubiquitin ligase enzyme (364). It is therefore possible that GzB could be indirectly promoting apoptosis in ALK+ ALCL by cleaving different signalling proteins, which in turn, regulate the activity or expression of pro- or anti-apoptotic proteins.

## **CHAPTER 5: THE HEAT SHOCK PROTEIN-90 CO-CHAPERONE, CYCLOPHILIN 40, PROMOTES ALK+ ALCL VIABILITY AND ITS EXPRESSION IS REGULATED BY THE NPM-ALK ONCOPROTEIN**

A portion of this chapter has been published:

**Pearson JD, Mohammed Z, Bacani JTC, Lai R, and Ingham RJ.** (2012) The heat shock protein-90 co-chaperone, Cyclophilin 40, promotes ALK-positive anaplastic large cell lymphoma and its regulation is regulated by the NPM-ALK oncoprotein. *BMC Cancer*. **12**:229.

All experiments contained within this chapter were performed by J. Pearson. Z. Mohammed performed some repeats of the luciferase assays in Figure 5.4A. Joyce Wu and Dr. R. Ingham generated the JunB shRNA stable Karpas 299 cell lines used in Figure 5.2. The original manuscript was written by J. Pearson and Dr. R. Ingham with minor editorial input from Z. Mohammed, Dr. J. Bacani and Dr. R. Lai.

## 5.1: INTRODUCTION

In the quantitative mass spectrometry screen to identify JunB-regulated proteins in ALK+ ALCL cell lines described in Chapter 3 we also identified the heat shock protein-90 (Hsp90) co-chaperone protein, Cyclophilin 40 (Cyp40), as a protein that was down-regulated in cells treated with JunB siRNA. We were particularly intrigued by this finding because the activity of the NPM-ALK oncoprotein in ALK+ ALCL is critically dependent on the molecular chaperone, Hsp90 (365-368).

Hsp90 is a ubiquitously expressed protein that assists in the proper folding and activity of many cellular proteins (369, 370). In ALK+ ALCL, Hsp90 has been shown to promote the stability of NPM-ALK (365-368), as treatment of cell lines with the Hsp90 inhibitor, 17-Allylamino-Demethoxygeldanamycin (17-AAG), resulted in proteasomal degradation of NPM-ALK (367). 17-AAG treatment also disrupted the association of NPM-ALK with Hsp90 (366), and resulted in enhanced association of newly synthesized NPM-ALK with the Hsp70 chaperone (366). This is similar to what has been observed for other tyrosine kinases, such as ErbB2 (371, 372), BCR-ABL and v-Src (373) that are degraded following Hsp90 inhibition. The carboxyl-terminus of Hsp70-interacting protein (CHIP) E3 ubiquitin ligase is often found to target Hsp70-bound client proteins for proteasomal degradation (374). In COS7 cells ectopically expressing NPM-ALK, CHIP associated with NPM-ALK (367), and CHIP over-expression promoted NPM-ALK ubiquitylation and reduced NPM-ALK levels in these cells (367), consistent with the notion that CHIP targets NPM-ALK for degradation.

Consistent with an important role for Hsp90 in regulating NPM-ALK expression, the treatment of ALK+ ALCL cell lines with 17-AAG results in cell cycle arrest and the induction of apoptosis (365, 368); however, these effects are likely due to more than just decreased NPM-ALK levels. Hsp90 inhibition was also shown to result in decreased levels of the pro-survival serine/threonine kinase Akt, and the cell cycle-associated proteins cyclin D1, cyclin-dependent kinase 4 and cyclin-

dependent kinase 6, as well as several other proteins in ALK+ ALCL (365, 368, 375). The treatment of ALK+ ALCL cell lines with 17-AAG also results in decreased phosphorylation of the serine/threonine kinase ERK without affecting ERK levels (365); however, this effect may be due to reduced NPM-ALK expression, as NPM-ALK signalling promotes ERK phosphorylation (191, 268-270). The importance of Hsp90 for regulating ALK fusion proteins is not restricted to NPM-ALK, as the engineered ALK fusion protein, TPR-ALK, was also degraded after treatment of cells with 17-AAG (366). Moreover, the treatment of ALK+ NSCLC cells with Hsp90 inhibitors resulted in degradation of the EML4-ALK oncoprotein and Akt, as well as ERK dephosphorylation in these tumours (376-378). Hsp90 inhibitors are also effective at inhibiting EML4-ALK-driven tumourigenesis *in vivo* in the mouse (376, 377), and the treatment of three ALK+ NSCLC patients with the Hsp90 inhibitor, IPI-504, resulted in a partial response in two patients and stable disease in the other (379). Importantly, Hsp90 inhibitors are effective against tumour cells expressing ALK fusion proteins that possess mutations that render them resistant to the ALK inhibitor, Crizotinib (378, 380). Thus, Hsp90 inhibitors may be useful in treating patients that develop resistance to ALK inhibitors.

One aspect of Hsp90 biology that is largely unstudied in ALK-expressing tumours is the role of Hsp90 co-chaperones. Co-chaperones mediate many aspects of Hsp90 function, including the association of Hsp90 with client proteins and the regulation of Hsp90 ATPase activity (369, 370). Cyp40 belongs to the immunophilin family of Hsp90 co-chaperones, which also includes FK506-binding protein (FKBP) 51, and FKBP52. This family is best characterized for association with Hsp90-steroid hormone receptor complexes containing client proteins such as the glucocorticoid, estrogen, progesterone, and androgen receptors (381-384). The individual immunophilin family members show some preference for specific hormone receptors, and they can both antagonize or promote the transcription mediated by these receptors. For example, FKBP51 inhibits the transcriptional activity of the glucocorticoid receptor (385-387), while FKBP52 is

important for promoting the transcriptional activity of this receptor (386-389). In addition to steroid hormone receptors, immunophilin co-chaperones have been found to complex with the Lck (390) and Fes (391) tyrosine kinases. As well, the expression and activity of ectopically expressed v-Src oncoprotein in *Saccharomyces cerevisiae* is dependent on the Cyp40 homolog, Cpr7 (392). Immunophilin co-chaperones are also important in cancer, as Cyp40 and FKBP51 have been shown to promote proliferation of androgen-independent prostate cancer cell lines and were required for proliferation of an androgen-dependent prostate cancer cell line in response to androgen treatment (393).

Here, we demonstrate that JunB and NPM-ALK promote the expression of Cyp40 in ALK+ ALCL. We further examined the regulation of the related immunophilin co-chaperones, FKBP51 and FKBP52, in ALK+ ALCL and found that while JunB does not regulate expression of these proteins, NPM-ALK does promote FKBP52 expression. Given the importance of co-chaperone proteins for Hsp90 function and the critical role of Hsp90 in ALK+ ALCL, we further examined the importance of the immunophilin co-chaperones in ALK+ ALCL. Knock-down of Cyp40, but not FKBP51 or FKBP52, reduced the viability of ALK+ ALCL cell lines; however, the mechanism by which Cyp40 does this has yet to be elucidated, as Cyp40 knock-down does not appear to regulate NPM-ALK expression or signalling.

## **5.2: JUNB PROMOTES CYP40, BUT NOT FKBP51 OR FKBP52, PROTEIN EXPRESSION IN ALK+ ALCL CELL LINES**

In the quantitative mass spectrometry screen discussed in section 3.2, we also identified Cyp40 as a down-regulated protein in cells transfected with JunB siRNA. In the two separate iTRAQ experiments, two peptides corresponding to Cyp40 were found in each experiment to have reduced abundance in cell lysates from both Karpas 299 and SUP-M2 cells transfected with JunB siRNA (Table 5.1), suggesting that JunB promotes the expression of Cyp40 in ALK+ ALCL.

|              | Cyp40 peptides used for quantification | Karpas 299           |                   | SUP-M2               |                  |
|--------------|--|----------------------|-------------------|----------------------|------------------|
|              |  | Relative Cyp40 Level | Rank              | Relative Cyp40 level | Rank             |
| Experiment 1 | 2                                      | 0.7316               | 7 <sup>th</sup>   | 0.8107               | 13 <sup>th</sup> |
| Experiment 2 | 2                                      | 0.9011               | 138 <sup>th</sup> | 0.9185               | 84 <sup>th</sup> |

**Table 5.1: Summary of Cyp40 quantitative mass spectrometry results.**

The summarized Cyp40 results from the two independent iTRAQ experiments are shown. The “relative Cyp40 level” is the ratio of Cyp40 protein in the JunB siRNA-treated cell lysate compared to control siRNA-treated cells. “Rank” indicates the rank order of Cyp40 on the list of down-regulated proteins in the Karpas 299 or SUP-M2 JunB siRNA-treated cell lysates for the indicated experiment.

Since Cyp40 was identified as a potential JunB-regulated protein in our mass spectrometry screen, we first wanted to confirm these findings. We used quantitative western blotting to examine Cyp40 protein expression in ALK+ ALCL cell lines transfected with JunB siRNA. Consistent with our mass spectrometry findings, we observed a decrease in Cyp40 protein expression after JunB knock-down in both the Karpas 299 and SUP-M2 ALK+ ALCL cell lines (Figure 5.1A). Because Cyp40 belongs to the immunophilin family of Hsp90 co-chaperone proteins, which includes FKBP51 and FKBP52, we next examined whether JunB also promotes the expression of these proteins. However, we found that JunB knock-down did not influence FKBP51 or FKBP52 protein expression in ALK+ ALCL cell lines (Figure 5.1B and C).

To confirm that the reduction in Cyp40 levels after JunB knock-down was not due to off-targeting by the pooled JunB siRNAs, we examined Cyp40 protein levels after JunB knock-down using Karpas 299 cells stably expressing an inducible JunB shRNA. Following treatment of these cells with IPTG to induce expression of the JunB shRNA, we observed a dose-dependent down-regulation of Cyp40 protein levels over 48 and 72 hrs (Figure 5.2). However, treatment of cells expressing a control (non-targeting) shRNA had no effect on Cyp40 levels (Figure 5.2), demonstrating that the reduction in Cyp40 levels was due to JunB knock-down.

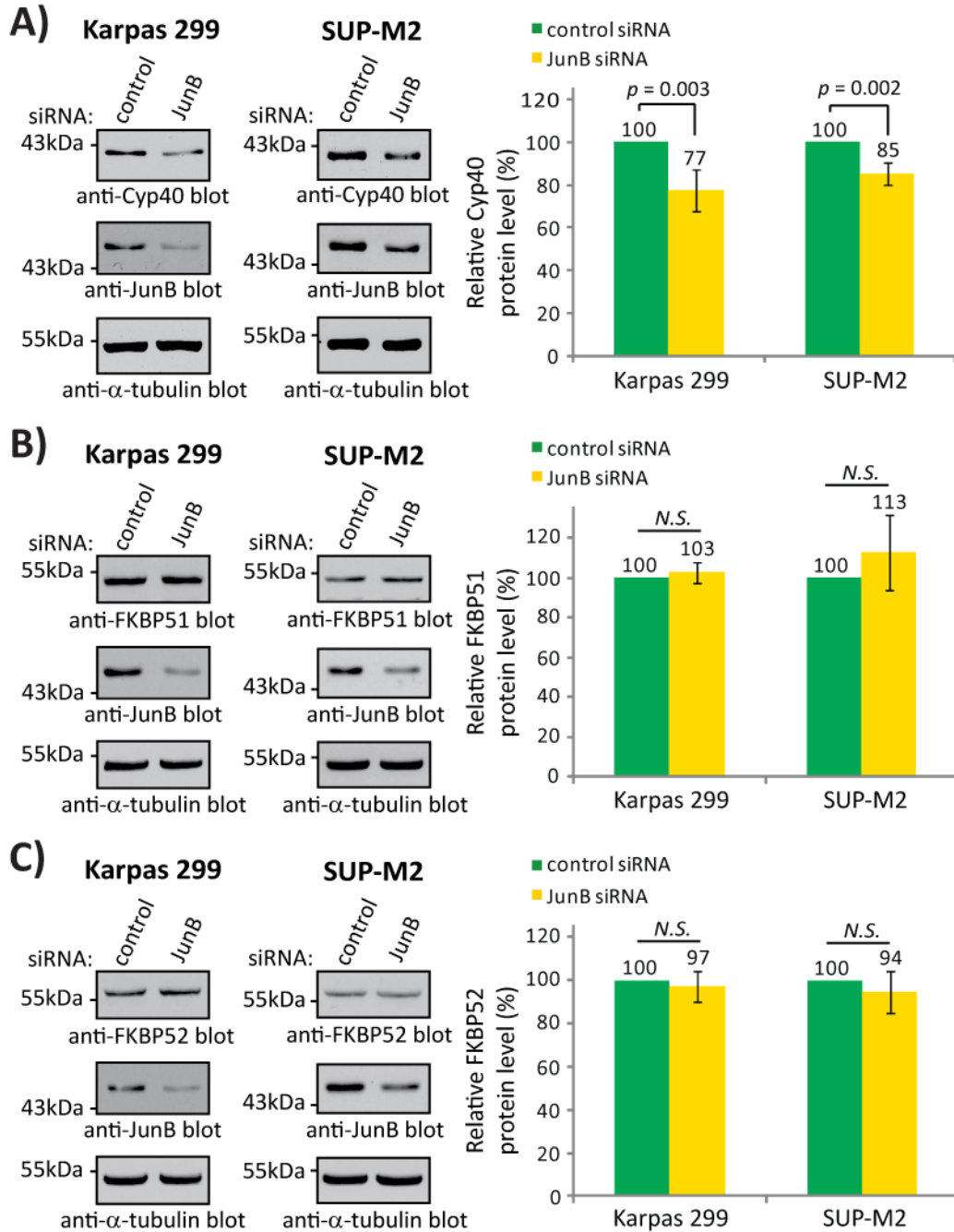


**Figure 5.1: JunB promotes Cyp40, but not FKBP51 or FKBP52, protein expression in ALK+ ALCL.**

Western blot analysis (left) and quantification (right) of Cyp40 (A), FKBP51 (B), and FKBP52 (C) levels in lysates collected from Karpas 299 and SUP-M2 cells treated with pooled control or JunB siRNA. Quantification represents the mean and standard deviation of five (Cyp40) or four (FKBP51 and FKBP52) experiments.  $p$  values were obtained using paired, one-tailed  $t$ -tests. N.S. indicates a  $p$  value > 0.05. Molecular mass markers are shown to the left of the blots.

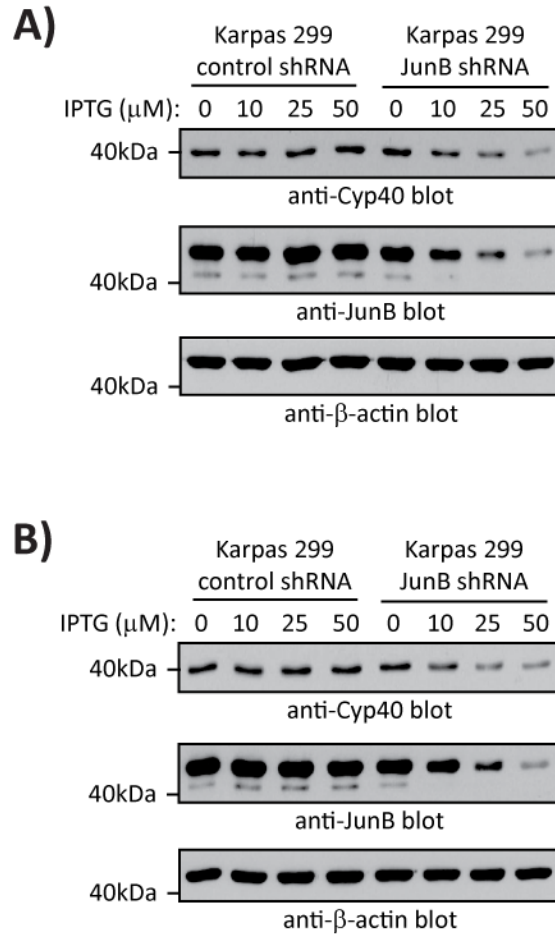


**Figure 5.2: shRNA-mediated knock-down of JunB results in reduced Cyp40 protein expression.**

Karpas 299 cells stably expressing an IPTG-inducible control (non-targeting) or JunB shRNA were treated with 10, 25 or 50  $\mu$ M IPTG or were left untreated for 48 hrs (**A**) or 72 hrs (**B**) to induce the shRNA. Lysates were then collected and JunB and Cyp40 protein levels were assessed using western blotting. Anti- $\beta$ -actin western blots demonstrate equivalent protein loading. Molecular mass markers are indicated to the left of the blots.

### 5.3: JUNB PROMOTES *CYP40* TRANSCRIPTION IN ALK+ ALCL CELL LINES

We next examined *Cyp40* mRNA levels after treatment of cells with JunB siRNA, and found that knock-down of JunB resulted in reduced *Cyp40* mRNA levels in Karpas 299 and SUP-M2 cells (Figure 5.3). To determine if JunB can promote transcription from the *Cyp40* promoter, we generated a firefly luciferase reporter construct under control of the human *Cyp40* proximal promoter. When transfected into Karpas 299 cells this construct exhibited strong luciferase activity, which was reduced when cells were co-transfected with JunB siRNA (Figure 5.4A). In addition, over-expression of Myc-tagged JunB promoted transcription from this luciferase reporter, further demonstrating that JunB promotes *Cyp40* transcription (Figure 5.4B). The *Cyp40* promoter contains a consensus sequence for AP-1 transcription factors (394) that could be recognized by JunB. Mutation of this site resulted in reduced luciferase activity (Figure 5.4C), demonstrating this site is important for regulating *Cyp40* transcription.

Since the AP-1 site was important for promoting transcription from the *Cyp40* promoter, we next used EMSA experiments to determine whether JunB can bind this site (Figure 5.5). We found that a protein(s) expressed by Karpas 299 cells associated with a biotinylated probe corresponding to the AP-1 site in the *Cyp40* promoter. This interaction was specific to the AP-1 site in the probe, because inclusion of an excess of an unlabelled wild type probe (wt competitor) blocked shifting of the biotinylated *Cyp40* promoter probe by Karpas 299 nuclear extract, whereas an unlabelled probe with a mutation in the AP-1 site (AP-1 mutant competitor) did not. We further found that JunB was a major component of the probe/protein complex(es) bound to the *Cyp40* promoter AP-1 site, as inclusion of an anti-JunB antibody in the binding reaction resulted in an almost complete super-shift of the probe/protein complex, while an isotype control antibody had no effect. Taken together, our results argue that JunB functions as a direct transcriptional activator of *Cyp40* in ALK+ ALCL.

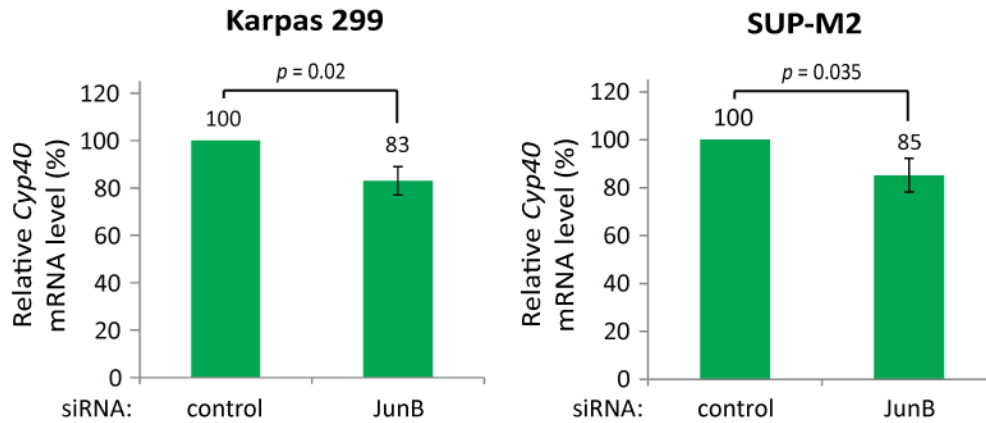


**Figure 5.3: siRNA-mediated knock-down of JunB results in reduced *Cyp40* mRNA expression in ALK+ ALCL cells.**

qRT-PCR analysis of *Cyp40* mRNA levels in Karpas 299 (left) and SUP-M2 (right) cells transfected with pooled control (non-targeting) or JunB siRNAs. *Cyp40* mRNA levels were normalized to the  $\beta$ -actin housekeeping gene. Quantification represents the mean and standard deviation of three independent experiments and *p* values were determined using paired, one-tailed *t*-tests.

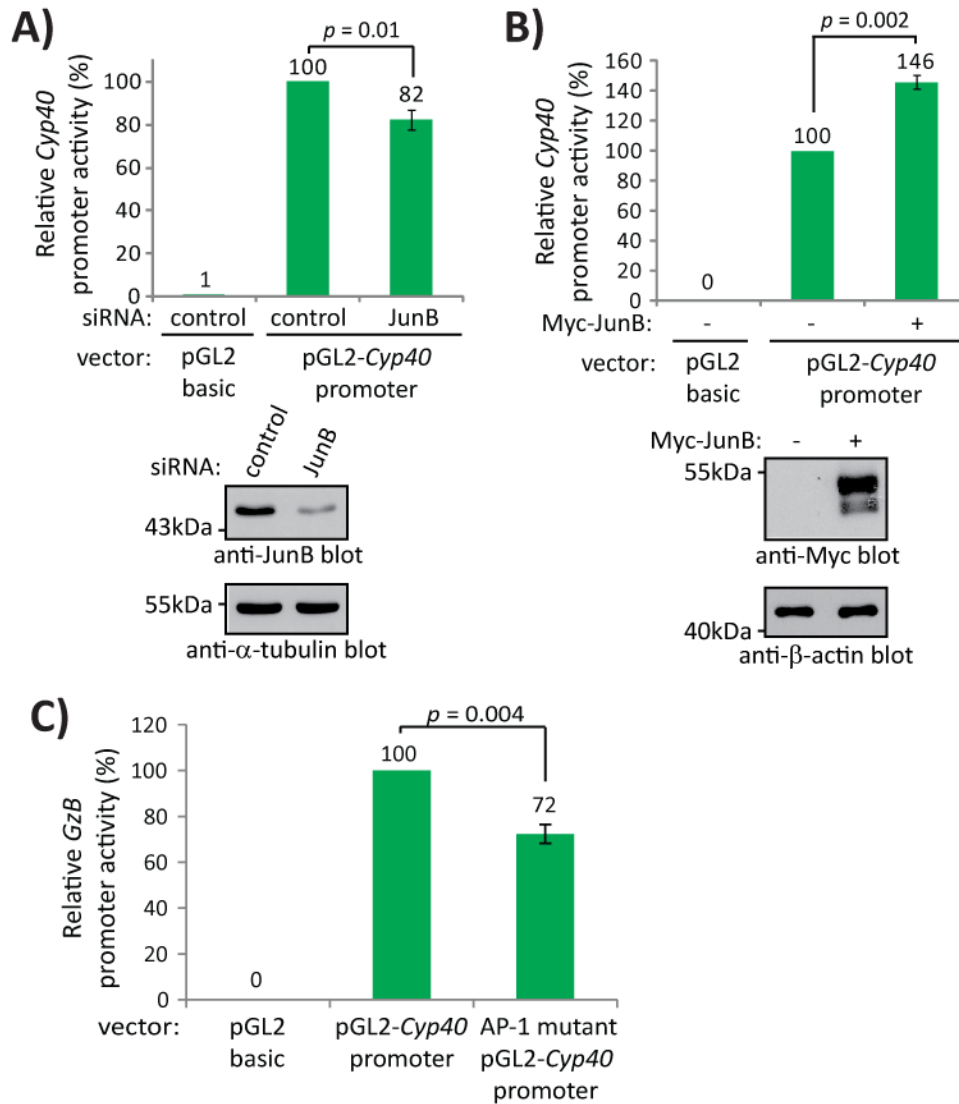


**Figure 5.4: JunB promotes transcription from the *Cyp40* promoter.**

**(A)** Luciferase activity was analysed in Karpas 299 cells transfected with a human *Cyp40* promoter-driven (pGL2-*Cyp40* promoter) or promoter-less (pGL2 basic) luciferase vector, and pooled control or JunB siRNA. Results are presented relative to cells co-transfected with pGL2-*Cyp40* promoter and control siRNA. A western blot demonstrating JunB silencing is shown below. **(B)** Luciferase activity was measured in Karpas 299 cells transfected with the luciferase constructs described in **(A)** along with empty vector (-) or Myc-tagged JunB (+) (top). A western blot illustrating expression of the Myc-tagged JunB is shown below. **(C)** Luciferase activity in Karpas 299 cells transfected with the pGL2 basic, pGL2-*Cyp40* promoter, or an AP-1 mutant pGL2-*Cyp40* promoter luciferase construct. Luciferase activity is expressed relative to the pGL2-*Cyp40* promoter transfected cells. Error bars represent the standard deviation of three independent experiments. *p* values were determined using paired, one-tailed *t*-tests.

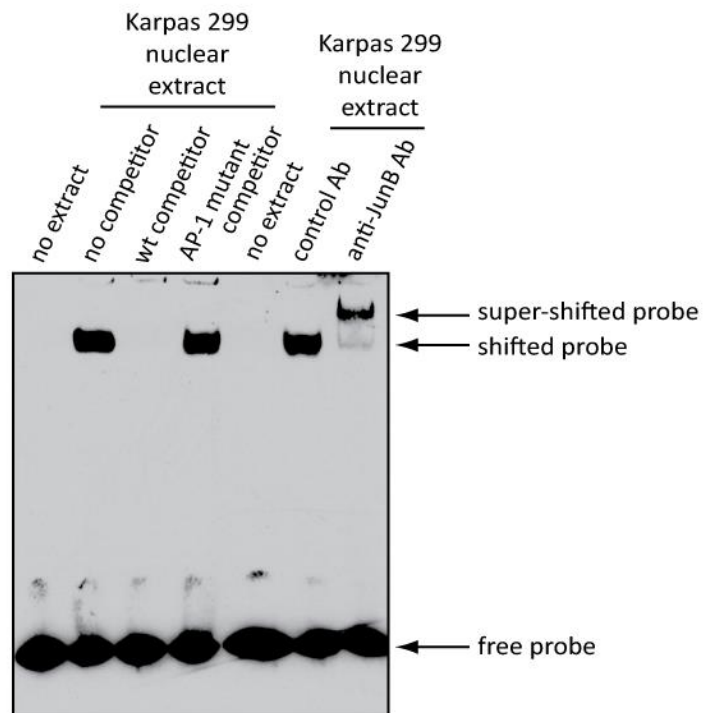


**Figure 5.5: JunB binds to the AP-1 site of the *Cyp40* promoter.**

EMSAs examining JunB binding to the AP-1 site in the *Cyp40* promoter were performed using a biotinylated *Cyp40* AP-1 probe and no competitor, an unlabelled *Cyp40* promoter AP-1 competitor (wt competitor) or an unlabelled *Cyp40* competitor with a mutation in the AP-1 site (AP-1 mutant competitor). For super-shift experiments, an isotype control (control) or an anti-JunB antibody (Ab) were included in the binding reaction. “No extract” represents a sample where no Karpas 299 nuclear extract was added to the binding reaction and demonstrates mobility of the biotinylated free probe.

#### **5.4: NPM-ALK PROMOTES CYP40 AND FKBP52, BUT NOT FKBP51, EXPRESSION**

The NPM-ALK oncoprotein drives much of the signalling underlying the pathogenesis of ALK+ ALCL (24, 190), including the elevated expression of JunB (51, 191, 395). Therefore, we next examined whether NPM-ALK promotes expression of the immunophilin co-chaperones in ALK+ ALCL. We found that knock-down of NPM-ALK in Karpas 299 and SUP-M2 cells resulted in significantly reduced Cyp40 protein levels (Figure 5.6A). Furthermore, NPM-ALK knock-down resulted in a substantial reduction in JunB levels, that was comparable to reduction in JunB observed after JunB siRNA treatment (compare Figure 5.1 to Figure 5.6A). Knock-down of NPM-ALK also resulted in decreased FKBP52 expression, but had no effect on the expression of FKBP51 (Figure 5.6B and C, respectively). Using qRT-PCR, we found that knock-down of NPM-ALK also reduced *Cyp40* (Figure 5.7A) and *FKBP52* (Figure 5.7B) mRNA expression in ALK+ ALCL cell lines. These findings suggest that both *Cyp40* and *FKBP52* are transcriptional targets of NPM-ALK signalling in ALK+ ALCL.

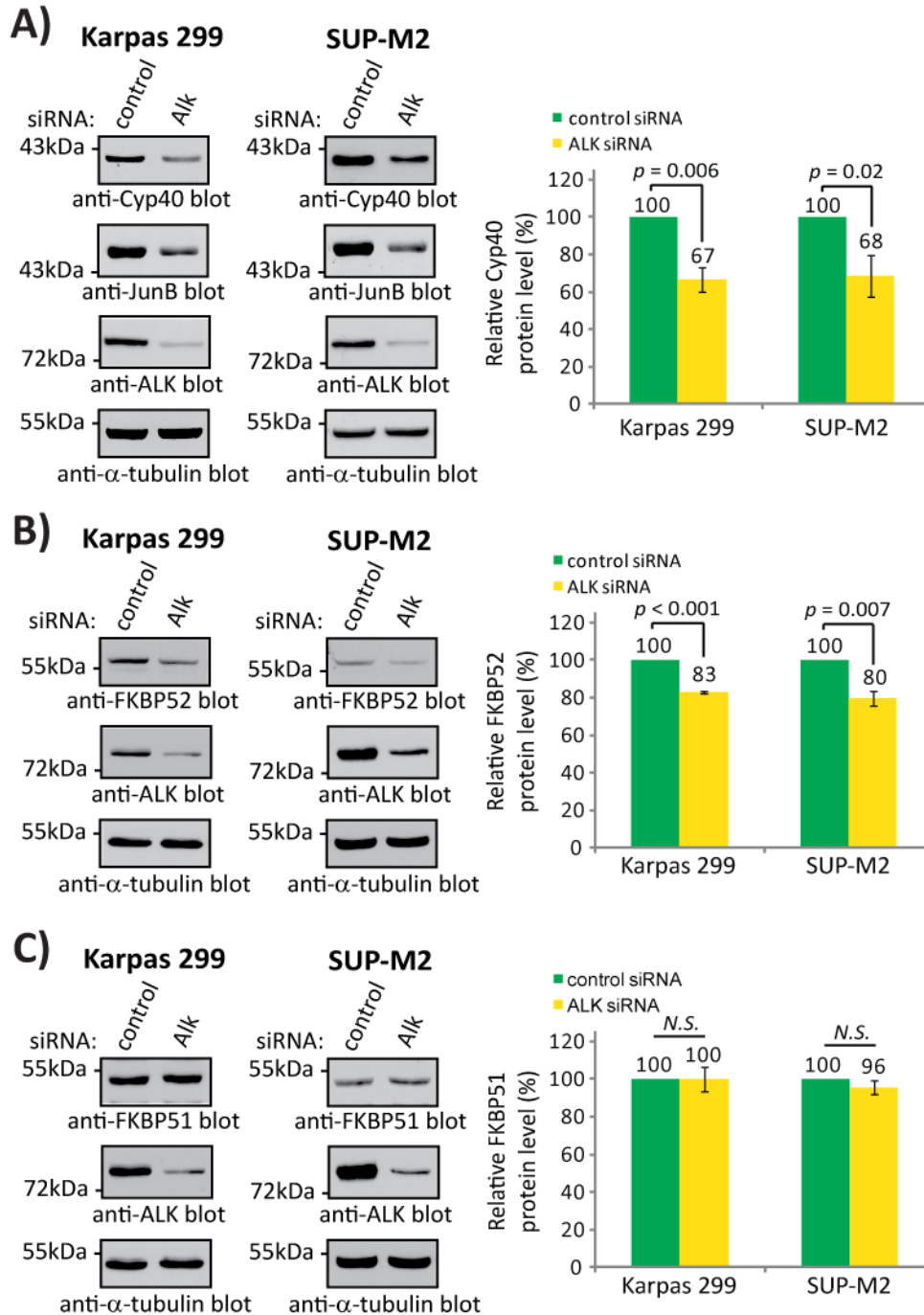


**Figure 5.6: NPM-ALK promotes Cyp40 and FKBP52, but not FKBP51, protein expression in ALK+ ALCL cell lines.**

Western blot analysis (left) and quantification (right) of Cyp40 **(A)**, FKBP52 **(B)**, and FKBP51 **(C)** protein levels in Karpas 299 and SUP-M2 cells transfected with pooled control or ALK siRNA. Error bars represent the standard deviation of the mean of three independent experiments.  $p$  values were obtained using paired, one-tailed  $t$ -tests. *N.S.* indicates a  $p$  value  $> 0.05$ .

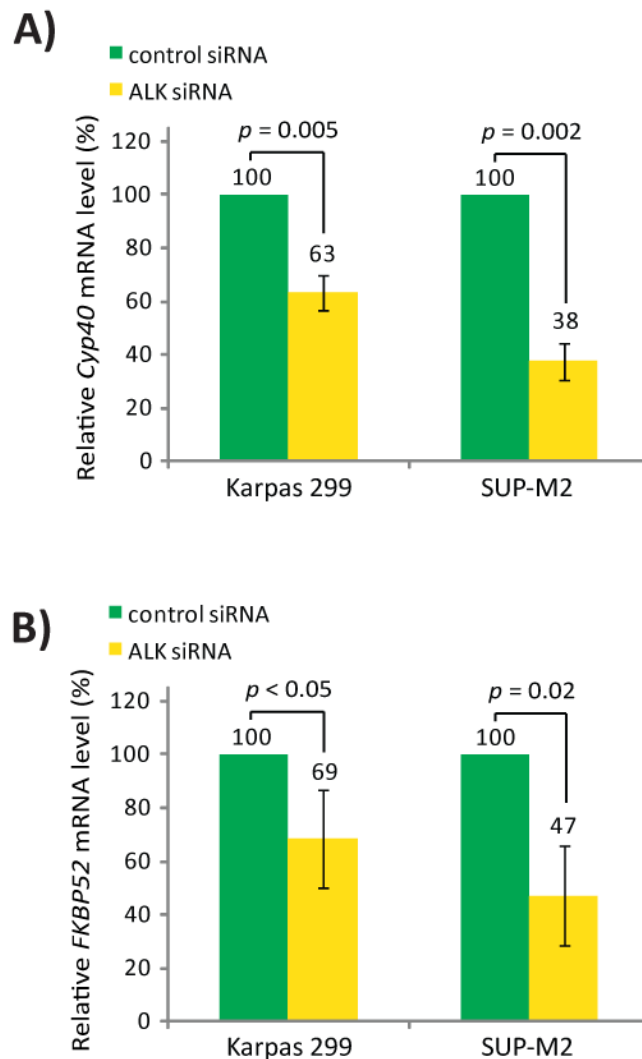


**Figure 5.7: NPM-ALK promotes *Cyp40* and *FKBP52* mRNA expression in ALK+ ALCL.**

qRT-PCR analysis of *Cyp40* (**A**) and *FKBP52* (**B**) mRNA expression in Karpas 299 and SUP-M2 cells transfected with pooled control or ALK siRNA. mRNA levels were normalized to the housekeeping gene  $\beta$ -*actin*. Quantification represents the mean and standard deviation of three independent experiments. *p* values were obtained using paired, one-tailed *t*-tests.

To further examine the regulation of the immunophilin co-chaperones by NPM-ALK, we treated ALK+ ALCL cell lines with the ALK inhibitor, Crizotinib, that has been shown to be useful in treating patients with ALK+ ALCL (175) and EML4-ALK+ NSCLC (176, 396, 397). Treatment of Karpas 299 and SUP-M2 cells with Crizotinib resulted in a dose- (Figure 5.8A) and time-dependent (Figure 5.8B) decrease in NPM-ALK phosphorylation on tyrosines 338, 342, and 343. These phosphorylation sites are located within the activation loop of the ALK kinase domain, and their phosphorylation correlates with NPM-ALK activation (398, 399). We also observed a strong reduction in phosphorylation of STAT3 on tyrosine 705 (Figure 5.8A and B), a known target of NPM-ALK signalling (400-402), after Crizotinib treatment, demonstrating the efficiency of the drug treatment. Furthermore, we observed a dose- (Figure 5.9) and time-dependent (Figure 5.10) decrease in Cyp40 and FKBP52 protein expression in both Karpas 299 and SUP-M2 cells after Crizotinib treatment. In contrast, Crizotinib treatment did not decrease FKBP51 expression in either cell line; however it did result in a modest increase in FKBP51 expression in the Karpas 299 cells at low Crizotinib doses (Figure 5.9A). Thus, similar to our NPM-ALK knock-down results, treatment of ALK+ ALCL cell lines with an NPM-ALK inhibitor resulted in reduced Cyp40 and FKBP52, but not FKBP51, expression.

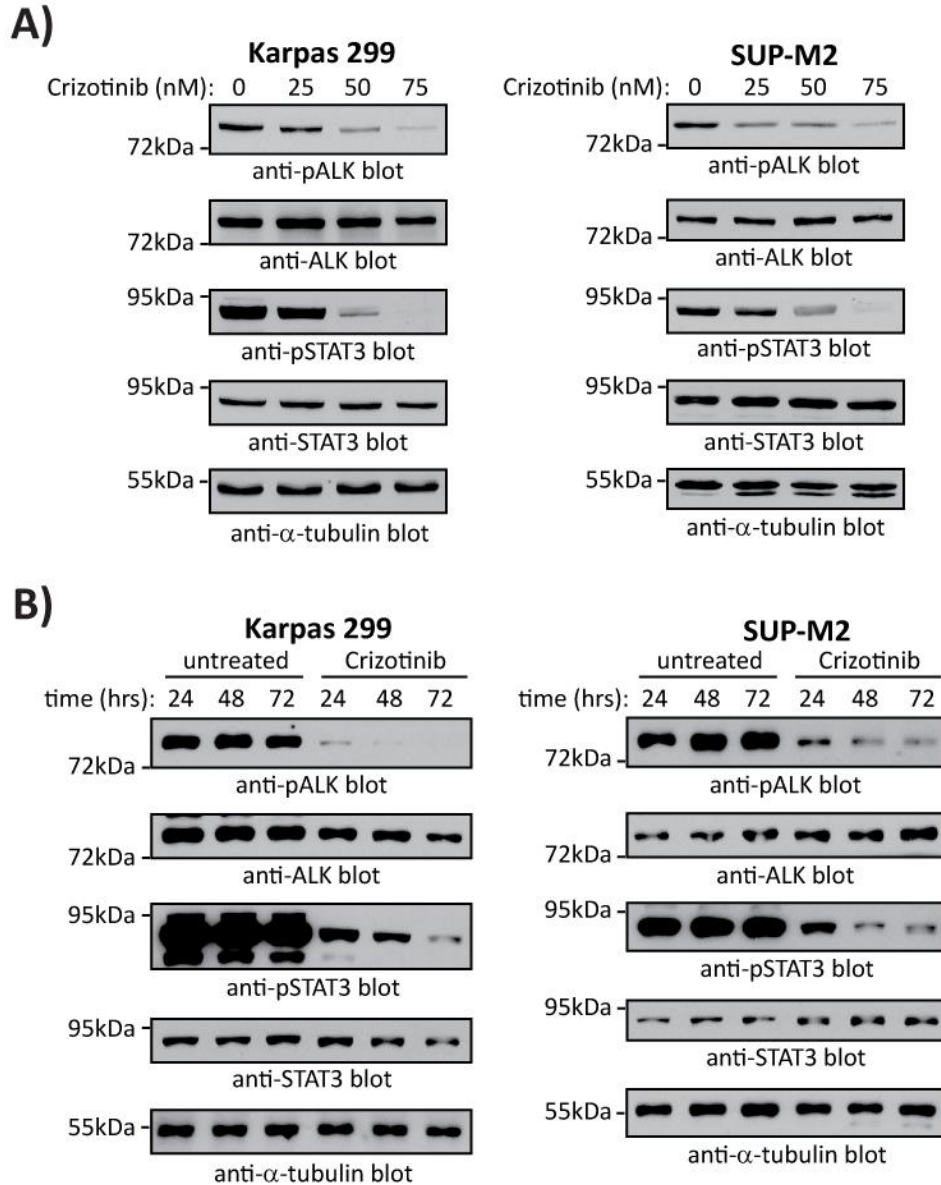


**Figure 5.8: Crizotinib efficiently inhibits NPM-ALK activity in ALK+ ALCL cell lines.**

**(A)** Western blot analysis examining NPM-ALK phosphorylation (anti-pALK blot) and STAT3 phosphorylation (anti-pSTAT3 blot) in Karpas 299 (left) or SUP-M2 (right) cells left untreated or treated with 25, 50 or 75 nM of the ALK inhibitor, Crizotinib, for 48 hrs. **(B)** NPM-ALK and STAT3 phosphorylation was analysed in Karpas 299 (left) or SUP-M2 (right) cells left untreated or treated with 75 nM Crizotinib for 24, 48 or 72 hrs. Anti-α-tubulin western blots demonstrate protein loading. Molecular mass markers are indicated to the left of the blots.

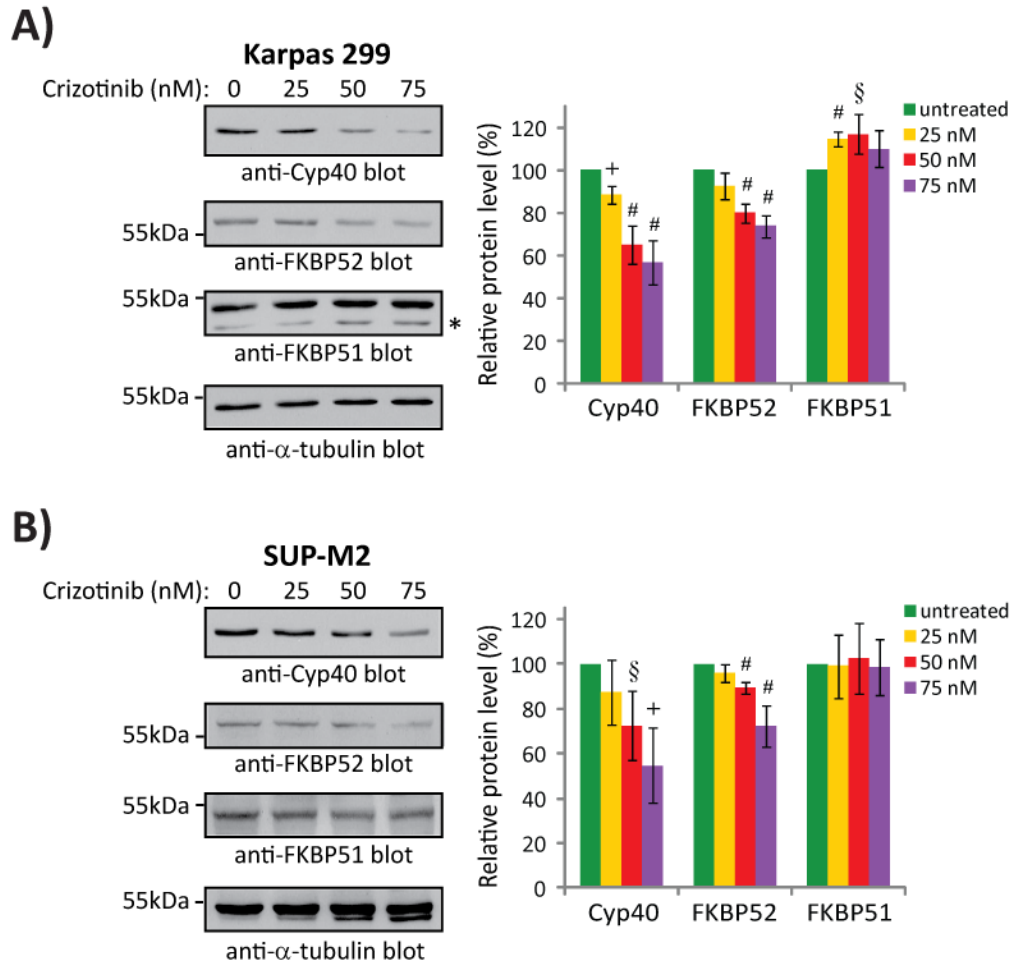


**Figure 5.9: Inhibition of NPM-ALK activity results in a dose-dependent reduction in Cyp40 and FKBP52 protein levels.**

Western blot analysis (left) and quantification (right) of Cyp40, FKBP52 and FKBP51 protein levels in Karpas 299 (A) or SUP-M2 (B) cells untreated or treated with 25, 50 or 75 nM Crizotinib for 48 hrs. \* indicates a non-specific band in the anti-FKBP51 blot. Quantification is presented relative to untreated cells (which were set to 100%), and represents the mean and standard deviation of four independent experiments.  $p$  values comparing untreated cells to cells treated with each concentration of Crizotinib were obtained using paired, one-tailed  $t$ -tests. §  $p < 0.05$ , +  $p < 0.01$ , #  $p < 0.005$ . The anti- $\alpha$ -tubulin blots are included to demonstrate protein loading. Molecular mass markers are shown to the left of blots.

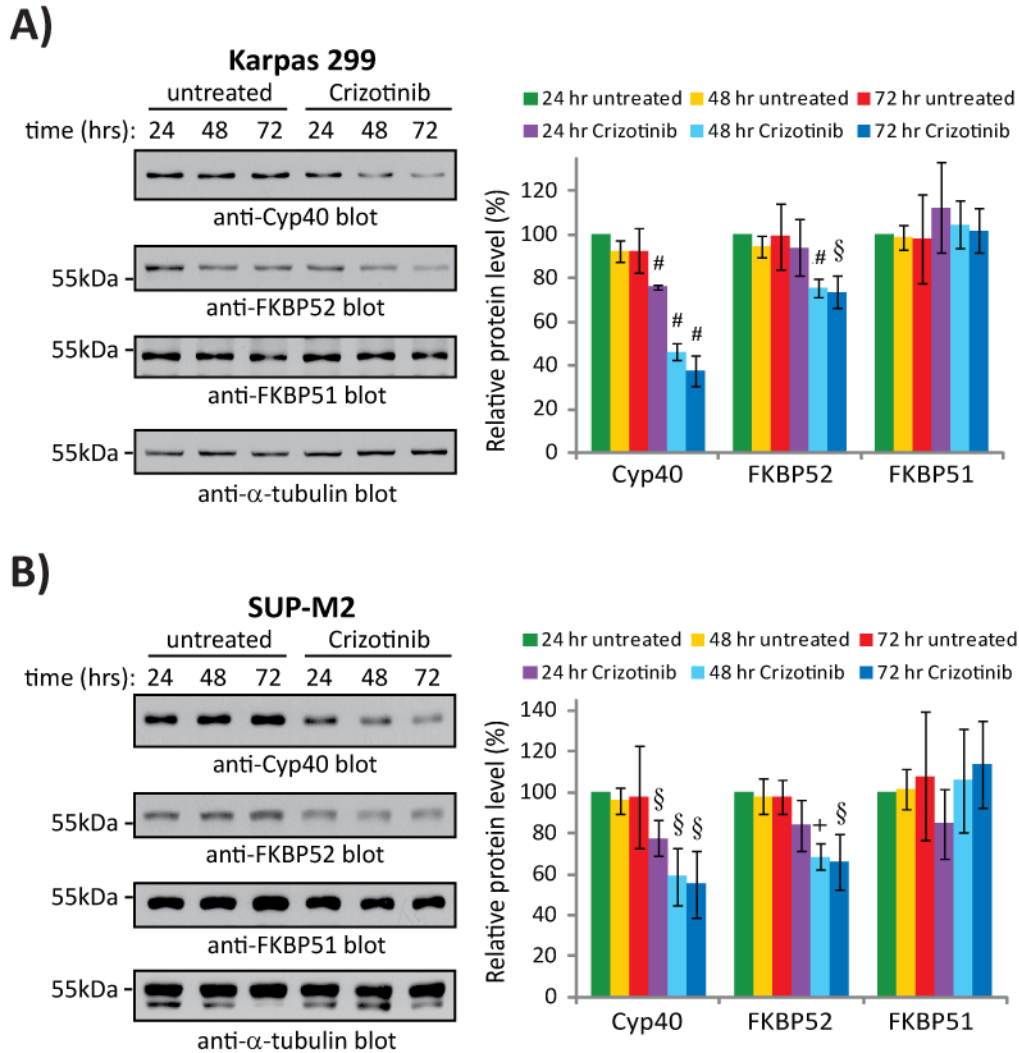


**Figure 5.10: Inhibition of NPM-ALK activity results in a time-dependent reduction in Cyp40 and FKBP52 protein levels.**

Western blot analysis (left) and quantification (right) of Cyp40, FKBP52 and FKBP51 protein levels in Karpas 299 (**A**) or SUP-M2 (**B**) cells untreated or treated with 75 nM Crizotinib for 24, 48 or 72 hrs. Quantification is presented relative to untreated cells at 24 hrs (which was set to 100%), and represents the mean and standard deviation of three independent experiments. *p* values comparing treated cells at each time point to untreated cells at the 24 hr time point were obtained using paired, one-tailed *t*-tests. § *p* < 0.05, + *p* < 0.01, # *p* < 0.005. Anti- $\alpha$ -tubulin western blots demonstrate equivalent protein loading. Molecular mass markers are indicated to the left of the blots.

## **5.5: KNOCK-DOWN OF CYP40 REDUCES THE VIABILITY OF ALK+ ALCL CELL LINES**

Hsp90 is vitally important for the proliferation and survival of ALK+ ALCL cell lines (365, 368), and is required for the expression and activation of NPM-ALK and other important signalling proteins in this lymphoma (365-368, 375). Therefore, we examined whether the immunophilin co-chaperones were similarly important in ALK+ ALCL by examining the effect of their knock-down on cellular viability. Treatment of cells with Cyp40 siRNA resulted in reduced viability of both Karpas 299 and SUP-M2 cells as measured by MTS assay (Figure 5.11). However, we found that reducing the expression of either FKBP51 or FKBP52 did not significantly affect the viability of these cell lines (Figure 5.11). The immunophilin co-chaperones are known to associate with Hsp90-client protein complexes containing over-lapping substrate proteins (391, 403, 404); therefore, we next sought examine whether knock-down of FKBP51 and FKBP52 in combination with Cyp40 resulted in a greater reduction in viability compared to knock-down of Cyp40 alone. To generate a pooled siRNA to knock-down all three immunophilin co-chaperones, we first tested four individual siRNAs for each of the immunophilin co-chaperones to identify the most effective siRNAs for each gene (Figure 5.12). While transfection of all four individual siRNAs into Karpas 299 cells resulted in knock-down of the expected protein, for Cyp40 and FKBP51 siRNA #1 and #2 were able to silence more efficiently than siRNA #3 and #4. We found that FKBP52 siRNA #2 silenced FKBP52 levels slightly more efficiently than the other three siRNAs, all of which reduced FKBP52 expression to a similar extent. We then generated a siRNA pool to target Cyp40, FKBP51 and FKBP52 in combination that consisted of siRNA #1 and #2 for each target. Knock-down of all three immunophilin family members in combination did not significantly reduce viability over Cyp40 knock-down alone in Karpas 299 and SUP-M2 cells (Figure 5.13). This finding argues that the reduced viability observed in these cell lines is predominantly due to decreased Cyp40 expression.

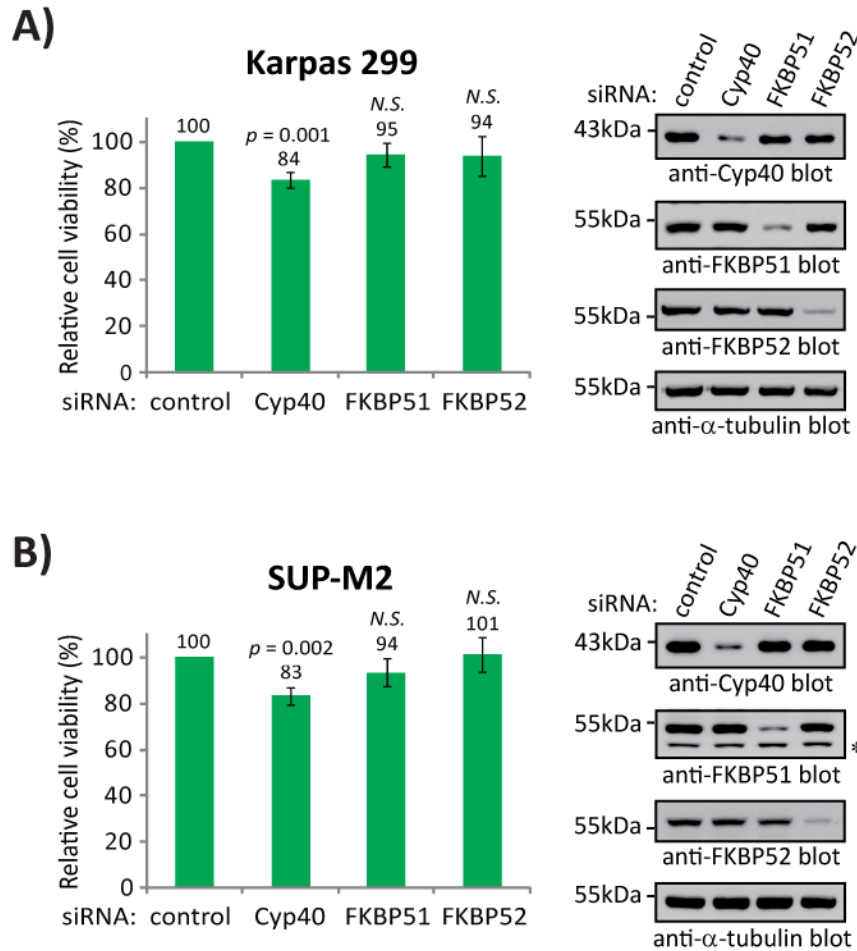


**Figure 5.11: Cyp40, but not FKBP51 or FKBP52, promotes ALK+ ALCL viability.**

The viability of Karpas 299 (A) or SUP-M2 (B) cells transfected with the indicated pooled siRNAs was measured using the MTS assay (left). Quantification represents the mean and standard deviation of four independent experiments. *p* values comparing cells transfected with the indicated siRNA to those transfected with control siRNA were obtained using paired, one-tailed *t*-tests. *N.S.* indicates a *p* value > 0.05. Western blots (right) demonstrate the silencing efficiency of the targeted proteins. Anti- $\alpha$ -tubulin western blots demonstrate equal protein loading and molecular mass markers are indicated to the left of the blots. \* indicates a non-specific band in the anti-FKBP51 blot.

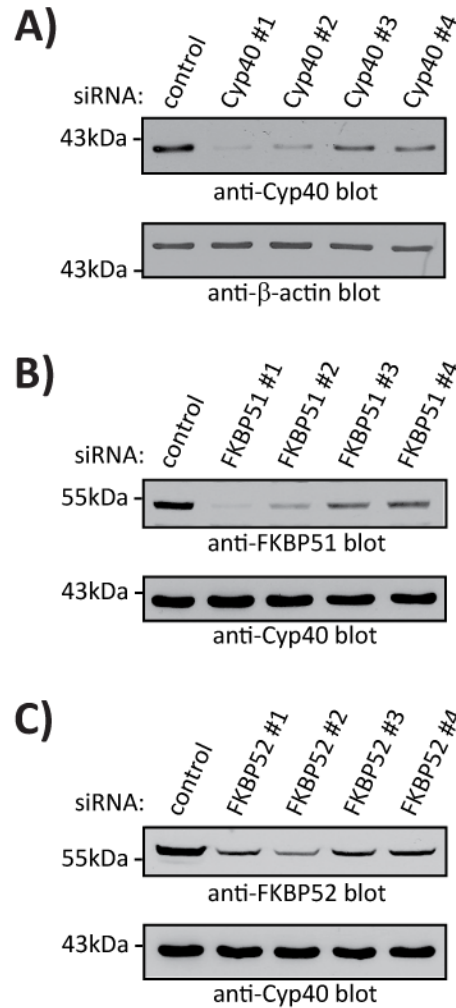


**Figure 5.12: Knock-down of Cyp40, FKBP51 and FKBP52 with individual siRNAs.**

Western blotting was used to assess knock-down of Cyp40 **(A)**, FKBP51 **(B)** or FKBP52 **(C)** in Karpas 299 cells transfected with four different individual siRNAs (#1 - #4) to silence each target. In **(A)**, the anti- $\beta$ -actin blot demonstrates equivalent loading. In **(B)** and **(C)**, the anti-Cyp40 blot demonstrates equivalent protein loading. Molecular mass markers are shown to the left of the western blots. Note that the experiments for FKBP51 **(B)** and FKBP52 **(C)** were performed only once.

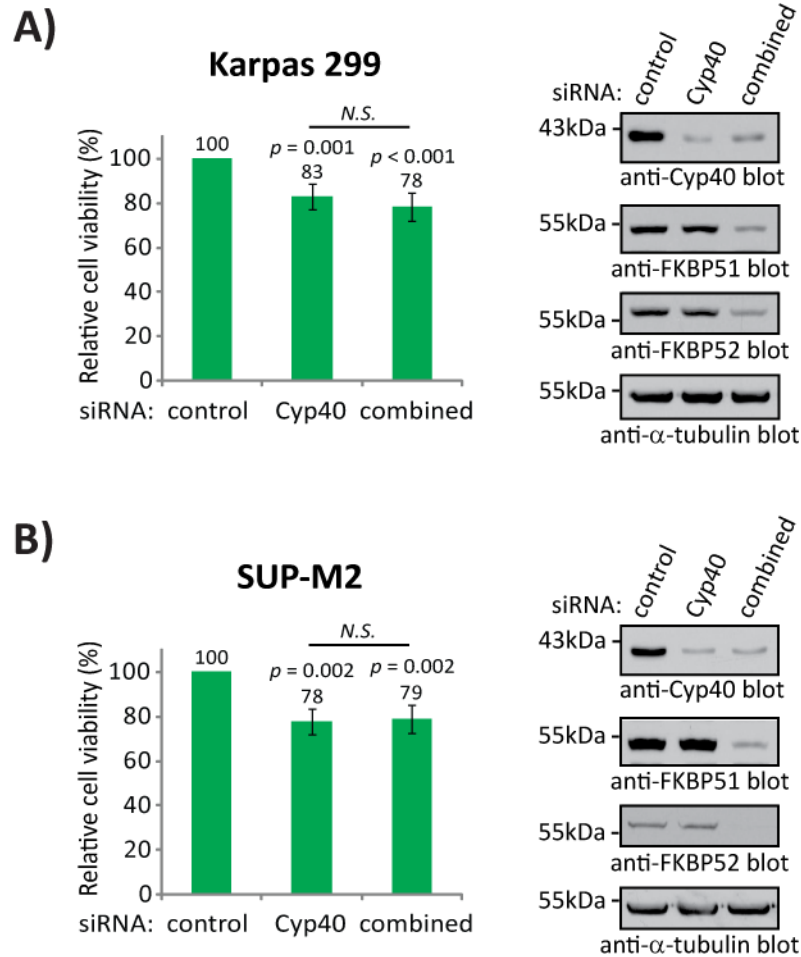


**Figure 5.13: Knock-down of Cyp40, FKBP51 and FKBP52 in combination does not reduce cell viability more than Cyp40 knock-down alone.**

Viability of Karpas 299 (A) or SUP-M2 (B) cells transfected with the indicated pooled siRNAs was measured using the MTS cell viability assay (left). Combined siRNA consists of siRNAs to target the three immunophilin co-chaperones, Cyp40, FKBP51 and FKBP52. Quantification represents the mean and standard deviation of four independent experiments.  $p$  values comparing cells transfected with the indicated siRNA to those transfected with control siRNA were obtained using paired, one-tailed  $t$ -tests.  $p$  values comparing cells transfected with Cyp40 or combined siRNA were obtained using unpaired, one-tailed  $t$ -tests. *N.S.* indicates a  $p$  value  $> 0.05$ . Western blots (right) are included to demonstrate silencing of the indicated proteins. Anti- $\alpha$ -tubulin blots demonstrate equivalent protein loading. Molecular mass makers are indicated to the left of the blots.

## **5.6: CYP40 KNOCK-DOWN DOES NOT AFFECT NPM-ALK LEVELS OR TYROSINE PHOSPHORYLATION, OR THE PHOSPHORYLATION OF CELLULAR PROTEINS**

Cyp40 is primarily noted for its role in co-chaperoning with Hsp90 in complex with steroid hormone receptors (381-384). However, Cyp40 has also been found in Hsp90-kinase client complexes. For example, Hsp90-Cyp40 complexes associate with the Lck (390) and Fes (391) tyrosine kinases, and the stability and signalling capacity of ectopically expressed v-Src in *S. cerevisiae* is dependent on the yeast Cyp40 homolog, Cpr7 (392). Therefore, we examined whether the decrease in viability due to Cyp40 knock-down could be attributed to a failure of Cyp40 to help Hsp90 stabilize NPM-ALK or allow NPM-ALK to signal. We observed no difference in NPM-ALK levels (Figure 5.14A), phosphorylation on tyrosines 338, 342, and 343 (Figure 5.14B), or overall tyrosine phosphorylation (Figure 5.14C) in Karpas 299 or SUP-M2 cells treated with Cyp40 siRNA. Moreover, we saw no significant alteration in the tyrosine phosphorylation of total cellular proteins after Cyp40 knock-down (Figure 5.15A). However, knock-down of NPM-ALK in these cell lines resulted in a dramatic reduction in the tyrosine phosphorylation of total cellular proteins (Figure 5.15A). We also observed no effect on phosphorylation of STAT3 on tyrosine 705 after knock-down of Cyp40 (Figure 5.15B). Phosphorylation of STAT3 on this residue is promoted by NPM-ALK signalling (400-402) and is critical for STAT3 DNA binding and transcriptional activity (405-407). We next examined the phosphorylation of ERK1/2 (on Thr 202 and Tyr 204) and expression of JunB and c-Jun, all of which are downstream targets of NPM-ALK signalling (51, 191, 194, 269, 270). We observed no alteration in the phosphorylation of ERK or the expression of these proteins after Cyp40 knock-down (Figure 5.15B). We also found no alteration in the level of Akt (Figure 5.15B), which is a known Hsp90 target in this lymphoma (365). Thus, while Cyp40 is important for the viability of ALK+ ALCL cell lines, our results argue that it does not appear to be influencing viability through regulating NPM-ALK levels or activity, or levels of the Hsp90 client protein Akt.

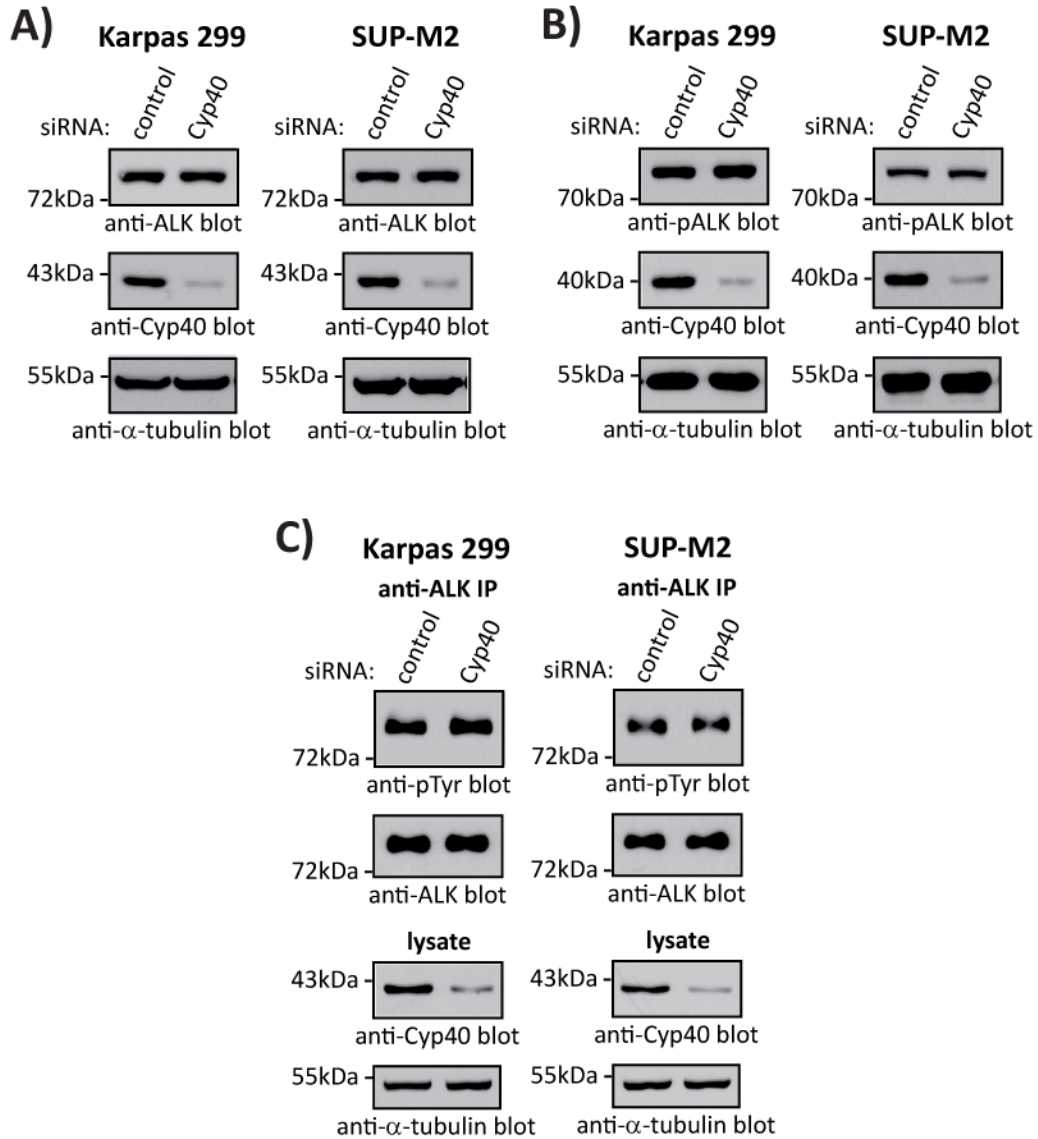


**Figure 5.14: Cyp40 knock-down does not influence NPM-ALK expression or tyrosine phosphorylation.**

**(A)** Western blot analysis of NPM-ALK protein levels (anti-ALK blots) in lysates collected from Karpas 299 and SUP-M2 cells after transfection with pooled control or Cyp40 siRNA. **(B)** Phosphorylation of NPM-ALK on tyrosines 338, 342, and 343 of the ALK kinase activation loop was assessed by western blotting (anti-pALK blots) in cells treated as in **(A)**. **(C)** The overall tyrosine phosphorylation status of NPM-ALK was analysed by immunoprecipitation of NPM-ALK (anti-ALK IP) followed by anti-phosphotyrosine (4G10) western blotting (anti-pTyr blot) in cells transfected with pooled control or Cyp40 siRNA. Anti- $\alpha$ -tubulin western blots of cell lysates are included to demonstrate equal protein loading. Molecular mass markers are indicated to the left of the western blots.

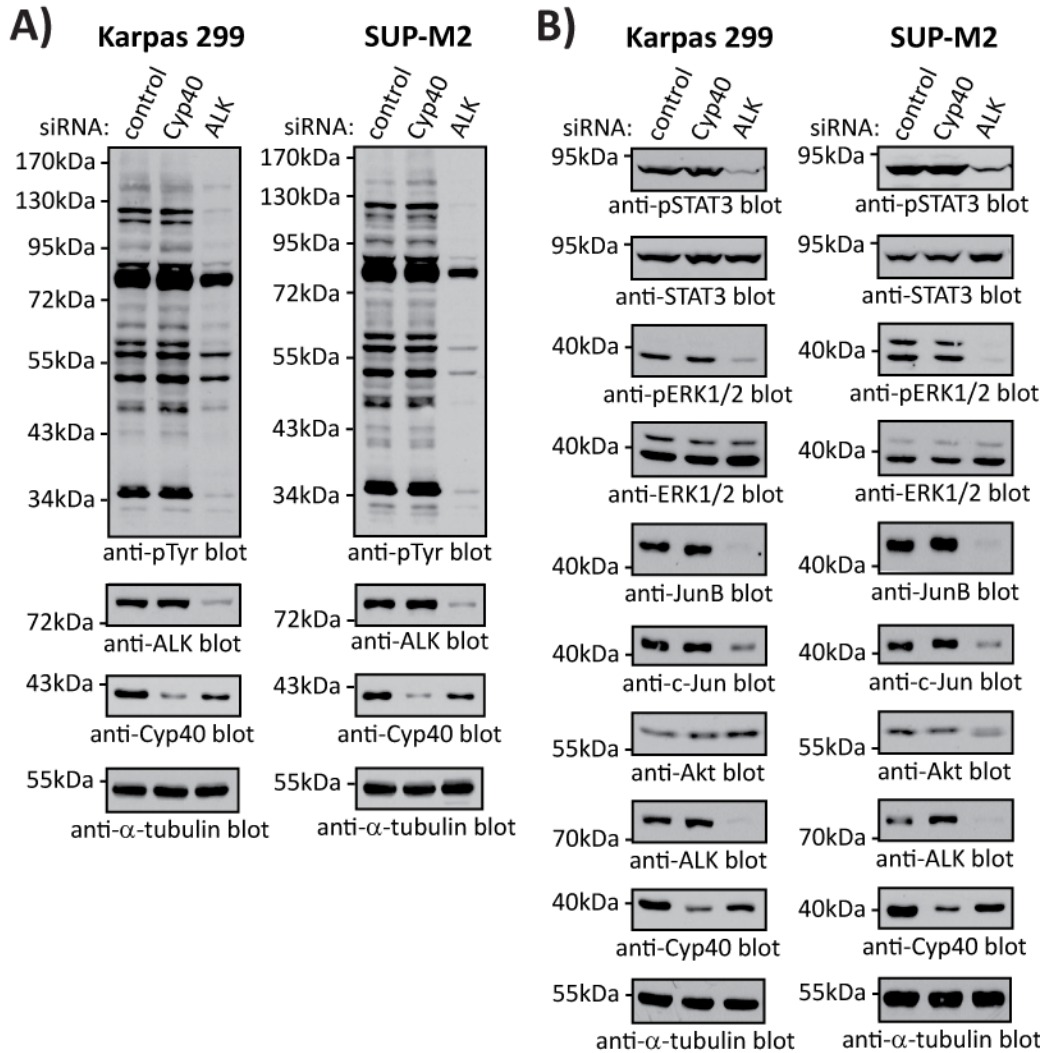


**Figure 5.15: Knock-down of Cyp40 does not affect phosphorylation of total cellular proteins or influence the phosphorylation and/or expression of STAT3, ERK1/2, JunB, c-Jun or Akt in ALK+ ALCL cell lines**

**(A)** The tyrosine phosphorylation status of total cellular proteins (anti-pTyr blot) was analysed by western blotting in lysates from cells transfected with pooled control, Cyp40 or ALK siRNA. **(B)** The tyrosine phosphorylation of STAT3 on Tyr 705 (anti-pSTAT3 blot), and the phosphorylation of ERK1/2 on Thr 202/Tyr 204 (anti-pERK1/2 blot) was assessed by western blotting in cells transfected with pooled control, Cyp40 or ALK siRNA. In addition, the total level of STAT3, ERK1/2, JunB, c-Jun and Akt was analysed in lysates collected from these same cells. In all experiments anti- $\alpha$ -tubulin blots demonstrate equal protein loading and molecular mass markers are indicated to the left of the blots.

## 5.7: DISCUSSION

ALK+ ALCL express the three related immunophilin co-chaperones, Cyp40, FKBP51, and FKBP52; however, our findings demonstrate their expression is distinctly regulated in this lymphoma (Figure 5.16). Signals originating from NPM-ALK promote the expression of Cyp40 and FKBP52, but not FKBP51; whereas the only immunophilin family member regulated by JunB in ALK+ ALCL is Cyp40. Since the expression of JunB is promoted by NPM-ALK in ALK+ ALCL (51, 191, 395), we think it is likely that NPM-ALK promotes the transcription of *Cyp40* largely through JunB. However, it is unresolved whether NPM-ALK regulates *Cyp40* transcription exclusively through JunB or via a combination of JunB-dependent and independent pathways. NPM-ALK knock-down results in a greater reduction in Cyp40 expression than JunB knock-down (compare Figures 5.1A and 5.3 to Figures 5.6A and 5.7A), despite a similar reduction in JunB levels in both instances, so we believe it is likely that other signalling pathways activated by NPM-ALK also contribute to Cyp40 expression. Moreover, since JunB does not influence FKBP52 expression, this demonstrates NPM-ALK signalling promotes the transcription of *FKBP52* through other downstream effectors. We were surprised by our finding that FKBP51 protein expression was modestly up-regulated in Karpas 299 cells treated with low concentrations of Crizotinib (Figure 5.9A). However, since we did not observe this increase in FKBP51 protein expression in Crizotinib-treated SUP-M2 cells (Figure 5.9B), or in Karpas 299 or SUP-M2 cells treated with ALK siRNA (Figure 5.6C), we are unsure of the significance of this observation.

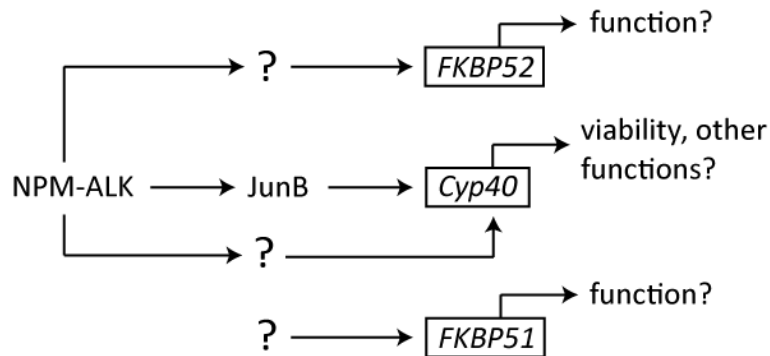


**Figure 5.16: Pathways influencing expression of the immunophilin family of co-chaperones in ALK+ ALCL.**

The transcription of *Cyp40* is promoted by signals initiated by NPM-ALK, and we postulate that up-regulation of JunB by NPM-ALK accounts for much of the increase in *Cyp40* transcription. However, additional signalling pathways activated by this oncoprotein likely also contribute to *Cyp40* expression. The transcription of *FKBP52* is promoted by NPM-ALK in ALK+ ALCL, but in a manner that is independent of JunB. Although expressed in ALK+ ALCL, FKBP51 expression is not regulated by NPM-ALK or JunB in this lymphoma.

While this is the first report to show an important role for an immunophilin co-chaperone in lymphoma, several reports have demonstrated that this family of proteins perform critical functions in other malignancies. For example, knock-down of either Cyp40 or FKBP51 in prostate cancer cell lines decreased cellular proliferation; this was particularly evident in androgen-dependent cell lines where these co-chaperones promote the transcriptional activity of the androgen receptor (393). Metastatic melanoma has high levels of FKBP51, and knock-down of FKBP51 sensitized the SAN melanoma cell line to ionizing radiation (408). This response was postulated to be due to decreased anti-apoptotic signalling through NF- $\kappa$ B in response to reduced FKBP51 levels (408). In contrast, reducing the expression of FKBP51 in breast, lung, and pancreatic cancer cell lines resulted in reduced sensitivity to chemotherapeutic agents (409). It was suggested in this study that activation of Akt was partially responsible for this decreased sensitivity. Thus, the immunophilin co-chaperones perform important functions in a number of cancers, and may represent attractive therapeutic targets in some malignancies.

An important unanswered question arising from our study is why reducing Cyp40 expression in ALK+ ALCL cell lines resulted in reduced viability (Figure 5.11 and Figure 5.12). This decrease in viability does not appear to be due to an impairment of NPM-ALK activity (Figure 5.14 and 5.15), and suggests that the dysregulation of another protein(s) is important for this phenotype. In addition to steroid hormone receptors and kinases, Cyp40 is known to associate with a number of other proteins with a variety of cellular functions including the c-Myb transcription factor (410), mutant forms of p53 (411), and the RACK1 scaffolding protein (412). Also, a genetic study in *Arabidopsis* identified an important role for the *Cyp40* orthologue, *SQUINT*, in microRNA biogenesis (413). Thus, there are several cellular activities whose disruption could account for the decreased viability observed when Cyp40 is knocked down in ALK+ALCL cell lines. Regardless of the exact cellular activity or activities regulated by Cyp40 that is

important for the viability of ALK+ ALCL cell lines, our findings demonstrate that these activities are not redundant with FKBP51 and FKBP52.

Our results show that Cyp40 does not regulate NPM-ALK levels or activity (Figure 5.14 and 5.15), but it is possible that other co-chaperones could be working with Hsp90 to regulate NPM-ALK activity. There are currently more than 20 known Hsp90 co-chaperones (369, 370). One of these proteins, Cdc37, co-chaperones for many kinase client proteins including Erb-B2, c-Raf, CDK4, CDK6 and Akt (414). Cdc37 was identified by mass spectrometry as an NPM-ALK associated protein (415), and has also been shown to complex with EML4-ALK in NSCLC (376). These studies however, did not examine whether these interactions are important for the activity of the respective ALK fusion proteins. If a co-chaperone protein that cooperates with Hsp90 to regulate NPM-ALK can be identified, it could represent a potential drug target to treat ALK+ ALCL, and other cancers expressing ALK fusion proteins, especially in situations where ALK mutations have resulted in resistance to conventional ALK inhibitors.

## **CHAPTER 6: DISCUSSION**

## 6.1: SUMMARY OF FINDINGS

The JunB transcription factor is highly expressed in ALK+ ALCL (242, 254, 255) and has been demonstrated to promote the proliferation of the ALK+ ALCL cell line, Karpas 299 (191). Despite this, JunB transcriptional targets were not well characterized in ALK+ ALCL. In order to better understand the role of JunB in ALK+ ALCL, we performed a quantitative iTRAQ mass spectrometry screen to identify potential JunB targets in this lymphoma. In this screen we identified GzB and Cyp40 as proteins whose expression was promoted by JunB in ALK+ ALCL. We confirmed these findings using quantitative western blotting and further found that JunB promoted transcription of *GzB* and *Cyp40*, likely through binding the AP-1 site in the promoter of these genes. Because NPM-ALK signalling promotes the expression of JunB in ALK+ ALCL, we examined whether NPM-ALK also functions upstream of GzB and Cyp40. Indeed we found that NPM-ALK promoted the expression of Cyp40 and GzB in ALK+ ALCL cell lines, and we feel it is likely that NPM-ALK promotes the expression of these proteins largely through up-regulating JunB.

GzB is one component of cytolytic granules present in ALK+ ALCL; however, it has also been found that these cells commonly express Perforin and TIA-1 (19, 28, 54-56). The expression of these proteins, along with GzB contributes to the cytotoxic phenotype observed in ALK+ ALCL tumour cells. To test whether JunB and NPM-ALK regulate other cytotoxic proteins in ALK+ ALCL we examined Perforin levels following JunB or NPM-ALK knock-down. While JunB did not appear to regulate Perforin expression, we found that NPM-ALK promoted Perforin expression in one cell line, but represses it in others. Together, these findings demonstrated that NPM-ALK and JunB signalling contributes to the cytotoxic phenotype in ALK+ ALCL (Figure 6.1).

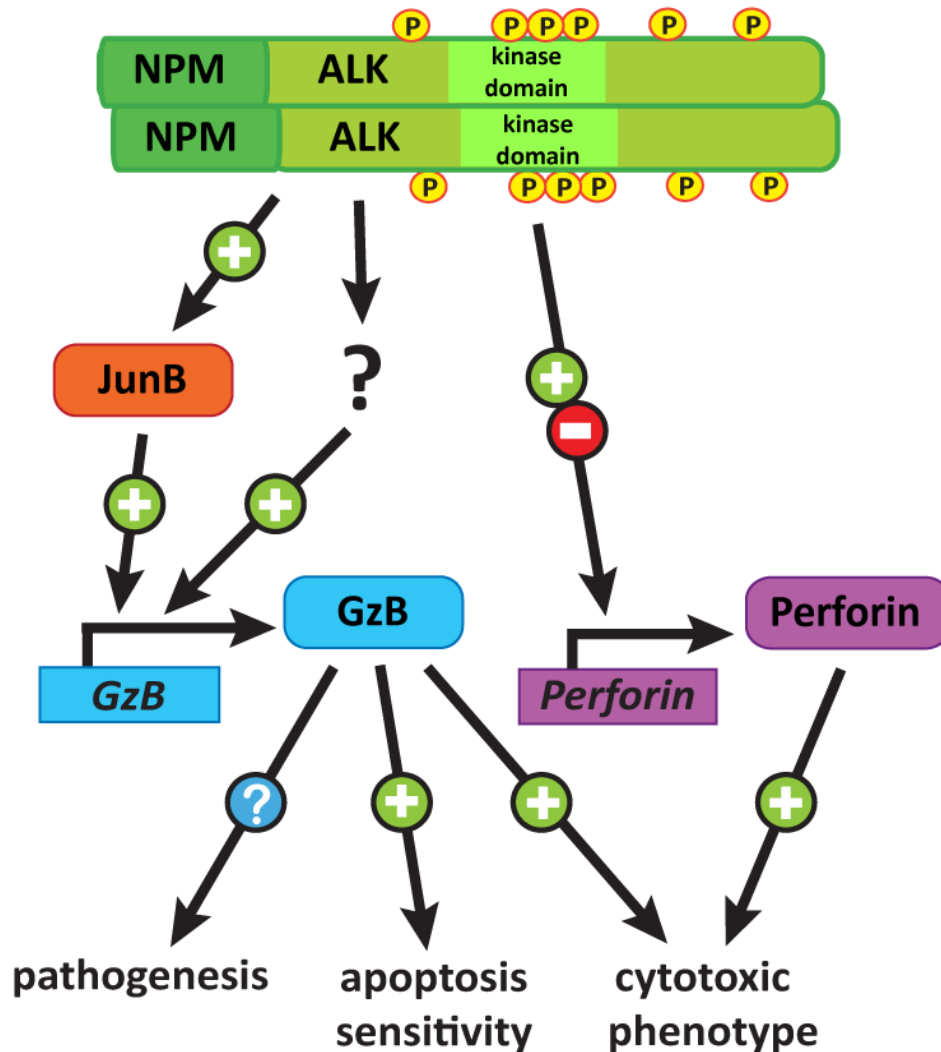


**Figure 6.1: NPM-ALK and JunB regulate the expression of cytotoxic proteins in ALK+ ALCL cell lines.**

NPM-ALK promotes the transcription of *GzB*, largely through the up-regulation of JunB, but potentially through other signalling pathways as well. NPM-ALK can also enhance or repress *Perforin* expression in a cell line-specific manner, independent of JunB. By regulating the expression of *GzB* and *Perforin*, NPM-ALK and JunB influence the cytotoxic phenotype of ALK+ ALCL. Furthermore, *GzB* expression appears to sensitize ALK+ ALCL cell lines to apoptosis following treatment with apoptosis-inducing drugs. Whether *GzB* also promotes the pathogenesis of ALK+ ALCL cells is currently an unanswered question.

We next examined if the up-regulation of GzB by NPM-ALK and JunB plays an important role in the pathogenesis ALK+ ALCL. One possibility was that GzB promotes the invasion of ALK+ ALCL cells, as has been demonstrated in bladder cancer cell lines (325). We found that ALK+ ALCL cell lines express and release enzymatically active GzB; however, we did not observe any alteration in the invasion of SUP-M2 cells *in vitro* following GzB knock-down (at least under the conditions tested). Interestingly, we found instead that GzB sensitizes ALK+ ALCL cell lines to apoptosis induced by the apoptosis-inducing agents, staurosporine and doxorubicin. This suggests that the expression of GzB by ALK+ ALCL lymphoma cells might be a contributing factor to why ALK+ ALCL patients are successfully treated with standard chemotherapy regimens containing apoptosis-inducing drugs such as doxorubicin (11-14, 29, 85).

Cyp40, along with FKBP51 and FKBP52, comprises the immunophilin family of Hsp90 co-chaperone proteins. While JunB promoted Cyp40 expression, it did not regulate the expression of either FKBP51 or FKBP52. However, NPM-ALK did promote the expression of FKBP52 (Figure 6.2). To determine if the immunophilin proteins represent important targets downstream of NPM-ALK and JunB, we examined cell viability following knock-down of these proteins individually or in combination. Cyp40 was found to promote the viability of ALK+ ALCL cell lines, while FKBP51 and FKBP52 did not influence the viability of these cells. Because Hsp90 plays a critical role in regulating NPM-ALK stability (365-368), we examined whether Cyp40 might promote ALK+ ALCL viability by stabilizing NPM-ALK expression. However, we did not observe any alterations in NPM-ALK expression or signalling following Cyp40 knock-down, so the mechanism by which Cyp40 promotes ALK+ ALCL viability is currently unknown.

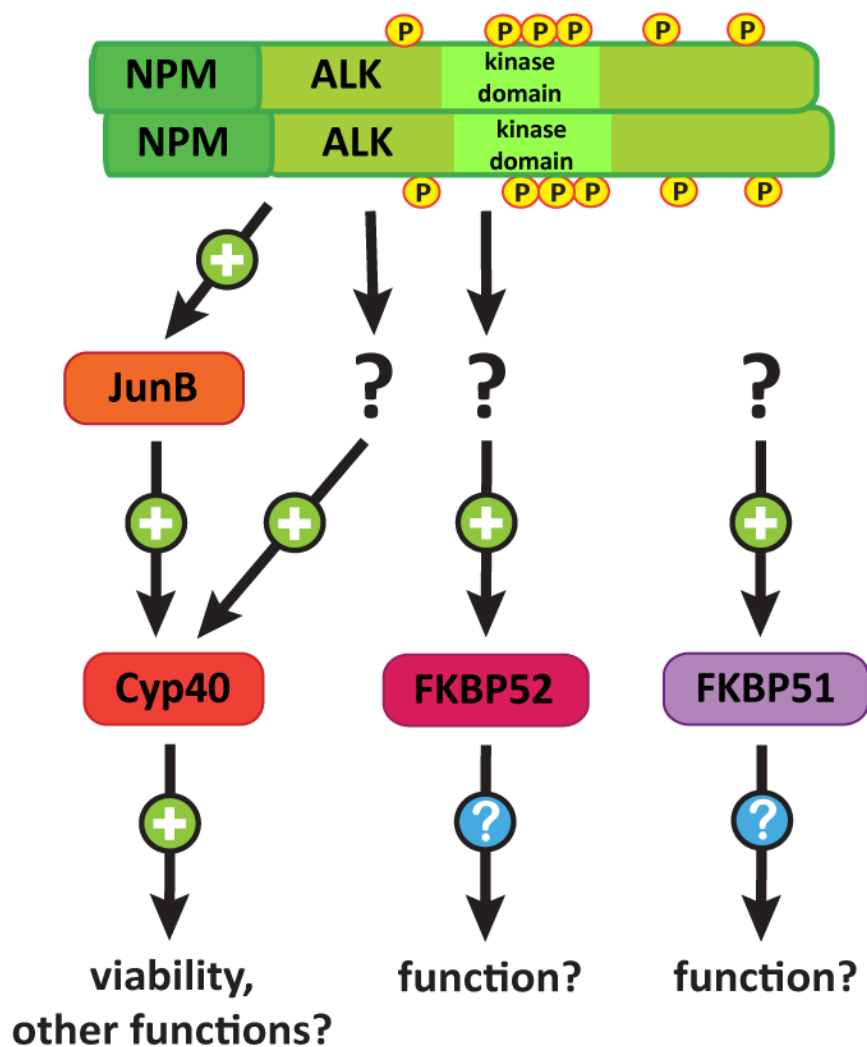


**Figure 6.2: Regulation and function of the immunophilin co-chaperone proteins in ALK+ ALCL.**

NPM-ALK promotes expression of *Cyp40* in ALK+ ALCL, which is likely largely through up-regulating JunB expression in this cancer. NPM-ALK, through a currently unknown pathway, also promotes the expression of *FKBP52*, but does not influence the expression of *FKBP51* in ALK+ ALCL. *Cyp40* was further found to promote the viability of ALK+ ALCL cell lines, while knock-down of *FKBP51* and *FKBP52* did not impact ALK+ ALCL viability.

## 6.2: OTHER POTENTIAL JUNB TARGETS IDENTIFIED IN THE iTRAQ SCREEN

In our iTRAQ mass spectrometry screen to identify JunB target proteins, we identified Cyp40 and GzB as proteins whose expression was promoted by JunB in both Karpas 299 and SUP-M2 cells. In this screen we focused our analysis on proteins that were found to be commonly regulated by JunB in Karpas 299 and SUP-M2 cells in both of the independent experiments that we performed. Based on these criteria we did not identify any other proteins up-regulated by JunB; however, we did identify Annexin A1 as a protein whose expression was repressed by JunB. To test whether JunB does repress the expression of Annexin A1, we examined Annexin A1 protein levels following JunB knock-down (Appendix A2). Consistent with the mass spectrometry data, we demonstrated that Annexin A1 protein levels were increased following JunB knock-down in Karpas 299 and SUP-M2 cells. Because we had found that JunB regulated *GzB* and *Cyp40* expression at the transcriptional level, we next examined whether JunB repressed expression of *Annexin A1* message in ALK+ ALCL cell lines. We found that JunB knock-down did result in increased *Annexin A1* mRNA expression (Appendix A2), suggesting that JunB might repress the transcription of *Annexin A1*. Consistent with this hypothesis, a region of the first untranslated exon and the first intron of the *Annexin A1* gene possesses two potential AP-1 binding sites (416), suggesting that JunB could function as a direct transcriptional repressor of Annexin A1 in ALK+ ALCL.

The mass spectrometry screen that we performed covered only a small proportion of the total proteins expressed in cells (less than 900 total proteins), and when we focused on proteins commonly identified in both replicates of this experiment the coverage was even smaller (342 total proteins). This suggested that we likely missed many JunB-regulated proteins in our original analysis, and we sought to determine if other proteins that were identified as potential JunB targets in only one repeat of the screen were regulated by JunB in ALK+ ALCL. In these experiments we still focused on proteins whose expression was similarly

regulated in both Karpas 299 and SUP-M2 cells in order to identify common JunB targets in this cancer. However, for simplicity sake we limited our studies to Karpas 299 cells. We selected the four most up-regulated targets and the three most down-regulated targets identified in the screen following JunB knock-down in only one replicate of the experiment. Since we demonstrated that *GzB*, *Cyp40* and *Annexin A1* were all regulated by JunB at the mRNA level, we used qPCR to examine the mRNA expression levels of the genes that encode for the selected proteins. The seven genes we examined, along with the primer sequences used are listed in Appendix A3. None of the genes expected to be promoted by JunB had reduced expression following JunB knock-down in Karpas 299 cells, and if anything, *N-ethylmaleimide-sensitive factor attachment protein, gamma (NAPG)* mRNA expression was slightly elevated following JunB knock-down (Appendix A4). Of the four genes predicted to be repressed by JunB, *UTP-glucose-1-phosphate uridylyltransferase 1 (UGP2)* was the only one found to have statistically significantly increased expression following JunB knock-down (Appendix A4). *Thymidine phosphorylase precursor (TYMP)* levels were also found to be elevated in cells treated with JunB siRNA; however, this increase was not statistically significant ( $p = 0.08$ ), likely due to the large variability observed for this target. More replicates of this experiment may help to resolve whether *TYMP* expression is repressed by JunB in Karpas 299 cells. While we did not observe alterations in the expression of many of the genes examined, these targets were initially identified as JunB-regulated proteins so it is possible that JunB regulates these proteins without influencing expression of their corresponding genes. At this time we cannot exclude this possibility, but given our findings with *Cyp40*, *GzB* and *Annexin A1*, we feel that it is unlikely that the majority of these proteins would be regulated by JunB at only the protein level. Thus, these findings suggest that many of the potential JunB targets identified in the mass spectrometry screen that were identified in only one replicate of the experiment are not likely to be true JunB targets in ALK+ ALCL. Therefore, we

decided not to further examine other targets identified in only a single replicate of the mass spectrometry screen.

While we did identify several novel JunB targets in ALK+ ALCL, there are likely many unidentified JunB targets in this lymphoma. Future work could focus on identifying more JunB targets in ALK+ ALCL and examining the role of these targets in the pathogenesis of ALK+ ALCL, both *in vitro* and *in vivo*. Identification of more JunB targets would likely be best accomplished using a microarray approach that would cover the entire genome, opposed to the ~800 total proteins that the iTRAQ technique identified. However, another important issue to address prior to conducting a microarray would be the limited JunB knock-down that we achieved using transient transfection with siRNAs. One possibility will be to use the cells with inducible JunB knock-down that we have generated (see Figures 3.3 and 4.3), which we have found give more efficient JunB knock-down than the JunB siRNAs.

### **6.3: JUNB REGULATES THE EXPRESSION OF PROTEINS THAT CONTRIBUTE TO MANY ASPECTS OF ALK+ ALCL BIOLOGY**

When we initiated our studies it was known that JunB promoted proliferation of the Karpas 299 ALK+ ALCL cell line. It had also been demonstrated that JunB promoted the transcription of *CD30* in ALK+ ALCL, contributing to a major phenotypic characteristic of this lymphoma. However, since CD30 signalling has been shown to inhibit proliferation and might also induce apoptosis in ALK+ ALCL cell lines, it is unlikely that CD30 represented a JunB target that promoted proliferation of ALK+ ALCL cells. Therefore, we hypothesized that JunB regulates the expression of many genes that play important roles in ALK+ ALCL, and we identified *GzB* and *Cyp40* as novel JunB transcriptional targets in this lymphoma. To the best of our knowledge, this is the first demonstration that JunB regulates the expression of these proteins, although it has previously been demonstrated

that AP-1 signalling is important for transcription from the *GzB* promoter in CTLs (290, 291).

In addition to our findings that JunB promoted the transcription of *GzB* and *Cyp40* in ALK+ ALCL cell lines, several other studies have identified novel JunB targets in ALK+ ALCL or NPM-ALK-driven lymphomas over the past few years. In mitotic ALK+ ALCL cells, JunB was shown to repress expression of DDX11 (193), a DNA helicase required for sister chromatid cohesion in mitotic cells (278). This was suggested to result in a cohesion defect in ALK+ ALCL cells, and the authors postulated that repression of DDX11 by JunB may contribute to the chromosomal abnormalities commonly observed in ALK+ ALCL (193). Furthermore, cyclin A2 protein expression was found to be reduced in Karpas 299 cells following JunB knock-down, suggesting that JunB promotes cyclin A2 expression (193). In this study it was not examined whether JunB directly promoted *cyclin A2* transcription in Karpas 299 cells (193). However, JunB has been shown to promote transcription from the CRE site in the murine *cyclin A2* promoter (229) (a site that is also found in the human *cyclin A2* promoter (417)), so it is quite possible that JunB does directly promote *cyclin A2* transcription in ALK+ ALCL. Given that cyclin A2 is known to promote cell cycle transition and proliferation in various cell types (418), it is likely that it would perform a similar function in ALK+ ALCL.

Finally, in a transgenic mouse model of NPM-ALK-induced lymphomagenesis, where NPM-ALK is expressed under control of the *CD4* promoter, it was recently demonstrated that knockout of both *JunB* and *c-Jun* significantly increased survival of these transgenic mice (279). JunB and c-Jun were further found to cooperate to promote transcription of *PDGFR $\beta$*  in this model (279). The importance of *PDGFR $\beta$*  expression in the pathogenesis of NPM-ALK transgenic mice was demonstrated by experiments showing that *PDGFR $\beta$*  inhibition increased survival of these mice, which was accompanied by reduced

proliferation and enhanced apoptosis of tumour cells (279). While ALK+ ALCL cell lines do not express PDGFR $\beta$ , it was found that PDGFR $\beta$  is expressed by tumour cells of many ALK+ ALCL patients, and treatment of one ALK+ ALCL patient with a PDGFR $\beta$  inhibitor resulted in clinical remission of the patient (279). While the authors did not test whether JunB promoted *PDGFR $\beta$*  transcription in human ALK+ ALCL, these findings suggested that PDGFR $\beta$  could potentially represent an important JunB target in ALK+ ALCL. Since c-Jun was also found to promote PDGFR $\beta$  expression in the NPM-ALK transgenic mice, PDGFR $\beta$  may also represent a target of c-Jun in ALK+ ALCL.

Taken together, our findings along with those of other studies demonstrate that JunB regulates the expression of proteins that contribute to different aspects of ALK+ ALCL biology (Figure 6.3). JunB contributes to multiple phenotypic characteristics of ALK+ ALCL by promoting transcription of *CD30* and *GzB*. By regulating the expression of *GzB*, JunB may also influence sensitivity of ALK+ ALCL cells to apoptosis-inducing agents. Furthermore, by repressing the expression of *DDX11*, JunB influences the chromosomal abnormalities observed in ALK+ ALCL. We found that JunB promotes the expression of *Cyp40*, and *Cyp40* was found to promote the viability of ALK+ ALCL cell lines (likely through promoting proliferation and/or survival). Finally, JunB appears to promote the expression of cyclin A2 and PDGFR $\beta$ , both of which likely promote the proliferation of ALK+ ALCL tumour cells. It is also probable that PDGFR $\beta$  promotes survival of ALK+ ALCL lymphoma cells. While the above mentioned JunB targets have been identified in ALK+ ALCL, it is quite likely that JunB regulates the expression of many other genes in this cancer. It will be interesting to determine whether other JunB targets impact these same aspects of ALK+ ALCL biology, or if they also influence other events such as cell migration and invasion.

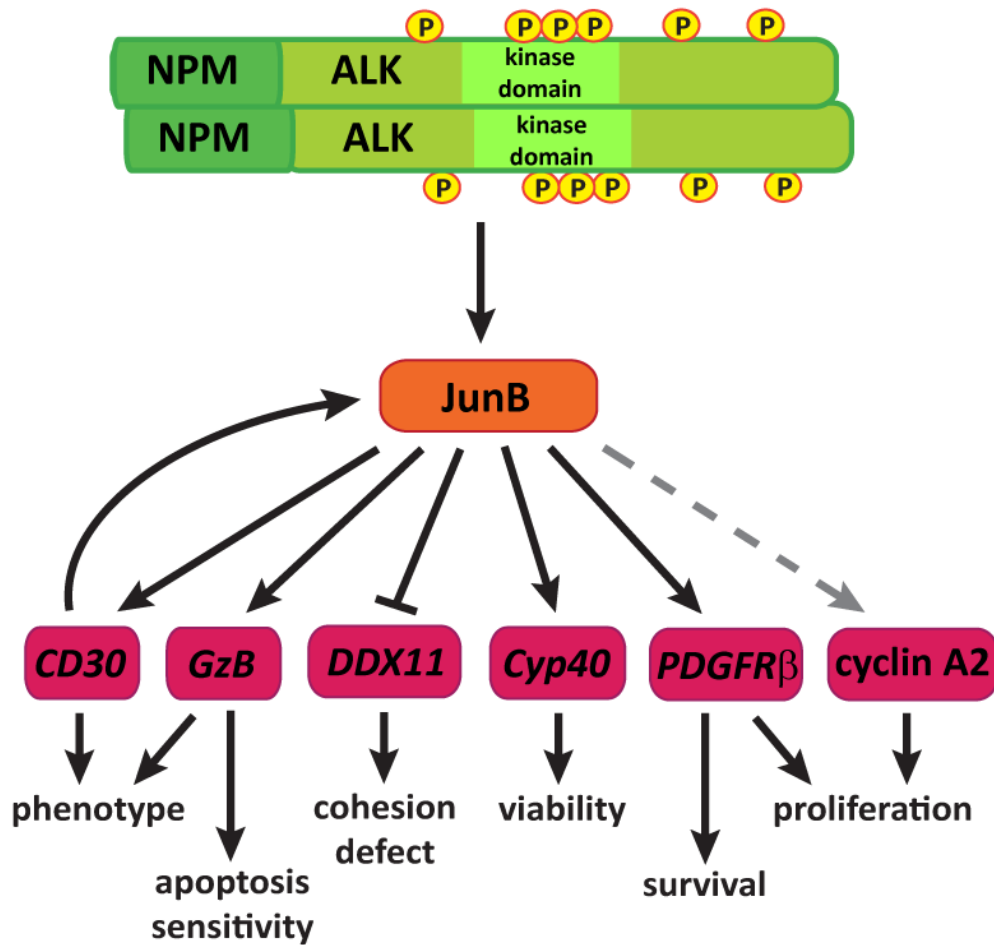


**Figure 6.3: JunB targets contribute to multiple aspects of ALK+ ALCL biology.**

JunB regulates the expression of multiple genes and proteins that affect different aspects of ALK+ ALCL. By promoting CD30 and GzB expression, JunB influences phenotypic characteristics of ALK+ ALCL. By enhancing the expression of Cyp40 and PDGFR $\beta$ , JunB promotes cell viability through regulating proteins that influence processes such as proliferation and survival. JunB may also promote cyclin A2 expression, which would likely promote cellular proliferation. Finally, through repressing the expression of DDX11, JunB may contribute to the chromosomal abnormalities observed in ALK+ ALCL.

#### **6.4: EXAMINING THE ROLE OF JUNB IN OTHER LYMPHOMAS**

While much work over the last few years has examined the function of JunB in ALK+ ALCL, JunB is also highly expressed in several other lymphomas. These include Hodgkin lymphoma (254, 255), ALK- ALCL (255) and CD30+ DLBCL (255), as well as the lymphoproliferative disorder, CD30+ lymphomatoid papulosis (255). However, little work has examined the function of JunB in these cancers. JunB was shown to bind an AP-1 site in the *CD30* promoter and was found to promote transcription from this promoter in Hodgkin lymphoma (256-258) and ALK- ALCL (256) cell lines (much like ALK+ ALCL). This suggests that JunB may have some similar functions in different lymphomas. It will be very interesting to determine whether JunB plays similar roles and regulates the expression of many of the same genes in different lymphomas where it is highly expressed. One interesting question is whether JunB promotes GzB expression in some of these lymphomas. ALK- ALCL tumour cells are often found to express GzB (28, 56) and a small proportion of patients with Hodgkin lymphoma also possess tumour cells that express GzB (419-421). Interestingly, some studies have suggested that the expression of cytotoxic molecules may have prognostic value in some lymphomas. In Hodgkin-like ALCL (a disease with characteristics of both Hodgkin lymphoma and ALK- ALCL) it has been found that the presence of a cytotoxic phenotype (GzB and TIA-1 expression) correlated with poor outcome (422). Furthermore, in a large study of patients with classical Hodgkin lymphoma, the expression of cytotoxic molecules and other T cell markers correlated with a significantly poorer prognosis (420). While a correlation was noted in these studies, it is not clear if GzB directly influences the prognosis of these patients, or if GzB expression is associated with other factors that play important roles in the progression of the disease. Furthermore, two other studies did not observe any correlation between the expression of cytotoxic molecules and the clinical outcome of ALCL (56) or Hodgkin lymphoma (419) patients, so the prognostic value of GzB in these diseases is not entirely clear.

## **6.5: THE FUNCTION OF JUNB IN OTHER ALK-EXPRESSING MALIGNANCIES**

In ALK+ ALCL JunB expression is promoted by NPM-ALK signalling (51, 192, 267), and ectopic expression of NPM-ALK in different cell types results in enhanced JunB levels (51, 191). This suggests that JunB is a common target of NPM-ALK signalling, and leads to the possibility that JunB is likely a target of ALK signalling in other cancers where ALK fusions are expressed. However, the function of JunB has not been examined in other ALK-expressing malignancies, such as ALK+ NSCLC. The ALK+ NSCLC cell line, H2228, has been shown to express JunB, and JunB levels were reduced in these cells following transfection with microRNA-96, a treatment that also dramatically reduced EML4-ALK levels (423). However, it was not examined whether the reduced JunB levels were a result of reduced EML4-ALK expression following microRNA-96 transfection. EML4-ALK has been reported to activate the ERK (424-427) and Akt (424, 426) signalling pathways in ALK+ NSCLC cell lines, although there is not complete agreement as to whether Akt is activated downstream of EML4-ALK (425, 427). Both the MEK/ERK and PI3K/Akt pathways contribute to JunB expression in ALK+ ALCL (191-193, 256), which further supports the possibility that ALK signalling may promote JunB expression in ALK-expressing malignancies other than ALK+ ALCL. Future work will be required to determine if JunB is commonly expressed in different ALK-expressing malignancies, and if so, whether JunB represents a target of ALK signalling in these cancers. Furthermore, it will be important to examine whether JunB plays a role in the pathogenesis of these cancers, using both *in vitro* and *in vivo* models.

## **6.6: THE ROLE OF OTHER AP-1 PROTEINS WITH RELATION TO JUNB FUNCTION IN ALK+ ALCL**

JunB has the ability to function as a homodimer or a heterodimer with other AP-1 proteins. However, whether JunB functions as a homodimer or heterodimer

(and if so, which AP-1 proteins it functions with) to regulate various genes in ALK+ ALCL is not well understood. Many AP-1 transcription factors are known to be expressed in ALK+ ALCL patient samples (254, 263-265), and NPM-ALK can enhance the expression and/or activity of many of these proteins (191, 266), suggesting that most other AP-1 transcription factors are likely available to function with JunB in ALK+ ALCL. It was suggested that JunB regulates *CD30* as a homodimer because an anti-JunB antibody was the only one found to strongly super-shift the *CD30* AP-1 probe in EMSA experiments, and JunB, but not c-Jun, over-expression could promote transcription from the *CD30* promoter in luciferase reporter assays (256). Using EMSA experiments, another study also found that JunB was the major AP-1 protein in ALK+ ALCL cells that could bind a synthetic AP-1 probe (191). However, using similar experiments it was demonstrated that both JunB and Fra2 were the major AP-1 components in ALK+ ALCL cell lines, and JunB and Fra2 were found to associate in these cell lines (265). We similarly found that JunB and Fra2 associate in ALK+ ALCL cell lines, and also demonstrated that JunB associates with c-Fos as well as other JunB molecules in these cells. Our findings using EMSA experiments with the *GzB* promoter AP-1 probe suggested that c-Fos may represent an important dimerization partner that functions with JunB to promote *GzB* expression in ALK+ ALCL; however, we could not determine whether c-Fos does promote *GzB* expression because we were unable to silence c-Fos expression in ALK+ ALCL cell lines using siRNA. It remains to be determined whether JunB primarily functions as a homodimer or a heterodimer to regulate important processes, such as promoting proliferation, in ALK+ ALCL, or whether different JunB dimers are important in this lymphoma. As more JunB targets are identified in ALK+ ALCL, specific knock-down experiments of other AP-1 proteins alone, or in combination with JunB, will be required to determine if other AP-1 factors are important for regulating the same genes as JunB. By better understanding which AP-1 factors JunB functions with in ALK+ ALCL, we will be better able to understand how this

important transcription factor functions in ALK+ ALCL and may also identify other molecules that are important in the pathogenesis of this lymphoma. Furthermore, given that ALK+ ALCL cells express most (if not all) of the different AP-1 factors, ALK+ ALCL may represent an excellent system to dissect how JunB and other AP-1 factors function together.

Another interesting question is whether there is any redundancy between c-Jun and JunB in ALK+ ALCL. c-Jun and JunB are the most closely related of the Jun family proteins and it has been found that ectopic expression of JunB can rescue many of the defects observed in c-Jun knockout mice (221); however, it has also been shown that JunB can inhibit c-Jun function (224-227). In ALK+ ALCL cell lines, c-Jun over-expression did not activate the *CD30* promoter, whereas JunB over-expression could activate this promoter (256). Furthermore, Staber and colleagues found that JunB knock-down reduced Karpas 299 proliferation while c-Jun knock-down did not (191). These findings suggested that c-Jun and JunB may have largely non-redundant functions in ALK+ ALCL. However, a recent study in NPM-ALK transgenic mice demonstrated that knockout of either *c-Jun* or *JunB* had no significant impact on survival of these mice, whereas knockout of both *c-Jun* and *JunB* significantly prolonged survival of NPM-ALK transgenic mice (279). In these mice it was further found that knockout of either *c-Jun* or *JunB* reduced PDGFR $\beta$  expression by ~50%, and that knockout of both genes resulted in a further decrease in PDGFR $\beta$  expression (80-90% reduction). These results demonstrated that there is some redundancy between c-Jun and JunB in NPM-ALK-driven lymphomas. Further work using systems where both c-Jun and JunB expression can be efficiently reduced or inhibited in the same cells is required to fully determine if there is overlap between the function of JunB and c-Jun in human ALK+ ALCL, and if so, to what extent do their roles overlap in this lymphoma.

## 6.7: CONCLUSIONS

This thesis describes the identification of two novel JunB transcriptional targets in ALK+ ALCL, the serine protease *GzB* and the immunophilin Hsp90 co-chaperone protein *Cyp40*. This demonstrates that JunB influences the cytotoxic phenotype of ALK+ ALCL by promoting the expression of *GzB*, and we make the interesting observation that *GzB* sensitizes ALK+ ALCL cells to apoptosis following treatment of cells with apoptosis-inducing drugs. Furthermore, the up-regulation of *Cyp40* by JunB and NPM-ALK signalling might also contribute to the viability of ALK+ ALCL cells, as *Cyp40* knock-down reduced viability of these cells. Overall, these findings better clarify the function of an important transcription factor in ALK+ ALCL and uncover novel factors influencing different aspects of ALK+ ALCL biology.

## **CHAPTER 7: REFERENCES**

1. Stein, H., Mason, D. Y., Gerdes, J., O'Connor, N., Wainscoat, J., Pallesen, G., Gatter, K., Falini, B., Delsol, G., Lemke, H., and et al. (1985) The expression of the Hodgkin's disease associated antigen Ki-1 in reactive and neoplastic lymphoid tissue: evidence that Reed-Sternberg cells and histiocytic malignancies are derived from activated lymphoid cells. *Blood* **66**, 848-858
2. Fischer, P., Nacheva, E., Mason, D. Y., Sherrington, P. D., Hoyle, C., Hayhoe, F. G., and Karpas, A. (1988) A Ki-1 (CD30)-positive human cell line (Karpas 299) established from a high-grade non-Hodgkin's lymphoma, showing a 2;5 translocation and rearrangement of the T-cell receptor beta-chain gene. *Blood* **72**, 234-240
3. Morgan, R., Smith, S. D., Hecht, B. K., Christy, V., Mellentin, J. D., Warnke, R., and Cleary, M. L. (1989) Lack of involvement of the c-fms and N-myc genes by chromosomal translocation t(2;5)(p23;q35) common to malignancies with features of so-called malignant histiocytosis. *Blood* **73**, 2155-2164
4. Rimokh, R., Magaud, J. P., Berger, F., Samarut, J., Coiffier, B., Germain, D., and Mason, D. Y. (1989) A translocation involving a specific breakpoint (q35) on chromosome 5 is characteristic of anaplastic large cell lymphoma ('Ki-1 lymphoma'). *British journal of haematology* **71**, 31-36
5. Kaneko, Y., Frizzera, G., Edamura, S., Maseki, N., Sakurai, M., Komada, Y., Tanaka, H., Sasaki, M., Suchi, T., and et al. (1989) A novel translocation, t(2;5)(p23;q35), in childhood phagocytic large T-cell lymphoma mimicking malignant histiocytosis. *Blood* **73**, 806-813
6. Bitter, M. A., Franklin, W. A., Larson, R. A., McKeithan, T. W., Rubin, C. M., Le Beau, M. M., Stephens, J. K., and Vardiman, J. W. (1990) Morphology in Ki-1(CD30)-positive non-Hodgkin's lymphoma is correlated with clinical features and the presence of a unique chromosomal abnormality, t(2;5)(p23;q35). *The American journal of surgical pathology* **14**, 305-316
7. Le Beau, M. M., Bitter, M. A., Larson, R. A., Doane, L. A., Ellis, E. D., Franklin, W. A., Rubin, C. M., Kadin, M. E., and Vardiman, J. W. (1989) The t(2;5)(p23;q35): a recurring chromosomal abnormality in Ki-1-positive anaplastic large cell lymphoma. *Leukemia : official journal of the Leukemia Society of America, Leukemia Research Fund, U.K* **3**, 866-870
8. Morris, S. W., Kirstein, M. N., Valentine, M. B., Dittmer, K. G., Shapiro, D. N., Saltman, D. L., and Look, A. T. (1994) Fusion of a kinase gene, ALK, to a nucleolar protein gene, NPM, in non-Hodgkin's lymphoma. *Science* **263**, 1281-1284
9. Shiota, M., Fujimoto, J., Semba, T., Satoh, H., Yamamoto, T., and Mori, S. (1994) Hyperphosphorylation of a novel 80 kDa protein-tyrosine kinase similar to Ltk in a human Ki-1 lymphoma cell line, AMS3. *Oncogene* **9**, 1567-1574
10. Shiota, M., Nakamura, S., Ichinohasama, R., Abe, M., Akagi, T., Takeshita, M., Mori, N., Fujimoto, J., Miyauchi, J., Mikata, A., Nanba, K., Takami, T.,

- Yamabe, H., Takano, Y., Izumo, T., Nagatani, T., Mohri, N., Nasu, K., Satoh, H., Katano, H., Fujimoto, J., Yamamoto, T., and Mori, S. (1995) Anaplastic large cell lymphomas expressing the novel chimeric protein p80NPM/ALK: a distinct clinicopathologic entity. *Blood* **86**, 1954-1960
11. Falini, B., Pileri, S., Zinzani, P. L., Carbone, A., Zagonel, V., Wolf-Peeters, C., Verhoef, G., Menestrina, F., Todeschini, G., Paulli, M., Lazzarino, M., Giardini, R., Aiello, A., Foss, H. D., Araujo, I., Fizzotti, M., Pelicci, P. G., Flenghi, L., Martelli, M. F., and Santucci, A. (1999) ALK+ lymphoma: clinico-pathological findings and outcome. *Blood* **93**, 2697-2706
  12. Schmitz, N., Trumper, L., Ziepert, M., Nickelsen, M., Ho, A. D., Metzner, B., Peter, N., Loeffler, M., Rosenwald, A., and Pfreundschuh, M. (2010) Treatment and prognosis of mature T-cell and NK-cell lymphoma: an analysis of patients with T-cell lymphoma treated in studies of the German High-Grade Non-Hodgkin Lymphoma Study Group. *Blood* **116**, 3418-3425
  13. Savage, K. J., Harris, N. L., Vose, J. M., Ullrich, F., Jaffe, E. S., Connors, J. M., Rimsza, L., Pileri, S. A., Chhanabhai, M., Gascoyne, R. D., Armitage, J. O., Weisenburger, D. D., and International Peripheral, T. C. L. P. (2008) ALK- anaplastic large-cell lymphoma is clinically and immunophenotypically different from both ALK+ ALCL and peripheral T-cell lymphoma, not otherwise specified: report from the International Peripheral T-Cell Lymphoma Project. *Blood* **111**, 5496-5504
  14. Vose, J., Armitage, J., Weisenburger, D., and International, T. C. L. P. (2008) International peripheral T-cell and natural killer/T-cell lymphoma study: pathology findings and clinical outcomes. *Journal of clinical oncology : official journal of the American Society of Clinical Oncology* **26**, 4124-4130
  15. Pulford, K., Lamant, L., Morris, S. W., Butler, L. H., Wood, K. M., Stroud, D., Delsol, G., and Mason, D. Y. (1997) Detection of anaplastic lymphoma kinase (ALK) and nucleolar protein nucleophosmin (NPM)-ALK proteins in normal and neoplastic cells with the monoclonal antibody ALK1. *Blood* **89**, 1394-1404
  16. Falini, B., Bigerna, B., Fizzotti, M., Pulford, K., Pileri, S. A., Delsol, G., Carbone, A., Paulli, M., Magrini, U., Menestrina, F., Giardini, R., Pilotti, S., Mezzelani, A., Ugolini, B., Billi, M., Pucciarini, A., Pacini, R., Pelicci, P. G., and Flenghi, L. (1998) ALK expression defines a distinct group of T/null lymphomas ("ALK lymphomas") with a wide morphological spectrum. *The American journal of pathology* **153**, 875-886
  17. Lamant, L., Meggetto, F., al Saati, T., Brugieres, L., de Paillerets, B. B., Dastugue, N., Bernheim, A., Rubie, H., Terrier-Lacombe, M. J., Robert, A., Rigal, F., Schlaifer, D., Shiuta, M., Mori, S., and Delsol, G. (1996) High incidence of the t(2;5)(p23;q35) translocation in anaplastic large cell lymphoma and its lack of detection in Hodgkin's disease. Comparison of

- cytogenetic analysis, reverse transcriptase-polymerase chain reaction, and P-80 immunostaining. *Blood* **87**, 284-291
18. Brugieres, L., Deley, M. C., Pacquement, H., Meguerian-Bedoyan, Z., Terrier-Lacombe, M. J., Robert, A., Pondarre, C., Leverger, G., Devalck, C., Rodary, C., Delsol, G., and Hartmann, O. (1998) CD30(+) anaplastic large-cell lymphoma in children: analysis of 82 patients enrolled in two consecutive studies of the French Society of Pediatric Oncology. *Blood* **92**, 3591-3598
  19. d'Amore, E. S., Menin, A., Bonoldi, E., Bevilacqua, P., Cazzavillan, S., Donofrio, V., Gambini, C., Forni, M., Gentile, A., Magro, G., Boldrini, R., Pillon, M., Rosolen, A., and Alaggio, R. (2007) Anaplastic large cell lymphomas: a study of 75 pediatric patients. *Pediatr Dev Pathol* **10**, 181-191
  20. Delsol, G., Falini, B., Muller-Hermelink, H., Campo, E., Jaffe, E., Gascoyne, R., Stein, H., and Kinney M. (2008) Anaplastic Large Cell Lymphoma (ALCL), ALK-positive In *International Agency for Research on Cancer (IARC)* (Swerdlow, S., Campo, E., Harris, N., Jaffe, E., Pileri, S., Stein, H., Thiele, J., and Vardiman, J., ed) pp. 312-316, IARC Press, Lyon, France
  21. Fornari, A., Piva, R., Chiarle, R., Novero, D., and Inghirami, G. (2009) Anaplastic large cell lymphoma: one or more entities among T-cell lymphoma? *Hematological oncology* **27**, 161-170
  22. Benharroch, D., Meguerian-Bedoyan, Z., Lamant, L., Amin, C., Brugieres, L., Terrier-Lacombe, M. J., Haralambieva, E., Pulford, K., Pileri, S., Morris, S. W., Mason, D. Y., and Delsol, G. (1998) ALK-positive lymphoma: a single disease with a broad spectrum of morphology. *Blood* **91**, 2076-2084
  23. Gascoyne, R. D., Aoun, P., Wu, D., Chhanabhai, M., Skinnider, B. F., Greiner, T. C., Morris, S. W., Connors, J. M., Vose, J. M., Viswanatha, D. S., Coldman, A., and Weisenburger, D. D. (1999) Prognostic significance of anaplastic lymphoma kinase (ALK) protein expression in adults with anaplastic large cell lymphoma. *Blood* **93**, 3913-3921
  24. Amin, H. M., and Lai, R. (2007) Pathobiology of ALK+ anaplastic large-cell lymphoma. *Blood* **110**, 2259-2267
  25. Ambrogio, C., Martinengo, C., Voena, C., Tondat, F., Riera, L., di Celle, P. F., Inghirami, G., and Chiarle, R. (2009) NPM-ALK oncogenic tyrosine kinase controls T-cell identity by transcriptional regulation and epigenetic silencing in lymphoma cells. *Cancer research* **69**, 8611-8619
  26. Bonzheim, I., Geissinger, E., Roth, S., Zettl, A., Marx, A., Rosenwald, A., Muller-Hermelink, H. K., and Rudiger, T. (2004) Anaplastic large cell lymphomas lack the expression of T-cell receptor molecules or molecules of proximal T-cell receptor signaling. *Blood* **104**, 3358-3360
  27. Lamant, L., McCarthy, K., d'Amore, E., Klapper, W., Nakagawa, A., Fraga, M., Maldyk, J., Simonitsch-Klupp, I., Oschlies, I., Delsol, G., Mauguen, A., Brugieres, L., and Le Deley, M. C. (2011) Prognostic impact of morphologic and phenotypic features of childhood ALK-positive

- anaplastic large-cell lymphoma: results of the ALCL99 study. *Journal of clinical oncology : official journal of the American Society of Clinical Oncology* **29**, 4669-4676
28. Foss, H. D., Anagnostopoulos, I., Araujo, I., Assaf, C., Demel, G., Kummer, J. A., Hummel, M., and Stein, H. (1996) Anaplastic large-cell lymphomas of T-cell and null-cell phenotype express cytotoxic molecules. *Blood* **88**, 4005-4011
  29. Delsol, G., Brugieres, L., Gaulard, P., Espinos, E., and Lamant, L. (2009) Anaplastic large cell lymphoma, ALK-positive and anaplastic large cell lymphoma ALK-negative. *Hematology Meeting Reports* **3**, 51-57
  30. Kinney, M. C., Higgins, R. A., and Medina, E. A. (2011) Anaplastic large cell lymphoma: twenty-five years of discovery. *Arch Pathol Lab Med* **135**, 19-43
  31. Tabbo, F., Barreca, A., Piva, R., Inghirami, G., and European, T. C. L. S. G. (2012) ALK Signaling and Target Therapy in Anaplastic Large Cell Lymphoma. *Frontiers in oncology* **2**, 41
  32. Schwab, U., Stein, H., Gerdes, J., Lemke, H., Kirchner, H., Schaadt, M., and Diehl, V. (1982) Production of a monoclonal antibody specific for Hodgkin and Sternberg-Reed cells of Hodgkin's disease and a subset of normal lymphoid cells. *Nature* **299**, 65-67
  33. Stein, H., Gerdes, J., Schwab, U., Lemke, H., Mason, D. Y., Ziegler, A., Schienle, W., and Diehl, V. (1982) Identification of Hodgkin and Sternberg-reed cells as a unique cell type derived from a newly-detected small-cell population. *International journal of cancer. Journal international du cancer* **30**, 445-459
  34. Greer, J. P., Kinney, M. C., and Loughran, T. P., Jr. (2001) T cell and NK cell lymphoproliferative disorders. *Hematology / the Education Program of the American Society of Hematology. American Society of Hematology. Education Program*, 259-281
  35. Younes, A. (2011) CD30-targeted antibody therapy. *Current opinion in oncology* **23**, 587-593
  36. Younes, A., and Kadin, M. E. (2003) Emerging applications of the tumor necrosis factor family of ligands and receptors in cancer therapy. *Journal of clinical oncology : official journal of the American Society of Clinical Oncology* **21**, 3526-3534
  37. Hu, S., Xu-Monette, Z. Y., Balasubramanyam, A., Manyam, G. C., Visco, C., Tzankov, A., Liu, W. M., Miranda, R. N., Zhang, L., Montes-Moreno, S., Dybkaer, K., Chiu, A., Orazi, A., Zu, Y., Bhagat, G., Richards, K. L., Hsi, E. D., Choi, W. W., Han van Krieken, J., Huang, Q., Huh, J., Ai, W., Ponzoni, M., Ferreri, A. J., Zhao, X., Winter, J. N., Zhang, M., Li, L., Moller, M. B., Piris, M. A., Li, Y., Go, R. S., Wu, L., Medeiros, L. J., and Young, K. H. (2013) CD30 expression defines a novel subgroup of diffuse large B-cell lymphoma with favorable prognosis and distinct gene expression

- signature: a report from the International DLBCL Rituximab-CHOP Consortium Program Study. *Blood* **121**, 2715-2724
38. Durkop, H., Latza, U., Hummel, M., Eitelbach, F., Seed, B., and Stein, H. (1992) Molecular cloning and expression of a new member of the nerve growth factor receptor family that is characteristic for Hodgkin's disease. *Cell* **68**, 421-427
  39. Biswas, P., Smith, C. A., Goletti, D., Hardy, E. C., Jackson, R. W., and Fauci, A. S. (1995) Cross-linking of CD30 induces HIV expression in chronically infected T cells. *Immunity* **2**, 587-596
  40. McDonald, P. P., Cassatella, M. A., Bald, A., Maggi, E., Romagnani, S., Gruss, H. J., and Pizzolo, G. (1995) CD30 ligation induces nuclear factor-kappa B activation in human T cell lines. *European journal of immunology* **25**, 2870-2876
  41. Gruss, H. J., Boiani, N., Williams, D. E., Armitage, R. J., Smith, C. A., and Goodwin, R. G. (1994) Pleiotropic effects of the CD30 ligand on CD30-expressing cells and lymphoma cell lines. *Blood* **83**, 2045-2056
  42. Tian, Z. G., Longo, D. L., Funakoshi, S., Asai, O., Ferris, D. K., Widmer, M., and Murphy, W. J. (1995) In vivo antitumor effects of unconjugated CD30 monoclonal antibodies on human anaplastic large-cell lymphoma xenografts. *Cancer research* **55**, 5335-5341
  43. Wright, C. W., Rumble, J. M., and Duckett, C. S. (2007) CD30 activates both the canonical and alternative NF-kappaB pathways in anaplastic large cell lymphoma cells. *The Journal of biological chemistry* **282**, 10252-10262
  44. Hubinger, G., Scheffrahn, I., Muller, E., Bai, R., Duyster, J., Morris, S. W., Schrezenmeier, H., and Bergmann, L. (1999) The tyrosine kinase NPM-ALK, associated with anaplastic large cell lymphoma, binds the intracellular domain of the surface receptor CD30 but is not activated by CD30 stimulation. *Experimental hematology* **27**, 1796-1805
  45. Hubinger, G., Muller, E., Scheffrahn, I., Schneider, C., Hildt, E., Singer, B. B., Sigg, I., Graf, J., and Bergmann, L. (2001) CD30-mediated cell cycle arrest associated with induced expression of p21(CIP1/WAF1) in the anaplastic large cell lymphoma cell line Karpas 299. *Oncogene* **20**, 590-598
  46. Levi, E., Pfeifer, W. M., and Kadin, M. E. (2001) CD30-activation-mediated growth inhibition of anaplastic large-cell lymphoma cell lines: apoptosis or cell-cycle arrest? *Blood* **98**, 1630-1632
  47. Hirsch, B., Hummel, M., Bentink, S., Fouladi, F., Spang, R., Zollinger, R., Stein, H., and Durkop, H. (2008) CD30-induced signaling is absent in Hodgkin's cells but present in anaplastic large cell lymphoma cells. *The American journal of pathology* **172**, 510-520
  48. Pfeifer, W., Levi, E., Petrogiannis-Haliotis, T., Lehmann, L., Wang, Z., and Kadin, M. E. (1999) A murine xenograft model for human CD30+ anaplastic large cell lymphoma. Successful growth inhibition with an anti-

- CD30 antibody (HeFi-1). *The American journal of pathology* **155**, 1353-1359
49. Mir, S. S., Richter, B. W., and Duckett, C. S. (2000) Differential effects of CD30 activation in anaplastic large cell lymphoma and Hodgkin disease cells. *Blood* **96**, 4307-4312
  50. Mir, S. S., Richter, B. W. M., and Duckett, C. S. (2001) Strength of CD30 signal determines sensitivity to apoptosis. *Blood* **98**, 1631-1632
  51. Hsu, F. Y., Johnston, P. B., Burke, K. A., and Zhao, Y. (2006) The expression of CD30 in anaplastic large cell lymphoma is regulated by nucleophosmin-anaplastic lymphoma kinase-mediated JunB level in a cell type-specific manner. *Cancer research* **66**, 9002-9008
  52. Hubinger, G., Schneider, C., Stohr, D., Ruff, H., Kirchner, D., Schwanen, C., Schmid, M., Bergmann, L., and Muller, E. (2004) CD30-induced up-regulation of the inhibitor of apoptosis genes cIAP1 and cIAP2 in anaplastic large cell lymphoma cells. *Experimental hematology* **32**, 382-389
  53. Horie, R., Watanabe, M., Ishida, T., Koiwa, T., Aizawa, S., Itoh, K., Higashihara, M., Kadin, M. E., and Watanabe, T. (2004) The NPM-ALK oncoprotein abrogates CD30 signaling and constitutive NF-kappaB activation in anaplastic large cell lymphoma. *Cancer cell* **5**, 353-364
  54. Foss, H. D., Demel, G., Anagnostopoulos, I., Araujo, I., Hummel, M., and Stein, H. (1997) Uniform expression of cytotoxic molecules in anaplastic large cell lymphoma of null/T cell phenotype and in cell lines derived from anaplastic large cell lymphoma. *Pathobiology* **65**, 83-90
  55. Krenacs, L., Wellmann, A., Sorbara, L., Himmelmann, A. W., Bagdi, E., Jaffe, E. S., and Raffeld, M. (1997) Cytotoxic cell antigen expression in anaplastic large cell lymphomas of T- and null-cell type and Hodgkin's disease: evidence for distinct cellular origin. *Blood* **89**, 980-989
  56. Dukers, D. F., ten Berge, R. L., Oudejans, J. J., Pulford, K., Hayes, D., Misere, J. F., Ossenkoppele, G. J., Jaspars, L. H., Willemze, R., and Meijer, C. J. (1999) A cytotoxic phenotype does not predict clinical outcome in anaplastic large cell lymphomas. *J Clin Pathol* **52**, 129-136
  57. Anthony, D. A., Andrews, D. M., Watt, S. V., Trapani, J. A., and Smyth, M. J. (2010) Functional dissection of the granzyme family: cell death and inflammation. *Immunological reviews* **235**, 73-92
  58. Cullen, S. P., Brunet, M., and Martin, S. J. (2010) Granzymes in cancer and immunity. *Cell death and differentiation* **17**, 616-623
  59. Boivin, W. A., Cooper, D. M., Hiebert, P. R., and Granville, D. J. (2009) Intracellular versus extracellular granzyme B in immunity and disease: challenging the dogma. *Laboratory investigation; a journal of technical methods and pathology* **89**, 1195-1220
  60. Clark, R., and Griffiths, G. M. (2003) Lytic granules, secretory lysosomes and disease. *Current opinion in immunology* **15**, 516-521

61. Podack, E. R., and Konigsberg, P. J. (1984) Cytolytic T cell granules. Isolation, structural, biochemical, and functional characterization. *The Journal of experimental medicine* **160**, 695-710
62. Podack, E. R., Young, J. D., and Cohn, Z. A. (1985) Isolation and biochemical and functional characterization of perforin 1 from cytolytic T-cell granules. *Proceedings of the National Academy of Sciences of the United States of America* **82**, 8629-8633
63. Masson, D., and Tschopp, J. (1985) Isolation of a lytic, pore-forming protein (perforin) from cytolytic T-lymphocytes. *The Journal of biological chemistry* **260**, 9069-9072
64. Criado, M., Lindstrom, J. M., Anderson, C. G., and Dennert, G. (1985) Cytotoxic granules from killer cells: specificity of granules and insertion of channels of defined size into target membranes. *Journal of immunology* **135**, 4245-4251
65. Shi, L., Kraut, R. P., Aebersold, R., and Greenberg, A. H. (1992) A natural killer cell granule protein that induces DNA fragmentation and apoptosis. *The Journal of experimental medicine* **175**, 553-566
66. Shi, L., Kam, C. M., Powers, J. C., Aebersold, R., and Greenberg, A. H. (1992) Purification of three cytotoxic lymphocyte granule serine proteases that induce apoptosis through distinct substrate and target cell interactions. *The Journal of experimental medicine* **176**, 1521-1529
67. Froelich, C. J., Orth, K., Turbov, J., Seth, P., Gottlieb, R., Babior, B., Shah, G. M., Bleackley, R. C., Dixit, V. M., and Hanna, W. (1996) New paradigm for lymphocyte granule-mediated cytotoxicity. Target cells bind and internalize granzyme B, but an endosomolytic agent is necessary for cytosolic delivery and subsequent apoptosis. *The Journal of biological chemistry* **271**, 29073-29079
68. Pinkoski, M. J., Hobman, M., Heibin, J. A., Tomaselli, K., Li, F., Seth, P., Froelich, C. J., and Bleackley, R. C. (1998) Entry and trafficking of granzyme B in target cells during granzyme B-perforin-mediated apoptosis. *Blood* **92**, 1044-1054
69. Nakajima, H., Park, H. L., and Henkart, P. A. (1995) Synergistic roles of granzymes A and B in mediating target cell death by rat basophilic leukemia mast cell tumors also expressing cytolysin/perforin. *The Journal of experimental medicine* **181**, 1037-1046
70. Lowin, B., French, L., Martinou, J. C., and Tschopp, J. (1996) Expression of the CTL-associated protein TIA-1 during murine embryogenesis. *Journal of immunology* **157**, 1448-1454
71. Izquierdo, J. M., and Valcarcel, J. (2007) Two isoforms of the T-cell intracellular antigen 1 (TIA-1) splicing factor display distinct splicing regulation activities. Control of TIA-1 isoform ratio by TIA-1-related protein. *The Journal of biological chemistry* **282**, 19410-19417

72. Tian, Q., Streuli, M., Saito, H., Schlossman, S. F., and Anderson, P. (1991) A polyadenylate binding protein localized to the granules of cytolytic lymphocytes induces DNA fragmentation in target cells. *Cell* **67**, 629-639
73. Yeowell, H. N., Walker, L. C., Mauger, D. M., Seth, P., and Garcia-Blanco, M. A. (2009) TIA nuclear proteins regulate the alternate splicing of lysyl hydroxylase 2. *The Journal of investigative dermatology* **129**, 1402-1411
74. Yamasaki, S., Stoecklin, G., Kedersha, N., Simarro, M., and Anderson, P. (2007) T-cell intracellular antigen-1 (TIA-1)-induced translational silencing promotes the decay of selected mRNAs. *The Journal of biological chemistry* **282**, 30070-30077
75. Izquierdo, J. M., Alcalde, J., Carrascoso, I., Reyes, R., and Ludena, M. D. (2011) Knockdown of T-cell intracellular antigens triggers cell proliferation, invasion and tumour growth. *The Biochemical journal* **435**, 337-344
76. Gottschald, O. R., Malec, V., Krasteva, G., Hasan, D., Kamlah, F., Herold, S., Rose, F., Seeger, W., and Hanze, J. (2010) TIAR and TIA-1 mRNA-binding proteins co-aggregate under conditions of rapid oxygen decline and extreme hypoxia and suppress the HIF-1alpha pathway. *Journal of molecular cell biology* **2**, 345-356
77. Simarro, M., Giannattasio, G., Xing, W., Lundequist, E. M., Stewart, S., Stevens, R. L., Orduna, A., Boyce, J. A., and Anderson, P. J. (2012) The translational repressor T-cell intracellular antigen-1 (TIA-1) is a key modulator of Th2 and Th17 responses driving pulmonary inflammation induced by exposure to house dust mite. *Immunology letters* **146**, 8-14
78. Anderson, P., Nagler-Anderson, C., O'Brien, C., Levine, H., Watkins, S., Slayter, H. S., Blue, M. L., and Schlossman, S. F. (1990) A monoclonal antibody reactive with a 15-kDa cytoplasmic granule-associated protein defines a subpopulation of CD8+ T lymphocytes. *Journal of immunology* **144**, 574-582
79. Eckerle, S., Brune, V., Doring, C., Tiacci, E., Bohle, V., Sundstrom, C., Kodet, R., Paulli, M., Falini, B., Klapper, W., Chaubert, A. B., Willenbrock, K., Metzler, D., Brauninger, A., Kuppers, R., and Hansmann, M. L. (2009) Gene expression profiling of isolated tumour cells from anaplastic large cell lymphomas: insights into its cellular origin, pathogenesis and relation to Hodgkin lymphoma. *Leukemia : official journal of the Leukemia Society of America, Leukemia Research Fund, U.K* **23**, 2129-2138
80. Sun, J., Bird, C. H., Sutton, V., McDonald, L., Coughlin, P. B., De Jong, T. A., Trapani, J. A., and Bird, P. I. (1996) A cytosolic granzyme B inhibitor related to the viral apoptotic regulator cytokine response modifier A is present in cytotoxic lymphocytes. *The Journal of biological chemistry* **271**, 27802-27809
81. ten Berge, R. L., Meijer, C. J., Dukers, D. F., Kummer, J. A., Bladergroen, B. A., Vos, W., Hack, C. E., Ossenkoppele, G. J., and Oudejans, J. J. (2002)

- Expression levels of apoptosis-related proteins predict clinical outcome in anaplastic large cell lymphoma. *Blood* **99**, 4540-4546
82. Kasprzycka, M., Marzec, M., Liu, X., Zhang, Q., and Wasik, M. A. (2006) Nucleophosmin/anaplastic lymphoma kinase (NPM/ALK) oncoprotein induces the T regulatory cell phenotype by activating STAT3. *Proceedings of the National Academy of Sciences of the United States of America* **103**, 9964-9969
  83. Matsuyama, H., Suzuki, H. I., Nishimori, H., Noguchi, M., Yao, T., Komatsu, N., Mano, H., Sugimoto, K., and Miyazono, K. (2011) miR-135b mediates NPM-ALK-driven oncogenicity and renders IL-17-producing immunophenotype to anaplastic large cell lymphoma. *Blood* **118**, 6881-6892
  84. Savan, R., McFarland, A. P., Reynolds, D. A., Feigenbaum, L., Ramakrishnan, K., Karwan, M., Shiota, H., Klinman, D. M., Dunleavy, K., Pittaluga, S., Anderson, S. K., Donnelly, R. P., Wilson, W. H., and Young, H. A. (2011) A novel role for IL-22R1 as a driver of inflammation. *Blood* **117**, 575-584
  85. Piccaluga, P. P., Gazzola, A., Mannu, C., Agostinelli, C., Bacci, F., Sabattini, E., Sagrarnoso, C., Piva, R., Roncolato, F., Inghirami, G., and Pileri, S. A. (2010) Pathobiology of anaplastic large cell lymphoma. *Advances in hematology*, 345053
  86. Fujimoto, J., Shiota, M., Iwahara, T., Seki, N., Satoh, H., Mori, S., and Yamamoto, T. (1996) Characterization of the transforming activity of p80, a hyperphosphorylated protein in a Ki-1 lymphoma cell line with chromosomal translocation t(2;5). *Proceedings of the National Academy of Sciences of the United States of America* **93**, 4181-4186
  87. Bischof, D., Pulford, K., Mason, D. Y., and Morris, S. W. (1997) Role of the nucleophosmin (NPM) portion of the non-Hodgkin's lymphoma-associated NPM-anaplastic lymphoma kinase fusion protein in oncogenesis. *Molecular and cellular biology* **17**, 2312-2325
  88. Ma, Z., Cools, J., Marynen, P., Cui, X., Siebert, R., Gesk, S., Schlegelberger, B., Peeters, B., De Wolf-Peeters, C., Wlodarska, I., and Morris, S. W. (2000) Inv(2)(p23q35) in anaplastic large-cell lymphoma induces constitutive anaplastic lymphoma kinase (ALK) tyrosine kinase activation by fusion to ATIC, an enzyme involved in purine nucleotide biosynthesis. *Blood* **95**, 2144-2149
  89. Trinej, M., Lanfrancone, L., Campo, E., Pulford, K., Mason, D. Y., Pelicci, P. G., and Falini, B. (2000) A new variant anaplastic lymphoma kinase (ALK)-fusion protein (ATIC-ALK) in a case of ALK-positive anaplastic large cell lymphoma. *Cancer research* **60**, 793-798
  90. Armstrong, F., Duplantier, M. M., Trepmpat, P., Hieblot, C., Lamant, L., Espinos, E., Racaud-Sultan, C., Allouche, M., Campo, E., Delsol, G., and Touriol, C. (2004) Differential effects of X-ALK fusion proteins on

- proliferation, transformation, and invasion properties of NIH3T3 cells. *Oncogene* **23**, 6071-6082
91. Chiarle, R., Gong, J. Z., Guasparri, I., Pesci, A., Cai, J., Liu, J., Simmons, W. J., Dhall, G., Howes, J., Piva, R., and Inghirami, G. (2003) NPM-ALK transgenic mice spontaneously develop T-cell lymphomas and plasma cell tumors. *Blood* **101**, 1919-1927
  92. Turner, S. D., Tooze, R., Maclennan, K., and Alexander, D. R. (2003) Vav-promoter regulated oncogenic fusion protein NPM-ALK in transgenic mice causes B-cell lymphomas with hyperactive Jun kinase. *Oncogene* **22**, 7750-7761
  93. Jager, R., Hahne, J., Jacob, A., Egert, A., Schenkel, J., Wernert, N., Schorle, H., and Wellmann, A. (2005) Mice transgenic for NPM-ALK develop non-Hodgkin lymphomas. *Anticancer research* **25**, 3191-3196
  94. Turner, S. D., and Alexander, D. R. (2005) What have we learnt from mouse models of NPM-ALK-induced lymphomagenesis? *Leukemia : official journal of the Leukemia Society of America, Leukemia Research Fund, U.K* **19**, 1128-1134
  95. Turner, S. D., Merz, H., Yeung, D., and Alexander, D. R. (2006) CD2 promoter regulated nucleophosmin-anaplastic lymphoma kinase in transgenic mice causes B lymphoid malignancy. *Anticancer research* **26**, 3275-3279
  96. Giuriato, S., Foisseau, M., Dejean, E., Felsher, D. W., Al Saati, T., Demur, C., Ragab, A., Kruczynski, A., Schiff, C., Delsol, G., and Meggetto, F. (2010) Conditional TPM3-ALK and NPM-ALK transgenic mice develop reversible ALK-positive early B-cell lymphoma/leukemia. *Blood* **115**, 4061-4070
  97. Lamant, L., Dastugue, N., Pulford, K., Delsol, G., and Mariame, B. (1999) A new fusion gene TPM3-ALK in anaplastic large cell lymphoma created by a (1;2)(q25;p23) translocation. *Blood* **93**, 3088-3095
  98. Siebert, R., Gesk, S., Harder, L., Steinemann, D., Grote, W., Schlegelberger, B., Tiemann, M., Wlodarska, I., and Schemmel, V. (1999) Complex variant translocation t(1;2) with TPM3-ALK fusion due to cryptic ALK gene rearrangement in anaplastic large-cell lymphoma. *Blood* **94**, 3614-3617
  99. Hernandez, L., Pinyol, M., Hernandez, S., Bea, S., Pulford, K., Rosenwald, A., Lamant, L., Falini, B., Ott, G., Mason, D. Y., Delsol, G., and Campo, E. (1999) TRK-fused gene (TFG) is a new partner of ALK in anaplastic large cell lymphoma producing two structurally different TFG-ALK translocations. *Blood* **94**, 3265-3268
  100. Hernandez, L., Bea, S., Bellosillo, B., Pinyol, M., Falini, B., Carbone, A., Ott, G., Rosenwald, A., Fernandez, A., Pulford, K., Mason, D., Morris, S. W., Santos, E., and Campo, E. (2002) Diversity of genomic breakpoints in TFG-ALK translocations in anaplastic large cell lymphomas: identification of a new TFG-ALK(XL) chimeric gene with transforming activity. *The American journal of pathology* **160**, 1487-1494

101. Colleoni, G. W., Bridge, J. A., Garicochea, B., Liu, J., Filippa, D. A., and Ladanyi, M. (2000) ATIC-ALK: A novel variant ALK gene fusion in anaplastic large cell lymphoma resulting from the recurrent cryptic chromosomal inversion, inv(2)(p23q35). *The American journal of pathology* **156**, 781-789
102. Touriol, C., Greenland, C., Lamant, L., Pulford, K., Bernard, F., Rousset, T., Mason, D. Y., and Delsol, G. (2000) Further demonstration of the diversity of chromosomal changes involving 2p23 in ALK-positive lymphoma: 2 cases expressing ALK kinase fused to CLTCL (clathrin chain polypeptide-like). *Blood* **95**, 3204-3207
103. Meech, S. J., McGavran, L., Odom, L. F., Liang, X., Meltesen, L., Gump, J., Wei, Q., Carlsen, S., and Hunger, S. P. (2001) Unusual childhood extramedullary hematologic malignancy with natural killer cell properties that contains tropomyosin 4--anaplastic lymphoma kinase gene fusion. *Blood* **98**, 1209-1216
104. Tort, F., Pinyol, M., Pulford, K., Roncador, G., Hernandez, L., Nayach, I., Kluin-Nelemans, H. C., Kluin, P., Touriol, C., Delsol, G., Mason, D., and Campo, E. (2001) Molecular characterization of a new ALK translocation involving moesin (MSN-ALK) in anaplastic large cell lymphoma. *Laboratory investigation; a journal of technical methods and pathology* **81**, 419-426
105. Tort, F., Campo, E., Pohlman, B., and Hsi, E. (2004) Heterogeneity of genomic breakpoints in MSN-ALK translocations in anaplastic large cell lymphoma. *Human pathology* **35**, 1038-1041
106. Cools, J., Wlodarska, I., Somers, R., Mentens, N., Pedeutour, F., Maes, B., De Wolf-Peeters, C., Pauwels, P., Hagemeijer, A., and Marynen, P. (2002) Identification of novel fusion partners of ALK, the anaplastic lymphoma kinase, in anaplastic large-cell lymphoma and inflammatory myofibroblastic tumor. *Genes Chromosomes Cancer* **34**, 354-362
107. Lamant, L., Gascoyne, R. D., Duplantier, M. M., Armstrong, F., Raghav, A., Chhanabhai, M., Rajcan-Separovic, E., Raghav, J., Delsol, G., and Espinos, E. (2003) Non-muscle myosin heavy chain (MYH9): a new partner fused to ALK in anaplastic large cell lymphoma. *Genes, chromosomes & cancer* **37**, 427-432
108. Morris, S. W., Naeve, C., Mathew, P., James, P. L., Kirstein, M. N., Cui, X., and Witte, D. P. (1997) ALK, the chromosome 2 gene locus altered by the t(2;5) in non-Hodgkin's lymphoma, encodes a novel neural receptor tyrosine kinase that is highly related to leukocyte tyrosine kinase (LTK). *Oncogene* **14**, 2175-2188
109. Iwahara, T., Fujimoto, J., Wen, D., Cupples, R., Bucay, N., Arakawa, T., Mori, S., Ratzkin, B., and Yamamoto, T. (1997) Molecular characterization of ALK, a receptor tyrosine kinase expressed specifically in the nervous system. *Oncogene* **14**, 439-449

110. Vernerissson, E., Khoo, N. K., Henriksson, M. L., Roos, G., Palmer, R. H., and Hallberg, B. (2006) Characterization of the expression of the ALK receptor tyrosine kinase in mice. *Gene Expr Patterns* **6**, 448-461
111. Souttou, B., Carvalho, N. B., Raulais, D., and Vigny, M. (2001) Activation of anaplastic lymphoma kinase receptor tyrosine kinase induces neuronal differentiation through the mitogen-activated protein kinase pathway. *The Journal of biological chemistry* **276**, 9526-9531
112. Moog-Lutz, C., Degoutin, J., Gouzi, J. Y., Frobert, Y., Brunet-de Carvalho, N., Bureau, J., Creminon, C., and Vigny, M. (2005) Activation and inhibition of anaplastic lymphoma kinase receptor tyrosine kinase by monoclonal antibodies and absence of agonist activity of pleiotrophin. *J Biol Chem* **280**, 26039-26048
113. Motegi, A., Fujimoto, J., Kotani, M., Sakuraba, H., and Yamamoto, T. (2004) ALK receptor tyrosine kinase promotes cell growth and neurite outgrowth. *J Cell Sci* **117**, 3319-3329
114. Gouzi, J. Y., Moog-Lutz, C., Vigny, M., and Brunet-de Carvalho, N. (2005) Role of the subcellular localization of ALK tyrosine kinase domain in neuronal differentiation of PC12 cells. *Journal of cell science* **118**, 5811-5823
115. Bilsland, J. G., Wheeldon, A., Mead, A., Znamenskiy, P., Almond, S., Waters, K. A., Thakur, M., Beaumont, V., Bonnert, T. P., Heavens, R., Whiting, P., McAllister, G., and Munoz-Sanjuan, I. (2008) Behavioral and neurochemical alterations in mice deficient in anaplastic lymphoma kinase suggest therapeutic potential for psychiatric indications. *Neuropsychopharmacology* **33**, 685-700
116. Weiss, J. B., Xue, C., Benice, T., Xue, L., Morris, S. W., and Raber, J. (2012) Anaplastic lymphoma kinase and leukocyte tyrosine kinase: functions and genetic interactions in learning, memory and adult neurogenesis. *Pharmacology, biochemistry, and behavior* **100**, 566-574
117. Bazigou, E., Apitz, H., Johansson, J., Loren, C. E., Hirst, E. M., Chen, P. L., Palmer, R. H., and Salecker, I. (2007) Anterograde Jelly belly and Alk receptor tyrosine kinase signaling mediates retinal axon targeting in *Drosophila*. *Cell* **128**, 961-975
118. Lasek, A. W., Lim, J., Kliethermes, C. L., Berger, K. H., Joslyn, G., Brush, G., Xue, L., Robertson, M., Moore, M. S., Vranizan, K., Morris, S. W., Schuckit, M. A., White, R. L., and Heberlein, U. (2011) An evolutionary conserved role for anaplastic lymphoma kinase in behavioral responses to ethanol. *PLoS One* **6**, e22636
119. Palmer, R. H., Vernerissson, E., Grabbe, C., and Hallberg, B. (2009) Anaplastic lymphoma kinase: signalling in development and disease. *The Biochemical journal* **420**, 345-361
120. Wang, K. S., Liu, X., Zhang, Q., Pan, Y., Aragam, N., and Zeng, M. (2011) A meta-analysis of two genome-wide association studies identifies 3 new

- loci for alcohol dependence. *Journal of psychiatric research* **45**, 1419-1425
121. Kunugi, H., Hashimoto, R., Okada, T., Hori, H., Nakabayashi, T., Baba, A., Kudo, K., Omori, M., Takahashi, S., Tsukue, R., Anami, K., Hirabayashi, N., Kosuga, A., Tatsumi, M., Kamijima, K., Asada, T., Harada, S., Arima, K., and Saitoh, O. (2006) Possible association between nonsynonymous polymorphisms of the anaplastic lymphoma kinase (ALK) gene and schizophrenia in a Japanese population. *J Neural Transm* **113**, 1569-1573
  122. Englund, C., Loren, C. E., Grabbe, C., Varshney, G. K., Deleuil, F., Hallberg, B., and Palmer, R. H. (2003) Jeb signals through the Alk receptor tyrosine kinase to drive visceral muscle fusion. *Nature* **425**, 512-516
  123. Lee, H. H., Norris, A., Weiss, J. B., and Frasch, M. (2003) Jelly belly protein activates the receptor tyrosine kinase Alk to specify visceral muscle pioneers. *Nature* **425**, 507-512
  124. Stute, C., Schimmelpfeng, K., Renkawitz-Pohl, R., Palmer, R. H., and Holz, A. (2004) Myoblast determination in the somatic and visceral mesoderm depends on Notch signalling as well as on milliways(mili(Alk)) as receptor for Jeb signalling. *Development* **131**, 743-754
  125. Stoica, G. E., Kuo, A., Aigner, A., Sunitha, I., Souttou, B., Malerczyk, C., Caughey, D. J., Wen, D., Karavanov, A., Riegel, A. T., and Wellstein, A. (2001) Identification of anaplastic lymphoma kinase as a receptor for the growth factor pleiotrophin. *J Biol Chem* **276**, 16772-16779
  126. Powers, C., Aigner, A., Stoica, G. E., McDonnell, K., and Wellstein, A. (2002) Pleiotrophin signaling through anaplastic lymphoma kinase is rate-limiting for glioblastoma growth. *The Journal of biological chemistry* **277**, 14153-14158
  127. Bowden, E. T., Stoica, G. E., and Wellstein, A. (2002) Anti-apoptotic signaling of pleiotrophin through its receptor, anaplastic lymphoma kinase. *The Journal of biological chemistry* **277**, 35862-35868
  128. Lu, K. V., Jong, K. A., Kim, G. Y., Singh, J., Dia, E. Q., Yoshimoto, K., Wang, M. Y., Cloughesy, T. F., Nelson, S. F., and Mischel, P. S. (2005) Differential induction of glioblastoma migration and growth by two forms of pleiotrophin. *The Journal of biological chemistry* **280**, 26953-26964
  129. Stoica, G. E., Kuo, A., Powers, C., Bowden, E. T., Sale, E. B., Riegel, A. T., and Wellstein, A. (2002) Midkine binds to anaplastic lymphoma kinase (ALK) and acts as a growth factor for different cell types. *J Biol Chem* **277**, 35990-35998
  130. Kuo, A. H., Stoica, G. E., Riegel, A. T., and Wellstein, A. (2007) Recruitment of insulin receptor substrate-1 and activation of NF-kappaB essential for midkine growth signaling through anaplastic lymphoma kinase. *Oncogene* **26**, 859-869
  131. Lorente, M., Torres, S., Salazar, M., Carracedo, A., Hernandez-Tiedra, S., Rodriguez-Fornes, F., Garcia-Taboada, E., Melendez, B., Mollejo, M., Campos-Martin, Y., Lakatos, S. A., Barcia, J., Guzman, M., and Velasco, G.

- (2011) Stimulation of the midkine/ALK axis renders glioma cells resistant to cannabinoid antitumoral action. *Cell death and differentiation* **18**, 959-973
132. Mathivet, T., Mazot, P., and Vigny, M. (2007) In contrast to agonist monoclonal antibodies, both C-terminal truncated form and full length form of Pleiotrophin failed to activate vertebrate ALK (anaplastic lymphoma kinase)? *Cellular signalling* **19**, 2434-2443
  133. Perez-Pinera, P., Zhang, W., Chang, Y., Vega, J. A., and Deuel, T. F. (2007) Anaplastic lymphoma kinase is activated through the pleiotrophin/receptor protein-tyrosine phosphatase beta/zeta signaling pathway: an alternative mechanism of receptor tyrosine kinase activation. *J Biol Chem* **282**, 28683-28690
  134. Mouri, J., Benard, A., Lourenco, F. C., Monnet, C., Greenland, C., Moog-Lutz, C., Racaud-Sultan, C., Gonzalez-Dunia, D., Vigny, M., Mehlen, P., Delsol, G., and Allouche, M. (2006) Anaplastic lymphoma kinase is a dependence receptor whose proapoptotic functions are activated by caspase cleavage. *Mol Cell Biol* **26**, 6209-6222
  135. Mehlen, P., and Bredesen, D. E. (2004) The dependence receptor hypothesis. *Apoptosis* **9**, 37-49
  136. Pearson, J. D., Lee, J. K., Bacani, J. T., Lai, R., and Ingham, R. J. (2012) NPM-ALK: The Prototypic Member of a Family of Oncogenic Fusion Tyrosine Kinases. *Journal of signal transduction* **2012**, 123253
  137. Arber, D. A., Sun, L. H., and Weiss, L. M. (1996) Detection of the t(2;5)(p23;q35) chromosomal translocation in large B-cell lymphomas other than anaplastic large cell lymphoma. *Hum Pathol* **27**, 590-594
  138. De Paepe, P., Baens, M., van Krieken, H., Verhasselt, B., Stul, M., Simons, A., Poppe, B., Laureys, G., Brons, P., Vandenberghe, P., Speleman, F., Praet, M., De Wolf-Peeters, C., Marynen, P., and Wlodarska, I. (2003) ALK activation by the CLTC-ALK fusion is a recurrent event in large B-cell lymphoma. *Blood* **102**, 2638-2641
  139. Gascoyne, R. D., Lamant, L., Martin-Subero, J. I., Lestou, V. S., Harris, N. L., Muller-Hermelink, H. K., Seymour, J. F., Campbell, L. J., Horsman, D. E., Auvigne, I., Espinos, E., Siebert, R., and Delsol, G. (2003) ALK-positive diffuse large B-cell lymphoma is associated with Clathrin-ALK rearrangements: report of 6 cases. *Blood* **102**, 2568-2573
  140. Chikatsu, N., Kojima, H., Suzukawa, K., Shinagawa, A., Nagasawa, T., Ozawa, H., Yamashita, Y., and Mori, N. (2003) ALK+, CD30-, CD20- large B-cell lymphoma containing anaplastic lymphoma kinase (ALK) fused to clathrin heavy chain gene (CLTC). *Mod Pathol* **16**, 828-832
  141. Van Roosbroeck, K., Cools, J., Dierickx, D., Thomas, J., Vandenberghe, P., Stul, M., Delabie, J., De Wolf-Peeters, C., Marynen, P., and Wlodarska, I. (2010) ALK-positive large B-cell lymphomas with cryptic SEC31A-ALK and NPM1-ALK fusions. *Haematologica* **95**, 509-513

142. Bedwell, C., Rowe, D., Moulton, D., Jones, G., Bown, N., and Bacon, C. M. (2011) Cytogenetically complex SEC31A-ALK fusions are recurrent in ALK-positive large B-cell lymphomas. *Haematologica* **96**, 343-346
143. Takeuchi, K., Soda, M., Togashi, Y., Ota, Y., Sekiguchi, Y., Hatano, S., Asaka, R., Noguchi, M., and Mano, H. (2011) Identification of a novel fusion, SQSTM1-ALK, in ALK-positive large B-cell lymphoma. *Haematologica* **96**, 464-467
144. Wang, W. Y., Gu, L., Liu, W. P., Li, G. D., Liu, H. J., and Ma, Z. G. (2011) ALK-positive extramedullary plasmacytoma with expression of the CLTC-ALK fusion transcript. *Pathol Res Pract* **207**, 587-591
145. Barreca, A., Lasorsa, E., Riera, L., Machiorlatti, R., Piva, R., Ponzoni, M., Kwee, I., Bertoni, F., Piccaluga, P. P., Pileri, S. A., Inghirami, G., and European, T. C. L. S. G. (2011) Anaplastic lymphoma kinase in human cancer. *Journal of molecular endocrinology* **47**, R11-23
146. Roskoski, R., Jr. (2013) Anaplastic lymphoma kinase (ALK): structure, oncogenic activation, and pharmacological inhibition. *Pharmacological research : the official journal of the Italian Pharmacological Society* **68**, 68-94
147. Lin, E., Li, L., Guan, Y., Soriano, R., Rivers, C. S., Mohan, S., Pandita, A., Tang, J., and Modrusan, Z. (2009) Exon array profiling detects EML4-ALK fusion in breast, colorectal, and non-small cell lung cancers. *Mol Cancer Res* **7**, 1466-1476
148. Zhang, X., Zhang, S., Yang, X., Yang, J., Zhou, Q., Yin, L., An, S., Lin, J., Chen, S., Xie, Z., Zhu, M., Zhang, X., and Wu, Y. L. (2010) Fusion of EML4 and ALK is associated with development of lung adenocarcinomas lacking EGFR and KRAS mutations and is correlated with ALK expression. *Molecular cancer* **9**, 188
149. Soda, M., Choi, Y. L., Enomoto, M., Takada, S., Yamashita, Y., Ishikawa, S., Fujiwara, S., Watanabe, H., Kurashina, K., Hatanaka, H., Bando, M., Ohno, S., Ishikawa, Y., Aburatani, H., Niki, T., Sohara, Y., Sugiyama, Y., and Mano, H. (2007) Identification of the transforming EML4-ALK fusion gene in non-small-cell lung cancer. *Nature* **448**, 561-566
150. Rikova, K., Guo, A., Zeng, Q., Possemato, A., Yu, J., Haack, H., Nardone, J., Lee, K., Reeves, C., Li, Y., Hu, Y., Tan, Z., Stokes, M., Sullivan, L., Mitchell, J., Wetzel, R., Macneill, J., Ren, J. M., Yuan, J., Bakalarski, C. E., Villen, J., Kornhauser, J. M., Smith, B., Li, D., Zhou, X., Gygi, S. P., Gu, T. L., Polakiewicz, R. D., Rush, J., and Comb, M. J. (2007) Global survey of phosphotyrosine signaling identifies oncogenic kinases in lung cancer. *Cell* **131**, 1190-1203
151. Inamura, K., Takeuchi, K., Togashi, Y., Nomura, K., Ninomiya, H., Okui, M., Satoh, Y., Okumura, S., Nakagawa, K., Soda, M., Choi, Y. L., Niki, T., Mano, H., and Ishikawa, Y. (2008) EML4-ALK fusion is linked to histological characteristics in a subset of lung cancers. *Journal of thoracic oncology :*

*official publication of the International Association for the Study of Lung Cancer* **3**, 13-17

152. Wong, D. W., Leung, E. L., So, K. K., Tam, I. Y., Sihoe, A. D., Cheng, L. C., Ho, K. K., Au, J. S., Chung, L. P., Pik Wong, M., and University of Hong Kong Lung Cancer Study, G. (2009) The EML4-ALK fusion gene is involved in various histologic types of lung cancers from nonsmokers with wild-type EGFR and KRAS. *Cancer* **115**, 1723-1733
153. Griffin, C. A., Hawkins, A. L., Dvorak, C., Henkle, C., Ellingham, T., and Perlman, E. J. (1999) Recurrent involvement of 2p23 in inflammatory myofibroblastic tumors. *Cancer research* **59**, 2776-2780
154. Lawrence, B., Perez-Atayde, A., Hibbard, M. K., Rubin, B. P., Dal Cin, P., Pinkus, J. L., Pinkus, G. S., Xiao, S., Yi, E. S., Fletcher, C. D., and Fletcher, J. A. (2000) TPM3-ALK and TPM4-ALK oncogenes in inflammatory myofibroblastic tumors. *Am J Pathol* **157**, 377-384
155. Debiec-Rychter, M., Marynen, P., Hagemeyer, A., and Pauwels, P. (2003) ALK-AT1C fusion in urinary bladder inflammatory myofibroblastic tumor. *Genes Chromosomes Cancer* **38**, 187-190
156. Bridge, J. A., Kanamori, M., Ma, Z., Pickering, D., Hill, D. A., Lydiatt, W., Lui, M. Y., Colleoni, G. W., Antonescu, C. R., Ladanyi, M., and Morris, S. W. (2001) Fusion of the ALK gene to the clathrin heavy chain gene, CLTC, in inflammatory myofibroblastic tumor. *Am J Pathol* **159**, 411-415
157. Ma, Z., Hill, D. A., Collins, M. H., Morris, S. W., Sumegi, J., Zhou, M., Zuppan, C., and Bridge, J. A. (2003) Fusion of ALK to the Ran-binding protein 2 (RANBP2) gene in inflammatory myofibroblastic tumor. *Genes Chromosomes Cancer* **37**, 98-105
158. Panagopoulos, I., Nilsson, T., Domanski, H. A., Isaksson, M., Lindblom, P., Mertens, F., and Mandahl, N. (2006) Fusion of the SEC31L1 and ALK genes in an inflammatory myofibroblastic tumor. *Int J Cancer* **118**, 1181-1186
159. Takeuchi, K., Soda, M., Togashi, Y., Sugawara, E., Hatano, S., Asaka, R., Okumura, S., Nakagawa, K., Mano, H., and Ishikawa, Y. (2011) Pulmonary inflammatory myofibroblastic tumor expressing a novel fusion, PPF1BP1-ALK: reappraisal of anti-ALK immunohistochemistry as a tool for novel ALK fusion identification. *Clin Cancer Res* **17**, 3341-3348
160. Lipson, D., Capelletti, M., Yelensky, R., Otto, G., Parker, A., Jarosz, M., Curran, J. A., Balasubramanian, S., Bloom, T., Brennan, K. W., Donahue, A., Downing, S. R., Frampton, G. M., Garcia, L., Juhn, F., Mitchell, K. C., White, E., White, J., Zwirko, Z., Peretz, T., Nechushtan, H., Soussan-Gutman, L., Kim, J., Sasaki, H., Kim, H. R., Park, S. I., Ercan, D., Sheehan, C. E., Ross, J. S., Cronin, M. T., Janne, P. A., and Stephens, P. J. (2012) Identification of new ALK and RET gene fusions from colorectal and lung cancer biopsies. *Nat Med*
161. Debelenko, L. V., Raimondi, S. C., Daw, N., Shivakumar, B. R., Huang, D., Nelson, M., and Bridge, J. A. (2011) Renal cell carcinoma with novel VCL-

- ALK fusion: new representative of ALK-associated tumor spectrum. *Mod Pathol* **24**, 430-442
162. Marino-Enriquez, A., Ou, W. B., Weldon, C. B., Fletcher, J. A., and Perez-Atayde, A. R. (2011) ALK rearrangement in sickle cell trait-associated renal medullary carcinoma. *Genes, chromosomes & cancer* **50**, 146-153
  163. Sugawara, E., Togashi, Y., Kuroda, N., Sakata, S., Hatano, S., Asaka, R., Yuasa, T., Yonese, J., Kitagawa, M., Mano, H., Ishikawa, Y., and Takeuchi, K. (2012) Identification of anaplastic lymphoma kinase fusions in renal cancer: Large-scale immunohistochemical screening by the intercalated antibody-enhanced polymer method. *Cancer*
  164. Jazii, F. R., Najafi, Z., Malekzadeh, R., Conrads, T. P., Ziaee, A. A., Abnet, C., Yazdznbod, M., Karkhane, A. A., and Salekdeh, G. H. (2006) Identification of squamous cell carcinoma associated proteins by proteomics and loss of beta tropomyosin expression in esophageal cancer. *World J Gastroenterol* **12**, 7104-7112
  165. Du, X. L., Hu, H., Lin, D. C., Xia, S. H., Shen, X. M., Zhang, Y., Luo, M. L., Feng, Y. B., Cai, Y., Xu, X., Han, Y. L., Zhan, Q. M., and Wang, M. R. (2007) Proteomic profiling of proteins dysregulated in Chinese esophageal squamous cell carcinoma. *J Mol Med (Berl)* **85**, 863-875
  166. Perez-Pinera, P., Chang, Y., Astudillo, A., Mortimer, J., and Deuel, T. F. (2007) Anaplastic lymphoma kinase is expressed in different subtypes of human breast cancer. *Biochem Biophys Res Commun* **358**, 399-403
  167. Schoppmann, S. F., Streubel, B., and Birner, P. (2013) Amplification but not translocation of anaplastic lymphoma kinase is a frequent event in oesophageal cancer. *European journal of cancer*
  168. Lamant, L., Pulford, K., Bischof, D., Morris, S. W., Mason, D. Y., Delsol, G., and Mariame, B. (2000) Expression of the ALK tyrosine kinase gene in neuroblastoma. *Am J Pathol* **156**, 1711-1721
  169. Janoueix-Lerosey, I., Lequin, D., Brugieres, L., Ribeiro, A., de Pontual, L., Combaret, V., Raynal, V., Puisieux, A., Schleiermacher, G., Pierron, G., Valteau-Couanet, D., Frebourg, T., Michon, J., Lyonnet, S., Amiel, J., and Delattre, O. (2008) Somatic and germline activating mutations of the ALK kinase receptor in neuroblastoma. *Nature* **455**, 967-970
  170. Chen, Y., Takita, J., Choi, Y. L., Kato, M., Ohira, M., Sanada, M., Wang, L., Soda, M., Kikuchi, A., Igarashi, T., Nakagawara, A., Hayashi, Y., Mano, H., and Ogawa, S. (2008) Oncogenic mutations of ALK kinase in neuroblastoma. *Nature* **455**, 971-974
  171. George, R. E., Sanda, T., Hanna, M., Frohling, S., Luther, W., 2nd, Zhang, J., Ahn, Y., Zhou, W., London, W. B., McGrady, P., Xue, L., Zozulya, S., Gregor, V. E., Webb, T. R., Gray, N. S., Gilliland, D. G., Diller, L., Greulich, H., Morris, S. W., Meyerson, M., and Look, A. T. (2008) Activating mutations in ALK provide a therapeutic target in neuroblastoma. *Nature* **455**, 975-978

172. Caren, H., Abel, F., Kogner, P., and Martinsson, T. (2008) High incidence of DNA mutations and gene amplifications of the ALK gene in advanced sporadic neuroblastoma tumours. *Biochem J* **416**, 153-159
173. Mosse, Y. P., Laudenslager, M., Longo, L., Cole, K. A., Wood, A., Attiyeh, E. F., Laquaglia, M. J., Sennett, R., Lynch, J. E., Perri, P., Laureys, G., Speleman, F., Kim, C., Hou, C., Hakonarson, H., Torkamani, A., Schork, N. J., Brodeur, G. M., Tonini, G. P., Rappaport, E., Devoto, M., and Maris, J. M. (2008) Identification of ALK as a major familial neuroblastoma predisposition gene. *Nature* **455**, 930-935
174. Murugan, A. K., and Xing, M. (2011) Anaplastic thyroid cancers harbor novel oncogenic mutations of the ALK gene. *Cancer Res* **71**, 4403-4411
175. Gambacorti-Passerini, C., Messa, C., and Pogliani, E. M. (2011) Crizotinib in anaplastic large-cell lymphoma. *N Engl J Med* **364**, 775-776
176. Kwak, E. L., Bang, Y. J., Camidge, D. R., Shaw, A. T., Solomon, B., Maki, R. G., Ou, S. H., Dezube, B. J., Janne, P. A., Costa, D. B., Varella-Garcia, M., Kim, W. H., Lynch, T. J., Fidias, P., Stubbs, H., Engelman, J. A., Sequist, L. V., Tan, W., Gandhi, L., Mino-Kenudson, M., Wei, G. C., Shreeve, S. M., Ratain, M. J., Settleman, J., Christensen, J. G., Haber, D. A., Wilner, K., Salgia, R., Shapiro, G. I., Clark, J. W., and Iafrate, A. J. (2010) Anaplastic lymphoma kinase inhibition in non-small-cell lung cancer. *N Engl J Med* **363**, 1693-1703
177. Shaw, A. T., Yeap, B. Y., Solomon, B. J., Riely, G. J., Gainor, J., Engelman, J. A., Shapiro, G. I., Costa, D. B., Ou, S. H., Butaney, M., Salgia, R., Maki, R. G., Varella-Garcia, M., Doebele, R. C., Bang, Y. J., Kulig, K., Selaru, P., Tang, Y., Wilner, K. D., Kwak, E. L., Clark, J. W., Iafrate, A. J., and Camidge, D. R. (2011) Effect of crizotinib on overall survival in patients with advanced non-small-cell lung cancer harbouring ALK gene rearrangement: a retrospective analysis. *The lancet oncology* **12**, 1004-1012
178. Camidge, D. R., Bang, Y. J., Kwak, E. L., Iafrate, A. J., Varella-Garcia, M., Fox, S. B., Riely, G. J., Solomon, B., Ou, S. H., Kim, D. W., Salgia, R., Fidias, P., Engelman, J. A., Gandhi, L., Janne, P. A., Costa, D. B., Shapiro, G. I., Lorusso, P., Ruffner, K., Stephenson, P., Tang, Y., Wilner, K., Clark, J. W., and Shaw, A. T. (2012) Activity and safety of crizotinib in patients with ALK-positive non-small-cell lung cancer: updated results from a phase 1 study. *The lancet oncology* **13**, 1011-1019
179. Butrynski, J. E., D'Adamo, D. R., Hornick, J. L., Dal Cin, P., Antonescu, C. R., Jhanwar, S. C., Ladanyi, M., Capelletti, M., Rodig, S. J., Ramaiya, N., Kwak, E. L., Clark, J. W., Wilner, K. D., Christensen, J. G., Janne, P. A., Maki, R. G., Demetri, G. D., and Shapiro, G. I. (2010) Crizotinib in ALK-rearranged inflammatory myofibroblastic tumor. *N Engl J Med* **363**, 1727-1733
180. La Madrid, A. M., Campbell, N., Smith, S., Cohn, S. L., and Salgia, R. (2012) Targeting ALK: a promising strategy for the treatment of non-small cell lung cancer, non-Hodgkin's lymphoma, and neuroblastoma. *Targeted oncology* **7**, 199-210

181. Takeuchi, K., Choi, Y. L., Togashi, Y., Soda, M., Hatano, S., Inamura, K., Takada, S., Ueno, T., Yamashita, Y., Satoh, Y., Okumura, S., Nakagawa, K., Ishikawa, Y., and Mano, H. (2009) KIF5B-ALK, a novel fusion oncokine identified by an immunohistochemistry-based diagnostic system for ALK-positive lung cancer. *Clinical cancer research : an official journal of the American Association for Cancer Research* **15**, 3143-3149
182. Togashi, Y., Soda, M., Sakata, S., Sugawara, E., Hatano, S., Asaka, R., Nakajima, T., Mano, H., and Takeuchi, K. (2012) KLC1-ALK: a novel fusion in lung cancer identified using a formalin-fixed paraffin-embedded tissue only. *PloS one* **7**, e31323
183. Debelenko, L. V., Arthur, D. C., Pack, S. D., Helman, L. J., Schrupp, D. S., and Tsokos, M. (2003) Identification of CARS-ALK fusion in primary and metastatic lesions of an inflammatory myofibroblastic tumor. *Laboratory investigation; a journal of technical methods and pathology* **83**, 1255-1265
184. Rodrigues, G. A., and Park, M. (1993) Dimerization mediated through a leucine zipper activates the oncogenic potential of the met receptor tyrosine kinase. *Molecular and cellular biology* **13**, 6711-6722
185. Chan, P. K. (1989) Cross-linkage of nucleophosmin in tumor cells by nitrogen mustard. *Cancer Res* **49**, 3271-3275
186. Yung, B. Y., and Chan, P. K. (1987) Identification and characterization of a hexameric form of nucleolar phosphoprotein B23. *Biochimica et biophysica acta* **925**, 74-82
187. Mano, H. (2008) Non-solid oncogenes in solid tumors: EML4-ALK fusion genes in lung cancer. *Cancer Sci* **99**, 2349-2355
188. Damm-Welk, C., Klapper, W., Oschlies, I., Gesk, S., Rottgers, S., Bradtke, J., Siebert, R., Reiter, A., and Woessmann, W. (2009) Distribution of NPM1-ALK and X-ALK fusion transcripts in paediatric anaplastic large cell lymphoma: a molecular-histological correlation. *British journal of haematology* **146**, 306-309
189. Armstrong, F., Lamant, L., Hieblot, C., Delsol, G., and Touriol, C. (2007) TPM3-ALK expression induces changes in cytoskeleton organisation and confers higher metastatic capacities than other ALK fusion proteins. *European journal of cancer* **43**, 640-646
190. Chiarle, R., Voena, C., Ambrogio, C., Piva, R., and Inghirami, G. (2008) The anaplastic lymphoma kinase in the pathogenesis of cancer. *Nat Rev Cancer* **8**, 11-23
191. Staber, P. B., Vesely, P., Haq, N., Ott, R. G., Funato, K., Bambach, I., Fuchs, C., Schauer, S., Linkesch, W., Hrzenjak, A., Dirks, W. G., Sexl, V., Bergler, H., Kadin, M. E., Sternberg, D. W., Kenner, L., and Hoefler, G. (2007) The oncoprotein NPM-ALK of anaplastic large-cell lymphoma induces JUNB transcription via ERK1/2 and JunB translation via mTOR signaling. *Blood* **110**, 3374-3383

192. Watanabe, M., Itoh, K., Togano, T., Kadin, M. E., Watanabe, T., Higashihara, M., and Horie, R. (2012) Ets-1 activates overexpression of JunB and CD30 in Hodgkin's lymphoma and anaplastic large-cell lymphoma. *The American journal of pathology* **180**, 831-838
193. Perez-Benavente, B., Garcia, J. L., Rodriguez, M. S., Pineda-Lucena, A., Piechaczyk, M., Font de Mora, J., and Farras, R. (2012) GSK3-SCF(FBXW7) targets JunB for degradation in G2 to preserve chromatid cohesion before anaphase. *Oncogene*
194. Leventaki, V., Drakos, E., Medeiros, L. J., Lim, M. S., Elenitoba-Johnson, K. S., Claret, F. X., and Rassidakis, G. Z. (2007) NPM-ALK oncogenic kinase promotes cell-cycle progression through activation of JNK/cJun signaling in anaplastic large-cell lymphoma. *Blood* **110**, 1621-1630
195. Shaulian, E., and Karin, M. (2001) AP-1 in cell proliferation and survival. *Oncogene* **20**, 2390-2400
196. Shaulian, E., and Karin, M. (2002) AP-1 as a regulator of cell life and death. *Nat Cell Biol* **4**, E131-136
197. Shaulian, E. (2010) AP-1--The Jun proteins: Oncogenes or tumor suppressors in disguise? *Cellular signalling* **22**, 894-899
198. Kouzarides, T., and Ziff, E. (1988) The role of the leucine zipper in the fos-jun interaction. *Nature* **336**, 646-651
199. Hai, T. W., Liu, F., Coukos, W. J., and Green, M. R. (1989) Transcription factor ATF cDNA clones: an extensive family of leucine zipper proteins able to selectively form DNA-binding heterodimers. *Genes & development* **3**, 2083-2090
200. Nakabeppu, Y., Ryder, K., and Nathans, D. (1988) DNA binding activities of three murine Jun proteins: stimulation by Fos. *Cell* **55**, 907-915
201. Schuermann, M., Neuberg, M., Hunter, J. B., Jenuwein, T., Ryseck, R. P., Bravo, R., and Muller, R. (1989) The leucine repeat motif in Fos protein mediates complex formation with Jun/AP-1 and is required for transformation. *Cell* **56**, 507-516
202. Turner, R., and Tjian, R. (1989) Leucine repeats and an adjacent DNA binding domain mediate the formation of functional cFos-cJun heterodimers. *Science* **243**, 1689-1694
203. Angel, P., Imagawa, M., Chiu, R., Stein, B., Imbra, R. J., Rahmsdorf, H. J., Jonat, C., Herrlich, P., and Karin, M. (1987) Phorbol ester-inducible genes contain a common cis element recognized by a TPA-modulated trans-acting factor. *Cell* **49**, 729-739
204. Piette, J., Hirai, S., and Yaniv, M. (1988) Constitutive synthesis of activator protein 1 transcription factor after viral transformation of mouse fibroblasts. *Proceedings of the National Academy of Sciences of the United States of America* **85**, 3401-3405
205. Hai, T., and Curran, T. (1991) Cross-family dimerization of transcription factors Fos/Jun and ATF/CREB alters DNA binding specificity. *Proceedings*

- of the National Academy of Sciences of the United States of America **88**, 3720-3724
206. Smith, S. E., Papavassiliou, A. G., and Bohmann, D. (1993) Different TRE-related elements are distinguished by sets of DNA-binding proteins with overlapping sequence specificity. *Nucleic acids research* **21**, 1581-1585
  207. Chiu, R., Boyle, W. J., Meek, J., Smeal, T., Hunter, T., and Karin, M. (1988) The c-Fos protein interacts with c-Jun/AP-1 to stimulate transcription of AP-1 responsive genes. *Cell* **54**, 541-552
  208. Sassone-Corsi, P., Der, C. J., and Verma, I. M. (1989) ras-induced neuronal differentiation of PC12 cells: possible involvement of fos and jun. *Molecular and cellular biology* **9**, 3174-3183
  209. Chida, K., and Vogt, P. K. (1992) Nuclear translocation of viral Jun but not of cellular Jun is cell cycle dependent. *Proceedings of the National Academy of Sciences of the United States of America* **89**, 4290-4294
  210. Hibi, M., Lin, A., Smeal, T., Minden, A., and Karin, M. (1993) Identification of an oncoprotein- and UV-responsive protein kinase that binds and potentiates the c-Jun activation domain. *Genes & development* **7**, 2135-2148
  211. Derijard, B., Hibi, M., Wu, I. H., Barrett, T., Su, B., Deng, T., Karin, M., and Davis, R. J. (1994) JNK1: a protein kinase stimulated by UV light and Ha-Ras that binds and phosphorylates the c-Jun activation domain. *Cell* **76**, 1025-1037
  212. Smeal, T., Binetruy, B., Mercola, D. A., Birrer, M., and Karin, M. (1991) Oncogenic and transcriptional cooperation with Ha-Ras requires phosphorylation of c-Jun on serines 63 and 73. *Nature* **354**, 494-496
  213. Narayanan, K., Srinivas, R., Peterson, M. C., Ramachandran, A., Hao, J., Thimmapaya, B., Scherer, P. E., and George, A. (2004) Transcriptional regulation of dentin matrix protein 1 by JunB and p300 during osteoblast differentiation. *The Journal of biological chemistry* **279**, 44294-44302
  214. Alani, R., Brown, P., Binetruy, B., Dosaka, H., Rosenberg, R. K., Angel, P., Karin, M., and Birrer, M. J. (1991) The transactivating domain of the c-Jun proto-oncoprotein is required for cotransformation of rat embryo cells. *Molecular and cellular biology* **11**, 6286-6295
  215. Metz, R., Kouzarides, T., and Bravo, R. (1994) A C-terminal domain in FosB, absent in FosB/SF and Fra-1, which is able to interact with the TATA binding protein, is required for altered cell growth. *The EMBO journal* **13**, 3832-3842
  216. McBride, K., and Nemer, M. (1998) The C-terminal domain of c-fos is required for activation of an AP-1 site specific for jun-fos heterodimers. *Molecular and cellular biology* **18**, 5073-5081
  217. Wisdom, R., Yen, J., Rashid, D., and Verma, I. M. (1992) Transformation by FosB requires a trans-activation domain missing in FosB2 that can be substituted by heterologous activation domains. *Genes & development* **6**, 667-675

218. Wisdom, R., and Verma, I. M. (1993) Transformation by Fos proteins requires a C-terminal transactivation domain. *Molecular and cellular biology* **13**, 7429-7438
219. Ryder, K., Lau, L. F., and Nathans, D. (1988) A gene activated by growth factors is related to the oncogene v-jun. *Proceedings of the National Academy of Sciences of the United States of America* **85**, 1487-1491
220. Schorpp-Kistner, M., Wang, Z. Q., Angel, P., and Wagner, E. F. (1999) JunB is essential for mammalian placentation. *The EMBO journal* **18**, 934-948
221. Passegue, E., Jochum, W., Behrens, A., Ricci, R., and Wagner, E. F. (2002) JunB can substitute for Jun in mouse development and cell proliferation. *Nature genetics* **30**, 158-166
222. Hirai, S. I., Ryseck, R. P., Mechta, F., Bravo, R., and Yaniv, M. (1989) Characterization of junD: a new member of the jun proto-oncogene family. *The EMBO journal* **8**, 1433-1439
223. Kovary, K., and Bravo, R. (1991) Expression of different Jun and Fos proteins during the G0-to-G1 transition in mouse fibroblasts: in vitro and in vivo associations. *Molecular and cellular biology* **11**, 2451-2459
224. Deng, T., and Karin, M. (1993) JunB differs from c-Jun in its DNA-binding and dimerization domains, and represses c-Jun by formation of inactive heterodimers. *Genes & development* **7**, 479-490
225. Chiu, R., Angel, P., and Karin, M. (1989) Jun-B differs in its biological properties from, and is a negative regulator of, c-Jun. *Cell* **59**, 979-986
226. Schutte, J., Viallet, J., Nau, M., Segal, S., Fedorko, J., and Minna, J. (1989) jun-B inhibits and c-fos stimulates the transforming and trans-activating activities of c-jun. *Cell* **59**, 987-997
227. Bakiri, L., Lallemand, D., Bossy-Wetzel, E., and Yaniv, M. (2000) Cell cycle-dependent variations in c-Jun and JunB phosphorylation: a role in the control of cyclin D1 expression. *The EMBO journal* **19**, 2056-2068
228. Kovary, K., and Bravo, R. (1991) The jun and fos protein families are both required for cell cycle progression in fibroblasts. *Molecular and cellular biology* **11**, 4466-4472
229. Andrecht, S., Kolbus, A., Hartenstein, B., Angel, P., and Schorpp-Kistner, M. (2002) Cell cycle promoting activity of JunB through cyclin A activation. *The Journal of biological chemistry* **277**, 35961-35968
230. Kenner, L., Hoebertz, A., Beil, F. T., Keon, N., Karreth, F., Eferl, R., Scheuch, H., Szremska, A., Amling, M., Schorpp-Kistner, M., Angel, P., and Wagner, E. F. (2004) Mice lacking JunB are osteopenic due to cell-autonomous osteoblast and osteoclast defects. *The Journal of cell biology* **164**, 613-623
231. Passegue, E., and Wagner, E. F. (2000) JunB suppresses cell proliferation by transcriptional activation of p16(INK4a) expression. *The EMBO journal* **19**, 2969-2979
232. Passegue, E., Jochum, W., Schorpp-Kistner, M., Mohle-Steinlein, U., and Wagner, E. F. (2001) Chronic myeloid leukemia with increased

- granulocyte progenitors in mice lacking junB expression in the myeloid lineage. *Cell* **104**, 21-32
233. Wang, Z. Q., Ovitt, C., Grigoriadis, A. E., Mohle-Steinlein, U., Ruther, U., and Wagner, E. F. (1992) Bone and haematopoietic defects in mice lacking c-fos. *Nature* **360**, 741-745
234. Johnson, R. S., Spiegelman, B. M., and Papaioannou, V. (1992) Pleiotropic effects of a null mutation in the c-fos proto-oncogene. *Cell* **71**, 577-586
235. Grigoriadis, A. E., Wang, Z. Q., Cecchini, M. G., Hofstetter, W., Felix, R., Fleisch, H. A., and Wagner, E. F. (1994) c-Fos: a key regulator of osteoclast-macrophage lineage determination and bone remodeling. *Science* **266**, 443-448
236. Santaguida, M., Schepers, K., King, B., Sabnis, A. J., Forsberg, E. C., Attema, J. L., Braun, B. S., and Passegue, E. (2009) JunB protects against myeloid malignancies by limiting hematopoietic stem cell proliferation and differentiation without affecting self-renewal. *Cancer cell* **15**, 341-352
237. Passegue, E., Wagner, E. F., and Weissman, I. L. (2004) JunB deficiency leads to a myeloproliferative disorder arising from hematopoietic stem cells. *Cell* **119**, 431-443
238. Murphy, K. M., and Reiner, S. L. (2002) The lineage decisions of helper T cells. *Nature reviews. Immunology* **2**, 933-944
239. Li, B., Tournier, C., Davis, R. J., and Flavell, R. A. (1999) Regulation of IL-4 expression by the transcription factor JunB during T helper cell differentiation. *The EMBO journal* **18**, 420-432
240. Fang, D., Elly, C., Gao, B., Fang, N., Altman, Y., Joazeiro, C., Hunter, T., Copeland, N., Jenkins, N., and Liu, Y. C. (2002) Dysregulation of T lymphocyte function in itchy mice: a role for Itch in TH2 differentiation. *Nat Immunol* **3**, 281-287
241. Venuprasad, K., Elly, C., Gao, M., Salek-Ardakani, S., Harada, Y., Luo, J. L., Yang, C., Croft, M., Inoue, K., Karin, M., and Liu, Y. C. (2006) Convergence of Itch-induced ubiquitination with MEKK1-JNK signaling in Th2 tolerance and airway inflammation. *J Clin Invest* **116**, 1117-1126
242. Szremska, A. P., Kenner, L., Weisz, E., Ott, R. G., Passegue, E., Artwohl, M., Freissmuth, M., Stoxreiter, R., Theussl, H. C., Parzer, S. B., Moriggl, R., Wagner, E. F., and Sexl, V. (2003) JunB inhibits proliferation and transformation in B-lymphoid cells. *Blood* **102**, 4159-4165
243. Mao, X., and Orchard, G. (2008) Abnormal AP-1 protein expression in primary cutaneous B-cell lymphomas. *The British journal of dermatology* **159**, 145-151
244. Ott, R. G., Simma, O., Kollmann, K., Weisz, E., Zebedin, E. M., Schorpp-Kistner, M., Heller, G., Zochbauer, S., Wagner, E. F., Freissmuth, M., and Sexl, V. (2007) JunB is a gatekeeper for B-lymphoid leukemia. *Oncogene* **26**, 4863-4871
245. Steidl, U., Rosenbauer, F., Verhaak, R. G., Gu, X., Ebralidze, A., Otu, H. H., Klippel, S., Steidl, C., Bruns, I., Costa, D. B., Wagner, K., Aivado, M., Kobbe,

- G., Valk, P. J., Passegue, E., Libermann, T. A., Delwel, R., and Tenen, D. G. (2006) Essential role of Jun family transcription factors in PU.1 knockdown-induced leukemic stem cells. *Nature genetics* **38**, 1269-1277
246. Rosenbauer, F., Wagner, K., Kutok, J. L., Iwasaki, H., Le Beau, M. M., Okuno, Y., Akashi, K., Fiering, S., and Tenen, D. G. (2004) Acute myeloid leukemia induced by graded reduction of a lineage-specific transcription factor, PU.1. *Nature genetics* **36**, 624-630
247. Nakamura, T., Largaespada, D. A., Lee, M. P., Johnson, L. A., Ohyashiki, K., Toyama, K., Chen, S. J., Willman, C. L., Chen, I. M., Feinberg, A. P., Jenkins, N. A., Copeland, N. G., and Shaughnessy, J. D., Jr. (1996) Fusion of the nucleoporin gene NUP98 to HOXA9 by the chromosome translocation t(7;11)(p15;p15) in human myeloid leukaemia. *Nature genetics* **12**, 154-158
248. Lawrence, H. J., Rozenfeld, S., Cruz, C., Matsukuma, K., Kwong, A., Komuves, L., Buchberg, A. M., and Largman, C. (1999) Frequent co-expression of the HOXA9 and MEIS1 homeobox genes in human myeloid leukemias. *Leukemia : official journal of the Leukemia Society of America, Leukemia Research Fund, U.K* **13**, 1993-1999
249. Kroon, E., Kros, J., Thorsteinsdottir, U., Baban, S., Buchberg, A. M., and Sauvageau, G. (1998) Hoxa9 transforms primary bone marrow cells through specific collaboration with Meis1a but not Pbx1b. *The EMBO journal* **17**, 3714-3725
250. Dorsam, S. T., Ferrell, C. M., Dorsam, G. P., Derynck, M. K., Vijapurkar, U., Khodabakhsh, D., Pau, B., Bernstein, H., Haqq, C. M., Largman, C., and Lawrence, H. J. (2004) The transcriptome of the leukemogenic homeoprotein HOXA9 in human hematopoietic cells. *Blood* **103**, 1676-1684
251. Yang, M. Y., Liu, T. C., Chang, J. G., Lin, P. M., and Lin, S. F. (2003) JunB gene expression is inactivated by methylation in chronic myeloid leukemia. *Blood* **101**, 3205-3211
252. Hoshino, K., Quintas-Cardama, A., Radich, J., Dai, H., Yang, H., and Garcia-Manero, G. (2009) Downregulation of JUNB mRNA expression in advanced phase chronic myelogenous leukemia. *Leukemia research* **33**, 1361-1366
253. Strathdee, G., Ferguson, S., Sim, A., and Brown, R. (2010) DNA methylation does not regulate JUNB expression in CML: comment on "Downregulation of JUNB mRNA expression in advanced phase chronic myelogenous leukemia" by Hoshino et al. [Leuk. Res. 33 (2009) 1361-1366]. *Leukemia research* **34**, 685-686
254. Mathas, S., Hinz, M., Anagnostopoulos, I., Krappmann, D., Lietz, A., Jundt, F., Bommert, K., Mehta-Grigoriou, F., Stein, H., Dorken, B., and Scheidereit, C. (2002) Aberrantly expressed c-Jun and JunB are a hallmark of Hodgkin lymphoma cells, stimulate proliferation and synergize with NF-kappa B. *The EMBO journal* **21**, 4104-4113

255. Rassidakis, G. Z., Thomaidis, A., Atwell, C., Ford, R., Jones, D., Claret, F. X., and Medeiros, L. J. (2005) JunB expression is a common feature of CD30+ lymphomas and lymphomatoid papulosis. *Modern pathology : an official journal of the United States and Canadian Academy of Pathology, Inc* **18**, 1365-1370
256. Watanabe, M., Sasaki, M., Itoh, K., Higashihara, M., Umezawa, K., Kadin, M. E., Abraham, L. J., Watanabe, T., and Horie, R. (2005) JunB induced by constitutive CD30-extracellular signal-regulated kinase 1/2 mitogen-activated protein kinase signaling activates the CD30 promoter in anaplastic large cell lymphoma and reed-sternberg cells of Hodgkin lymphoma. *Cancer research* **65**, 7628-7634
257. Watanabe, M., Ogawa, Y., Itoh, K., Koiwa, T., Kadin, M. E., Watanabe, T., Okayasu, I., Higashihara, M., and Horie, R. (2008) Hypomethylation of CD30 CpG islands with aberrant JunB expression drives CD30 induction in Hodgkin lymphoma and anaplastic large cell lymphoma. *Laboratory investigation; a journal of technical methods and pathology* **88**, 48-57
258. Watanabe, M., Ogawa, Y., Ito, K., Higashihara, M., Kadin, M. E., Abraham, L. J., Watanabe, T., and Horie, R. (2003) AP-1 mediated relief of repressive activity of the CD30 promoter microsatellite in Hodgkin and Reed-Sternberg cells. *The American journal of pathology* **163**, 633-641
259. Horie, R., Watanabe, T., Morishita, Y., Ito, K., Ishida, T., Kanegae, Y., Saito, I., Higashihara, M., Mori, S., Kadin, M. E., and Watanabe, T. (2002) Ligand-independent signaling by overexpressed CD30 drives NF-kappaB activation in Hodgkin-Reed-Sternberg cells. *Oncogene* **21**, 2493-2503
260. Watanabe, M., Nakano, K., Togano, T., Nakashima, M., Higashihara, M., Kadin, M. E., Watanabe, T., and Horie, R. (2011) Targeted repression of overexpressed CD30 downregulates NF-kappaB and ERK1/2 pathway in Hodgkin lymphoma cell lines. *Oncology research* **19**, 463-469
261. Horie, R., Higashihara, M., and Watanabe, T. (2003) Hodgkin's lymphoma and CD30 signal transduction. *International journal of hematology* **77**, 37-47
262. Olive, M., Krylov, D., Echlin, D. R., Gardner, K., Taparowsky, E., and Vinson, C. (1997) A dominant negative to activation protein-1 (AP1) that abolishes DNA binding and inhibits oncogenesis. *The Journal of biological chemistry* **272**, 18586-18594
263. Drakos, E., Leventaki, V., Schlette, E. J., Jones, D., Lin, P., Medeiros, L. J., and Rassidakis, G. Z. (2007) c-Jun expression and activation are restricted to CD30+ lymphoproliferative disorders. *The American journal of surgical pathology* **31**, 447-453
264. Geissinger, E., Sadler, P., Roth, S., Grieb, T., Puppe, B., Muller, N., Reimer, P., Vetter-Kauczok, C. S., Wenzel, J., Bonzheim, I., Rudiger, T., Muller-Hermelink, H. K., and Rosenwald, A. (2010) Disturbed expression of the T-cell receptor/CD3 complex and associated signaling molecules in CD30+ T-cell lymphoproliferations. *Haematologica* **95**, 1697-1704

265. Mathas, S., Kreher, S., Meaburn, K. J., Johrens, K., Lamprecht, B., Assaf, C., Sterry, W., Kadin, M. E., Daibata, M., Joos, S., Hummel, M., Stein, H., Janz, M., Anagnostopoulos, I., Schrock, E., Misteli, T., and Dorken, B. (2009) Gene deregulation and spatial genome reorganization near breakpoints prior to formation of translocations in anaplastic large cell lymphoma. *Proceedings of the National Academy of Sciences of the United States of America* **106**, 5831-5836
266. Turner, S. D., Yeung, D., Hadfield, K., Cook, S. J., and Alexander, D. R. (2007) The NPM-ALK tyrosine kinase mimics TCR signalling pathways, inducing NFAT and AP-1 by RAS-dependent mechanisms. *Cellular signalling* **19**, 740-747
267. Ito, M., Zhao, N., Zeng, Z., Chang, C. C., and Zu, Y. (2010) Synergistic growth inhibition of anaplastic large cell lymphoma cells by combining cellular ALK gene silencing and a low dose of the kinase inhibitor U0126. *Cancer gene therapy* **17**, 633-644
268. Ritter, U., Damm-Welk, C., Fuchs, U., Bohle, R. M., Borkhardt, A., and Woessmann, W. (2003) Design and evaluation of chemically synthesized siRNA targeting the NPM-ALK fusion site in anaplastic large cell lymphoma (ALCL). *Oligonucleotides* **13**, 365-373
269. Marzec, M., Kasprzycka, M., Liu, X., Raghunath, P. N., Wlodarski, P., and Wasik, M. A. (2007) Oncogenic tyrosine kinase NPM/ALK induces activation of the MEK/ERK signaling pathway independently of c-Raf. *Oncogene* **26**, 813-821
270. Christensen, J. G., Zou, H. Y., Arango, M. E., Li, Q., Lee, J. H., McDonnell, S. R., Yamazaki, S., Alton, G. R., Mroczkowski, B., and Los, G. (2007) Cytoreductive antitumor activity of PF-2341066, a novel inhibitor of anaplastic lymphoma kinase and c-Met, in experimental models of anaplastic large-cell lymphoma. *Mol Cancer Ther* **6**, 3314-3322
271. Bai, R. Y., Ouyang, T., Miething, C., Morris, S. W., Peschel, C., and Duyster, J. (2000) Nucleophosmin-anaplastic lymphoma kinase associated with anaplastic large-cell lymphoma activates the phosphatidylinositol 3-kinase/Akt antiapoptotic signaling pathway. *Blood* **96**, 4319-4327
272. Slupianek, A., Nieborowska-Skorska, M., Hoser, G., Morrione, A., Majewski, M., Xue, L., Morris, S. W., Wasik, M. A., and Skorski, T. (2001) Role of phosphatidylinositol 3-kinase-Akt pathway in nucleophosmin/anaplastic lymphoma kinase-mediated lymphomagenesis. *Cancer research* **61**, 2194-2199
273. Gu, T. L., Tothova, Z., Scheijen, B., Griffin, J. D., Gilliland, D. G., and Sternberg, D. W. (2004) NPM-ALK fusion kinase of anaplastic large-cell lymphoma regulates survival and proliferative signaling through modulation of FOXO3a. *Blood* **103**, 4622-4629
274. Marzec, M., Kasprzycka, M., Liu, X., El-Salem, M., Halasa, K., Raghunath, P. N., Bucki, R., Wlodarski, P., and Wasik, M. A. (2007) Oncogenic tyrosine

- kinase NPM/ALK induces activation of the rapamycin-sensitive mTOR signaling pathway. *Oncogene* **26**, 5606-5614
275. Vega, F., Medeiros, L. J., Leventaki, V., Atwell, C., Cho-Vega, J. H., Tian, L., Claret, F. X., and Rassidakis, G. Z. (2006) Activation of mammalian target of rapamycin signaling pathway contributes to tumor cell survival in anaplastic lymphoma kinase-positive anaplastic large cell lymphoma. *Cancer research* **66**, 6589-6597
276. Cross, D. A., Alessi, D. R., Cohen, P., Andjelkovich, M., and Hemmings, B. A. (1995) Inhibition of glycogen synthase kinase-3 by insulin mediated by protein kinase B. *Nature* **378**, 785-789
277. McDonnell, S. R., Hwang, S. R., Basrur, V., Conlon, K. P., Fermin, D., Wey, E., Murga-Zamalloa, C., Zeng, Z., Zu, Y., Elenitoba-Johnson, K. S., and Lim, M. S. (2012) NPM-ALK signals through glycogen synthase kinase 3beta to promote oncogenesis. *Oncogene* **31**, 3733-3740
278. Parish, J. L., Rosa, J., Wang, X., Lahti, J. M., Doxsey, S. J., and Androphy, E. J. (2006) The DNA helicase ChIR1 is required for sister chromatid cohesion in mammalian cells. *Journal of cell science* **119**, 4857-4865
279. Laimer, D., Dolznig, H., Kollmann, K., Vesely, P. W., Schlederer, M., Merkel, O., Schiefer, A. I., Hassler, M. R., Heider, S., Amenitsch, L., Thallinger, C., Staber, P. B., Simonitsch-Klupp, I., Artaker, M., Lagger, S., Turner, S. D., Pileri, S., Piccaluga, P. P., Valent, P., Messana, K., Landra, I., Weichhart, T., Knapp, S., Shehata, M., Todaro, M., Sexl, V., Hofler, G., Piva, R., Medico, E., Ruggeri, B. A., Cheng, M., Eferl, R., Egger, G., Penninger, J. M., Jaeger, U., Moriggl, R., Inghirami, G., and Kenner, L. (2012) PDGFR blockade is a rational and effective therapy for NPM-ALK-driven lymphomas. *Nat Med* **18**, 1699-1704
280. Su, I. J., Balk, S. P., and Kadin, M. E. (1988) Molecular basis for the aberrant expression of T cell antigens in postthymic T cell malignancies. *The American journal of pathology* **132**, 192-198
281. Drexler, H. G., and MacLeod, R. A. (2004) Malignant hematopoietic cell lines: in vitro models for the study of anaplastic large-cell lymphoma. *Leukemia : official journal of the Leukemia Society of America, Leukemia Research Fund, U.K* **18**, 1569-1571
282. Kamesaki, H., Fukuhara, S., Tatsumi, E., Uchino, H., Yamabe, H., Miwa, H., Shirakawa, S., Hatanaka, M., and Honjo, T. (1986) Cytochemical, immunologic, chromosomal, and molecular genetic analysis of a novel cell line derived from Hodgkin's disease. *Blood* **68**, 285-292
283. Ross, P. L., Huang, Y. N., Marchese, J. N., Williamson, B., Parker, K., Hattan, S., Khainovski, N., Pillai, S., Dey, S., Daniels, S., Purkayastha, S., Juhász, P., Martin, S., Bartlett-Jones, M., He, F., Jacobson, A., and Pappin, D. J. (2004) Multiplexed protein quantitation in *Saccharomyces cerevisiae* using amine-reactive isobaric tagging reagents. *Mol Cell Proteomics* **3**, 1154-1169

284. Shilov, I. V., Seymour, S. L., Patel, A. A., Loboda, A., Tang, W. H., Keating, S. P., Hunter, C. L., Nuwaysir, L. M., and Schaeffer, D. A. (2007) The Paragon Algorithm, a next generation search engine that uses sequence temperature values and feature probabilities to identify peptides from tandem mass spectra. *Mol Cell Proteomics* **6**, 1638-1655
285. Livak, K. J., and Schmittgen, T. D. (2001) Analysis of relative gene expression data using real-time quantitative PCR and the 2<sup>-</sup>(Delta Delta C(T)) Method. *Methods* **25**, 402-408
286. Bradford, M. M. (1976) A rapid and sensitive method for the quantitation of microgram quantities of protein utilizing the principle of protein-dye binding. *Analytical biochemistry* **72**, 248-254
287. Ewen, C., Kane, K. P., Shostak, I., Griebel, P. J., Bertram, E. M., Watts, T. H., Bleackley, R. C., and McElhane, J. E. (2003) A novel cytotoxicity assay to evaluate antigen-specific CTL responses using a colorimetric substrate for Granzyme B. *J Immunol Methods* **276**, 89-101
288. McDermott, U., Iafrate, A. J., Gray, N. S., Shioda, T., Classon, M., Maheswaran, S., Zhou, W., Choi, H. G., Smith, S. L., Dowell, L., Ulkus, L. E., Kuhlmann, G., Greninger, P., Christensen, J. G., Haber, D. A., and Settleman, J. (2008) Genomic alterations of anaplastic lymphoma kinase may sensitize tumors to anaplastic lymphoma kinase inhibitors. *Cancer research* **68**, 3389-3395
289. Glimcher, L. H., Townsend, M. J., Sullivan, B. M., and Lord, G. M. (2004) Recent developments in the transcriptional regulation of cytolytic effector cells. *Nature reviews. Immunology* **4**, 900-911
290. Hanson, R. D., Grisolano, J. L., and Ley, T. J. (1993) Consensus AP-1 and CRE motifs upstream from the human cytotoxic serine protease B (CSP-B/CGL-1) gene synergize to activate transcription. *Blood* **82**, 2749-2757
291. Babichuk, C. K., and Bleackley, R. C. (1997) Mutational analysis of the murine granzyme B gene promoter in primary T cells and a T cell clone. *The Journal of biological chemistry* **272**, 18564-18571
292. Wargnier, A., Legros-Maida, S., Bosselut, R., Bourge, J. F., Lafaurie, C., Ghysdael, C. J., Sasportes, M., and Paul, P. (1995) Identification of human granzyme B promoter regulatory elements interacting with activated T-cell-specific proteins: implication of Ikaros and CBF binding sites in promoter activation. *Proceedings of the National Academy of Sciences of the United States of America* **92**, 6930-6934
293. Wargnier, A., Lafaurie, C., Legros-Maida, S., Bourge, J. F., Sigaux, F., Sasportes, M., and Paul, P. (1998) Down-regulation of human granzyme B expression by glucocorticoids. Dexamethasone inhibits binding to the Ikaros and AP-1 regulatory elements of the granzyme B promoter. *The Journal of biological chemistry* **273**, 35326-35331
294. Pakala, S. B., Singh, K., Reddy, S. D., Ohshiro, K., Li, D. Q., Mishra, L., and Kumar, R. (2011) TGF-beta1 signaling targets metastasis-associated protein 1, a new effector in epithelial cells. *Oncogene* **30**, 2230-2241

295. Kaminska, B., Kaczmarek, L., and Chaudhuri, A. (1996) Visual stimulation regulates the expression of transcription factors and modulates the composition of AP-1 in visual cortex. *The Journal of neuroscience : the official journal of the Society for Neuroscience* **16**, 3968-3978
296. Baumann, S., Hess, J., Eichhorst, S. T., Krueger, A., Angel, P., Krammer, P. H., and Kirchhoff, S. (2003) An unexpected role for FosB in activation-induced cell death of T cells. *Oncogene* **22**, 1333-1339
297. Kong, H. K., Yoon, S., and Park, J. H. (2012) The regulatory mechanism of the LY6K gene expression in human breast cancer cells. *The Journal of biological chemistry* **287**, 38889-38900
298. Zhang, Q., Wang, H. Y., Liu, X., Bhutani, G., Kantekure, K., and Wasik, M. (2011) IL-2R common gamma-chain is epigenetically silenced by nucleophosphin-anaplastic lymphoma kinase (NPM-ALK) and acts as a tumor suppressor by targeting NPM-ALK. *Proceedings of the National Academy of Sciences of the United States of America* **108**, 11977-11982
299. Zhang, Q., Wang, H. Y., Marzec, M., Raghunath, P. N., Nagasawa, T., and Wasik, M. A. (2005) STAT3- and DNA methyltransferase 1-mediated epigenetic silencing of SHP-1 tyrosine phosphatase tumor suppressor gene in malignant T lymphocytes. *Proceedings of the National Academy of Sciences of the United States of America* **102**, 6948-6953
300. Khoury, J. D., Rassidakis, G. Z., Medeiros, L. J., Amin, H. M., and Lai, R. (2004) Methylation of SHP1 gene and loss of SHP1 protein expression are frequent in systemic anaplastic large cell lymphoma. *Blood* **104**, 1580-1581
301. Han, Y., Amin, H. M., Frantz, C., Franko, B., Lee, J., Lin, Q., and Lai, R. (2006) Restoration of shp1 expression by 5-AZA-2'-deoxycytidine is associated with downregulation of JAK3/STAT3 signaling in ALK-positive anaplastic large cell lymphoma. *Leukemia : official journal of the Leukemia Society of America, Leukemia Research Fund, U.K* **20**, 1602-1609
302. Hagn, M., Schwesinger, E., Ebel, V., Sontheimer, K., Maier, J., Beyer, T., Syrovets, T., Laumonnier, Y., Fabricius, D., Simmet, T., and Jahrsdorfer, B. (2009) Human B cells secrete granzyme B when recognizing viral antigens in the context of the acute phase cytokine IL-21. *Journal of immunology* **183**, 1838-1845
303. Jahrsdorfer, B., Vollmer, A., Blackwell, S. E., Maier, J., Sontheimer, K., Beyer, T., Mandel, B., Lunov, O., Tron, K., Nienhaus, G. U., Simmet, T., Debatin, K. M., Weiner, G. J., and Fabricius, D. (2010) Granzyme B produced by human plasmacytoid dendritic cells suppresses T-cell expansion. *Blood* **115**, 1156-1165
304. Manyak, C. L., Norton, G. P., Lobe, C. G., Bleackley, R. C., Gershenfeld, H. K., Weissman, I. L., Kumar, V., Sigal, N. H., and Koo, G. C. (1989) IL-2 induces expression of serine protease enzymes and genes in natural killer and nonspecific T killer cells. *Journal of immunology* **142**, 3707-3713

305. DeBlaker-Hohe, D. F., Yamauchi, A., Yu, C. R., Horvath-Arcidiacono, J. A., and Bloom, E. T. (1995) IL-12 synergizes with IL-2 to induce lymphokine-activated cytotoxicity and perforin and granzyme gene expression in fresh human NK cells. *Cell Immunol* **165**, 33-43
306. Prakash, M. D., Bird, C. H., and Bird, P. I. (2009) Active and zymogen forms of granzyme B are constitutively released from cytotoxic lymphocytes in the absence of target cell engagement. *Immunol Cell Biol* **87**, 249-254
307. Buzza, M. S., Zamurs, L., Sun, J., Bird, C. H., Smith, A. I., Trapani, J. A., Froelich, C. J., Nice, E. C., and Bird, P. I. (2005) Extracellular matrix remodeling by human granzyme B via cleavage of vitronectin, fibronectin, and laminin. *The Journal of biological chemistry* **280**, 23549-23558
308. Boivin, W. A., Shackelford, M., Vanden Hoek, A., Zhao, H., Hackett, T. L., Knight, D. A., and Granville, D. J. (2012) Granzyme B cleaves decorin, biglycan and soluble betaglycan, releasing active transforming growth factor-beta1. *PloS one* **7**, e33163
309. Froelich, C. J., Zhang, X., Turbov, J., Hudig, D., Winkler, U., and Hanna, W. L. (1993) Human granzyme B degrades aggrecan proteoglycan in matrix synthesized by chondrocytes. *Journal of immunology* **151**, 7161-7171
310. Ganor, Y., Teichberg, V. I., and Levite, M. (2007) TCR activation eliminates glutamate receptor GluR3 from the cell surface of normal human T cells, via an autocrine/paracrine granzyme B-mediated proteolytic cleavage. *Journal of immunology* **178**, 683-692
311. Cullen, S. P., Adrain, C., Luthi, A. U., Duriez, P. J., and Martin, S. J. (2007) Human and murine granzyme B exhibit divergent substrate preferences. *The Journal of cell biology* **176**, 435-444
312. Barry, M., Heibin, J. A., Pinkoski, M. J., Lee, S. F., Moyer, R. W., Green, D. R., and Bleackley, R. C. (2000) Granzyme B short-circuits the need for caspase 8 activity during granule-mediated cytotoxic T-lymphocyte killing by directly cleaving Bid. *Molecular and cellular biology* **20**, 3781-3794
313. Heibin, J. A., Goping, I. S., Barry, M., Pinkoski, M. J., Shore, G. C., Green, D. R., and Bleackley, R. C. (2000) Granzyme B-mediated cytochrome c release is regulated by the Bcl-2 family members bid and Bax. *The Journal of experimental medicine* **192**, 1391-1402
314. Sutton, V. R., Davis, J. E., Cancilla, M., Johnstone, R. W., Ruefli, A. A., Sedelies, K., Browne, K. A., and Trapani, J. A. (2000) Initiation of apoptosis by granzyme B requires direct cleavage of bid, but not direct granzyme B-mediated caspase activation. *The Journal of experimental medicine* **192**, 1403-1414
315. Pinkoski, M. J., Waterhouse, N. J., Heibin, J. A., Wolf, B. B., Kuwana, T., Goldstein, J. C., Newmeyer, D. D., Bleackley, R. C., and Green, D. R. (2001) Granzyme B-mediated apoptosis proceeds predominantly through a Bcl-2-inhibitable mitochondrial pathway. *The Journal of biological chemistry* **276**, 12060-12067

316. Han, J., Goldstein, L. A., Gastman, B. R., Froelich, C. J., Yin, X. M., and Rabinowich, H. (2004) Degradation of Mcl-1 by granzyme B: implications for Bim-mediated mitochondrial apoptotic events. *The Journal of biological chemistry* **279**, 22020-22029
317. Adrain, C., Murphy, B. M., and Martin, S. J. (2005) Molecular ordering of the caspase activation cascade initiated by the cytotoxic T lymphocyte/natural killer (CTL/NK) protease granzyme B. *The Journal of biological chemistry* **280**, 4663-4673
318. Martin, S. J., Amarante-Mendes, G. P., Shi, L., Chuang, T. H., Casiano, C. A., O'Brien, G. A., Fitzgerald, P., Tan, E. M., Bokoch, G. M., Greenberg, A. H., and Green, D. R. (1996) The cytotoxic cell protease granzyme B initiates apoptosis in a cell-free system by proteolytic processing and activation of the ICE/CED-3 family protease, CPP32, via a novel two-step mechanism. *The EMBO journal* **15**, 2407-2416
319. Darmon, A. J., Nicholson, D. W., and Bleackley, R. C. (1995) Activation of the apoptotic protease CPP32 by cytotoxic T-cell-derived granzyme B. *Nature* **377**, 446-448
320. Medema, J. P., Toes, R. E., Scaffidi, C., Zheng, T. S., Flavell, R. A., Melief, C. J., Peter, M. E., Offringa, R., and Krammer, P. H. (1997) Cleavage of FLICE (caspase-8) by granzyme B during cytotoxic T lymphocyte-induced apoptosis. *European journal of immunology* **27**, 3492-3498
321. Gu, Y., Sarnecki, C., Fleming, M. A., Lippke, J. A., Bleackley, R. C., and Su, M. S. (1996) Processing and activation of CMH-1 by granzyme B. *The Journal of biological chemistry* **271**, 10816-10820
322. Zhang, D., Beresford, P. J., Greenberg, A. H., and Lieberman, J. (2001) Granzymes A and B directly cleave lamins and disrupt the nuclear lamina during granule-mediated cytolysis. *Proceedings of the National Academy of Sciences of the United States of America* **98**, 5746-5751
323. Thomas, D. A., Du, C., Xu, M., Wang, X., and Ley, T. J. (2000) DFF45/ICAD can be directly processed by granzyme B during the induction of apoptosis. *Immunity* **12**, 621-632
324. Froelich, C. J., Hanna, W. L., Poirier, G. G., Duriez, P. J., D'Amours, D., Salvesen, G. S., Alnemri, E. S., Earnshaw, W. C., and Shah, G. M. (1996) Granzyme B/perforin-mediated apoptosis of Jurkat cells results in cleavage of poly(ADP-ribose) polymerase to the 89-kDa apoptotic fragment and less abundant 64-kDa fragment. *Biochemical and biophysical research communications* **227**, 658-665
325. D'Eliseo, D., Pisu, P., Romano, C., Tubaro, A., De Nunzio, C., Morrone, S., Santoni, A., Stoppacciaro, A., and Velotti, F. (2010) Granzyme B is expressed in urothelial carcinoma and promotes cancer cell invasion. *International journal of cancer. Journal international du cancer* **127**, 1283-1294
326. Lagarrigue, F., Dupuis-Coronas, S., Ramel, D., Delsol, G., Tronchere, H., Payrastre, B., and Gaits-Iacovoni, F. (2010) Matrix Metalloproteinase-9 Is

Upregulated in Nucleophosmin-Anaplastic Lymphoma Kinase-Positive Anaplastic Lymphomas and Activated at the Cell Surface by the Chaperone Heat Shock Protein 90 to Promote Cell Invasion. *Cancer research*

327. Rassidakis, G. Z., Sarris, A. H., Herling, M., Ford, R. J., Cabanillas, F., McDonnell, T. J., and Medeiros, L. J. (2001) Differential expression of BCL-2 family proteins in ALK-positive and ALK-negative anaplastic large cell lymphoma of T/null-cell lineage. *The American journal of pathology* **159**, 527-535
328. Drakos, E., Rassidakis, G. Z., Lai, R., Herling, M., O'Connor, S. L., Schmitt-Graeff, A., McDonnell, T. J., and Medeiros, L. J. (2004) Caspase-3 activation in systemic anaplastic large-cell lymphoma. *Modern pathology : an official journal of the United States and Canadian Academy of Pathology, Inc* **17**, 109-116
329. Rassidakis, G. Z., Jones, D., Thomaidis, A., Sen, F., Lai, R., Cabanillas, F., McDonnell, T. J., and Medeiros, L. J. (2002) Apoptotic rate in peripheral T-cell lymphomas. A study using a tissue microarray with validation on full tissue sections. *American journal of clinical pathology* **118**, 328-334
330. Zhang, B., Zhang, J., and Tian, Z. (2008) Comparison in the effects of IL-2, IL-12, IL-15 and IFNalpha on gene regulation of granzymes of human NK cell line NK-92. *International immunopharmacology* **8**, 989-996
331. Wu, L., Zhang, C., and Zhang, J. (2011) HMBOX1 negatively regulates NK cell functions by suppressing the NKG2D/DAP10 signaling pathway. *Cellular & molecular immunology* **8**, 433-440
332. Caputo, A., Garner, R. S., Winkler, U., Hudig, D., and Bleackley, R. C. (1993) Activation of recombinant murine cytotoxic cell proteinase-1 requires deletion of an amino-terminal dipeptide. *The Journal of biological chemistry* **268**, 17672-17675
333. Smyth, M. J., McGuire, M. J., and Thia, K. Y. (1995) Expression of recombinant human granzyme B. A processing and activation role for dipeptidyl peptidase I. *Journal of immunology* **154**, 6299-6305
334. Pham, C. T., Thomas, D. A., Mercer, J. D., and Ley, T. J. (1998) Production of fully active recombinant murine granzyme B in yeast. *The Journal of biological chemistry* **273**, 1629-1633
335. Sutton, V. R., Waterhouse, N. J., Browne, K. A., Sedelies, K., Ciccone, A., Anthony, D., Koskinen, A., Mullbacher, A., and Trapani, J. A. (2007) Residual active granzyme B in cathepsin C-null lymphocytes is sufficient for perforin-dependent target cell apoptosis. *The Journal of cell biology* **176**, 425-433
336. Pham, C. T., and Ley, T. J. (1999) Dipeptidyl peptidase I is required for the processing and activation of granzymes A and B in vivo. *Proceedings of the National Academy of Sciences of the United States of America* **96**, 8627-8632

337. D'Angelo, M. E., Bird, P. I., Peters, C., Reinheckel, T., Trapani, J. A., and Sutton, V. R. (2010) Cathepsin H is an additional convertase of pro-granzyme B. *The Journal of biological chemistry* **285**, 20514-20519
338. Nebenfuhr, A., Ritzenthaler, C., and Robinson, D. G. (2002) Brefeldin A: deciphering an enigmatic inhibitor of secretion. *Plant Physiol* **130**, 1102-1108
339. Colomba, A., Giuriato, S., Dejean, E., Thornber, K., Delsol, G., Tronchere, H., Meggetto, F., Payrastre, B., and Gaits-iacovoni, F. (2011) Inhibition of Rac controls NPM-ALK-dependent lymphoma development and dissemination. *Blood cancer journal* **1**, e21
340. Gelebart, P., Hegazy, S. A., Wang, P., Bone, K. M., Anand, M., Sharon, D., Hitt, M., Pearson, J. D., Ingham, R. J., Ma, Y., and Lai, R. (2012) Aberrant expression and biological significance of Sox2, an embryonic stem cell transcriptional factor, in ALK-positive anaplastic large cell lymphoma. *Blood cancer journal* **2**, e82
341. Goping, I. S., Sawchuk, T., Underhill, D. A., and Bleackley, R. C. (2006) Identification of  $\alpha$ -tubulin as a granzyme B substrate during CTL-mediated apoptosis. *Journal of cell science* **119**, 858-865
342. Adrain, C., Duriez, P. J., Brumatti, G., Delivani, P., and Martin, S. J. (2006) The cytotoxic lymphocyte protease, granzyme B, targets the cytoskeleton and perturbs microtubule polymerization dynamics. *The Journal of biological chemistry* **281**, 8118-8125
343. Ko, Y. H., Park, S., Jin, H., Woo, H., Lee, H., Park, C., and Kim, K. (2007) Granzyme B leakage-induced apoptosis is a crucial mechanism of cell death in nasal-type NK/T-cell lymphoma. *Laboratory investigation; a journal of technical methods and pathology* **87**, 241-250
344. Ida, H., Nakashima, T., Kedersha, N. L., Yamasaki, S., Huang, M., Izumi, Y., Miyashita, T., Origuchi, T., Kawakami, A., Migita, K., Bird, P. I., Anderson, P., and Eguchi, K. (2003) Granzyme B leakage-induced cell death: a new type of activation-induced natural killer cell death. *European journal of immunology* **33**, 3284-3292
345. Nicholson, D. W., Ali, A., Thornberry, N. A., Vaillancourt, J. P., Ding, C. K., Gallant, M., Gareau, Y., Griffin, P. R., Labelle, M., Lazebnik, Y. A., and et al. (1995) Identification and inhibition of the ICE/CED-3 protease necessary for mammalian apoptosis. *Nature* **376**, 37-43
346. Tewari, M., Quan, L. T., O'Rourke, K., Desnoyers, S., Zeng, Z., Beidler, D. R., Poirier, G. G., Salvesen, G. S., and Dixit, V. M. (1995) Yama/CPP32 beta, a mammalian homolog of CED-3, is a CrmA-inhibitable protease that cleaves the death substrate poly(ADP-ribose) polymerase. *Cell* **81**, 801-809
347. Kaufmann, S. H., Desnoyers, S., Ottaviano, Y., Davidson, N. E., and Poirier, G. G. (1993) Specific proteolytic cleavage of poly(ADP-ribose) polymerase: an early marker of chemotherapy-induced apoptosis. *Cancer research* **53**, 3976-3985

348. Lazebnik, Y. A., Kaufmann, S. H., Desnoyers, S., Poirier, G. G., and Earnshaw, W. C. (1994) Cleavage of poly(ADP-ribose) polymerase by a proteinase with properties like ICE. *Nature* **371**, 346-347
349. Lippke, J. A., Gu, Y., Sarnecki, C., Caron, P. R., and Su, M. S. (1996) Identification and characterization of CPP32/Mch2 homolog 1, a novel cysteine protease similar to CPP32. *The Journal of biological chemistry* **271**, 1825-1828
350. Slee, E. A., Adrain, C., and Martin, S. J. (2001) Executioner caspase-3, -6, and -7 perform distinct, non-redundant roles during the demolition phase of apoptosis. *The Journal of biological chemistry* **276**, 7320-7326
351. Gavrieli, Y., Sherman, Y., and Ben-Sasson, S. A. (1992) Identification of programmed cell death in situ via specific labeling of nuclear DNA fragmentation. *The Journal of cell biology* **119**, 493-501
352. Gorczyca, W., Bigman, K., Mittelman, A., Ahmed, T., Gong, J., Melamed, M. R., and Darzynkiewicz, Z. (1993) Induction of DNA strand breaks associated with apoptosis during treatment of leukemias. *Leukemia : official journal of the Leukemia Society of America, Leukemia Research Fund, U.K* **7**, 659-670
353. Gold, R., Schmied, M., Giegerich, G., Breitschopf, H., Hartung, H. P., Toyka, K. V., and Lassmann, H. (1994) Differentiation between cellular apoptosis and necrosis by the combined use of in situ tailing and nick translation techniques. *Laboratory investigation; a journal of technical methods and pathology* **71**, 219-225
354. Hsu, F. Y., Zhao, Y., Anderson, W. F., and Johnston, P. B. (2007) Downregulation of NPM-ALK by siRNA causes anaplastic large cell lymphoma cell growth inhibition and augments the anti cancer effects of chemotherapy in vitro. *Cancer investigation* **25**, 240-248
355. Grossman, W. J., Verbsky, J. W., Tollefsen, B. L., Kemper, C., Atkinson, J. P., and Ley, T. J. (2004) Differential expression of granzymes A and B in human cytotoxic lymphocyte subsets and T regulatory cells. *Blood* **104**, 2840-2848
356. Bade, B., Boettcher, H. E., Lohrmann, J., Hink-Schauer, C., Bratke, K., Jenne, D. E., Virchow, J. C., Jr., and Luttmann, W. (2005) Differential expression of the granzymes A, K and M and perforin in human peripheral blood lymphocytes. *International immunology* **17**, 1419-1428
357. Bratke, K., Kuepper, M., Bade, B., Virchow, J. C., Jr., and Luttmann, W. (2005) Differential expression of human granzymes A, B, and K in natural killer cells and during CD8+ T cell differentiation in peripheral blood. *European journal of immunology* **35**, 2608-2616
358. Griffiths, G. M., and Isaaz, S. (1993) Granzymes A and B are targeted to the lytic granules of lymphocytes by the mannose-6-phosphate receptor. *The Journal of cell biology* **120**, 885-896
359. Sato, T., Yamochi, T., Aytac, U., Ohnuma, K., McKee, K. S., Morimoto, C., and Dang, N. H. (2005) CD26 regulates p38 mitogen-activated protein

- kinase-dependent phosphorylation of integrin beta1, adhesion to extracellular matrix, and tumorigenicity of T-anaplastic large cell lymphoma Karpas 299. *Cancer research* **65**, 6950-6956
360. Loeb, C. R., Harris, J. L., and Craik, C. S. (2006) Granzyme B proteolyzes receptors important to proliferation and survival, tipping the balance toward apoptosis. *The Journal of biological chemistry* **281**, 28326-28335
361. van Tetering, G., Bovenschen, N., Meeldijk, J., van Diest, P. J., and Vooijs, M. (2011) Cleavage of Notch1 by granzyme B disables its transcriptional activity. *The Biochemical journal* **437**, 313-322
362. Hostetter, D. R., Loeb, C. R., Chu, F., and Craik, C. S. (2007) Hip is a pro-survival substrate of granzyme B. *The Journal of biological chemistry* **282**, 27865-27874
363. Bredemeyer, A. J., Lewis, R. M., Malone, J. P., Davis, A. E., Gross, J., Townsend, R. R., and Ley, T. J. (2004) A proteomic approach for the discovery of protease substrates. *Proceedings of the National Academy of Sciences of the United States of America* **101**, 11785-11790
364. Mahoney, J. A., Odin, J. A., White, S. M., Shaffer, D., Koff, A., Casciola-Rosen, L., and Rosen, A. (2002) The human homologue of the yeast polyubiquitination factor Ufd2p is cleaved by caspase 6 and granzyme B during apoptosis. *The Biochemical journal* **361**, 587-595
365. Georgakis, G. V., Li, Y., Rassidakis, G. Z., Medeiros, L. J., and Younes, A. (2006) The HSP90 inhibitor 17-AAG synergizes with doxorubicin and U0126 in anaplastic large cell lymphoma irrespective of ALK expression. *Experimental hematology* **34**, 1670-1679
366. Bonvini, P., Gastaldi, T., Falini, B., and Rosolen, A. (2002) Nucleophosmin-anaplastic lymphoma kinase (NPM-ALK), a novel Hsp90-client tyrosine kinase: down-regulation of NPM-ALK expression and tyrosine phosphorylation in ALK(+) CD30(+) lymphoma cells by the Hsp90 antagonist 17-allylamino,17-demethoxygeldanamycin. *Cancer research* **62**, 1559-1566
367. Bonvini, P., Dalla Rosa, H., Vignes, N., and Rosolen, A. (2004) Ubiquitination and proteasomal degradation of nucleophosmin-anaplastic lymphoma kinase induced by 17-allylamino-demethoxygeldanamycin: role of the co-chaperone carboxyl heat shock protein 70-interacting protein. *Cancer research* **64**, 3256-3264
368. Schumacher, J. A., Crockett, D. K., Elenitoba-Johnson, K. S., and Lim, M. S. (2007) Proteome-wide changes induced by the Hsp90 inhibitor, geldanamycin in anaplastic large cell lymphoma cells. *Proteomics* **7**, 2603-2616
369. Trepel, J., Mollapour, M., Giaccone, G., and Neckers, L. (2010) Targeting the dynamic HSP90 complex in cancer. *Nat Rev Cancer* **10**, 537-549
370. Taipale, M., Jarosz, D. F., and Lindquist, S. (2010) HSP90 at the hub of protein homeostasis: emerging mechanistic insights. *Nat Rev Mol Cell Biol* **11**, 515-528

371. Xu, W., Mimnaugh, E., Rosser, M. F., Nicchitta, C., Marcu, M., Yarden, Y., and Neckers, L. (2001) Sensitivity of mature ErbB2 to geldanamycin is conferred by its kinase domain and is mediated by the chaperone protein Hsp90. *The Journal of biological chemistry* **276**, 3702-3708
372. Xu, W., Marcu, M., Yuan, X., Mimnaugh, E., Patterson, C., and Neckers, L. (2002) Chaperone-dependent E3 ubiquitin ligase CHIP mediates a degradative pathway for c-ErbB2/Neu. *Proceedings of the National Academy of Sciences of the United States of America* **99**, 12847-12852
373. An, W. G., Schulte, T. W., and Neckers, L. M. (2000) The heat shock protein 90 antagonist geldanamycin alters chaperone association with p210bcr-abl and v-src proteins before their degradation by the proteasome. *Cell growth & differentiation : the molecular biology journal of the American Association for Cancer Research* **11**, 355-360
374. McDonough, H., and Patterson, C. (2003) CHIP: a link between the chaperone and proteasome systems. *Cell stress & chaperones* **8**, 303-308
375. Theodoraki, M. A., Kunjappu, M., Sternberg, D. W., and Caplan, A. J. (2007) Akt shows variable sensitivity to an Hsp90 inhibitor depending on cell context. *Experimental cell research* **313**, 3851-3858
376. Chen, Z., Sasaki, T., Tan, X., Carretero, J., Shimamura, T., Li, D., Xu, C., Wang, Y., Adelmant, G. O., Capelletti, M., Lee, H. J., Rodig, S. J., Borgman, C., Park, S. I., Kim, H. R., Padera, R., Marto, J. A., Gray, N. S., Kung, A. L., Shapiro, G. I., Janne, P. A., and Wong, K. K. (2010) Inhibition of ALK, PI3K/MEK, and HSP90 in murine lung adenocarcinoma induced by EML4-ALK fusion oncogene. *Cancer Res* **70**, 9827-9836
377. Normant, E., Paez, G., West, K. A., Lim, A. R., Slocum, K. L., Tunkey, C., McDougall, J., Wylie, A. A., Robison, K., Caliri, K., Palombella, V. J., and Fritz, C. C. (2011) The Hsp90 inhibitor IPI-504 rapidly lowers EML4-ALK levels and induces tumor regression in ALK-driven NSCLC models. *Oncogene* **30**, 2581-2586
378. Katayama, R., Khan, T. M., Benes, C., Lifshits, E., Ebi, H., Rivera, V. M., Shakespeare, W. C., Iafrate, A. J., Engelman, J. A., and Shaw, A. T. (2011) Therapeutic strategies to overcome crizotinib resistance in non-small cell lung cancers harboring the fusion oncogene EML4-ALK. *Proceedings of the National Academy of Sciences of the United States of America* **108**, 7535-7540
379. Sequist, L. V., Gettinger, S., Senzer, N. N., Martins, R. G., Janne, P. A., Lilenbaum, R., Gray, J. E., Iafrate, A. J., Katayama, R., Hafeez, N., Sweeney, J., Walker, J. R., Fritz, C., Ross, R. W., Grayzel, D., Engelman, J. A., Borger, D. R., Paez, G., and Natale, R. (2010) Activity of IPI-504, a novel heat-shock protein 90 inhibitor, in patients with molecularly defined non-small-cell lung cancer. *Journal of clinical oncology : official journal of the American Society of Clinical Oncology* **28**, 4953-4960
380. Sasaki, T., Okuda, K., Zheng, W., Butrynski, J., Capelletti, M., Wang, L., Gray, N. S., Wilner, K., Christensen, J. G., Demetri, G., Shapiro, G. I., Rodig,

- S. J., Eck, M. J., and Janne, P. A. (2010) The neuroblastoma-associated F1174L ALK mutation causes resistance to an ALK kinase inhibitor in ALK-translocated cancers. *Cancer research* **70**, 10038-10043
381. Ratajczak, T., Ward, B. K., and Minchin, R. F. (2003) Immunophilin chaperones in steroid receptor signalling. *Curr Top Med Chem* **3**, 1348-1357
382. Ratajczak, T., Ward, B. K., Cluning, C., and Allan, R. K. (2009) Cyclophilin 40: an Hsp90-cochaperone associated with apo-steroid receptors. *Int J Biochem Cell Biol* **41**, 1652-1655
383. Davies, T. H., and Sanchez, E. R. (2005) Fkbp52. *Int J Biochem Cell Biol* **37**, 42-47
384. Li, L., Lou, Z., and Wang, L. (2011) The role of FKBP5 in cancer aetiology and chemoresistance. *British journal of cancer* **104**, 19-23
385. Denny, W. B., Valentine, D. L., Reynolds, P. D., Smith, D. F., and Scammell, J. G. (2000) Squirrel monkey immunophilin FKBP51 is a potent inhibitor of glucocorticoid receptor binding. *Endocrinology* **141**, 4107-4113
386. Riggs, D. L., Roberts, P. J., Chirillo, S. C., Cheung-Flynn, J., Prapapanich, V., Ratajczak, T., Gaber, R., Picard, D., and Smith, D. F. (2003) The Hsp90-binding peptidylprolyl isomerase FKBP52 potentiates glucocorticoid signaling in vivo. *The EMBO journal* **22**, 1158-1167
387. Wochnik, G. M., Ruegg, J., Abel, G. A., Schmidt, U., Holsboer, F., and Rein, T. (2005) FK506-binding proteins 51 and 52 differentially regulate dynein interaction and nuclear translocation of the glucocorticoid receptor in mammalian cells. *The Journal of biological chemistry* **280**, 4609-4616
388. Warriar, M., Hinds, T. D., Jr., Ledford, K. J., Cash, H. A., Patel, P. R., Bowman, T. A., Stechschulte, L. A., Yong, W., Shou, W., Najjar, S. M., and Sanchez, E. R. (2010) Susceptibility to diet-induced hepatic steatosis and glucocorticoid resistance in FK506-binding protein 52-deficient mice. *Endocrinology* **151**, 3225-3236
389. Davies, T. H., Ning, Y. M., and Sanchez, E. R. (2005) Differential control of glucocorticoid receptor hormone-binding function by tetratricopeptide repeat (TPR) proteins and the immunosuppressive ligand FK506. *Biochemistry* **44**, 2030-2038
390. Scroggins, B. T., Prince, T., Shao, J., Uma, S., Huang, W., Guo, Y., Yun, B. G., Hedman, K., Matts, R. L., and Hartson, S. D. (2003) High affinity binding of Hsp90 is triggered by multiple discrete segments of its kinase clients. *Biochemistry* **42**, 12550-12561
391. Nair, S. C., Toran, E. J., Rimerman, R. A., Hjermstad, S., Smithgall, T. E., and Smith, D. F. (1996) A pathway of multi-chaperone interactions common to diverse regulatory proteins: estrogen receptor, Fes tyrosine kinase, heat shock transcription factor Hsf1, and the aryl hydrocarbon receptor. *Cell stress & chaperones* **1**, 237-250

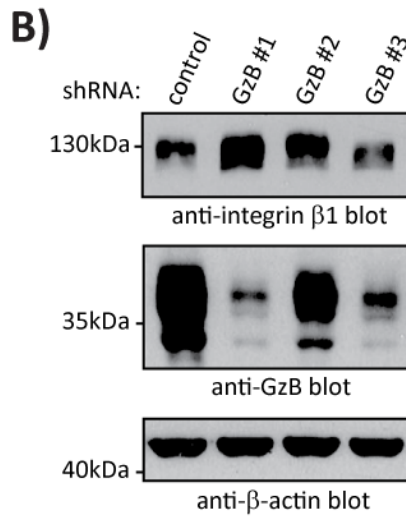
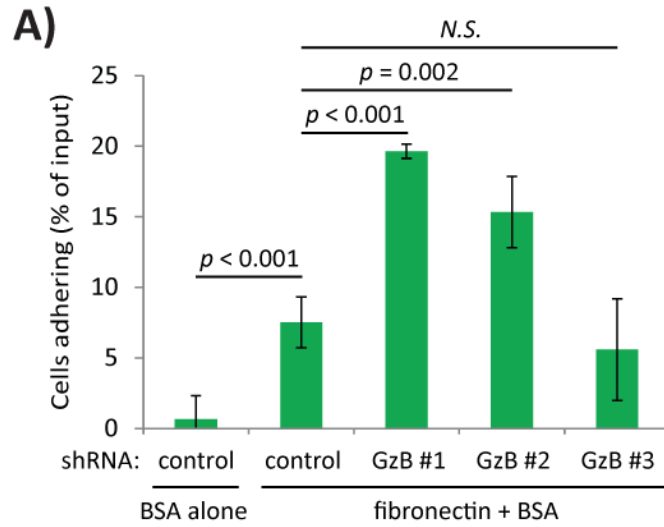
392. Duina, A. A., Chang, H. C., Marsh, J. A., Lindquist, S., and Gaber, R. F. (1996) A cyclophilin function in Hsp90-dependent signal transduction. *Science* **274**, 1713-1715
393. Periyasamy, S., Hinds, T., Jr., Shemshedini, L., Shou, W., and Sanchez, E. R. (2010) FKBP51 and Cyp40 are positive regulators of androgen-dependent prostate cancer cell growth and the targets of FK506 and cyclosporin A. *Oncogene* **29**, 1691-1701
394. Kumar, P., Ward, B. K., Minchin, R. F., and Ratajczak, T. (2001) Regulation of the Hsp90-binding immunophilin, cyclophilin 40, is mediated by multiple sites for GA-binding protein (GABP). *Cell stress & chaperones* **6**, 78-91
395. Pearson, J. D., Lee, J. K., Bacani, J. T., Lai, R., and Ingham, R. J. (2011) NPM-ALK and the JunB transcription factor regulate the expression of cytotoxic molecules in ALK-positive, anaplastic large cell lymphoma. *Int J Clin Exp Pathol* **4**, 124-133
396. Kimura, H., Nakajima, T., Takeuchi, K., Soda, M., Mano, H., Iizasa, T., Matsui, Y., Yoshino, M., Shingyoji, M., Itakura, M., Itami, M., Ikebe, D., Yokoi, S., Kageyama, H., Ohira, M., and Nakagawara, A. (2012) ALK fusion gene positive lung cancer and 3 cases treated with an inhibitor for ALK kinase activity. *Lung Cancer* **75**, 66-72
397. Kijima, T., Takeuchi, K., Tetsumoto, S., Shimada, K., Takahashi, R., Hirata, H., Nagatomo, I., Hoshino, S., Takeda, Y., Kida, H., Goya, S., Tachibana, I., and Kawase, I. (2011) Favorable response to crizotinib in three patients with echinoderm microtubule-associated protein-like 4-anaplastic lymphoma kinase fusion-type oncogene-positive non-small cell lung cancer. *Cancer Sci* **102**, 1602-1604
398. Tartari, C. J., Gunby, R. H., Coluccia, A. M., Sottocornola, R., Cimbro, B., Scapozza, L., Donella-Deana, A., Pinna, L. A., and Gambacorti-Passerini, C. (2008) Characterization of some molecular mechanisms governing autoactivation of the catalytic domain of the anaplastic lymphoma kinase. *The Journal of biological chemistry* **283**, 3743-3750
399. Wang, P., Wu, F., Ma, Y., Li, L., Lai, R., and Young, L. C. (2010) Functional characterization of the kinase activation loop in nucleophosmin (NPM)-anaplastic lymphoma kinase (ALK) using tandem affinity purification and liquid chromatography-mass spectrometry. *The Journal of biological chemistry* **285**, 95-103
400. Zhang, Q., Raghunath, P. N., Xue, L., Majewski, M., Carpentieri, D. F., Odum, N., Morris, S., Skorski, T., and Wasik, M. A. (2002) Multilevel dysregulation of STAT3 activation in anaplastic lymphoma kinase-positive T/null-cell lymphoma. *Journal of immunology* **168**, 466-474
401. Zamo, A., Chiarle, R., Piva, R., Howes, J., Fan, Y., Chilosi, M., Levy, D. E., and Inghirami, G. (2002) Anaplastic lymphoma kinase (ALK) activates Stat3 and protects hematopoietic cells from cell death. *Oncogene* **21**, 1038-1047

402. Wan, W., Albom, M. S., Lu, L., Quail, M. R., Becknell, N. C., Weinberg, L. R., Reddy, D. R., Holskin, B. P., Angeles, T. S., Underiner, T. L., Meyer, S. L., Hudkins, R. L., Dorsey, B. D., Ator, M. A., Ruggeri, B. A., and Cheng, M. (2006) Anaplastic lymphoma kinase activity is essential for the proliferation and survival of anaplastic large-cell lymphoma cells. *Blood* **107**, 1617-1623
403. Nair, S. C., Rimerman, R. A., Toran, E. J., Chen, S., Prapapanich, V., Butts, R. N., and Smith, D. F. (1997) Molecular cloning of human FKBP51 and comparisons of immunophilin interactions with Hsp90 and progesterone receptor. *Molecular and cellular biology* **17**, 594-603
404. Barent, R. L., Nair, S. C., Carr, D. C., Ruan, Y., Rimerman, R. A., Fulton, J., Zhang, Y., and Smith, D. F. (1998) Analysis of FKBP51/FKBP52 chimeras and mutants for Hsp90 binding and association with progesterone receptor complexes. *Mol Endocrinol* **12**, 342-354
405. Schaefer, T. S., Sanders, L. K., Park, O. K., and Nathans, D. (1997) Functional differences between Stat3alpha and Stat3beta. *Molecular and cellular biology* **17**, 5307-5316
406. Schaefer, L. K., Wang, S., and Schaefer, T. S. (1999) c-Src activates the DNA binding and transcriptional activity of Stat3 molecules: serine 727 is not required for transcriptional activation under certain circumstances. *Biochemical and biophysical research communications* **266**, 481-487
407. Kaptein, A., Paillard, V., and Saunders, M. (1996) Dominant negative stat3 mutant inhibits interleukin-6-induced Jak-STAT signal transduction. *The Journal of biological chemistry* **271**, 5961-5964
408. Romano, S., D'Angelillo, A., Pacelli, R., Staibano, S., De Luna, E., Bisogni, R., Eskelinen, E. L., Mascolo, M., Cali, G., Arra, C., and Romano, M. F. (2010) Role of FK506-binding protein 51 in the control of apoptosis of irradiated melanoma cells. *Cell death and differentiation* **17**, 145-157
409. Pei, H., Li, L., Fridley, B. L., Jenkins, G. D., Kalari, K. R., Lingle, W., Petersen, G., Lou, Z., and Wang, L. (2009) FKBP51 affects cancer cell response to chemotherapy by negatively regulating Akt. *Cancer cell* **16**, 259-266
410. Levenson, J. D., and Ness, S. A. (1998) Point mutations in v-Myb disrupt a cyclophilin-catalyzed negative regulatory mechanism. *Mol Cell* **1**, 203-211
411. Whitesell, L., Sutphin, P. D., Pulcini, E. J., Martinez, J. D., and Cook, P. H. (1998) The physical association of multiple molecular chaperone proteins with mutant p53 is altered by geldanamycin, an hsp90-binding agent. *Molecular and cellular biology* **18**, 1517-1524
412. Park, M. S., Chu, F., Xie, J., Wang, Y., Bhattacharya, P., and Chan, W. K. (2011) Identification of cyclophilin-40-interacting proteins reveals potential cellular function of cyclophilin-40. *Analytical biochemistry* **410**, 257-265
413. Smith, M. R., Willmann, M. R., Wu, G., Berardini, T. Z., Moller, B., Weijers, D., and Poethig, R. S. (2009) Cyclophilin 40 is required for microRNA

- activity in Arabidopsis. *Proceedings of the National Academy of Sciences of the United States of America* **106**, 5424-5429
414. Smith, J. R., Clarke, P. A., de Billy, E., and Workman, P. (2009) Silencing the cochaperone CDC37 destabilizes kinase clients and sensitizes cancer cells to HSP90 inhibitors. *Oncogene* **28**, 157-169
415. Wu, F., Wang, P., Young, L. C., Lai, R., and Li, L. (2009) Proteome-wide identification of novel binding partners to the oncogenic fusion gene protein, NPM-ALK, using tandem affinity purification and mass spectrometry. *The American journal of pathology* **174**, 361-370
416. Solito, E., de Coupade, C., Parente, L., Flower, R. J., and Russo-Marie, F. (1998) Human annexin 1 is highly expressed during the differentiation of the epithelial cell line A 549: involvement of nuclear factor interleukin 6 in phorbol ester induction of annexin 1. *Cell growth & differentiation : the molecular biology journal of the American Association for Cancer Research* **9**, 327-336
417. Nakamura, T., Okuyama, S., Okamoto, S., Nakajima, T., Sekiya, S., and Oda, K. (1995) Down-regulation of the cyclin A promoter in differentiating human embryonal carcinoma cells is mediated by depletion of ATF-1 and ATF-2 in the complex at the ATF/CRE site. *Experimental cell research* **216**, 422-430
418. Yam, C. H., Fung, T. K., and Poon, R. Y. (2002) Cyclin A in cell cycle control and cancer. *Cellular and molecular life sciences : CMLS* **59**, 1317-1326
419. Oudejans, J. J., Kummer, J. A., Jiwa, M., van der Valk, P., Ossenkoppele, G. J., Kluin, P. M., Kluin-Nelemans, J. C., and Meijer, C. J. (1996) Granzyme B expression in Reed-Sternberg cells of Hodgkin's disease. *The American journal of pathology* **148**, 233-240
420. Asano, N., Oshiro, A., Matsuo, K., Kagami, Y., Ishida, F., Suzuki, R., Kinoshita, T., Shimoyama, Y., Tamaru, J., Yoshino, T., Kitamura, K., Fukutani, H., Morishima, Y., and Nakamura, S. (2006) Prognostic significance of T-cell or cytotoxic molecules phenotype in classical Hodgkin's lymphoma: a clinicopathologic study. *Journal of clinical oncology : official journal of the American Society of Clinical Oncology* **24**, 4626-4633
421. Sakuma, I., Yoshino, T., Omonishi, K., Nishiuchi, R., Teramoto, N., Yanai, H., Kawahara, K., Kubonishi, I., Matsuo, Y., and Akagi, T. (1999) CD95 ligand is expressed in Reed-Sternberg cells of Hodgkin's disease. *Pathology international* **49**, 103-109
422. Asano, N., Suzuki, R., Matsuo, K., Kagami, Y., Ishida, F., Tamaru, J. I., Jin, G. S., Sato, Y., Shimoyama, Y., Yoshino, T., Morishima, Y., and Nakamura, S. (2007) Cytotoxic molecule expression is predictive of prognosis in Hodgkin's-like anaplastic large cell lymphoma. *Histopathology* **50**, 705-715
423. Vishwamitra, D., Li, Y., Wilson, D., Manshour, R., Curry, C. V., Shi, B., Tang, X. M., Sheehan, A. M., Wistuba, II, Shi, P., and Amin, H. M. (2012)

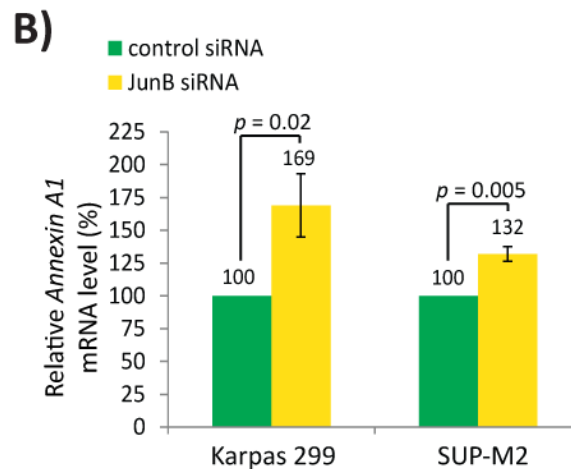
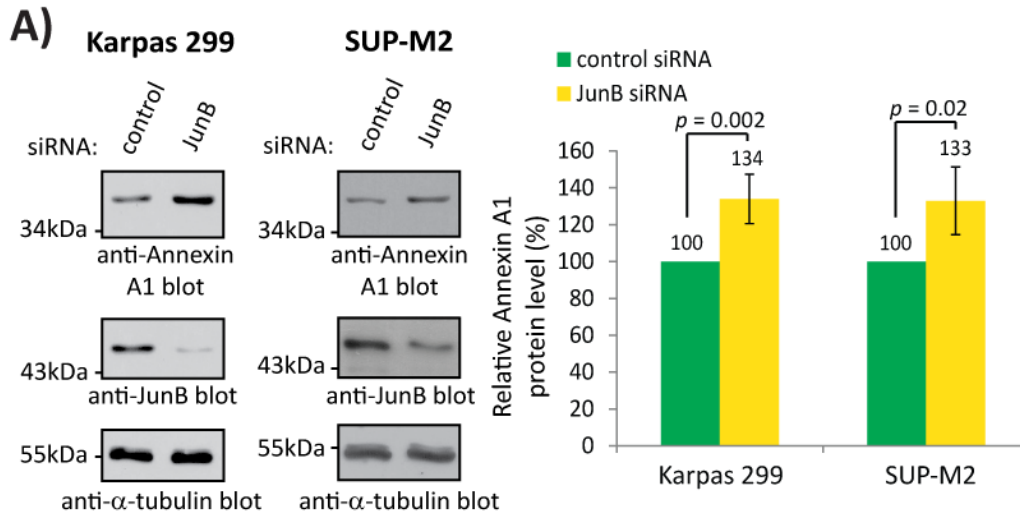
- MicroRNA 96 is a post-transcriptional suppressor of anaplastic lymphoma kinase expression. *The American journal of pathology* **180**, 1772-1780
424. Li, Y., Ye, X., Liu, J., Zha, J., and Pei, L. (2011) Evaluation of EML4-ALK fusion proteins in non-small cell lung cancer using small molecule inhibitors. *Neoplasia* **13**, 1-11
425. Takezawa, K., Okamoto, I., Nishio, K., Janne, P. A., and Nakagawa, K. (2011) Role of ERK-BIM and STAT3-survivin signaling pathways in ALK inhibitor-induced apoptosis in EML4-ALK-positive lung cancer. *Clinical cancer research : an official journal of the American Association for Cancer Research* **17**, 2140-2148
426. Koivunen, J. P., Mermel, C., Zejnullahu, K., Murphy, C., Lifshits, E., Holmes, A. J., Choi, H. G., Kim, J., Chiang, D., Thomas, R., Lee, J., Richards, W. G., Sugarbaker, D. J., Ducko, C., Lindeman, N., Marcoux, J. P., Engelman, J. A., Gray, N. S., Lee, C., Meyerson, M., and Janne, P. A. (2008) EML4-ALK fusion gene and efficacy of an ALK kinase inhibitor in lung cancer. *Clinical cancer research : an official journal of the American Association for Cancer Research* **14**, 4275-4283
427. Tanizaki, J., Okamoto, I., Takezawa, K., Sakai, K., Azuma, K., Kuwata, K., Yamaguchi, H., Hatashita, E., Nishio, K., Janne, P. A., and Nakagawa, K. (2012) Combined effect of ALK and MEK inhibitors in EML4-ALK-positive non-small-cell lung cancer cells. *British journal of cancer* **106**, 763-767

## **APPENDIX A: ADDITIONAL DATA**



### Appendix A1: Adhesion of Karpas 299 cells to fibronectin.

**(A)** Karpas 299 cells expressing control or different GzB shRNA constructs (#1-3) were incubated for 1.5 hrs in plates coated with fibronectin (then blocked with 5% BSA) or 5% BSA alone. Non-adhering cells were washed away and the proportion of cells adhering to the plate were quantified by incubating cells with 44  $\mu$ M resazurin (Sigma-Aldrich) for 4 hrs and measuring fluorescence (excitation - 544 nm, emission - 590 nm). Results are presented as a percentage of adhering cells relative to the input.  $p$  values were obtained using unpaired, one-tailed  $t$ -tests for four independent experiments. *N.S.* - not significant ( $p > 0.05$ ). **(B)** Western blot analysis of integrin  $\beta$ 1 protein levels in lysates from Karpas 299 cells stably expressing the indicated shRNAs. The anti-GzB blot demonstrates GzB knock-down and the  $\beta$ -actin blot demonstrates protein loading. Molecular mass markers are indicated to the left of blots.



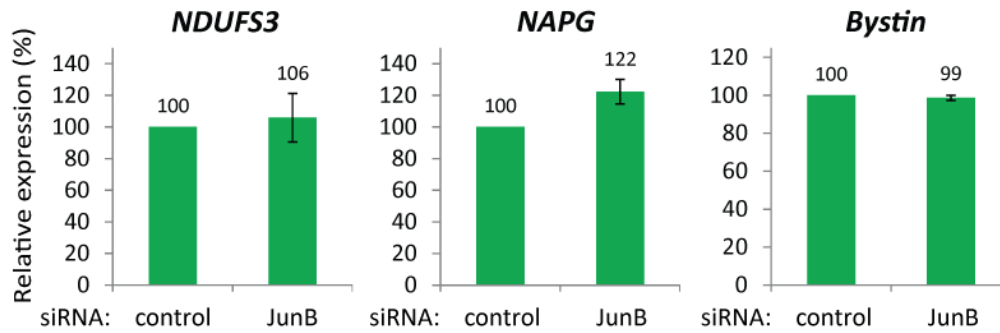
### Appendix A2: Annexin A1 expression is repressed by JunB in ALK+ ALCL cells.

**(A)** Western blot analysis of Annexin A1 levels following JunB knock-down in Karpas 299 and SUP-M2 cells (left). JunB blots demonstrate JunB knock-down and  $\alpha$ -tubulin blots demonstrate equivalent protein loading. Quantification of Annexin A1 protein levels in cells transfected with control or JunB siRNA is also included (right). **(B)** qRT-PCR analysis of *Annexin A1* message in ALK+ ALCL cells with JunB knock-down (*Annexin A1* forward primer - GCAGGCCTGGTTTATTGAAA; *Annexin A1* reverse primer - GCTGTGCATTGTTTCGCTTA). *Annexin A1* levels were normalized to  $\beta$ -actin. Note that these experiments were conducted with cells transfected with 600 nM pooled control or JunB siRNA. *p* values were obtained using paired, one-tailed *t*-tests for five (**A**, Karpas 299), four (**A**, SUP-M2) or three (**B**) independent experiments.

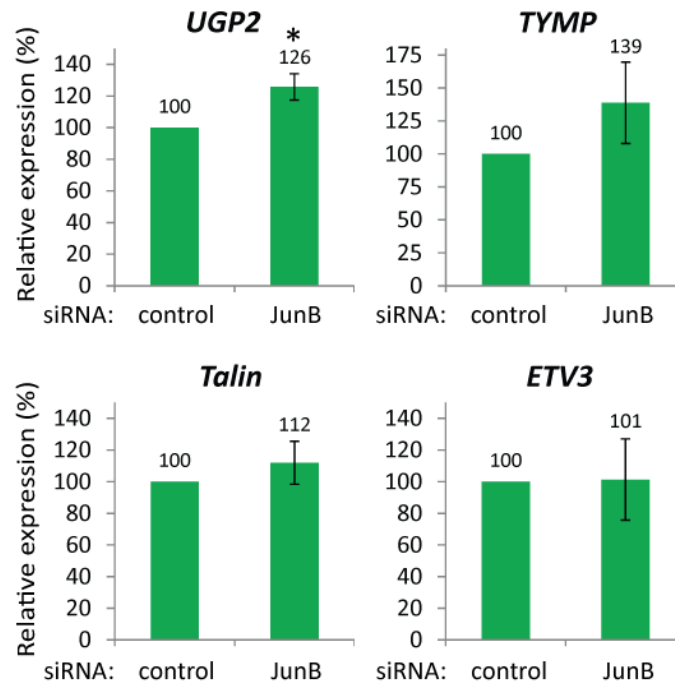
**Appendix A3: Primers used for qRT-PCR analysis of additional JunB targets.**

| <b>Target gene</b>   | <b>Forward primer sequence</b> | <b>Reverse primer sequence</b> |
|--|--------------------------------|--------------------------------|
| <b>Potentially promoted by JunB</b>  |                                |                                |
| <i>NADH-ubiquinone oxidoreductase 30 kDa subunit, mitochondrial precursor (NDUFS3)</i> | GTT CAA GGC AGC<br>CAA CTG GT  | AAG GAT GTC CCT<br>CGA AGC CA  |
| <i>N-ethylmaleimide-sensitive factor attachment protein, gamma (NAPG)</i>              | TAA ACG AGG GGC<br>TGG AAC AC  | CCT CAG GCA GGC<br>ATC TTT TG  |
| <i>Bystin</i>  | GAG AAG GCT GCC<br>ACA ATG ACA | CTG GCA GGA GGG<br>TTC TTG TTC |
| <b>Potentially repressed by JunB</b>   |                                |                                |
| <i>UTP-glucose-1-phosphate uridylyltransferase 1 (UGP2)</i>                            | ATC TGG GTG CCA<br>CAG TGG AT  | GTG AGT GTC CCG<br>CCC TTT AC  |
| <i>Thymidine phosphorylase precursor (TYMP)</i>  | ACA CAG GAG GCA<br>CCT TGG AT  | GGC TGT CAC ATC TCT<br>GGC TG  |
| <i>Talin 1</i>   | GCA GGC ACG AGA<br>TGA CAT CC  | CGC TCT CCC TTC TGC<br>TTC AC  |
| <i>ETS variant 3, isoform 1 (ETV3)</i>   | AGA GCA GCG AGG<br>AGT CAG CAC | TCC TCT TCA ATG GTC<br>CTG CTT |

### Expected to be promoted by JunB



### Expected to be repressed by JunB



#### Appendix A4: Analysis of potential JunB-regulated genes from proteins identified in a single repeat of the iTRAQ screen.

qRT-PCR analysis of the indicated targets was performed on RNA collected from Karpas 299 cells transfected with 600 nM pooled control or JunB siRNAs. Gene expression was normalized to the housekeeping gene  $\beta$ -actin. Results are the mean and standard deviation of two (expected to be promoted by JunB) or three (expected to be repressed by JunB) independent experiments. \*  $p < 0.05$ . No other targets were found to have significantly altered expression following JunB knock-down ( $p > 0.05$ ).  $p$  values were obtained using paired, one-tailed  $t$ -tests.